Evaluation of the inorganic water chemistry of the Vaal River

A Möhr

21082286

Dissertation submitted in fulfilment of the requirements for the degree *Magister Scientiae* in Environmental Sciences at the Potchefstroom Campus of the North-West University

Supervisor: Prof I Dennis

Co-supervisor: Prof JM Huizenga

May 2015

ACKNOWLEDGEMENTS

I would like to express my sincere gratitude and appreciation to:

- My supervisor Prof I Dennis
- My co-supervisor Prof JM Huizenga
- The Geology Department of the North West University for granting me this opportunity
- Dr R Dennis for the assistance in the AGIS maps
- Dr A Wood and Mr Rob Rhodes-Houghton for the editing corrections
- My mother for all her patience and moral support, and
- My Creator and Anchor in life.

Angelika Möhr

ABSTRACT

One of the most essential resources for life on our planet is water. A concern for water resource sustainability has shifted towards the sustainable development of clean water body resource (SWDF, 2009). Data for the Vaal River water chemistry is in abundance. However, research on the historic natural conditions influencing the inorganic water quality, is not as extensive. Inorganic data was obtained from the Department of Water Affairs, for the period 1972 to 2011, for identified monitoring stations along the Vaal River. Water quality was evaluated using various geochemical techniques to analyse the data.

The results of the study indicate that the water chemistry of the Vaal River is controlled by:

1. Chemical weathering of siliceous sediment, intrusive igneous rocks and metamorphic rocks (Na^+, K^+, Mg^{2+}, Ca^{2+} and $(HCO_3)^-$).
2. Anthropogenic influences increasing the sulphate (SO_4) concentration

There is no major increase in ion concentrations for the stations. However the concentrations of bicarbonate $(HCO_3)^-$ and SO_4 change as it progresses downstream from the first upstream station to the last downstream station. Based on the chemical characterisation, three groups have been identified.

(1) Group 1 stations appear to suggest a higher influence in chemical weathering than the group 2 stations. (2) Group 2 stations appear to suggest a greater influence from SO_4. (3) Group 3 stations appear to suggest an influence from both the bicarbonate and the SO_4 influences.

Geographically the chemical weathering is an indication of the three different groups with strong anthropogenic influences in the middle group. The water chemistry for the Vaal River is controlled by two processes, namely chemical weathering and anthropogenic influences. The prominent indication of the difference in these two influences can be seen between group 1 and group 2. A secondary conclusion indicates that a total dissolved solid (TDS) alone is not an accurate representation of anthropogenic influence (or poor water quality) on inorganic water quality of the Vaal River. The natural weathering or geological influences appears to play a more dominant role in certain sections or catchments with lower contributions from anthropogenic influences.

Key words:

Chemical weathering, HCO_3, anthropogenic, water quality, acid mine drainage, geochemical influence, groundwater, surface water.

ABBREVIATIONS AND ACRONYMS

AGIS	Agricultural Georeferenced Information System
AMD	Acid Mine Drainage
Carb	Carbonate rocks
CB	Charge Balance
DEAT	Department of Environmental Affairs and Tourism
DWA	Department of Water Affairs
DWAF	Department of Water Affairs and Forestry
K_a	Equilibrium constant
K_w	Dissociation constant
SANSP	South African National Scientific Programmes
SWDF	Safe Water Drinking Foundation
WMA	Water Management Area

Chemical parameters

Ca	Calcium
Cl	Chlorine
CO_3	Carbonate
EC	Electrical conductivity
F	Fluorine
HCO_3	Bicarbonate
K	Potassium
Mg	Magnesium
Na	Sodium
NH_4	Ammonia
NO_3	Nitrate

NO_2	Nitrite
pH	Chemical logarithm of hydronium ion concentration (the acidity or basicity of an aqueous solution)
PO_4	Phosphate
Si	Silica
∑Z+	Sum of all anions
∑Z-	Sum of all cations
SO_4	Sulphate
TAL	Total alkalinity in mol/L
TDS	Total Dissolved Solids

UNITS OF MEASUREMENT

kg/annum	kilogram per annum
km	kilometre
km^2	square kilometre
m^3	cubic metre
meq/ℓ	mili-equivalent per litre
mg/ℓ	milligrams per litre
mmol/ℓ	mili-moles per litre
mm/a	millimetre per annum
Mm^3/a	million cubic meters per annum
mS/m	mili-siemens per meter
µS/cm	micro-siemens per centimetre

TABLE OF CONTENTS

LIST OF FIGURES

LIST OF TABLES

1 INTRODUCTION

1.1 PREAMBLE

One of the most essential resources for life on our planet is water. A significant concern for water resource sustainability has shifted from the limited availability of water sources, particularly in South Africa, towards the sustainable development of clean, uncontaminated streams, rivers, oceans and any other large water body resource (SWDF, 2009). Without water; biodiversity, social and economic development is impossible to maintain (Ashton, 2002). Due to rapidly increased population growth and urbanisation, there has been a prompt increase in water demand in South Africa (King, 2004).

According to King (2004), whilst most of the commercial heart of South Africa is based in Gauteng Province and neighbouring provinces, they are all dependent upon the Vaal River system for water supply. A complicating factor is that the majority of the region has an arid to semi-arid climate. Another critical factor is the rainfall in the region is also unevenly distributed as shown in Figure 1-1 (King, 2004). These variations in rainfall are due to the Hadley cell effect, from the Drakensberg high altitude in the east with the warm Indian Ocean and the colder Atlantic Ocean on the west coast with a much lower altitude (O'Keeffe *et al.,* 1992). According to DEAT (2007), due to high evaporation rates the surface water recharge only yields 60% from the mean annual runoff. It is estimated that 20% of the runoff has to remain in the rivers to support the ecological components in the environment. A substantial portion of the surface water resource is abstracted for agricultural use (approximately 60%), leaving limited water supply available to industrial, commercial and residential use (DEAT, 2007).

The majority of South African water requirements are currently supplied by surface water (rivers and dams). Surface water resources are highly developed throughout the country, but are unevenly distributed. As a result, a significant amount of the water is transported both nationally and internationally via inter-basin transfer schemes (DEAT, 2007). To assist in water supply and management, South African surface water resources are divided into 9 primary catchment areas. The Vaal River falls within the Vaal Catchment, primary catchment C. The primary catchments have further been divided into quaternary catchment regions with reference to smaller tributaries draining into the primary rivers.

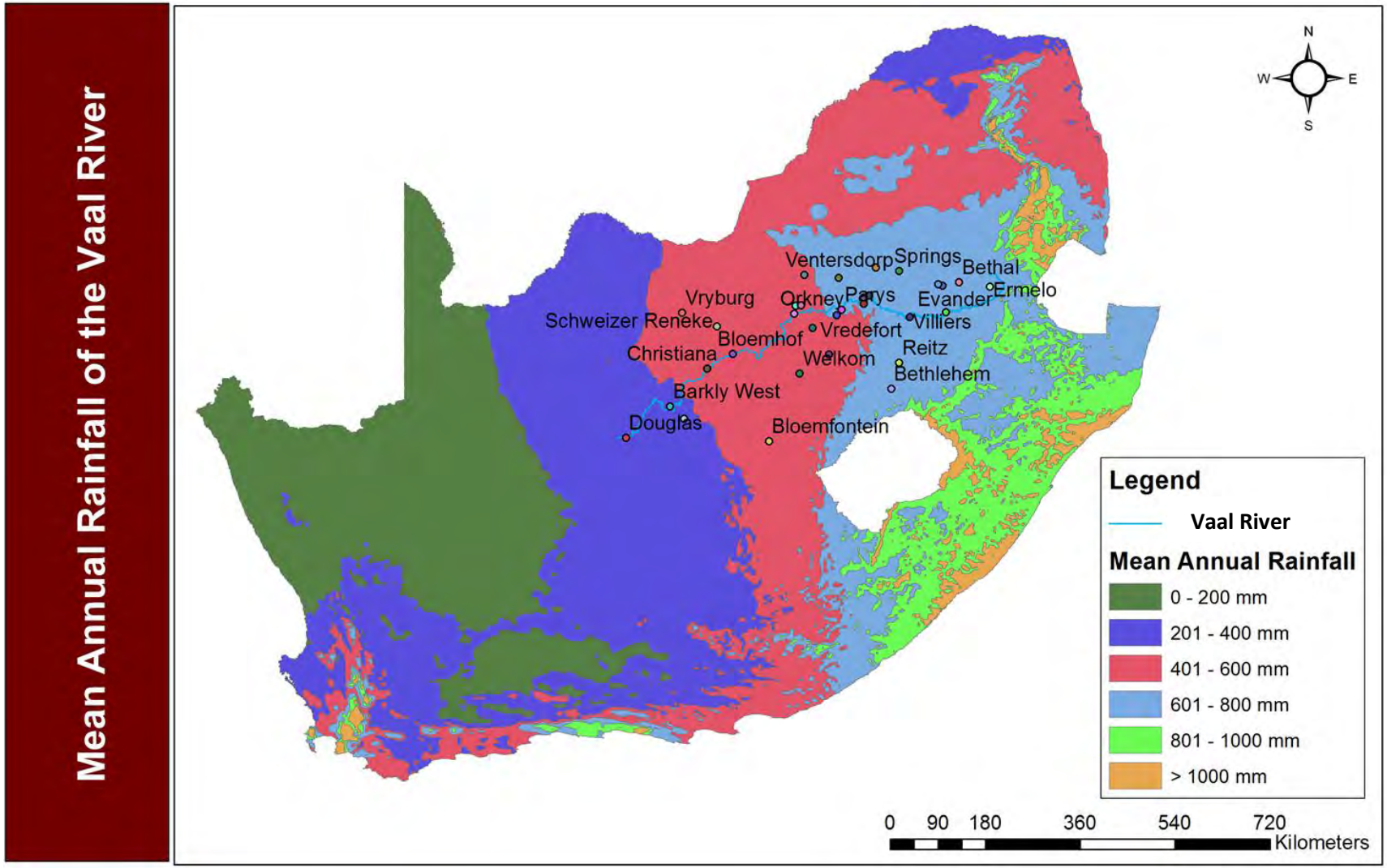

FIGURE 1-1: MEAN ANNUAL RAINFALL AND RAINFALL VARIATION OF SOUTH AFRICA WITH THE VAAL RIVER INDICATED (AGIS, 2009)

The Vaal River is the second largest river system (after the Orange River system) in South Africa, supplying approximately 16% of the country's population with water (DEAT, 2007). The different uses for the Vaal River are summarised in Table 1-1. Table 1-2 and show the importance of the Vaal River for agricultural and domestic use, mining, industry and power generation. This understandably leads to high water usage and pollution.

TABLE 1-1: WATER REQUIREMENTS FOR THE YEAR 2000 (MILLION M^3 PER ANNUM) FOR THE VAAL RIVER MANAGEMENT AREA (DEAT, 2007)

Water management area	Irrigation	Urban	Rural	Mining and bulk industrial	Power generation	Afforestation	Total local requirements
Total Vaal	798	796	119	264	80	0	2057
Total for South Africa	7920	2897	574	755	297	428	12871

TABLE 1-2: WATER REQUIREMENTS FOR THE YEAR 2000 FOR THE VAAL RIVER MANAGEMENT AREA (DEAT, 2007)

Water management area	Irrigation	Urban	Rural	Mining and bulk industrial	Power generation	Total local requirements for the area
Upper Vaal	6%	31%	2%	8%	4%	**51%**
Middle Vaal	7%	5%	2%	4%	0%	**18%**
Lower Vaal	25%	3%	2%	1%	0%	**31%**
Total Vaal (million m^3 per annum)	798	796	119	264	80	2057

1.2 SCOPE OF RESEARCH

The study focus is on the characterisation of the water quality for the Vaal River. The Department of Water Affairs (DWA) intensely monitors the Vaal River water quality, which has resulted in a large dataset for the Vaal River Catchment. A historic evaluation of the Vaal River water quality has, however, not been undertaken. A study by DWAF (2009), focussed mainly on total dissolved solids (TDS) and pH, without going into considerable detail with regards to the geographical differences in water quality or distinguishing between natural and anthropogenic factors contributing to the water quality.

Therefore the hypothesis of this study was initiated to focus on two principal issues: (1) How does the water quality of the Vaal River vary geographically, and (2) what are the controlling factors of the Vaal River water chemistry.

The hypothesis is that the geological and geochemical influences determine the quality of the water in the Vaal River.

The results of this study can be used as a basis for future studies on the Vaal River, and planning for management of water contamination and associated salinisation.

1.3 LAYOUT OF THE DISSERTATION

The body of the dissertation is organised into 5 chapters namely:

- Chapter 1 which provides an introduction and discusses the scope of the work.
- Chapter 2 presents the methods used in this study, including data manipulation and an explanation of the diagrams used for data interpretation.
- Chapter 3 introduces the factors influencing water chemistry, with specific reference to South Africa. The influencing factors being chemical weathering, climate and anthropogenic activities. The focus is on the influence of chemical weathering on the water chemistry.
- Chapters 4 presents detailed interpretation of the results.
- Chapter 5 follows with associated conclusions that can be drawn from the results, as well as recommendations based on the interpretations and conclusions.

1.4 DESCRIPTION OF STUDY AREA

The Vaal River is 1120 kilometer (km) in length, and is the largest tributary of the Orange River in South Africa with a 192 000 square kilometre (km^2) catchment surface area, as shown in Figure 1-2 (Braune and Rogers, 1987 and DEAT, 2007). The Vaal River originates in the western slopes of the Drakensberg mountains in Mpumalanga, approximately 240 km from the Indian Ocean. It flows 900 km west-south-west across the interior plateau to join the Orange River near Douglas, southwest of Kimberley in the Northern Cape Province. The Vaal River forms the border between Gauteng, Mpumalanga and the North West Provinces on the northern bank and the Free State on the southern bank. It flows east of Johannesburg and approximately 30 km north of Ermelo (Braune and Rogers, 1987).

Major tributaries of the Vaal River catchment are rivers draining from the Drakensberg in the east, Witwatersrand in the north and the Maluti Mountains in the south. Due to the underlying dolomites and associated geological structures in the Pretoria-Witwatersrand-Vereeniging area, the basin could potentially be considered as a source of groundwater. Options have been studied for the usage of this water for emergency or continuous abstraction and artificial recharge (DWA[1], 2011). According to DWA (2011), a complicating factor associated with the groundwater recharge, is the poor water quality associated with

the recharge from the coal and gold mines. This causes pollution of the groundwater and, when discharged to the surface, pollution of the Vaal River and associated catchment.

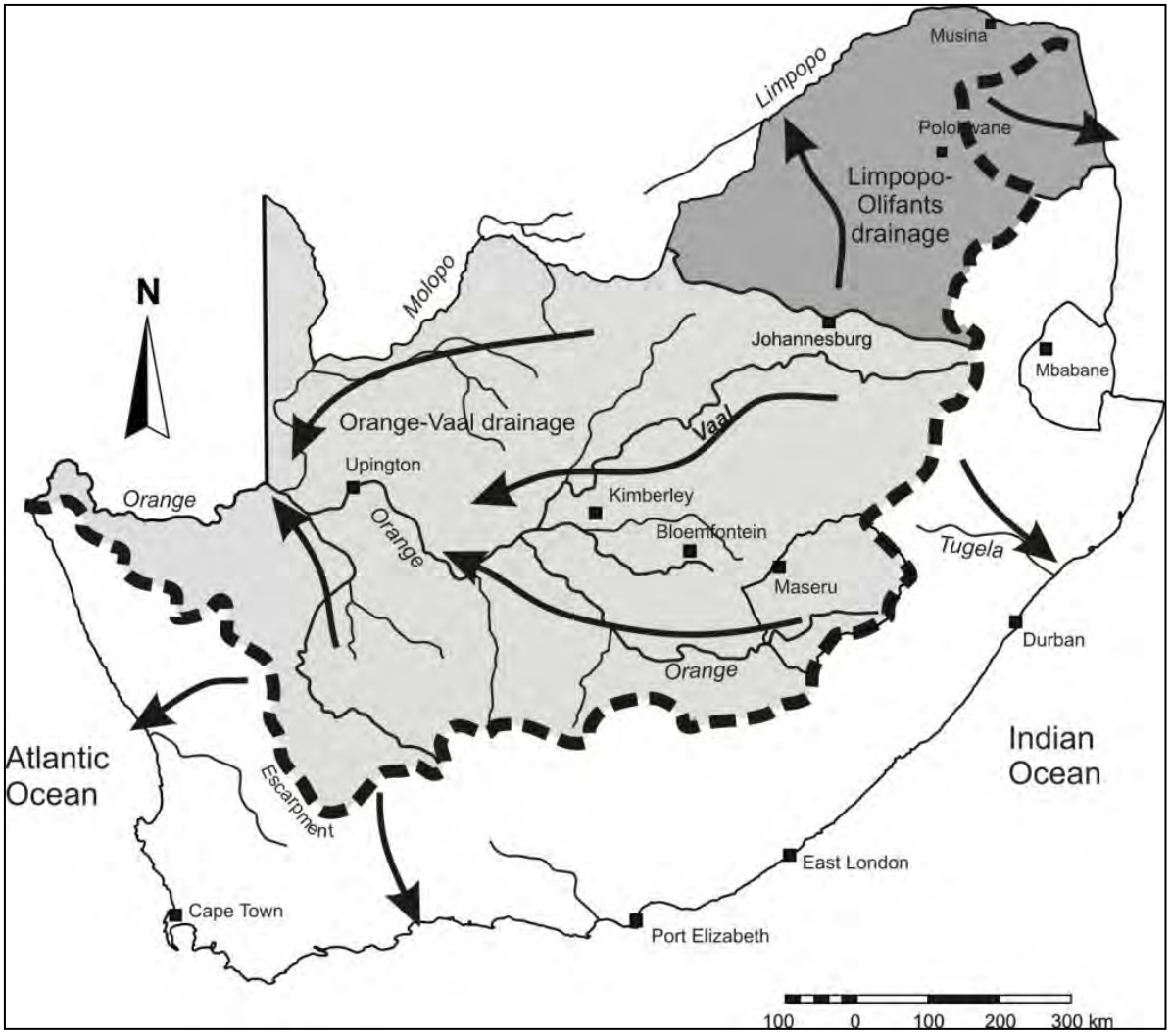

FIGURE 1-2: ORANGE-VAAL RIVER CATCHMENT WITHIN SOUTH AFRICA. DRAINAGE IS TOWARDS THE ATLANTIC OCEAN (Huizenga, 2011)

The Vaal catchment is subdivided into three larger areas: (1) Upper Vaal Water Management Area (WMA), with a water flow of 180 million cubic meters (m^3) per annum, (2) the Middle Vaal WMA, with a flow of 34 million m^3 per annum, and (3) the Lower Vaal WMA, with a flow of 30 million m^3 per annum. Subsequently the Vaal catchment is subdivided into 9 sub-catchment areas (Figure 1-3). The Vaal River produces 8% of the total annual runoff in South Africa per year (Braune and Rogers, 1987). Allegedly, 244 million m^3 per annum of water is being used unlawfully in the catchment, as well as pollution increasing (DWA[2], 2011), thereby exacerbating the problem.

The Vaal River catchment rainfall ranges from 800 mm per annum (mm/a) in the East to 200 mm/a in the West (Figure 1-4). The Vaal River originates in the Drakensberg area, near Breyten. The highest rainfall (600 to 800 mm/a) and the lowest evaporation occur in the Vaal River system. Following the river, the rainfall decreases and the evaporation steadily increases westward to 300 and 225 mm/a, respectively. This might have a significant implication on water quality, further research should be considered in this regard.

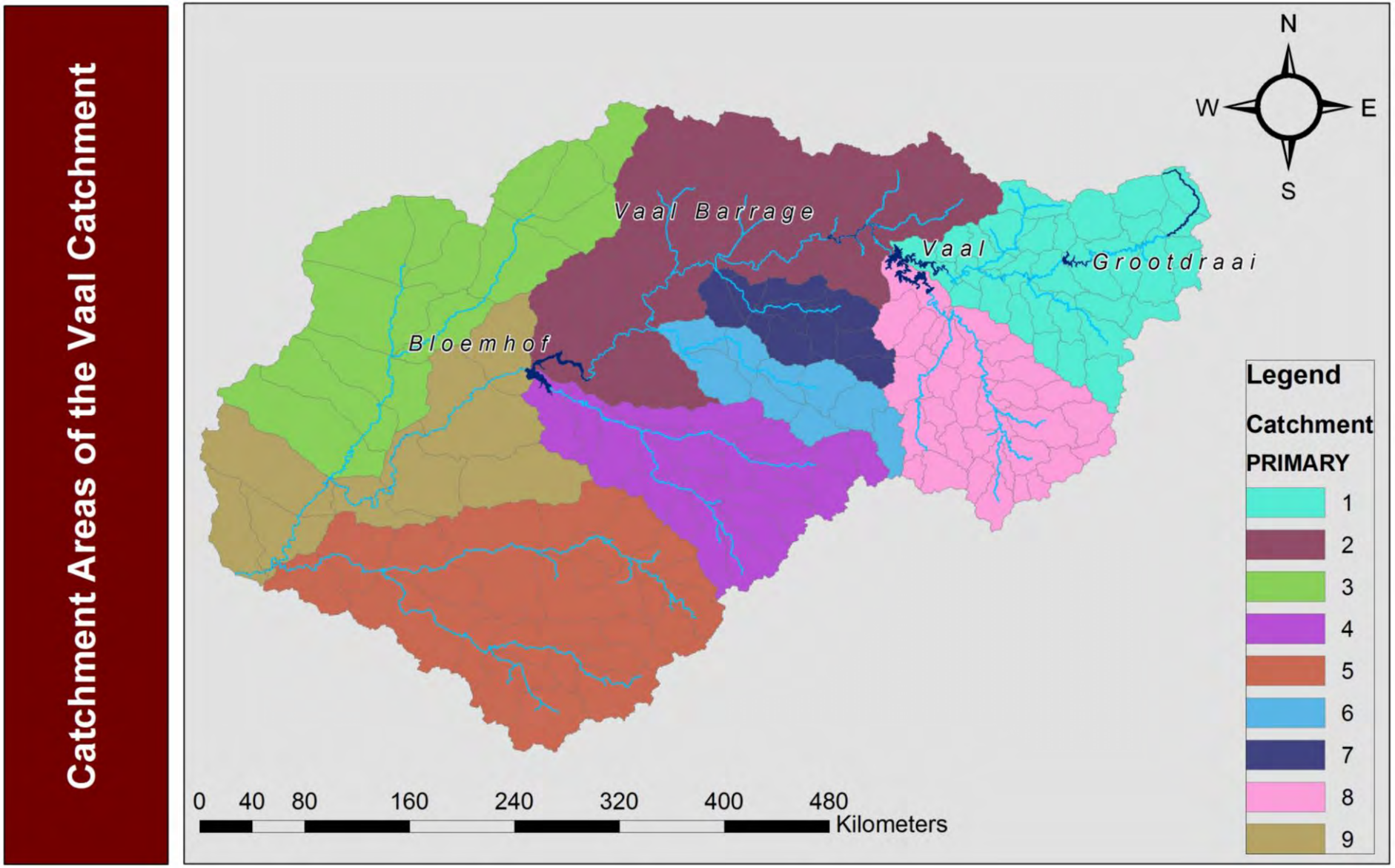

FIGURE 1-3: VAAL RIVER CATCHEMENT WITHIN SOUTH AFRICA (AGIS, 2009)

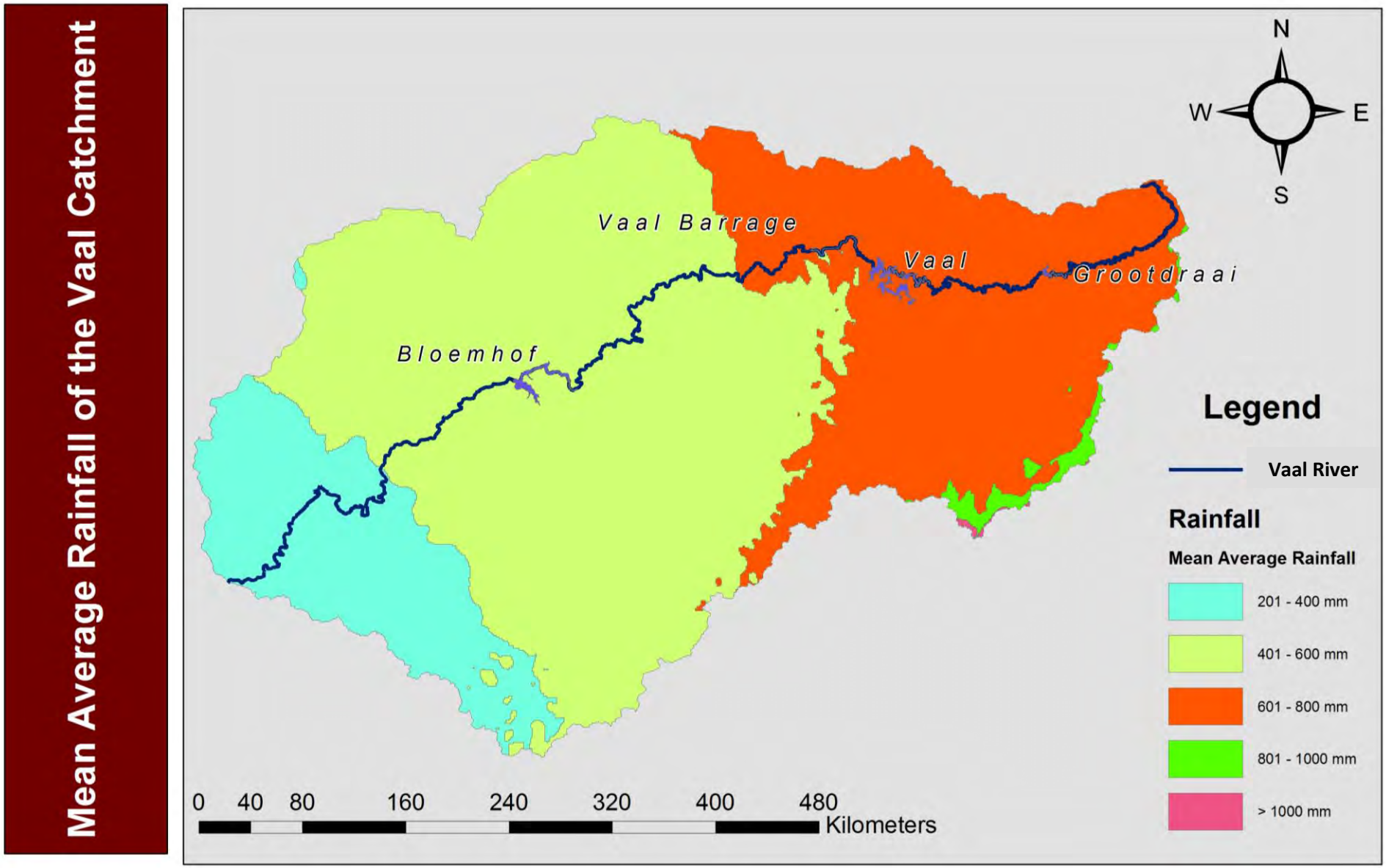

FIGURE 1-4: MEAN ANNUAL AVERAGE RAINFALL OF THE VAAL RIVER (AGIS, 2009).

The Vaal River catchment is situated in the economic heartland of South Africa (Figure 1-5), including the Pretoria-Witwatersrand-Vereeniging complex. The development of urban, industrial, mining and power generation industries in the catchment area is the greatest in South Africa (DEAT, 2007).

These activities require water and, in addition, also contribute to the pollution of the Vaal River system by their return flow. Concern for the near future is the imbalance between the supply and return flow, the growing demand for water and associated water pollution. The increasing water pollution associated with the Vaal River has attracted the attention of the public media such as NEWS 24 (2007), Carte Blanche (2009), The Times (2012) and Khakibos (2013).

According to Anthony Turton (The Times, 2012) "*South Africa has trapped so much of its water, massive blooms of toxic algae are able to flourish, posing a significant threat to our water supply. The Department of Water Affairs' emergency solution to the acid mine drainage crisis in Gauteng will leave the Vaal River so polluted that its water will not be fit for human consumption within two years (2014)*".

To aid the clean water availability reduction within the Vaal Barrage and the Vaal River, DWA introduced the Lesotho Highlands project, with phase two coming into effect in approximately 2024. The augmentation scheme can deliver water by 2019, however this will not be sufficient and water supply problems will still need to be addressed properly (DWAF, 2009).

Industrial activities in the catchment of the Vaal River include: steel, paper and pulp mills, chrome and ferrous metal smelters, petrochemical refineries, fertiliser and chemical manufacturers, food and beverage industries, breweries, metal finishing and plating activities, meat abattoirs, concrete manufacturers, industrial and municipal waste dumps, clay and sand quarries, and agricultural and residential areas, amongst many others.

According to Huizenga (2011) these specific activities, however, have not been identified as having a significant impact on the water quality as the current and projected near-future impacts of the coal, gold and mineral mining activities as well as the significant power generation related activities have been isolated in the catchment. Industry or industry density has not yet been isolated as the contributing factors (Huizenga, 2011) (see Table 1-3 for the list of mines and associated positions in Figure 1-5 in the near vicinity of the Vaal River).

TABLE 1-3: LIST OF ACTIVE MINES IN THE NEAR VICINITY OF THE VAAL RIVER (INTIERRARMG, 2013)

NAME OF MINE	COMMODITY	TYPE OF MINING	NEAREST TOWN	PROVINCE
Arnot colliery	Coal	Opencast/underground	Middelburg	Mpumalanga
Strathrae colliery	Coal	Opencast	Carolina	Mpumalanga
Eastside coal company	Coal	Opencast	Carolina	Mpumalanga
Tselentis colliery	Coal	Opencast/underground	Ermelo	Mpumalanga
Spitzkop mine	Coal	Opencast	Lydenburg	Mpumalanga
Golfview mine	Coal	Opencast/underground	Ermelo	Mpumalanga
Forzando Coal mines (Pty) Ltd	Coal	Underground	Bethal	Mpumalanga
Taaiboschspruit	Coal	Underground	Ermelo	Mpumalanga
New Denmark colliery	Coal	Underground	Standerton	Mpumalanga
Sasol Surface Services	Coal	Underground	Secunda	Mpumalanga
New Vaal colliery	Coal	Opencast	Sasolburg	Free State
Sigma colliery	Coal	Opencast/underground	Sasolburg	Free State
Driefontein colliery	Coal	Opencast	Witbank	Mpumalanga
Frank smith mine	Diamonds	Underground	Barkly west	Northern Cape
Loxton	Diamonds	Underground	Kimberley	Northern Cape
DuToitspan	Diamonds	Underground	Kimberley	Northern Cape
Libanon	Gold	Underground	Westonaria	Gauteng
Mponeng	Gold	Underground	Westonaria	Gauteng
Deelkraal	Gold	Underground	Westonaria	North West
Elandsrand	Gold	Underground	Westonaria	Gauteng
African Rainbow Minerals	Gold	Underground	Odendaalsrus	Free State
Moab Khotsong (Vaal Reefs)	Gold	Underground	Klerksdorp	Gauteng
Great Noligwa	Gold	Underground	Orkney	North West
Kopanang	Gold	Underground	Westonaria	Gauteng
Savuka	Gold	Underground	Carltonville	Gauteng
Vaal River Operations	Gold, cobalt , iron-pyrites, P.G.M., silver, sulphur, uranium	Underground	Klerksdorp	North West
Target operations	Gold, iron-pyrites, silver, sulphur	Underground	Odendaalsrus	Free State
Buffelsfontein	Gold, iron-pyrites, silver, sulphur, uranium	Underground	Klerksdorp	North West
Hartebeestfontein	Gold, iron-pyrites, silver, sulphur, uranium	Underground	Klerksdorp	North West
Blyvooruitzicht	Gold, P.G.M., silver, uranium	Underground	Oberholzer	Gauteng
Kloof - Driefontein	Gold, silver	Opencast/underground	Westonaria	Gauteng
Glen Douglas Dolomite mine	Limestone, aggregate	Opencast	Vereeniging	Gauteng
Afrisam - ULCO	Limestone, shale	Opencast	Barkly west	Northern Cape

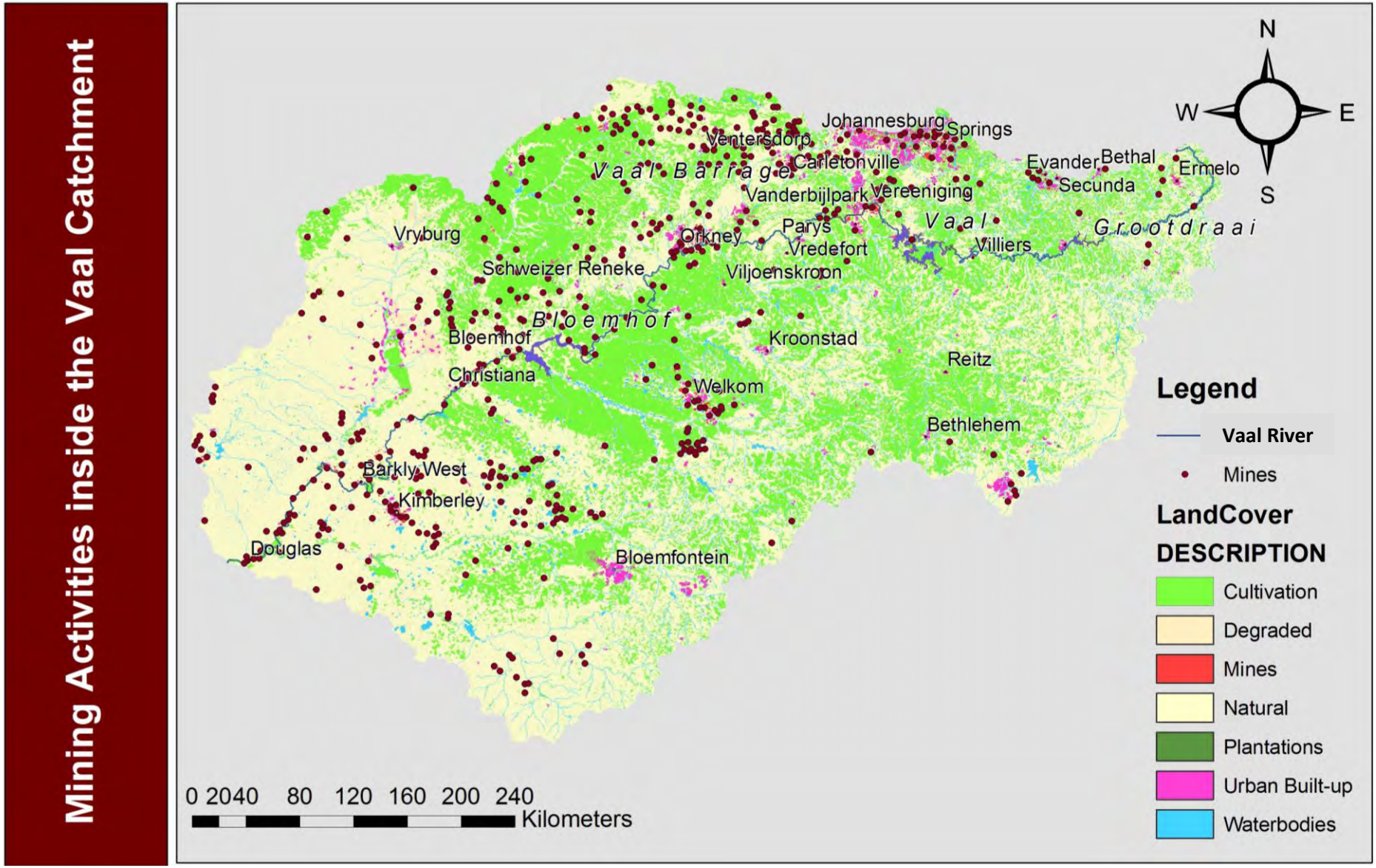

FIGURE 1-5: MINES SURROUNDING THE VAAL RIVER (AGIS, 2009)

1.5 GEOLOGY OF THE VAAL RIVER AREA

The water chemistry of the Vaal River is controlled to a large extent by the bedrock geology (Huizenga, 2011). The Vaal River meanders (from east to west), over-exposed rocks belonging to the Witwatersrand, Transvaal, Ventersdorp and the Karoo Supergroups (Figure 1-6) (McCarthy and Rubidge, 2005).

The dominant lithologies that are exposed within the Vaal catchment include the following:

- Banded Iron Formation (Witwatersrand Supergroup)
- Carbonate rocks (limestone and dolomite) (Transvaal Supergroup)
- Granites and granitic gneisses (Witwatersrand and Ventersdorp Supergroup, Archean granites)
- Felsic, mafic, and ultramafic volcanic rocks (Witwatersrand Supergroup)
- Siliclastic sediments (Karoo Supergroup)

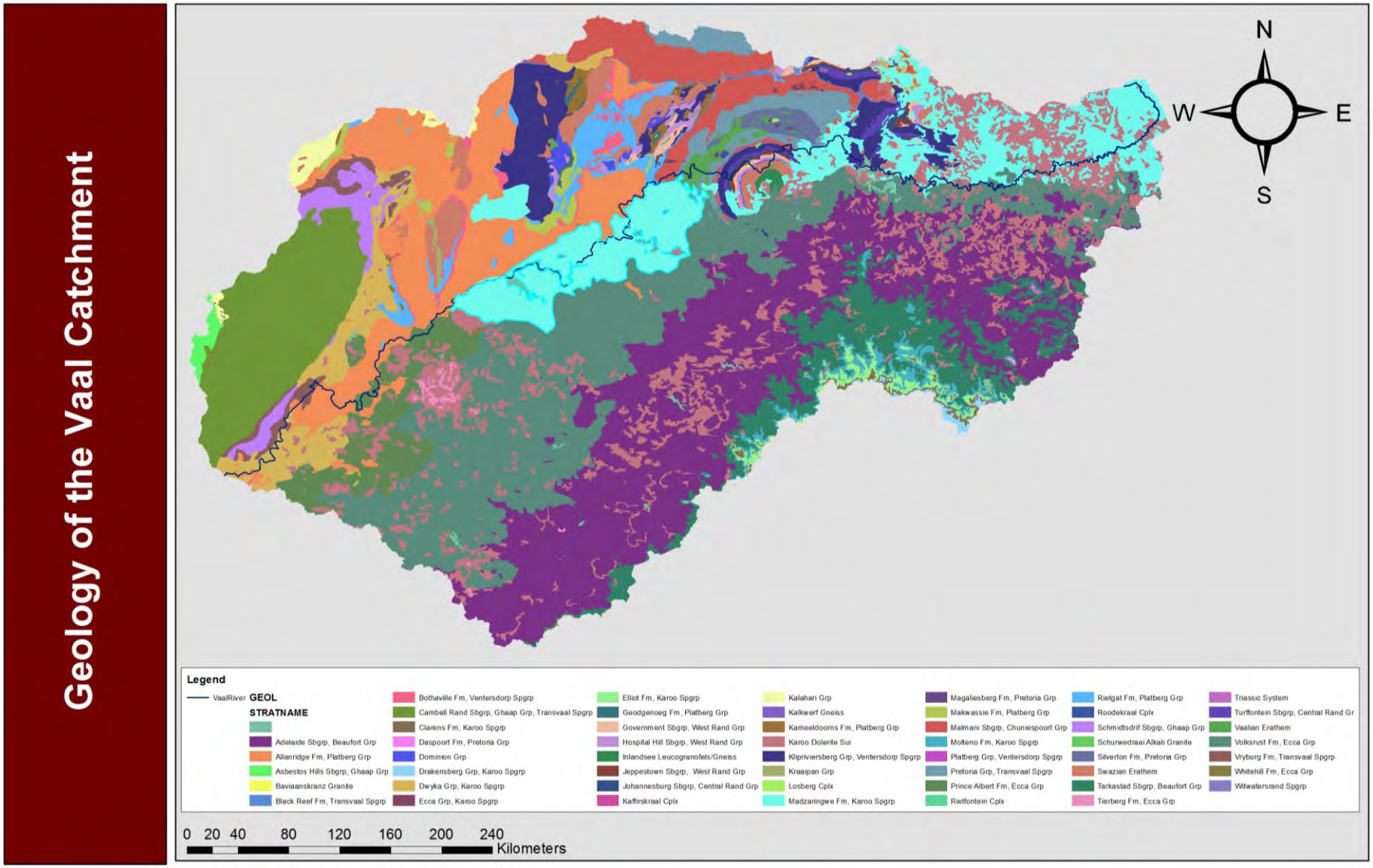

FIGURE 1-6: GEOLOGICAL MAP OF THE VAAL RIVER SHOWING THE DIFFERENT LITHOLOGIES (AGIS, 2009).

The influence of chemical weathering of these rock types on the Vaal River water chemistry is summarised in Table 1-4 and a simplified representation, taking into consideration Table 1-4, is depicted in Figure 1-7.

TABLE 1-4: LIST OF DOMINANT LITHOLOGIES IN THE VAAL RIVER CATCHMENT SHOWING TYPICAL CATIONS THAT WILL BE RELEASED INTO THE RIVER WATER DURING CHEMICAL WEATHERING

Lithologies	Dominant ions derived from chemical weathering	TDS concentration
Banded Iron Formations	N/A	Low
Carbonates	Ca, Mg, $(HCO_3)^-$	High
Granites / granitic gneiss	Na, K, $(HCO_3)^-$, ±Ca	Low
Felsic volcanic rocks	Na, Ca, K, $(HCO_3)^-$	Medium
Mafic and ultra-mafic volcanic rocks	Ca, Mg, $(HCO_3)^-$	Medium to high
Siliclastic sediments	Na, K, $(HCO_3)^-$, ±Ca	Low

Chapter 2 is an indication of the methodology applied during this study.

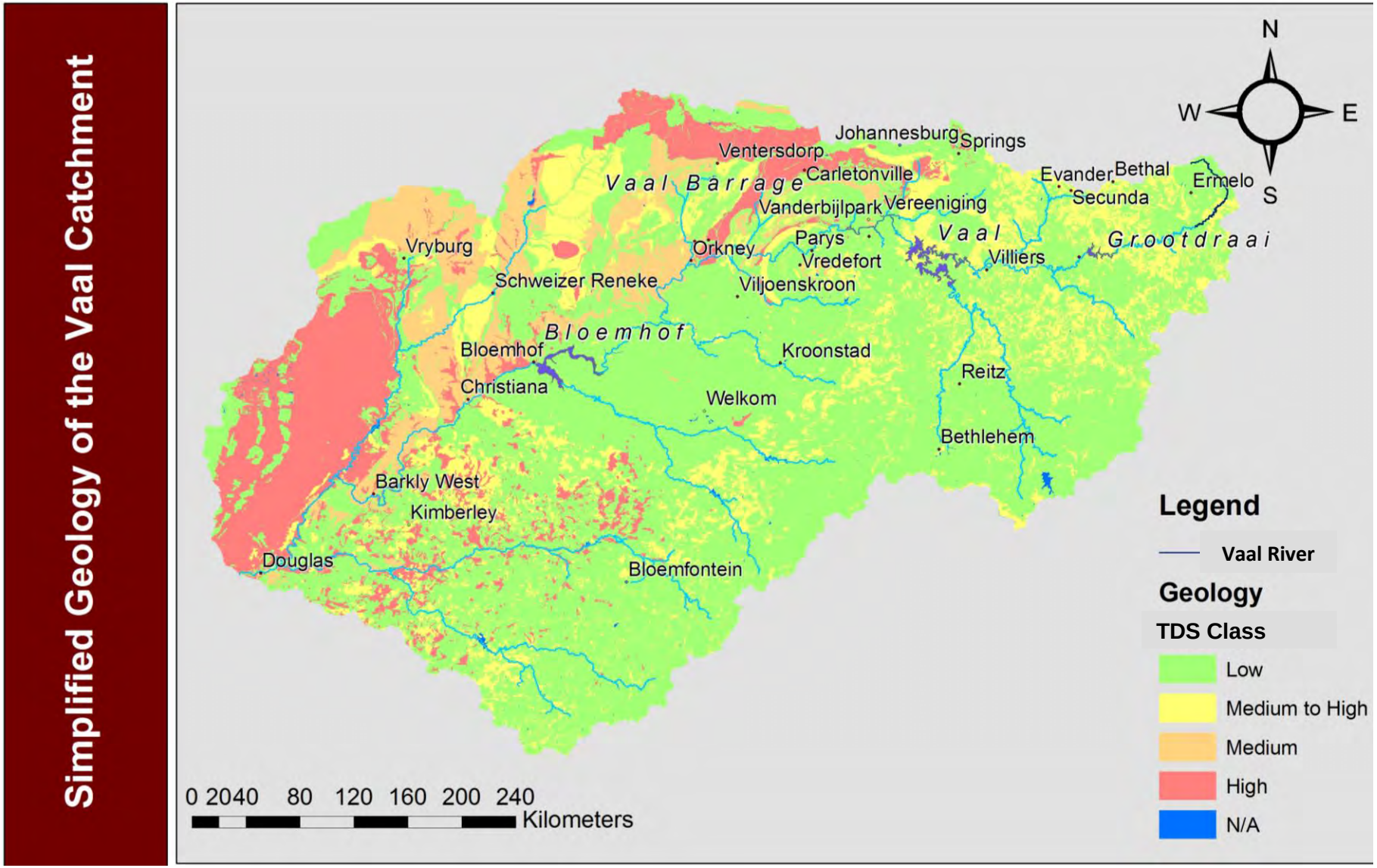

FIGURE 1-7: SIMPLIFIED GEOLOGY OF THE VAAL CATCHMENT (AGIS, 2009)

2 METHODOLOGY

2.1 INTRODUCTION

In this Chapter data collection and data manipulation are addressed. Furthermore, hydro-geochemical diagrams that are used to characterise the Vaal River water chemistry are introduced and explained.

2.2 DATA COLLECTION

Inorganic chemistry data (major elements, pH, electrical conductivity (EC), alkalinity, and TDS) were obtained from the DWA for sample stations along the Vaal River (191 stations in total). The data were imported into a database and monitoring points for the entire Vaal Catchment (Surface water Catchment C) were overlaid on top of the Vaal River and tributaries. The dataset was extremely large and the following methods were used to eliminate more of the stations 1) monitoring points located on the smaller secondary tributaries of the Vaal River were eliminated and 2) all primary river monitoring points with insufficient data were eliminated.

Because of the elimination of these monitoring points, a large portion of the westerly section of the Vaal River water quality has not been accounted for. The stations located west and near the confluence with the Orange River did not have sufficient data or monitoring stations. As these monitoring points on the lower Vaal River were insufficient to use, no background comparison could be made with water contained in the channels, and the canal monitoring stations were eliminated. A large section of the lower part of the Vaal catchment area was, as a result, not part of the monitoring data considered.

For this study 65 stations were identified in the Vaal River system, 20 on the Vaal River (primary river) and the remainder on primary tributaries. The sample stations that were used were in the following catchments, as listed in Appendix 1: catchments C1, C2, C3, C4, C6, C7, C8 and C9. Table 2-1 is an indication of differences considered for each of the catchment areas. Figure 2-1 shows the geographical distribution of the sample stations in the Vaal Catchment, with an indication of the main stations located along the Vaal River.

TABLE 2-1: A NUMBER OF DIFFERENCES CONSIDERED FOR THE CATCHMENT AREAS WITHIN THE VAAL RIVER CATCHMENT

Catchment	Rainfall (mm) (Figure 1-1)	Flow rates (average)	Simplified Geology Supergroups	Simplified TDS Class (Figure 1-7)	Potential pollution
C1	601 – 800	2.3 – 39.3	Archaean Granites Witwatersrand Ventersdorp Transvaal	Low Medium – High	Residential Agricultural
C2	601 – 800 401 – 600	38.9 – 89.6	Archaean Granites Witwatersrand Ventersdorp Transvaal	Medium High	Residential Industrial Mining
C3	401 – 600 201 - 400	N/A	Transvaal	Medium High	Residential Agricultural
C4	401 – 600	N/A	Ventersdorp Karoo	Low Medium – High	Residential Agricultural
C6	401 – 600	N/A	Ventersdorp Karoo	Low	Residential Agricultural
C7	401 – 600	N/A	Ventersdorp Karoo	Low Medium – High	Residential Agricultural
C8	601 – 800 401 – 600	N/A	Karoo	Low Medium – High	Residential Agricultural
C9	401 – 600 201 - 400	11.6 – 64.8	Ventersdorp Transvaal	Medium High	Residential Agricultural

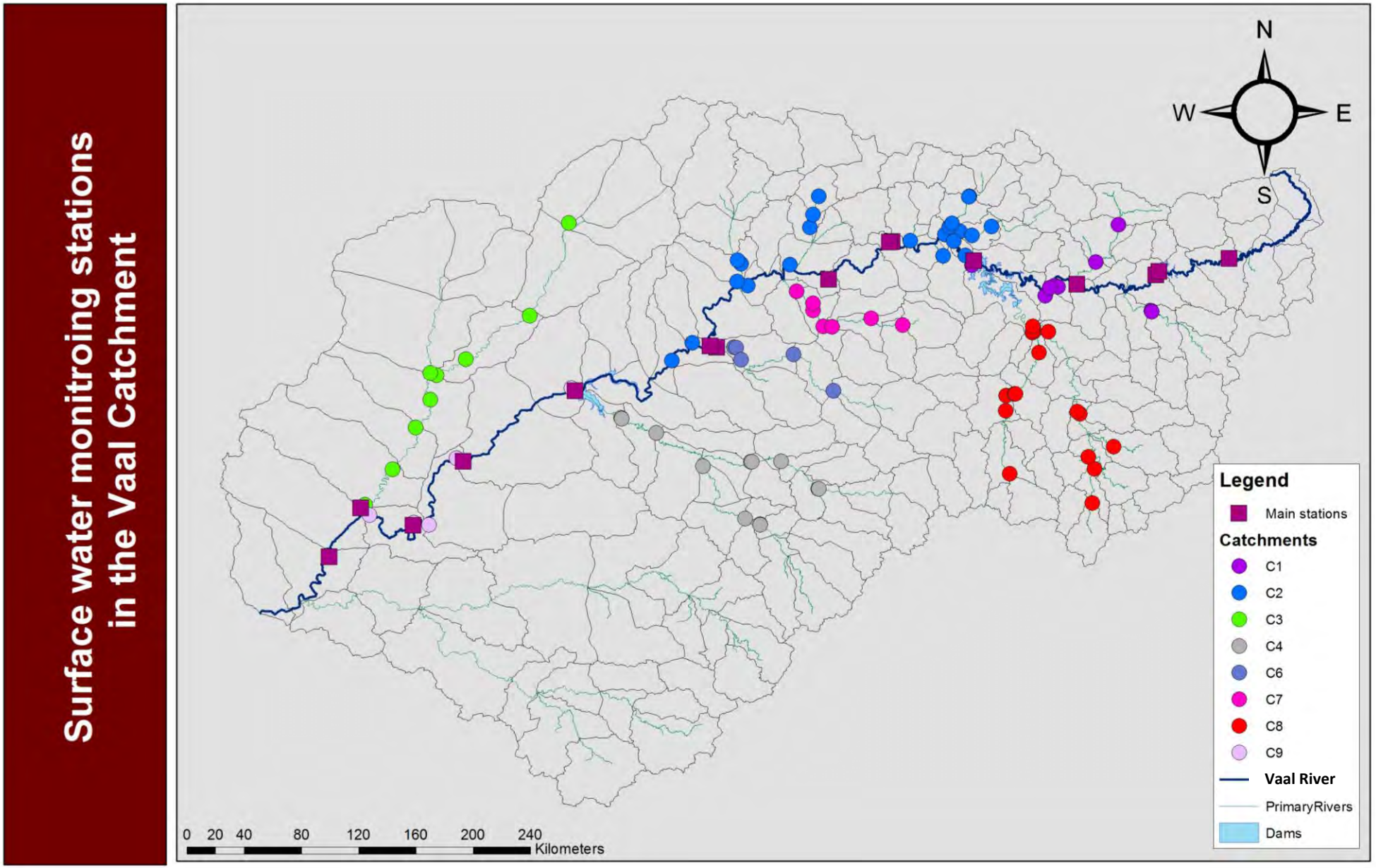

FIGURE 2-1: MAP INDICATING ALL SURFACE WATER SAMPLE STATIONS IN THE VAAL CATCHMENT, WITH INDICATION OF MAIN STATIONS ON THE VAAL RIVER (AGIS, 2009)

2.3 DATA MANIPULATION AND ACCURACY OF CHEMICAL ANALYSIS

The data set used for this study was provided by DWA. The analysis methods are not available, further information is also contained in Huizenga (2011). Accurate data from the original set were used to determine the water chemistry (a digital copy of the data included with Appendix 1). The accuracy was determined from the charge balance (CB), using the equation below (Appelo and Postma, 1993):

CB (%) = 100 × (|Σ [Cations] | - |Σ [Anions] |) / (|Σ [Cations] | + |Σ [Anions] |)

where the concentrations of the fluid species are expressed in meq/L (milli-equivalents per litre), which is the product of molar concentration with the relevant charge of the fluid species.

Carbonate $(HCO_3)^-$ and bicarbonate $(CO_3)^{2-}$ concentrations are necessary for the charge balance calculation. Concentrations of $(HCO_3)^-$ and $(CO_3)^{2-}$ (mol/L) were calculated from the total alkalinity (TAL in mol/L) and the pH, using the following equations, taken directly from Huizenga (2011) as per Appelo and Postma (2005):

$$[(HCO_3)^-] = 2 \times (TAL_{molar} - 10^{pH - pKw}) / (1 + 2 .10^{pH + pKa})$$

and

$$[(CO_3)^{2-}] = (TAL_{molar} - [(HCO_3)^-])/2$$

where K_w denotes the dissociation constant for water (10^{-14}) and K_a is the equilibrium constant ($10^{-10.3}$) for the reaction $(HCO_3)^- \leftrightarrow (CO_3)^{2-} + H^+$.

The total data set included 86 965 complete analyses. Only data with a charge balance between –5% and +5% were used in this study. Data for the 65 identified stations included 51298 complete analyses, 59% of all the data.

2.4 HYDRO-GEOCHEMICAL DIAGRAMS

For this study a number of diagrams were used to compare the water chemistry of the Vaal River on a temporal and spatial scale. In this section, these diagrams are introduced and briefly explained.

2.4.1 GIBBS DIAGRAM

The Gibbs diagram was introduced in 1970 and shows the two major mechanisms controlling surface water chemical composition. The dominant mechanisms are rock weathering and the evaporation-crystallisation processes. These two processes can be visualised as shown in Figure 2-2 in which TDS (mg/L) values are shown with respect to the $Na^+/(Ca^{2+} + Na^+)$ ratio (in mg/L). Rivers that are not affected by either chemical weathering or evaporation have an unaltered rain water composition (point C in Figure 2-2). The diagram shows three main end member compositions for river water:

- **Precipitation dominated end-member:** River water chemistry is controlled by rain water chemistry. The rocks present in the river do not supply dissolved salts to the water. These rivers are situated in the tropical areas of Africa and South America (point C in Figure 2-2).
- **The rock dominated end-member:** These surface waters have rocks and soils as their dominant source of dissolved salts. The relief and climate of the basin determine the exact composition, and these waters are mostly in equilibrium with their basin materials (point B in Figure 2-2, Gibbs, 1970).
- **Evaporation-fractional crystallisation dominated end-member:** Rivers and lakes situated in hot arid regions are characterised by high TDS concentrations and a high $Na^+/(Ca^{2+} + Na^+)$ mass ratio. This extends from Ca-rich medium salinity (freshwater) rock to the Na-rich high salinity. This is due to evaporation and the associated precipitation of calcite, which decreases the Ca-concentration relative to Na and increases the total salinity (point A in Figure 2-2, Gibbs, 1970).

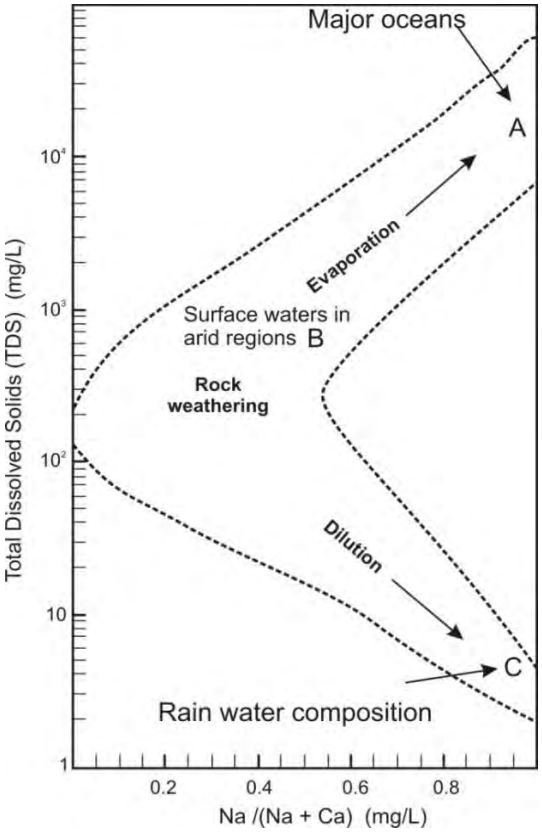

FIGURE 2-2: GIBBS DIAGRAM (GIBBS, 1970)

See text for further discussion.

2.4.2 GAILLARDET (MIXING) DIAGRAMS

Gaillardet *et al.,* (1999), constructed a diagram using data from 60 of the world's largest rivers. The diagram (Figure 2-3) uses Na^+ normalised Ca^{2+} and $(HCO_3)^-$ concentrations in order to eliminate the effect of dilution and evaporation. This diagram can be used to identify the main rock type (silicate, carbonate and evaporite rocks), that has been weathered by the river system.

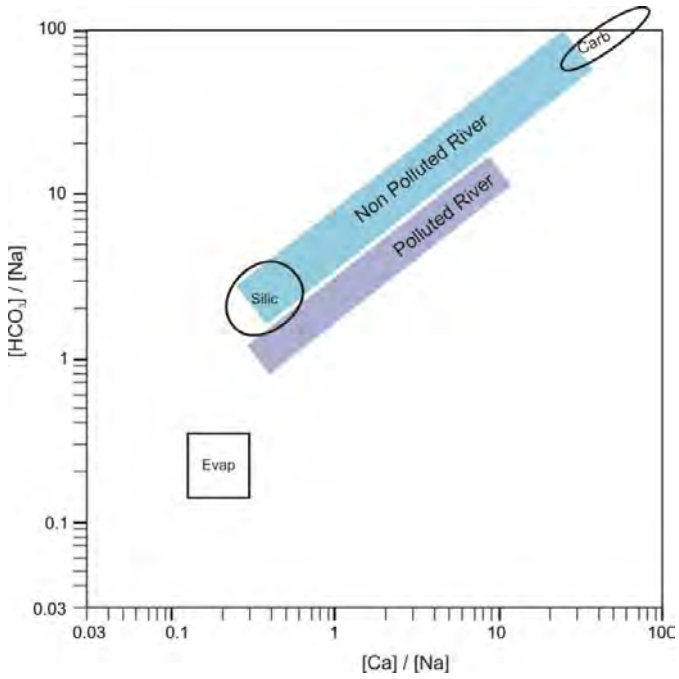

FIGURE 2-3: GAILLARDET DIAGRAM SHOWING THE FIELDS WHERE RIVERS ARE EXPECTED TO PLOT WHEN DRAINING SILICATE ROCKS (SILIC), CARBONATE ROCKS (CARB) OR EVAPORITIC ROCKS (EVAP). RIVERS THAT ARE POLLUTED ARE CHARACTERISED BY LOWER $[(HCO_3)^-]$/[NA] VALUES (GAILLARDET *et al.*, 1999)

2.4.3 ACTIVITY-ACTIVITY DIAGRAMS

Activity-activity diagrams are used as a graphical representation of the equilibrium between aqueous solutions and minerals. These diagrams (Figure 2-4) can be used to identify the intensity of chemical weathering.

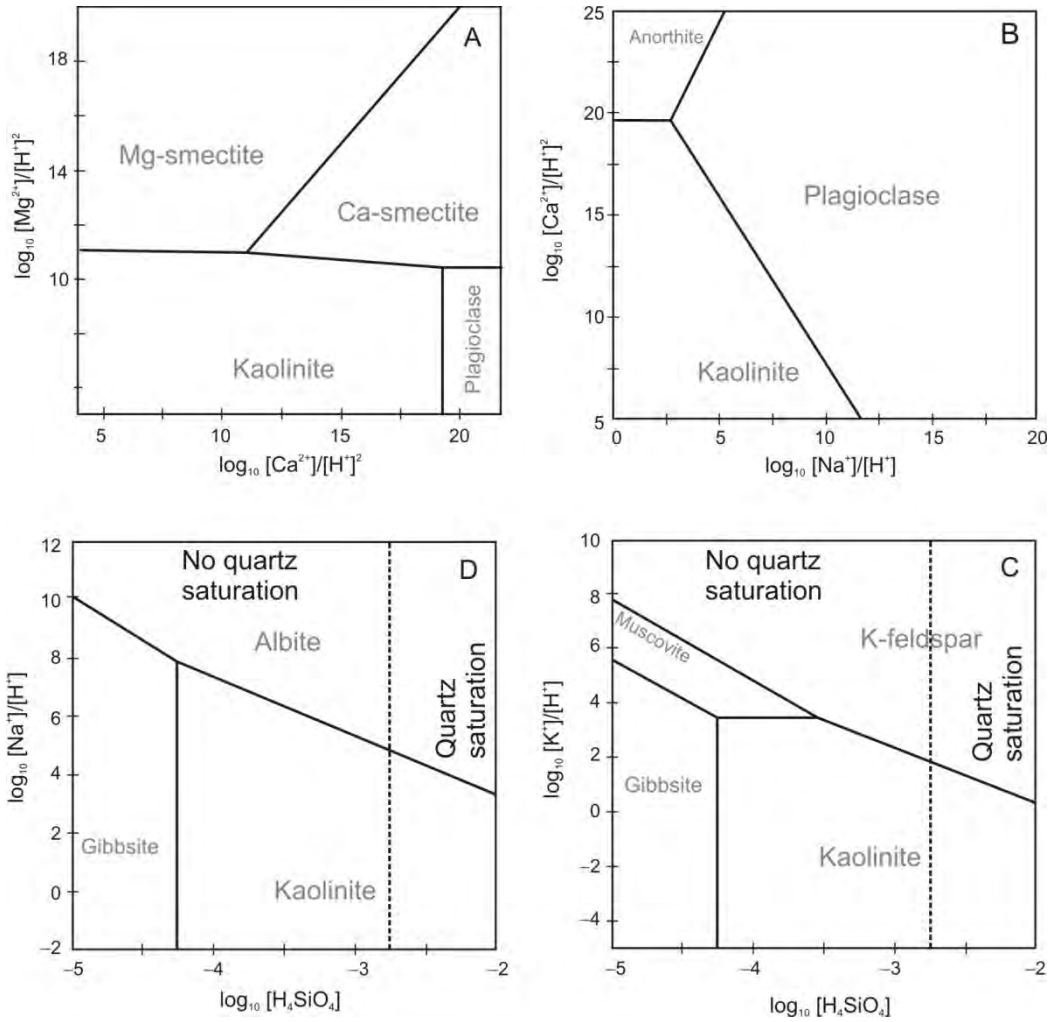

FIGURE 2-4: STABILITY (ACTIVITY) DIAGRAMS SHOWING THE STABILITY FIELDS OF THE PRIMARY AND SECONDARY (WEATHERING PRODUCTS) MINERAL PHASES

2.4.4 CONTAMINATION-WEATHERING DIAGRAMS

These diagrams are used to distinguish between silicate and carbonate weathering, and anthropogenic contaminations using $([Na^+] + [K^+])/[(HCO_3)^-]$ and $2([Mg^{2+}] + [Ca^{2+}])/ [(HCO_3)^-]$ as variables (Li *et al.,* 2009). Figure 2-5 shows that contamination results in $2([Mg^{2+}]+[Ca^{2+}])/[(HCO_3)^-] > 1$ due to sulphate and/or chloride contaminations. The vertical line of $2([Mg^{2+}]+[Ca^{2+}])/[(HCO_3)^-] = 1$ corresponds to river water chemistry, dominated by weathering of Ca and Mg dominated minerals (e.g., mafic minerals, calcite and dolomite). The (dashed) inclined line represents $[Na^+] + [K^+] + [Ca^{2+}] = [(HCO_3)^-]$ and rivers dominated by silicate chemical weathering should typically be situated on this line.

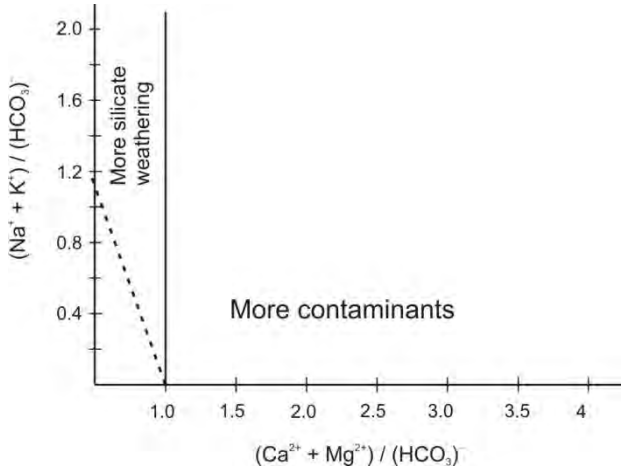

FIGURE 2-5: CONTAMINATION-WEATHERING DIAGRAM OF WATER CHEMISTRY (LI *et al*., 2009)

The contaminant weathering diagram can be used to illustrate the unnatural water quality of the Vaal River

2.4.5 TERNARY DIAGRAMS

Based on a statistical study performed by Huizenga (2011), three dominant factors are considered to characterise the surface water chemistry of natural waters in South Africa, and by implication taken into consideration when assessing the Vaal River system water quality. These include: Cl-salinisation, sulphate contamination and chemical weathering (reflected in the bicarbonate concentration).

Chloride salinisation is primarily due to saline soil and groundwater from salinisation, which is not identified as being a primary driver of water quality for the Vaal River (Rabie and Day, 2000). Secondary salinisation is caused by irrigation and removal of natural vegetation, which does occur in the Vaal River catchment, and near coastal regions seawater intrusions also contribute to salinisation (Rabie and Day, 2000; Flügel, 1995), but is not considered to be of significance in the Vaal River context.

Sources for sulphate in water include the dissolution and leaching of evaporates, oceanic water (aerosols), meteoric and atmospheric precipitation of sulphates and the oxidation of sulphide minerals such as pyrite (Cortecci *et al.,* 2002; Eby, 2004). In the Vaal River context, oceanic water aerosols are not a primary contributor, but pyrite oxidation is .

It has been identified that there are numerous anthropogenic sources that include industrial effluent from paper mills, fertilizer use contributing nitrates, domestic sewage, emissions from power stations, refineries, mines and other sources contributing H_2S to the atmosphere

and AMD. On a global scale the main source of $(SO_4)^{2-}$ contamination in water is due to anthropogenic activities (Cortecci *et al.,* 2002), and on a local scale for the Vaal River.

Considering these three factors, a ternary diagram (Figure 2-6) can be used as a visual aid for the composition of river water, where the apexes are defined by the three dominant controlling mechanisms: chemical weathering, Cl-salination and sulphate contamination. The following three equations were used to calculate the apex values:

$$[(HCO_3)^-]_{norm} = 100 \times [(HCO_3)^-] / [(HCO_3)^-] + [Cl^-] + 2\,[(SO_4)^{2-}]$$

$$[Cl^-]_{norm} = 100 \times [Cl^-] / [(HCO_3)^-] + [Cl^-] + 2[(SO_4)^{2-}]$$

$$2[(SO_4)^{2-}]_{norm} = 100 \times 2[(SO_4)^{2-}] / [(HCO_3)^-] + [Cl^-] + 2[(SO_4)^{2-}]$$

For the purpose of this study, chloride and sulphate are all considered to be mainly derived from anthropogenic sources and are thus defined as pollutants.

The ternary diagram is used to characterise the water quality of the Vaal River

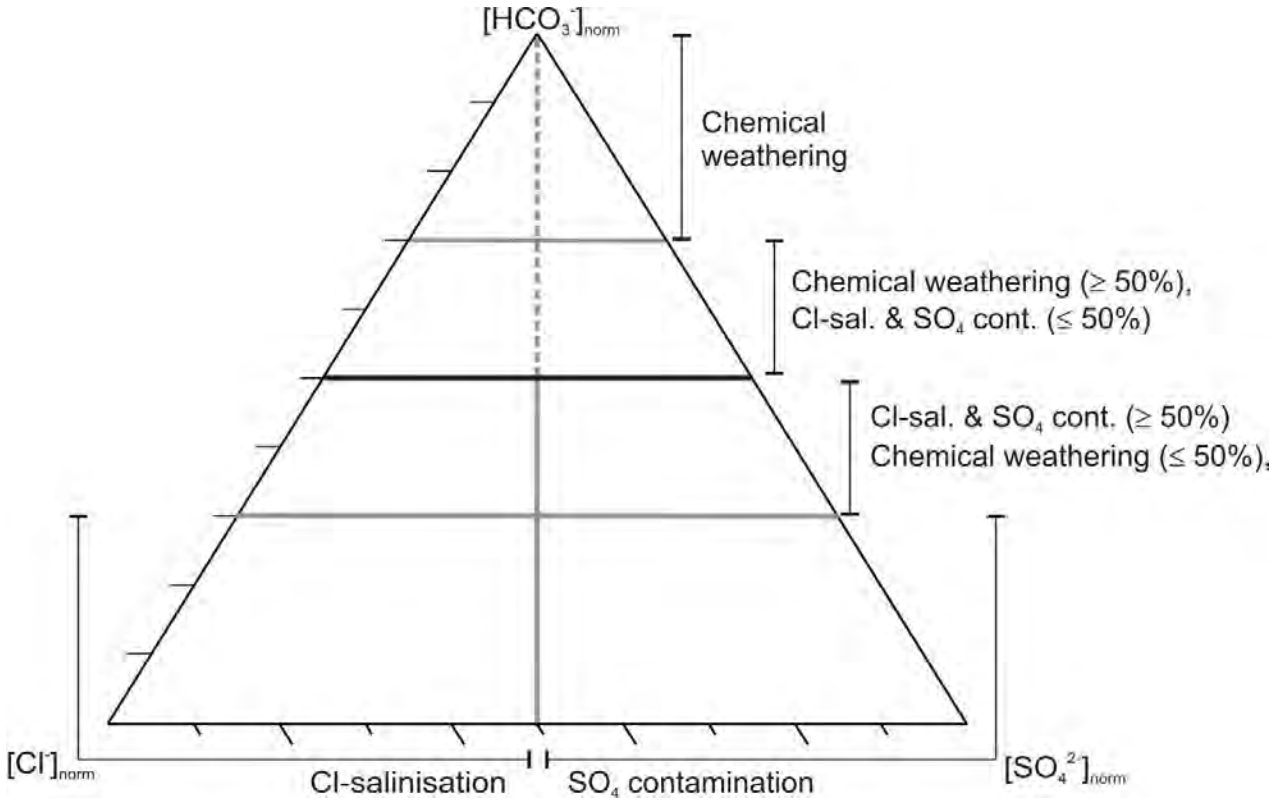

FIGURE 2-6: TERNARY DIAGRAM EXAMPLE FOR THE CHARACTERISATION OF THE INORGANIC WATER CHEMISTRY USING CHEMICAL WEATHERING, CHLORIDE SALINISATION, AND SULPHATE CONTAMINATION (FROM HUIZENGA, 2011)

2.4.6 STIFF DIAGRAMS

The Stiff diagram was introduced by Stiff in 1951. The diagram (Figure 2-7) represents the charge corrected concentrations (i.e., meq/L) of the various chemical species. The cation concentrations (i.e. Na, Ca and Mg) are plotted on the left side of the vertical axis, whereas anions (Cl, HCO_3 and SO_4) are plotted on the right. The shape of the Stiff pattern indicates how the cations and anions relate to each other, whereas the width of the pattern is an indication of the absolute concentration values of the cat- and anions (Stiff, 1951). Therefore, Stiff diagrams are ideal to compare the chemistry of major ions in space and time.

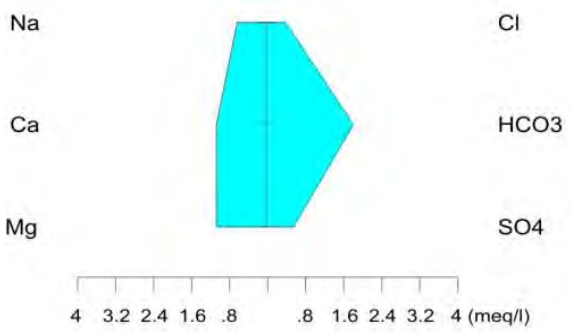

FIGURE 2-7: EXAMPLE OF A STIFF DIAGRAM FROM THE VAAL RIVER, SOUTH AFRICA.

The Stiff diagram can be used to characterise the water quality of the Vaal River in detail.

2.4.7 NATURAL VERSUS ANTHROPOGENIC EFFECT DIAGRAMS

The natural versus anthropogenic effect diagrams are used to show trends pertaining to TDS concentrations versus $[(HCO_3)^-] / [(HCO_3)^-] + [Cl^-] + [(SO_4)^{2-}]$ (denoted as $[(HCO_3)^-]_{norm}$). These diagrams can either show a negative trend or a positive trend. A negative trend implies that $[(HCO_3)^-]_{norm}$ is decreasing with increasing TDS. This means that the TDS increase is predominantly caused by pollution. A positive trend, on the other hand, implies an increasing TDS with increase in $[(HCO_3)^-]_{norm,}$ i.e. TDS increases as a result of an increasing chemical weathering rate (Figure 2-8) without any influence from pollution.

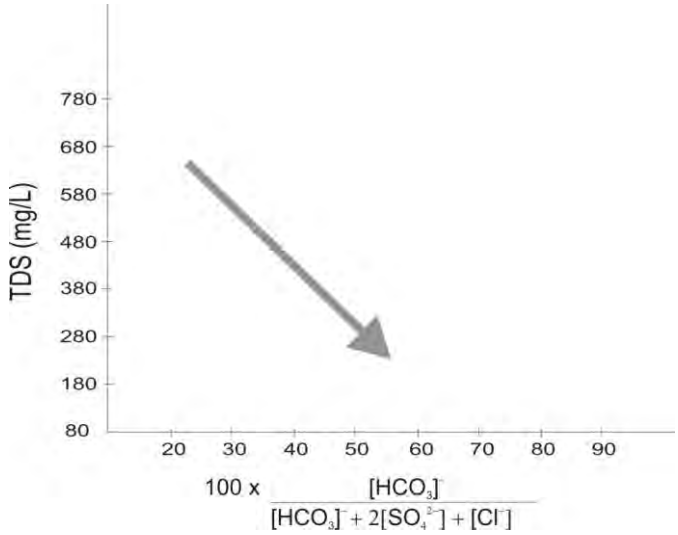

FIGURE 2-8: TDS VS. BICARBONATE DIAGRAM EXAMPLE, SHOWING A NEGATIVE TREND INDICATING THAT THE WATER CHEMISTRY IS MAINLY CAUSED BY POLLUTION.

2.5 SUMMARY

The **Gibbs diagram** was used to indicate the major mechanisms controlling surface water chemical composition, this was used to help classify the chemical-mechanisms controlling the Vaal River composition.

Gaillardet diagram was used to indicate the effect of dilution and evaporation, in order to indicate the main rock types (silicate, carbonate and evaporite rocks), that has been weathered by the river system, this diagram was used in order to confirm the rock types and other influences.

Activity-activity diagrams are used as a graphical representation of the equilibrium between aqueous solutions and minerals, to identify the intensity of chemical weathering. These diagrams were used to establish the level of chemical weathering expected in South African waters.

Contamination-weathering diagrams were used to distinguish between silicate and carbonate weathering, and anthropogenic contaminations, this tie in with the Gibbs and Gaillardet diagrams.

Ternary diagrams were used to characterise the surface water chemistry of natural waters in South Africa. The diagrams identified that there are numerous anthropogenic sources that contributing to the composition of the Vaal River. Specifically indicating the natural/inorganic characterisation by placing the water chemistry at one of the tree corners of the diagram, similar to a piper diagram.

The Stiff diagram represents the charge corrected concentrations of the various chemical species that could potentially interact. The shape of the Stiff pattern indicates how the cations and anions relate to each other, whereas the width of the pattern is an indication of the absolute concentration values of the cat- and anions The Stiff diagrams were ideal to compare the chemistry of major ions expected to be present in the Vaal River.

The **natural versus anthropogenic** effect diagrams are used to show trends pertaining to TDS concentrations. These diagrams can either show a negative trend or a positive trend. The diagram represents an indication of an increasing TDS or an increasing chemical weathering, without any influence from pollution.

Chapter 3 discusses the influence of chemical weathering on the water chemistry in more detail.

3 FACTORS INFLUENCING THE WATER CHEMISTRY OF THE VAAL RIVER

3.1 INTRODUCTION

The main factors that affect the Vaal River water chemistry include chemical weathering and pollution, in particular potential Acid Mine Drainage (AMD). In this Chapter the general principles of chemical weathering and AMD (with reference to the Vaal River) are described.

In Khakibos (2013), it is stated that the DWA needs an emergency solution for the AMD in Gauteng flowing into the Vaal River. Key water sources, the Vaal River in particular, will not be fit for drinking water for either animal or human consumption. The sulphate pollution is predicted to impact resources by mid-2013 to early 2014. "*DWA has plans to pump polluted water away from the mines in an effort to curb the issue by treating the water and re-introducing into streams which ultimately flow back to the Vaal River. Sulphates will still remain in the water at high concentrations*".

3.2 CHEMICAL WEATHERING

Chemical weathering is considered to be one of the dominant natural processes affecting the water chemistry of surface waters in South Africa. This is mainly due to the fact that the soil layer is very thin or non-existent as a result of the semi-arid climate (Figure 3-1). Chemical weathering in rivers is never in equilibrium as the system is a dynamic open system. The changes in variables and mixing of ions in these systems are usually rapid (Hem, 1989; Henderson, 1984).

Chemical weathering leads to the decomposition of minerals and the breakdown of rocks. This process is considered to be one of the major contributors of the dissolved ions in the water. The products of weathering reactions are secondary minerals and dissolved ions. There are different degrees of mineral resistance to weathering (Plant *et al.*, 2001; Eby, 2004, Hem, 1989) (Table 3-1).

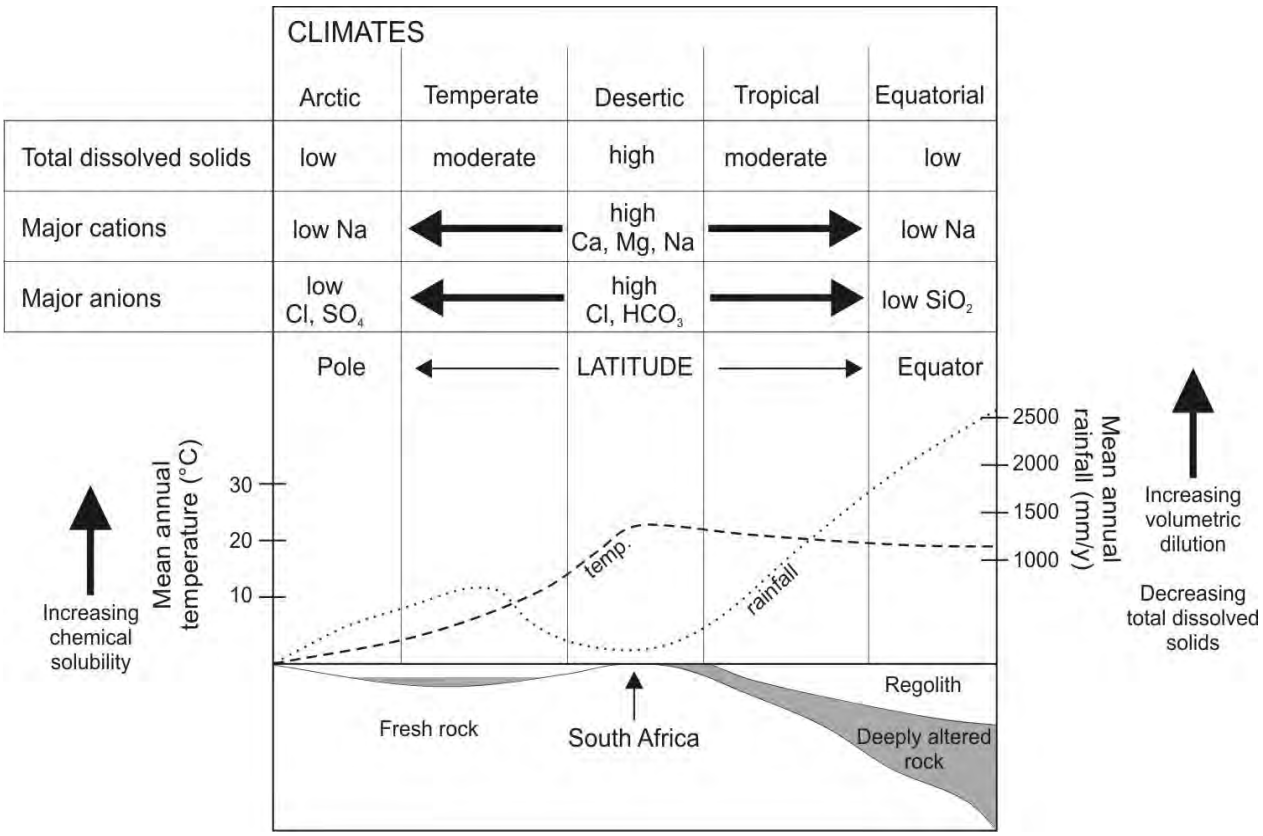

FIGURE 3-1: ILLUSTRATION OF THE RELATIONSHIP BETWEEN THE CLIMATIC FACTORS AND SURFACE WATER CHEMISTRY (MODIFIED FROM PLANT *et al*. 2001)

Table 3-1 lists rocks from their lowest resistance to highest resistance, with respect to chemical weathering. Due to the nature of the South African geology, soil, climate and weathering of carbonate and silicate minerals are the most important, in the case of the Vaal River system. Weathering of evaporite minerals, such as halite or gypsum, can be excluded, as evaporite rocks are hardly exposed in South Africa, or the Vaal River system (Eby, 2004).

TABLE 3-1: MINERAL WEATHERING LISTED IN ORDER OF INCREASING RESISTANCE TO WEATHERING (EBY, 2004).

Minerals	Rock type	Increasing Resistance
Calcite	Carbonate rocks	
Dolomite		
Volcanic glass	Silicate rocks	
Olivine		
Ca-plagioclase		
Pyroxenes		
Ca-Na plagioclase		
Amphiboles		
Na-plagioclase		
K-feldspar		
Mica		
Quartz		
Vermiculite, smectite	Clay minerals	
Kaolinite		
Gibbsite, hematite, goethite	Oxides	

Henderson (1984) identifies two types of dissolving reactions, namely congruent dissolution:

SiO_2 (quartz) + $2H_2O \leftrightarrow H_4SiO_4$

and incongruent dissolution:

$KAl_3Si_3O_{10}(OH)_2$(muscovite) + $5H_2O + 2CO_2 \rightarrow 3Al_3Si_2O_5(OH)_4$(kaolinite) + $2K^+ + 2(HCO_3)^-$

in which a solid residue (normally a Fe or Al enriched mineral phase depending on the mineral that is weathered), in addition to ions, is produced.

3.2.1 CHEMICAL WEATHERING OF CARBONATE ROCKS

All the larger rivers in the world are influenced by (congruent) carbonate dissolution (Appelo and Postma, 1993). Carbonate dissolution proceeds more rapidly than silicate dissolution (Table 3-1).

Rocks that typically have carbonate minerals are limestone, and are primarily composed of calcite, $CaCO_3$ and dolostones that comprise dolomite, $(Ca,Mg)(CO_3)_2$. The weathering results in high concentrations of Ca^{2+}, Mg^{2+}, and $(HCO_3)^-$ (Gaillardet *et al.*1999).

Calcite dissolution can be expressed by the following congruent reaction (Henderson, 1984):

$CaCO_3 + CO_2 + H_2O \rightarrow Ca^{2+} + 2(HCO_3)^-$

3.2.2 CHEMICAL WEATHERING OF SILICATES

The weathering of silicate minerals is responsible for 50% of the dissolved solid loads in rivers on the earth (Appelo and Postma, 1993). Silicate weathering can either be congruent or incongruent, but in most instances the reaction is incongruent. Chemical weathering of mineral phases formed at high temperatures and pressures are more susceptible to chemical weathering than minerals formed at lower pressure and temperatures. For example, minerals such as olivine ($(Mg,Fe)_2SiO_4$), pyroxene ($(Mg,Fe,Ca,Na)_2Si_2O_6$) and Ca-feldspar ($CaAl_2Si_2O_8$) dissociate quicker than minerals like K-feldspar and quartz that typically occur in granitic rocks (Appelo and Postma, 1993).

Silicate mineral phases undergo incongruent dissolution according to the generalised reaction:

Si-mineral + H_2O + CO_2 → Al/Fe – residue + $(HCO_3)^-$+ ions ± H_4SiO_4

For example, the weathering of K-feldspar to first muscovite and then kaolinite and gibbsite proceeds as follows:

$3KAlSi_3O_8$(K-feldspar) + $2H_2O$ + $2CO_2$ → $KAl_3Si_3O_{10}(OH)_2$(muscovite) + $6SiO_2$ +$2K^+$ + $2(HCO_3)^-$

$KAl_3Si_3O_{10}(OH)_2$(muscovite) + $5H_2O$ + $2CO_2$ → $3Al_3Si_2O_5(OH)_4$(kaolinite) + $2K^+$ + $2(HCO_3)^-$

$3Al_3Si_2O_5(OH)_4$(kaolinite)+ $5H_2O$ → $2Al(OH)_3$(gibbsite) + $2H_4SiO_4$

The secondary mineral phases are more insoluble aluminium-rich mineral phases.

The following characteristics apply to partial dissolution reactions involving silicate minerals (Appelo and Postma, 1993):

- Carbonic acid $(H_2CO_3)^-$ generally supplies the hydrogen protons, as a product of the reaction $H_2O + CO_2 \rightarrow H_2CO_3$ and $H_2CO_3 \rightarrow H^+ + (HCO_3)^-$, in which CO_2 is supplied by the atmosphere and biochemical processes in the soil.
- Iron and aluminium are left behind as insoluble mineral phases.
- Cations such as Mg^{2+}, Ca^{2+}, K^+ and Na^+, together with $(HCO_3)^-$ are released.

- The pH of the water is between 8 and 8.5 (basis) because of the release of bicarbonate (Figure 3-2).
- Kaolinite is the most common clay mineral residue.
- Precipitation of SiO_2 does not normally occur.

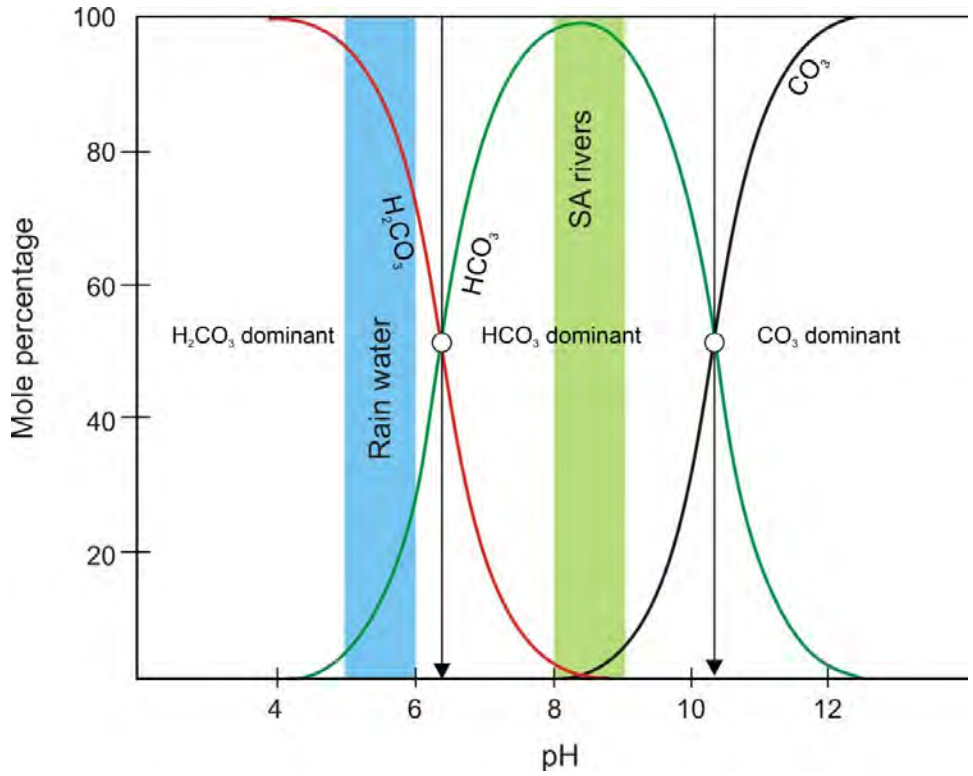

FIGURE 3-2: CARBONATE-BICARBONATE DISTRIBUTION AS A FUNCTION OF PH ILLUSTRATING THE EFFECT OF CHEMICAL WEATHERING ON THE PH OF SA RIVERS (ADAPTED FROM APPELO AND POSTMA, 1993)

Generally, the following can be stated of the river water chemistry, assuming that chemical weathering is the dominant controlling factor (Bluth and Kump, 1993; Hem, 1989), and by implication, contribute to the Vaal River system:

- Total dissolved solids are largely a function of runoff (where not contributed by industrial, mining and domestic contributions);
- Dissolution rates are controlled by basin lithology and soil and bedrock permeability;
- Anthropogenic influences on the quality in a stream are highly variable and most likely to affect the Na, Cl, SO_4 and NO_3 concentrations; and
- For the examination of the extent of chemical weathering, dissolved Si and bicarbonate seem to be the best species to look at, due to the fact that they are indicators of the progression of weathering in bedrock and soil. They are also the least affected by anthropogenic influences.

3.3 MINING ACTIVITIES INFLUENCING THE VAAL RIVER WATER QUALITY

The mining industry potentially has negative impacts on water resources, it might affect the availability of the water to other users, and may pollute the water.

Mining produces three main types of water pollution (McCarthy, 2011):

- Processing chemicals pollution;
- Erosion and sedimentation; and
- Associated mine water contamination

AMD has been identified as an important type with regards to the Vaal River catchment area, due to the presence of active and inactive coal, gold and uranium mines (see Table 1-3) and discharging pollutant loads into the Vaal River system.

3.4 INDIRECT IMPACTS ON WATER QUALITY

3.4.1 UNDERGROUND MINING HYDRAULICS

With regards to the gold mines in the Vaal River area, the mine residue facilities are again a major source of pyrite rainwater, the main cause of oxidation of pyrite at mine residue facilities. The sulphuric acid percolates through the mine residue dump, dissolving minerals that comprise heavy metals like uranium and enters the groundwater. This adds to the pollution plume in the groundwater (McCarthy, 2011).

Other metal contaminants and their concentrations associated with gold and coal mining are listed in Table 3-2. The contaminants are mostly found in the conglomerate composition of the gold bearing layers, or the surrounding host rock with regards to the coal layers (McCarthy, 2011).

TABLE 3-2: METAL CONTAMINANTS ASSOCIATED WITH GOLD AND COAL MINING (TUTU *et al.,* 2008).

Metal contaminants from mining	Concentrations (mg/L)	Mine type association
Al	60 – 600	Gold
Co	1 – 40	Gold
Cu	1 – 15	Gold
Mn	10 – 150	Gold
Ni	1 – 80	Gold
U	1 – 80	Gold
Zn	1 – 100	Gold, coal
SO_4^{2-}	100 – 5000	Gold, coal
Na	200 - 1500	Gold, coal
Mg	200 - 1500	Gold, coal

According to Dennis and Dennis (2012), it has become standard practice to pump water from the mine workings to allow the miners to work safely. However, in some cases, as underground mining ceases, and the active pumping of ground water ceases, the voids in the fractured rock fill with water and the groundwater level gradually rises. The fact that mine workings have been so extensive and crossed natural geological barriers, allows the returning groundwater to drain to a regional low level and gradually recover towards the surface. Since the natural barriers and natural decant points are removed, the groundwater will continue to rise to a point that will decant to the surface. The decant point is commonly associated with old mine shafts or adits, which provide conduit to the surface (Dennis and Dennis, 2012), as well as being dictated by head elevations versus surface elevations.

Whilst this may be a simplified generic concept, it may be further developed into two conceptual modelling approaches to predict the decanting scenario of mines. The first is a closed system where the mine void is isolated from the hanging aquifer as shown in Figure 3-3. This system is also more commonly known as the “U-Tube” and this type of system is guaranteed to decant if enough of an elevation difference exists between the ingress areas and possible decant points (Dennis and Dennis, 2012).

The closed system (U-Tube) is a theoretical scenario, as a completely closed system is seldom found in practice. Monitoring boreholes and shafts are seldom in hydraulic isolation from the surrounding aquifers. The effect of stratification also prohibits the mine void of being hydraulically isolated (Dennis and Dennis, 2012).

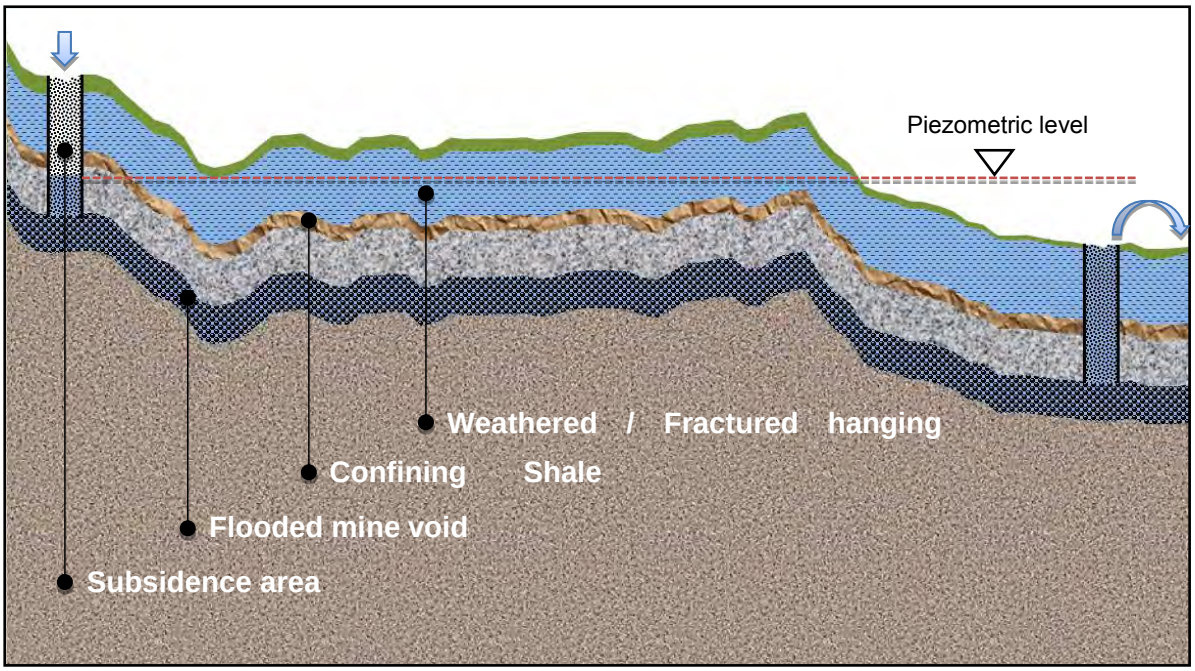

FIGURE 3-3: CLOSED SYSTEM THEORETICAL SCENARIO OF MINE VOID (DENNIS AND DENNIS, 2012)

The second type of conceptual model introduced is the leaky system (Figure 3-4).

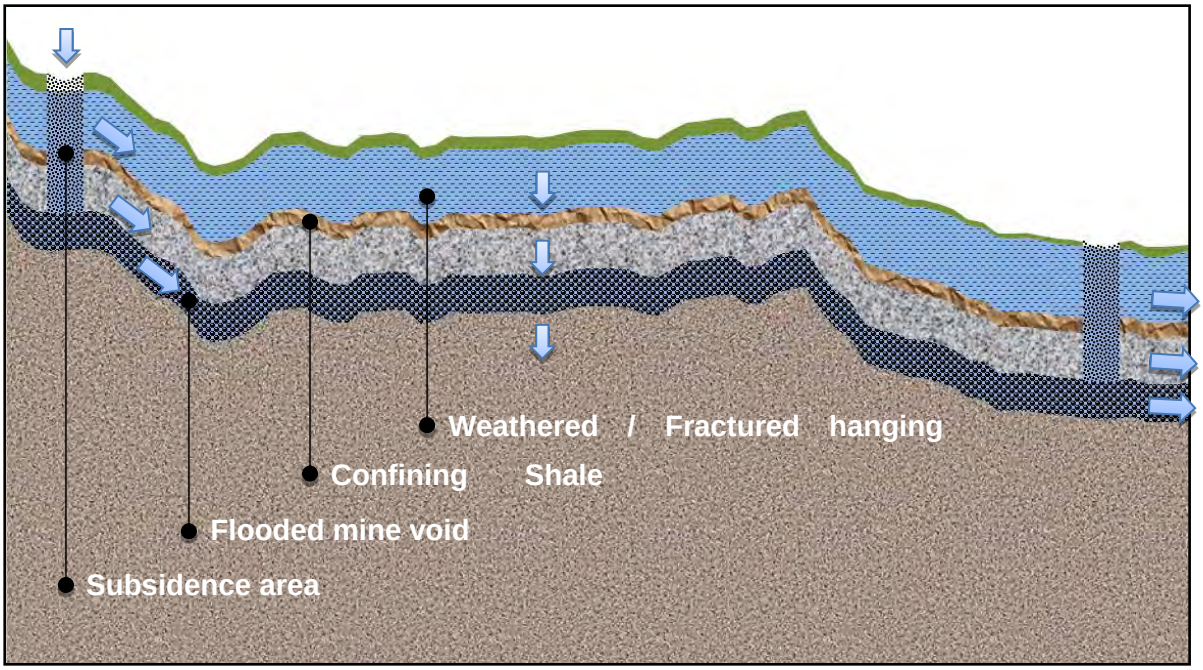

FIGURE 3-4: THEORETICAL SCENARIO OF A LEAKY SYSTEM (DENNIS AND DENNIS, 2012).

In the leaky system (Figure 3-4) the water level in the mine void will reach the water level in the hanging or regional aquifer and partial decant will take place into the groundwater. The leaky system does not rule out the potential for surface decant as this will be governed by the hydraulic parameters of the system (Dennis and Dennis, 2012).

3.4.2 OPENCAST MINES

Within the sedimentary rocks of the Karoo Supergroup there are numerous wide spread coal layers (Geldenhuis and Bell, 1998). Coal mining occurs either by extracting from underground or by opencast methods. Due to the coal being immediately removed from the site, the surface area for dumping of mineral residues is not as great as in the case of gold mining, but may be very material on a localized basis (Geldenhuis and Bell, 1998).

In opencast mining, the overlying soil and rocks (overburden and top soil) are removed to access the underlying coal layer. The overburden is then removed to the commercially extractable layer. Opencast overburden and coal is removed and stockpiled for use or rehabilitation. Not all coal is ever removed from an underground mine, due to low grade coal, other economic reasons or stability issues (pillars are occasionally left within the underground mining operations). Figure 3-5 and Figure 3-6 are an indication of the hydraulic state occurring in the region as mining progresses. Initially the groundwater and hydrology will follow a similar pattern to the topography; with a change in topography the groundwater will be affected. The open pit causes a depression and blasting can potentially cause fractures, the different aquifers are exposed and water can flow from the different layers (Dennis and Dennis, 2012).

For rehabilitating the open pit, the overburden and coal discard which has been removed, are backfilled into the open pit void and covered with soil removed during initial clearance. Thereafter, the terrain is landscaped and rehabilitated. Figure 3-7 again refers to the hydraulic state after rehabilitation. After rehabilitation, the groundwater flow should potentially mimic the surface topography (McCarthy, 2011, and Dennis and Dennis, 2012).

However, the surface covering and compaction of the backfill material has not been adequate to prevent rainwater infiltration into the soil and reach the backfill. The infiltration provides oxygen and water comes into contact with the residual pyrite in the backfilled material. This encourages the generation of AMD, which can subsequently decant onto the surface, or drain into the underlying groundwater resource (McCarthy, 2011).

It has been observed that, because opencast mines extend below the near surface aquifer, that as with underground mines, they can destroy the natural groundwater regime. This in turn alters the flow patterns and the interaction between groundwater and surface water (McCarthy, 2011).

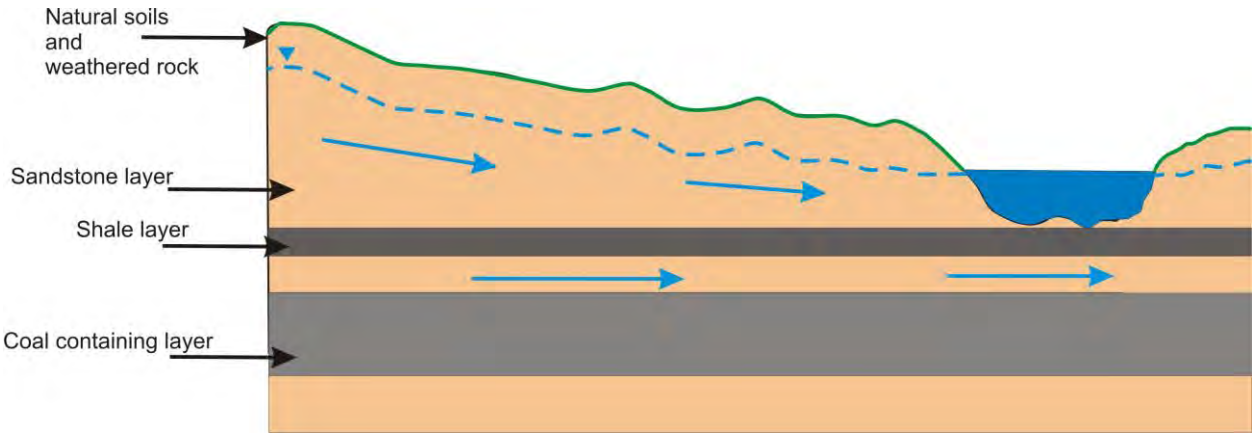

FIGURE 3-5: LAND BEFORE MINING HAS TAKEN PLACE

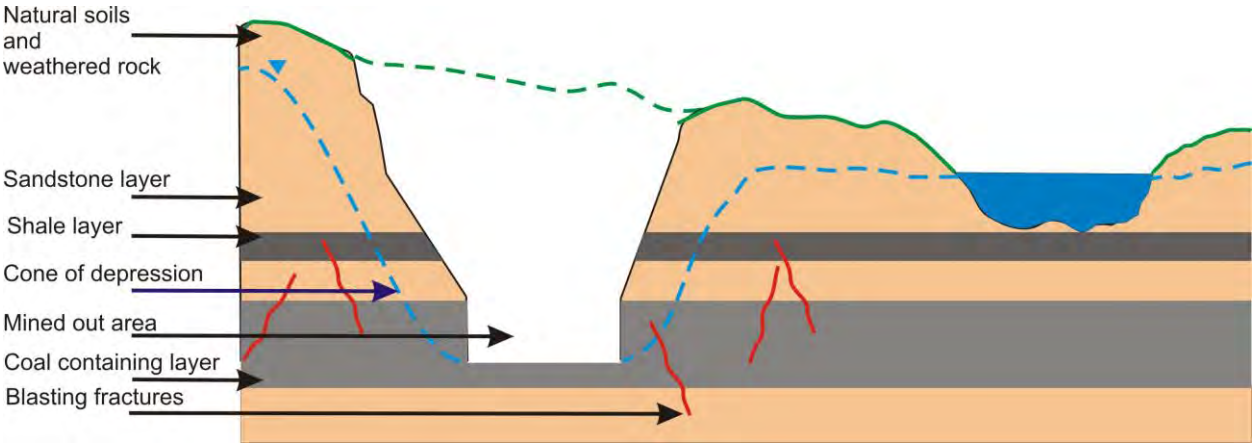

FIGURE 3-6: LAND WHILE OPENCAST MINING IS TAKING PLACE

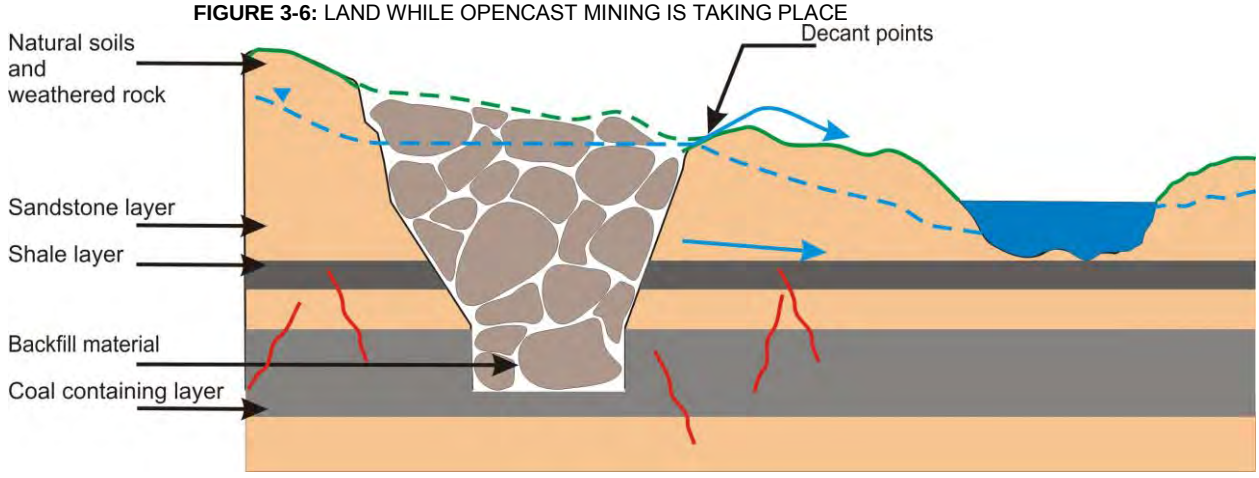

FIGURE 3-7: AFTER BACKFILL IS COMPLETED AND REHABILITATION OF THE OPENCAST MINE VOID, THE UNDERGROUND WATER MIGRATION PATH IS ALTERED BY THE BACKFILL MATERIAL FROM THE ORIGINAL ROCK. THE MATERIAL MAY BE ACIDIC, IRON AND CALCIUM-SULPHATE ENRICHED WHICH MAY LEAD TO AN ACIDIC POLLUTION PLUME FORMING AND CONTAMINATING THE LOCAL AND REGIONAL GROUND AND SURFACE WATER RESOURCES.

Contaminants commonly associated with coal mining are the pyrite components, iron and sulphate $(SO_4)^{2-}$ as well as other metals including Mn, Zn and elements as listed in Table 3-2 (Blowes *et al.,* 1998).

3.4.3 GROUNDWATER-SURFACE WATER INTERACTION

According to Tutu *et al.,* (2008), whatever the character of the mine drainage (acid or neutral), streams surrounding mine residue deposits tend to be heavily contaminated. Similarly, seepage or leachate from a mine residue deposit, an open pit operation or underground operation may contaminate the underlying groundwater. This contaminated water may finally emerge on the surface and decant into a stream or river contributing to the Vaal River (Tutu *et al.*, 2008). According to Tutu *et al., (2008),* over a great distance, dilution should take place and the contamination contribution to surface water should be of little significance. However, recirculation of neutralized water, from the Vaal Dam into the upper catchment could potentially have a significant impact on the water chemistry and lessens the effect of dilution over distance (Wood, 2013).

A contributing factor to the chemical load of the Vaal River is the fact that it is not just the isolated catchment of the mine residue deposits or open pits that are affecting the surface water tributaries, but also the groundwater from the regional areas that are constantly seeping into the mine workings (Tutu *et al.*, 2008). As mentioned previously, to prevent flooding, this groundwater infiltration or fissure water has to be pumped out. Tutu *et al.,* (2008), state that historically this extra water has either been used in the mining operations or was discharged into nearby streams after basic treatment to neutralize the acidity, without addressing the salt load. Where the mines have ceased operating, the pumping has also stopped. The groundwater level has rebounded or recovered and, decanting occurs from the lowest lying opening of the interconnected mine works. An example being the Western basin mine void in the Krugersdorp area, which has commenced decanting. In the near future, decanting of the Eastern Basin in the Nigel area and the Central Basin in the Johannesburg central business district area could also become an issue (Tutu *et al.*, 2008 and DWA, 2013).

According to McCarthy (2011) the water quality in the Vaal River is thought to be deteriorating in the direct vicinity of the mines or tailings. However, from the water analyses further downstream of the mines, it is evident that there is an improvement in water quality as well as in distal regions surrounding the mines (McCarthy, 2011). The presence of dolomite ($Ca,Mg(CO_3)_2$) from the Transvaal Supergroup, is the attributing factor to the improvement in the water quality (McCarthy, 2011).

3.4.4 ACID MINE DRAINAGE

AMD, as well as acid rock drainage, arises when sulphide bearing minerals such as pyrite, comes into contact with oxygenated water. With the discharge of acidic water to surface water, the oxidation of the pyrite, for example in the tailings, can be expressed as the following equation (Tutu *et al.,*2008);

$FeS_2 + 3½\ O_2 + H_2O \rightarrow 2(SO_4)^{2-} + Fe^{2+} + 2H^+$

Tutu *et al*. (2008) have shown that the general buffering capacity of the mine residues are insufficient to neutralise the acid and acidification occurs. During the oxidation reaction other minor minerals dissolve to elements such as U, As, Cu, Ni, Pb, Co and Zn. The acid water together with these minor constituents may be transported downwards by percolation to contaminate the underlying aquifers (Blowes *et al.,* 1998).

Where direct discharge of AMD to surface water tributaries occurs, and where contaminated groundwater decants to surface water tributaries, the exposure to oxygen causes further oxidation of Fe(II) to Fe(III) which may precipitate as the red sludge often seen where AMD is discharging (Espana *et al.* 2005):

$Fe^{2+} + ¼O_2 + H^+ \rightarrow Fe^{3+} + ½H_2O$

The pH of the water is the determining factor in the stability of the Fe(III). At a pH lower than 3.5, Fe(III) stays in solution and acts as an oxidising agent of pyrite according to the following reaction (Espana *et al.,* 2005):

$FeS_2 + 14Fe^{3+} + 8H_2O \rightarrow 15Fe^{2+} + (SO_4)^{2-} + 16H^+$

Fe(III) precipitates as $Fe(OH)_3$ (pH greater than 3.5)(Singer and Stumm,1970; Stumm and Morgan, 1996):

$Fe^{3+} + 3H_2O \rightarrow Fe(OH)_3 + 3H^+$ (Espana *et al.,* 2005)

and buffers the pH of the AMD between 2.5 and 3.5. There are two opposing consequences for this process: (1) the mobility and toxicity of metals increase due to the acidity; (2) the precipitation of the $Fe(OH)_3$ results in adsorption of metals in solution. The latter process is

considered to be the dominant process (Webster *et al.,* 1994; McGregor *et al.,* 1998; Espana *et al.,* 2005).

According to McCarthy (2011), during mining and mineral extraction processes, rock masses are crushed and fragmented, the mineral surface area that is exposed to water and oxygen is increased and, therefore, potentially resulting in an increase of the acid production rate. Host rocks that contain dolomite and/or calcite can (partially) neutralize the acid. This is, however, not the case for most of the coal and gold deposits in South Africa. The acid water may initially be introduced back into the system as groundwater, which then interacts with the surface water. This results in elevated metal concentrations, a relatively low pH and a high salinity of the river water. However, dilution will occur in the aquifer and the acid water should not create a major concern with the surface water, unless they are in close proximity, meaning the interaction between the surface and groundwater is narrowly spaced.

4 EVALUATION OF RESULTS

4.1 INTRODUCTION

As has been described in the introduction of this dissertation (Chapter 1), the objective of this study was to investigate (1) whether there are distinct geographical differences in the inorganic water chemistry along the Vaal River, and (2) whether it is possible to distinguish between natural and anthropogenic influences on the inorganic water chemistry.

In order to avoid too many data points on a single graph or diagram, median values of the inorganic water quality from the DWA monitoring stations along the Vaal River were used. All data considered were evaluated in detail, the data point considered plotted close together with regards to each station considering the time periods. Therefor for the purpose of this discussion points could be grouped together and median values could be used.

4.2 GENERAL CHARACTERISATION OF THE VAAL RIVER INORGANIC WATER CHEMISTRY

The general Vaal River inorganic water chemistry can be described using the Gibbs and Gaillardet mixing diagrams (Gibbs, 1970; Gaillardet *et al.*, 1999). The entire set of DWA monitoring stations plot in the rock dominated weathering region in the Gibb's diagram, with some having slightly higher TDS values, representative of the middle and westerly part of the Vaal River (Figure 4-1). The data show similar $Na^+/(Na^+ + Ca^{2+})$ ratio's while the TDS concentrations varies. The median for all the constituents used for all figures are attached in Appendix 1, standard deviation was not included in the appendices as the data would become excessive. The two outliers considered within catchment 2 not conforming to the trend suggest the natural weathering process has a higher influence regarding those particular stations, with higher Ca values compared to the Na values.

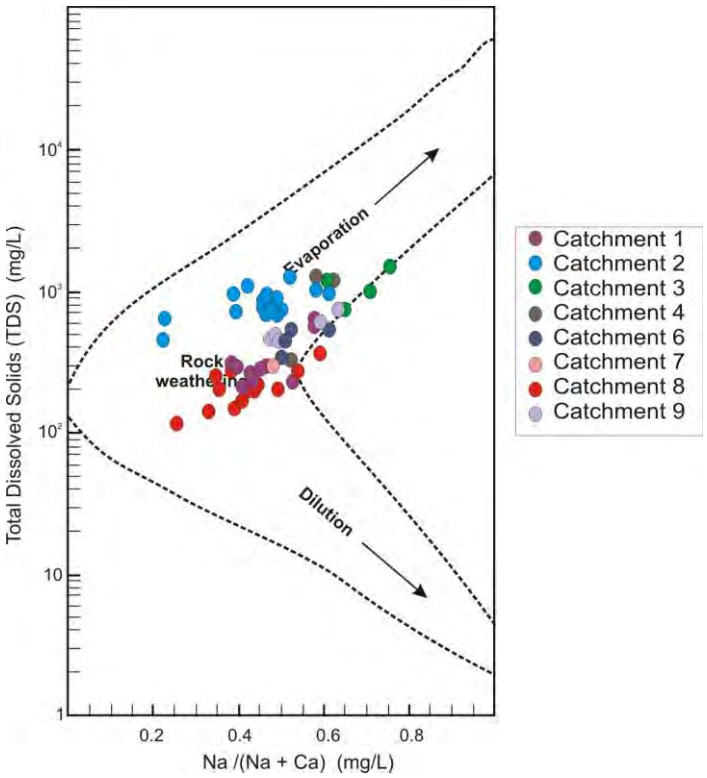

FIGURE 4-1: GIBBS DIAGRAM SHOWING THE MEDIAN DATA FOR EACH DWA MONITORING STATION ALONG THE VAAL RIVER

The Gaillardet's mixing diagram (Figure 4-2) shows that monitoring stations' data points plot in two regions, namely near the silicates weathering field, and in between the fields of silicate and evaporate weathering. The most westerly stations' data plot in the natural, or inferred non-pollution field, as indicated by the blues hade. The polluted area is/was representative of polluted rivers in Europe (Gaillardet *et al*., 1999), and generally the rivers, or in this case the DWA monitoring stations on the Vaal River, represent low $[(HCO_3)^-]/[Na^+]$ values. The two outliers considered within catchment 2 not conforming to the trend suggests the natural weathering process has a higher influence regarding those particular stations, with lower HCO_3 values compared to the Na values. Both Gibbs and Giallardet compared suggest the natural weathering influence higher with regards to the two stations.

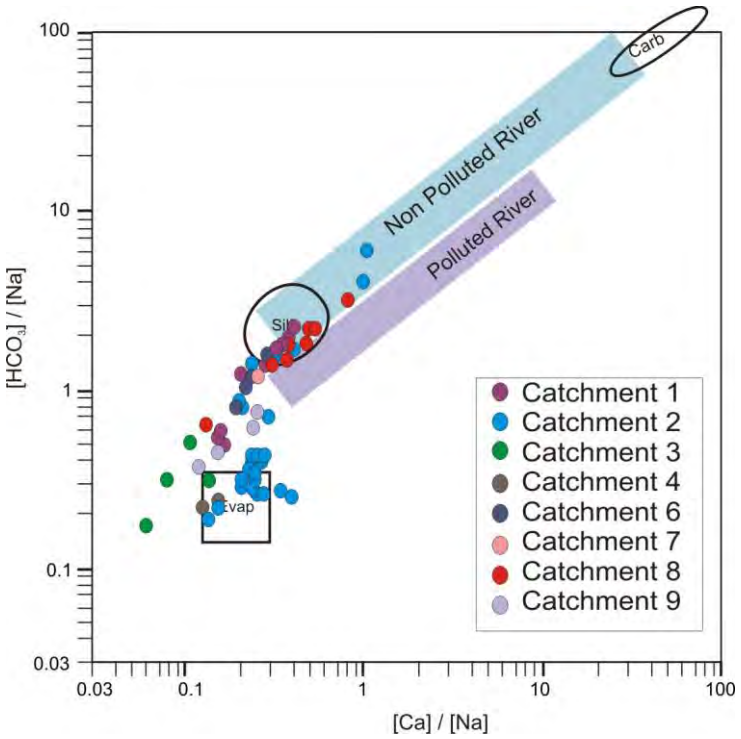

FIGURE 4-2: MIXING DIAGRAMS AFTER GAILLARDET *et al.* (1999) SHOWING, THE MEDIAN DATA FOR EACH DWA MONITORING STATION ALONG THE VAAL RIVER

The activity-activity diagrams (Figure 4-3) imply that the primary weathering product is kaolinite. This implies that chemical weathering is not advanced, which is confirmed by the generally high bicarbonate concentrations and the pH being greater than 8.

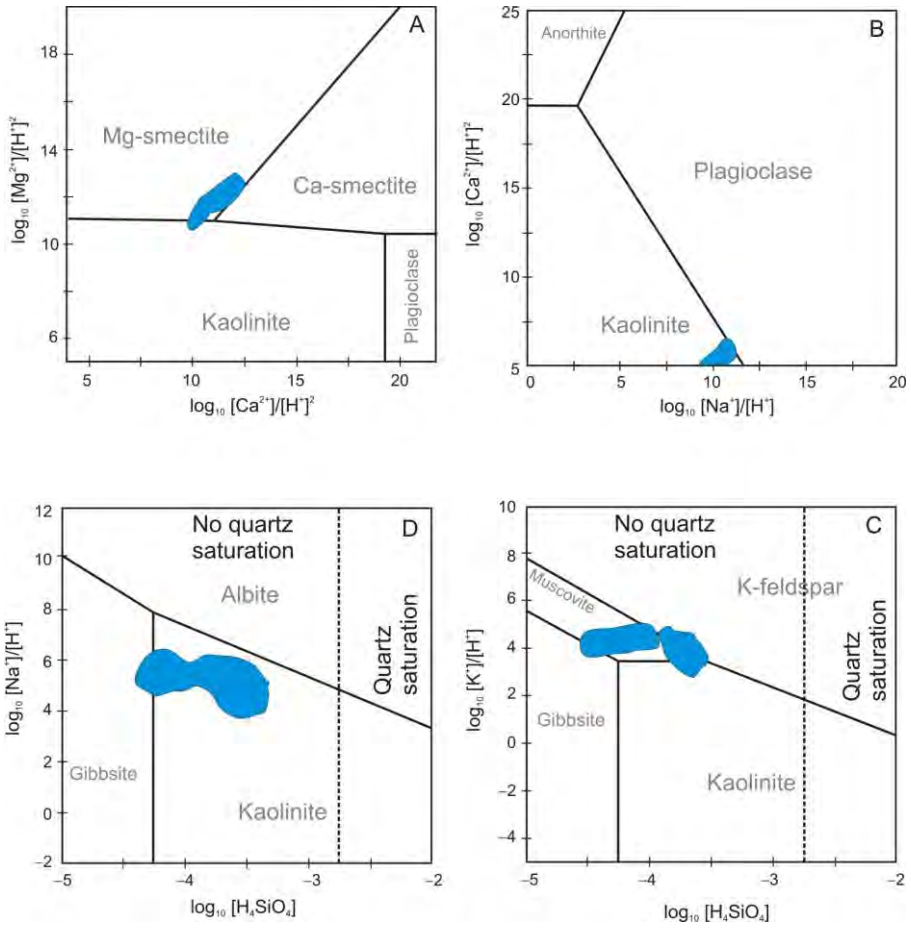

FIGURE 4-3: ACTIVITY-ACTIVITY DIAGRAMS SHOWING THE MEDIAN DATA FOR EACH DWA MONITORING STATION ALONG THE VAAL RIVER FOR THE MINERAL STABILITY FIELDS OF WEATHERING PRODUCTS.

Figure 4-4 is used to distinguish between silicate and carbonate weathering and anthropogenic contamination. Two regions of these diagrams are silicate weathering left of the $2([Mg^{2+}]+[Ca^{2+}])/[(HCO_3)]= 1$ corresponding straight line, and imply contamination right of the line.

There are two implied trends in the diagrams from the Vaal River monitoring stations data. The first is from the data plot in the 2nd quadrant along the $[Na^+] + [K^+]+ [Mg^{2+}] + [Ca^{2+}] = [(HCO_3)]$ dashed line (catchments C1, C6, C7 and C8). This is considered to reflect the contribution of silicate weathering to chemical weathering. The other trend is in the 1st quadrant where more contamination is inferred, for catchments C2, C3, C4 and C9, where an excess of $[Mg^{2+}] + [Ca^{2+}]$ relative to $[(HCO_3)]$ is taken to be likely related to anthropogenic activities.

With regards to the Contamination-Weathering diagrams the difference in geological and anthropogenic influences were taken into account. The influence of the geology alone is not taken into consideration as that is not the intent of the diagram.

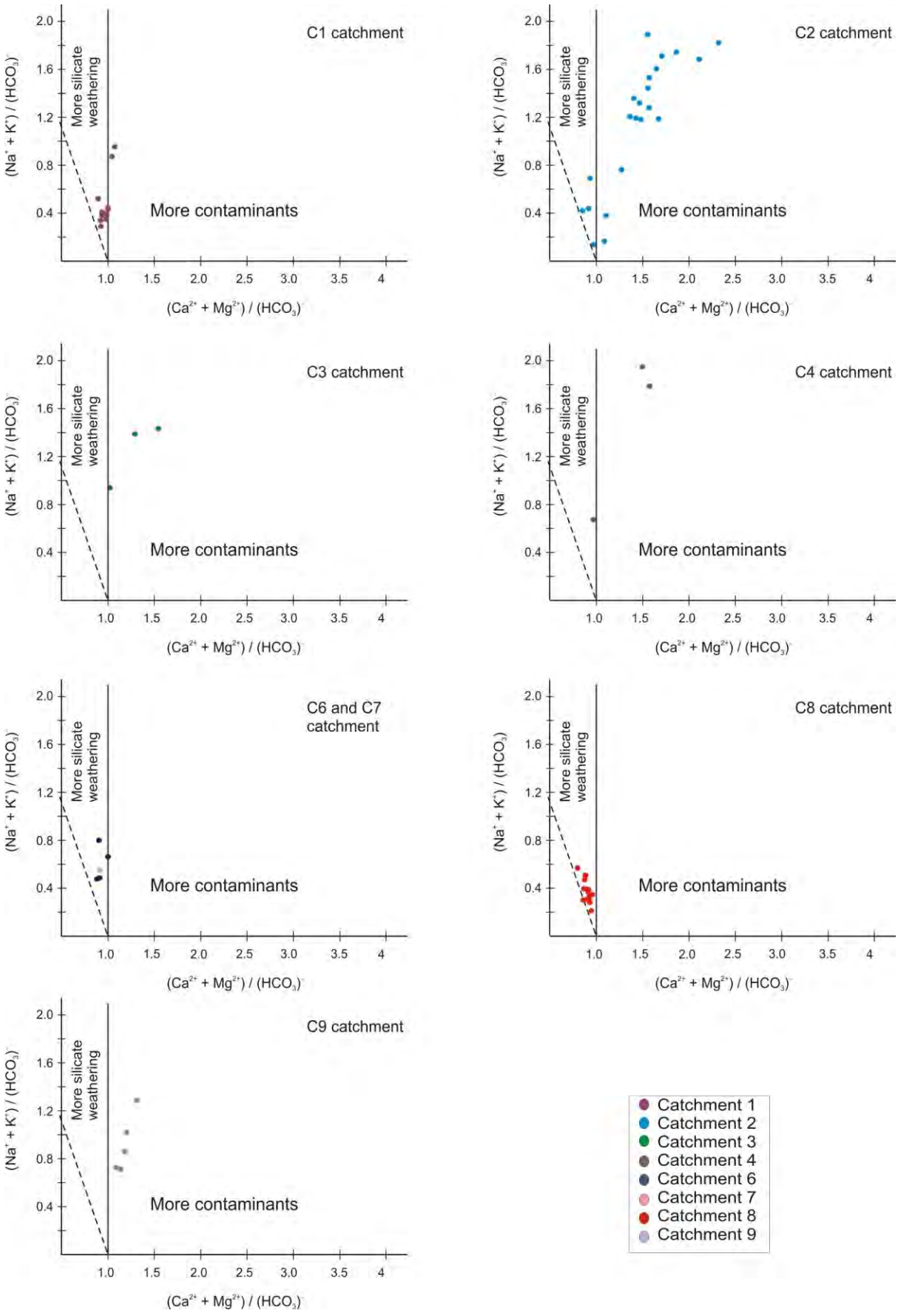

FIGURE 4-4 : CONTAMINATION-WEATHERING DIAGRAMS FOR DWA MONITORING STATION IN SELECTED CATCHMENTS

4.3 TERNARY DIAGRAMS

To assess the existence of geographical variation in inorganic water quality along the Vaal River, two diagrams were used: the ternary and Stiff diagrams. Different trends were observed in the ternary diagrams, chemical weather dominant, anthropogenic influences dominant, as well as an intermediate phase. Figure 4-5 summarises the ternary diagrams for each station to indicate the change in inorganic water chemistry geographically along the Vaal River.

There are three inferred trends visible from the ternary diagrams, the first group, catchment C1, C6, C7 and C8 (refer to Appendix 2 for detailed diagrams) (Figure 4-5) plot close to $[(HCO_3)^-]_{norm}$, indicating that rock weathering is taken to be the dominant factor contributing to the inorganic water chemistry. Catchment C1 is situated near the natural source, implying that water from the Lesotho Highlands system is transferred into the Vaal River system below the natural source. The first station (C1H007) is situated near Amersfoort and the last station for the C1 catchment is, station C1H017 on the Vaal River, situated well down the Vaal River near Villiers.

Catchment C2, the second group, indicates trends toward the $SO_{4\ norm}$ region (Figure 4-5). This is taken to indicate increasing anthropogenic influences on the water chemistry. The first station for the second group, (C2H122 on the Vaal River), is in the middle region of the river, situated after the Vaal Dam near Deneysville. The last station for the group, C2H61, is situated near the confluence with the Vals River, near Klipplaatdrift.

The third implied group includes catchment C9. It is indicated as a separate group, as influences from catchment C2 on C9 cannot be ignored, and cannot be excluded. Possible influences from the C2 catchment include a number of mines located in the catchment as well as the Vaal Dam within the catchment, possible chemical load changes could be associated with the Vaal Dam and the mine in close proximity. However, the C2 catchment covers the largest part of the study are, other potential influences such as industrial complexes as well as residential areas could contribute to the change in chemical composition that carries through to catchment C9 and could potentially influence the water chemistry. The ternary diagrams show an implied trend away from the SO_4 region. This can be seen with catchment C3 and C4 as well. This indicates that the SO_4 influence is still present but implied dilution is taking place. The first station for the third group, (C9H021) is situated near the town of Port Arlington and the last station in the group (C9H024) is situated near Schmidtsdrift. There are no usable data for points further west downstream near the confluence with the Orange River near Douglas.

Generally, the ternary diagrams imply that the anthropogenic effect becomes more pronounced towards the west, and lower reaches of the Vaal River. Here water use is dominated by agricultural activities, and not as pronounced for the upper (easterly) Vaal River where the primary industrial, commercial and urban activities are undertaken.

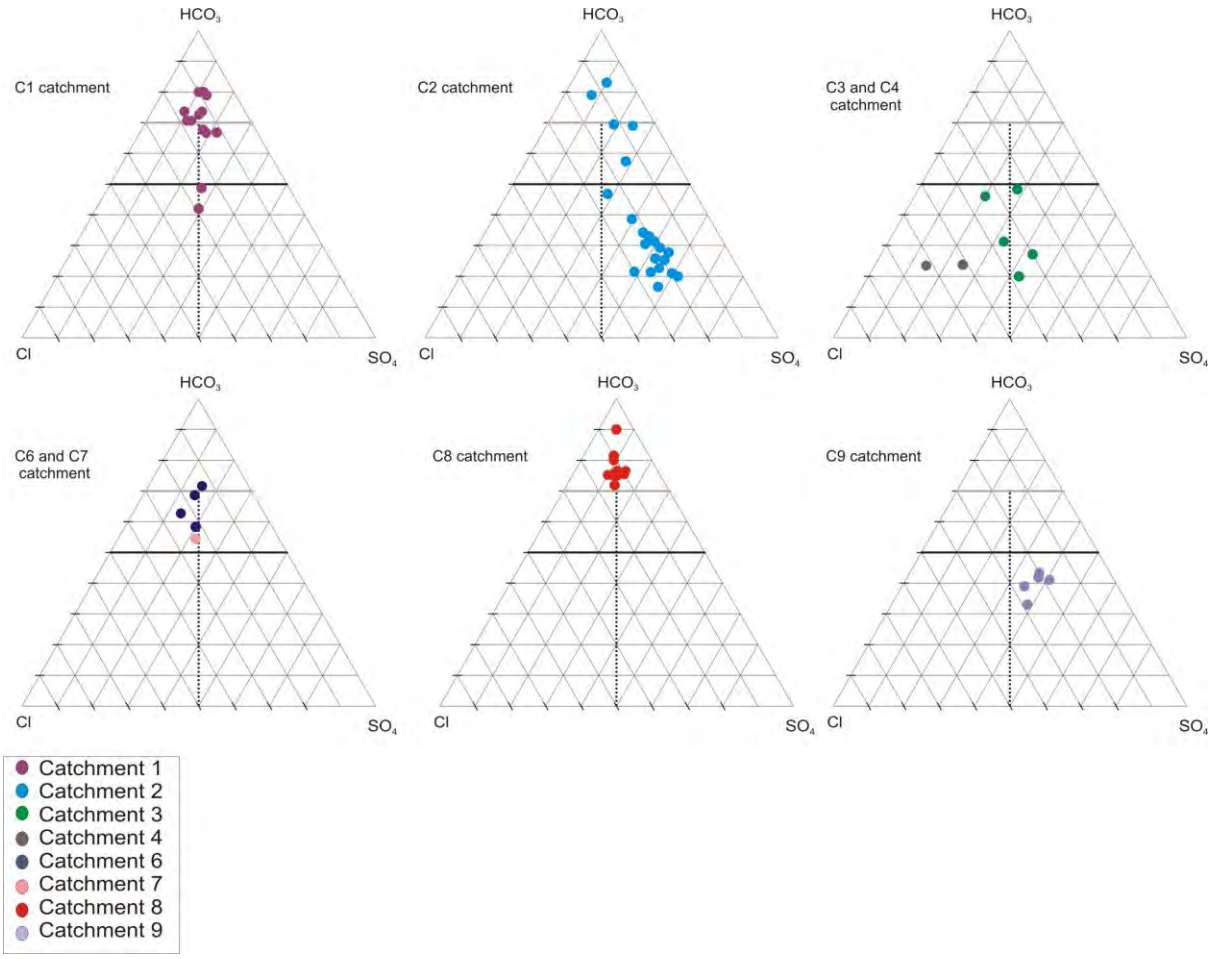

FIGURE 4-5: COMBINED TERNARY DIAGRAMS FOR CATCHMENTS C1, C2, C3, C4, C6, C7, C8 AND C9

4.4 STIFF DIAGRAMS

Further investigating the geographical trends in inorganic water quality, the Stiff diagrams are placed in the order from east to west; from primary source area flowing downstream. The diagrams are a collective representation of all the data from the ternary diagrams, together with the (HCO_3), $(SO_4)^2$ and Cl values, and include Na, Ca and Mg values. The groups are divided into three groups, however the two dominant implied differences are distinctively represented in the Stiff diagrams (Figure 4-6 and Figure 4-7).

The first group of stations (C1 catchment, Appendix 2) show high $(HCO_3)^-$ values, with lower $(SO_4)^2$ and Cl values. The Ca-values are higher than the Mg and Na in some of the stations, but overall the cations vary, also illustrated in Figure 4-6. The shape of the diagrams for

group one monitoring station data is also narrower than the group two data, suggesting lower overall ion concentrations in comparison with each other, with the width being the absolute concentrations of the ions.

The second group (C2 catchment, Appendix 2) shows an immense increase in the overall concentrations of all constituents. The $(SO_4)^2$ concentrations begin very high (C2H061) and as the monitoring stations move westward (downstream) the concentration decreases (C9H021). The $(HCO_3)^-$ value remains more or less the same from station C2H061 to C9H021. The Ca concentrations are also higher than group one, followed by the Na and then Mg concentrations (Figure 4-6). The shape of the Stiff diagrams for the group two monitoring stations data are thicker, suggesting that the overall ion concentrations has increased compared to the first group. This could be inferred from the influence of the activities upstream within the C2 catchment, such as the mining industry and Vaal Dam.

The third group (C9 catchment, Appendix 2) Stiff diagram representation, varies considerably with regards to the overall ion concentrations. This could be inferred from the influence of the upstream C2 catchment, such as the mining industry and Vaal Dam in the catchment. Figure 4-7 is a visual representation of the stations situated on the Vaal River, and the geographical positioning of the stations.

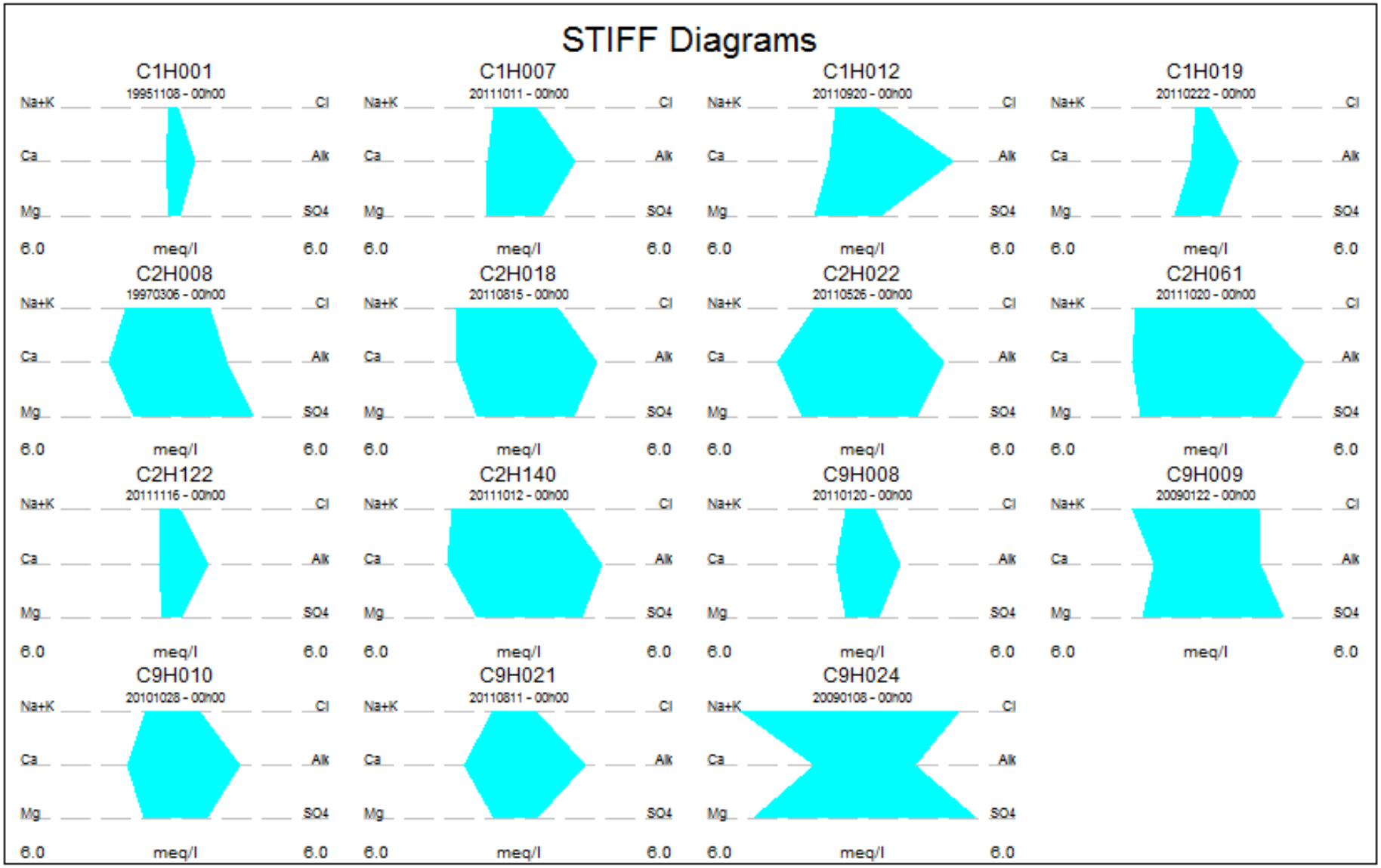

FIGURE 4-6: STIFF DIAGRAMS USING THE AVERAGE CONCENTRATION VALUES FOR THE CATIONS AND ANIONS FOR STATIONS LOCATED ON THE VAAL RIVER

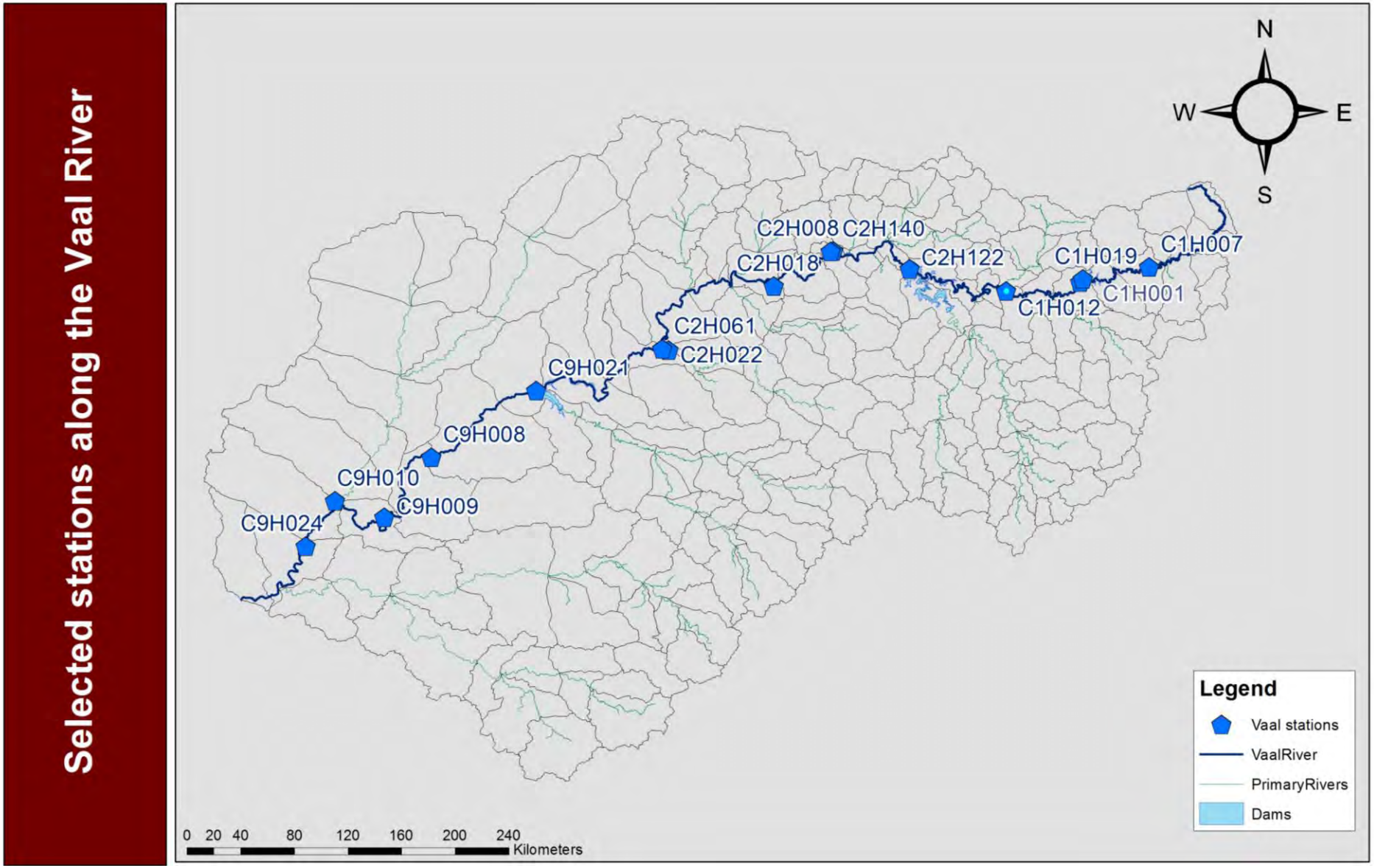

FIGURE 4-7: STIFF DIAGRAMS FOR STATIONS AND THEIR RELATIVE GEOGRAPHICAL POSITIONS ON THE VAAL RIVER

4.5 NATURAL VERSUS ANTHROPOGENIC EFFECT

In order to determine the relative importance of pollution, or anthropogenic effect, in addition to natural chemical weathering of the Vaal River water quality, TDS versus normalised bicarbonate concentrations were used as an indicator (Figure 4-8). By using these diagrams, in conjunction with the diagrams utilised to assess the chemical weathering effect on inorganic water chemistry, it is considered to be possible to establish whether the assumption that anthropogenic effect has a significant impact on the inorganic water quality of the Vaal River is supported by the use of TDS as an indicator of pollution.

For the individual monitoring stations (Appendix 3), stations C1H007, C2H007, C2H061, C9H021, C9H008 and C9H009 suggest the inferred negative trend, and an indication that the $[(HCO_3)]_{norm}$ increases with a decrease in TDS values, which is taken to be commonly associated with the increase in the $2[(SO_4)^2]_{norm}$ concentrations, except with regards to C1H007 where the influence of rainfall could be considered as a contributing factor. This can be contributed due to higher rainfall and thus having a dilution effect on the system at that point.

In contrast, stations C1H021 and C1H017 indicate an inferred positive slope, indicating a decrease in $HCO_{3\ norm}$ values with a decrease in TDS values. The last trend observed at stations C1H019, C1H020 and C1H122 has no obvious pattern, as the values remain the same and are spaced close together.

From these two inferred divergent trends (Figure 4-8, Stations C1H012 and C9H021) were identified and evaluated further. Stiff diagrams were populated to show the relative trends with regards to water chemistry and TDS variations. These diagrams have been created with data from each year, and were placed in a sequence of increasing $[(HCO_3)^-]$ concentrations for the two divergent stations selected (Figure 4-9 and Figure 4-10).

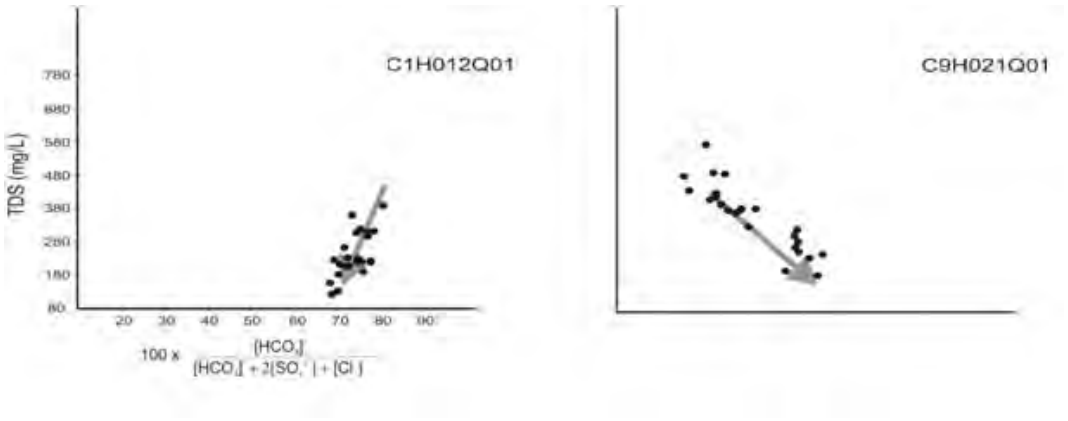

FIGURE 4-8: NATURAL VERSUS ANTHROPOGENIC DIAGRAMS CREATED FOR TWO DIVERGENT MONITORING STATIONS,SHOWING THE VALUES FOR THE TDS VERSUS BICARBONATE CONCENTRATIONS

C1H012Q01-2009
pH = 8.1
$[HCO_3^-]_{NORM}$ = 66%

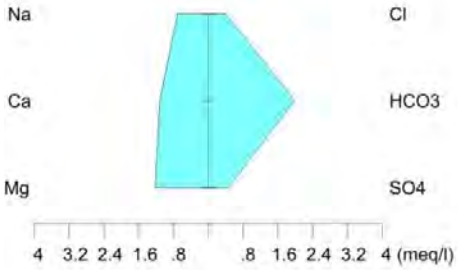

C1H012Q01-1993
pH = 8.0
TDS = 158 mg/L
$[HCO_3^-]_{NORM}$ = 68.5%

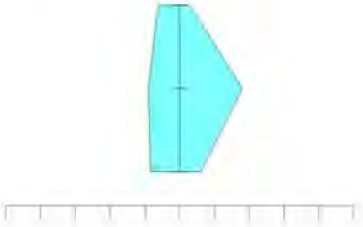

C1H012Q01-1986
pH = 7.5
TDS = 125 mg/L
$[HCO_3^-]_{NORM}$ = 68.9%

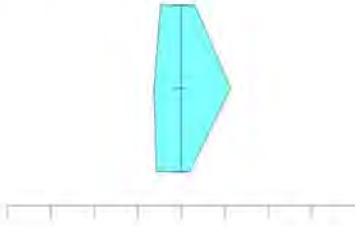

C1H012Q01-2007
pH = 8.1
TDS = 228 mg/L
$[HCO_3^-]_{NORM}$ = 69.4%

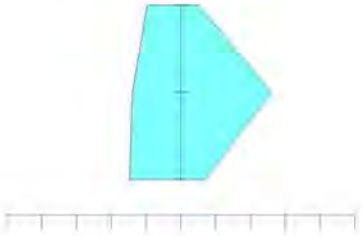

C1H012Q01-1987
pH = 7.2
TDS = 133 mg/L
$[HCO_3^-]_{NORM}$ = 70%

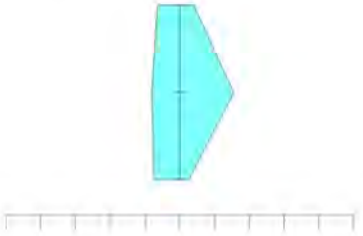

C1H012Q01-1991
pH = 8.1
TDS = 184 mg/L
$[HCO_3^-]_{NORM}$ = 70.3%

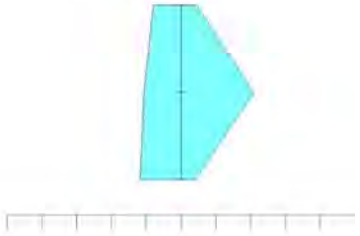

C1H012Q01-2008
pH = 8.0
TDS = 213 mg/L
$[HCO_3^-]_{NORM}$ = 70.7%

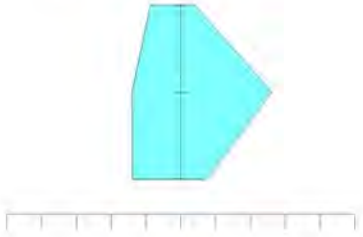

C1H012Q01-2003
pH = 8.2
TDS = 262 mg/L
$[HCO_3^-]_{NORM}$ = 71.8%

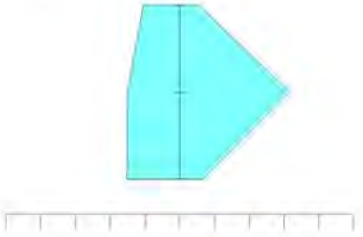

C1H012Q01-1990
pH = 8.1
TDS = 209 mg/L
$[HCO_3^-]_{NORM}$ = 72.3%

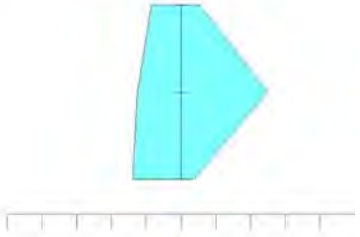

C1H012Q01-2004
pH = 8.1
TDS = 233 mg/L
$[HCO_3^-]_{NORM}$ = 72.4%

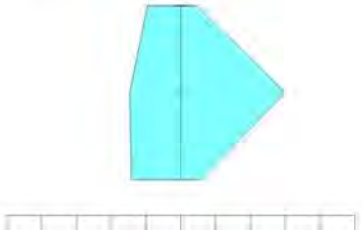

C1H012Q01-2000
pH = 8.2
TDS = 208 mg/L
$[HCO_3^-]_{NORM}$ = 72.5%

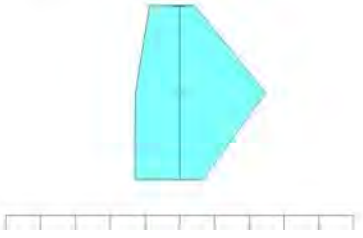

C1H012Q01-2010
pH = 8.1
TDS = 363 mg/L
$[HCO_3^-]_{NORM}$ = 73.7%

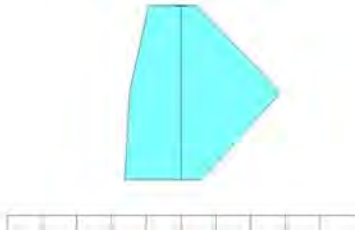

FIGURE 4-9: STIFF DIAGRAMS FOR STATION C1H012Q01 PLACED IN ORDER OF INCREASING $[(HCO_3)]_{NORM}$ VALUES. THIS STATION SHOWS AN INCREASE IN TDS WITH INCREASING $[(HCO_3)]_{NORM}$, WHICH REFLECTS A CHEMICAL WEATHERING TREND

C9H021Q01-1986
pH = 7.8
TDS = 484 mg/L
$[HCO_3^-]_{NORM}$ = 25.5%

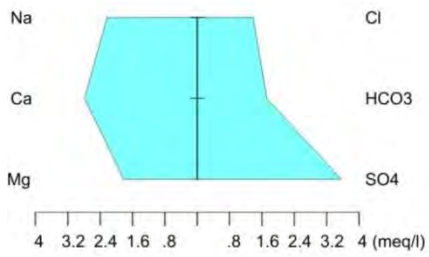

C9H021Q01-1987
pH = 7.4
TDS = 440 mg/L
$[HCO_3^-]_{NORM}$ = 26.7%

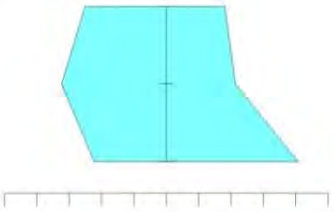

C9H021Q01-2004
pH = 8.0
TDS = 577 mg/L
$[HCO_3^-]_{NORM}$ = 30.7%

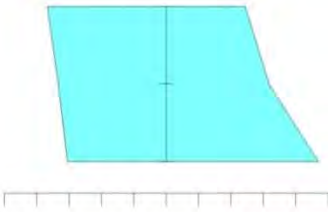

C9H021Q01-2008
pH = 8.0
TDS = 411 mg/L
$[HCO_3^-]_{NORM}$ = 31.8%

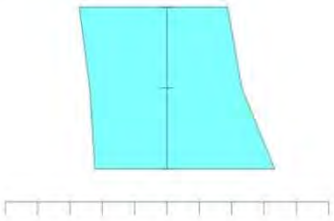

C9H021Q01-2005
pH = 8.0
TDS = 494 mg/L
$[HCO_3^-]_{NORM}$ = 32.3%

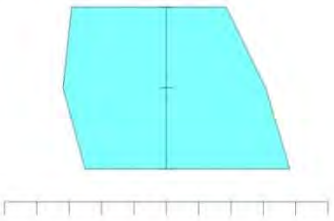

C9H021Q01-2003
pH = 8.2
TDS = 431 mg/L
$[HCO_3^-]_{NORM}$ = 33.1%

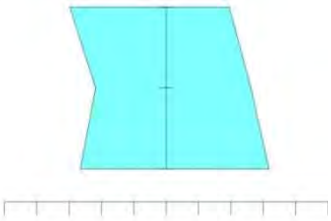

C9H021Q01-1991
pH = 8.2
TDS = 421 mg/L
$[HCO_3^-]_{NORM}$ = 33.1%

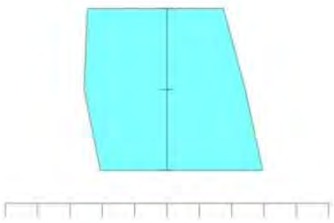

C9H021Q01-1999
pH = 8.3
TDS = 400 mg/L
$[HCO_3^-]_{NORM}$ = 34.2%

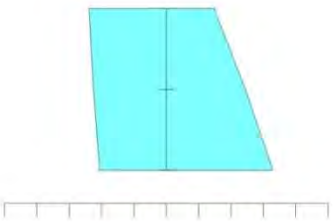

C9H021Q01-1992
pH = 8.4
TDS = 490 mg/L
$[HCO_3^-]_{NORM}$ = 34.6%

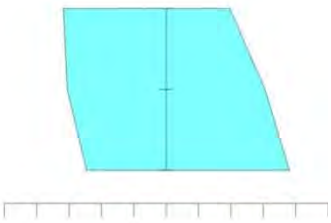

C9H021Q01-1990
pH = 8.3
TDS = 381 mg/L
$[HCO_3^-]_{NORM}$ = 35.9%

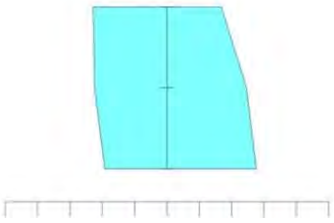

C9H021Q01-2007
pH = 8.0
TDS = 374 mg/L
$[HCO_3^-]_{NORM}$ = 37.5%

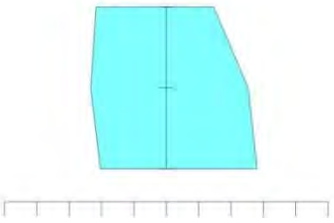

C9H021Q01-1994
pH = 8.3
TDS = 383 mg/L
$[HCO_3^-]_{NORM}$ = 38.7%

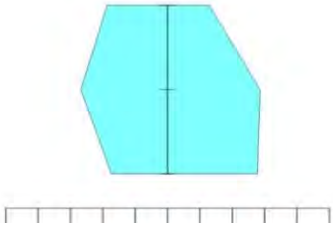

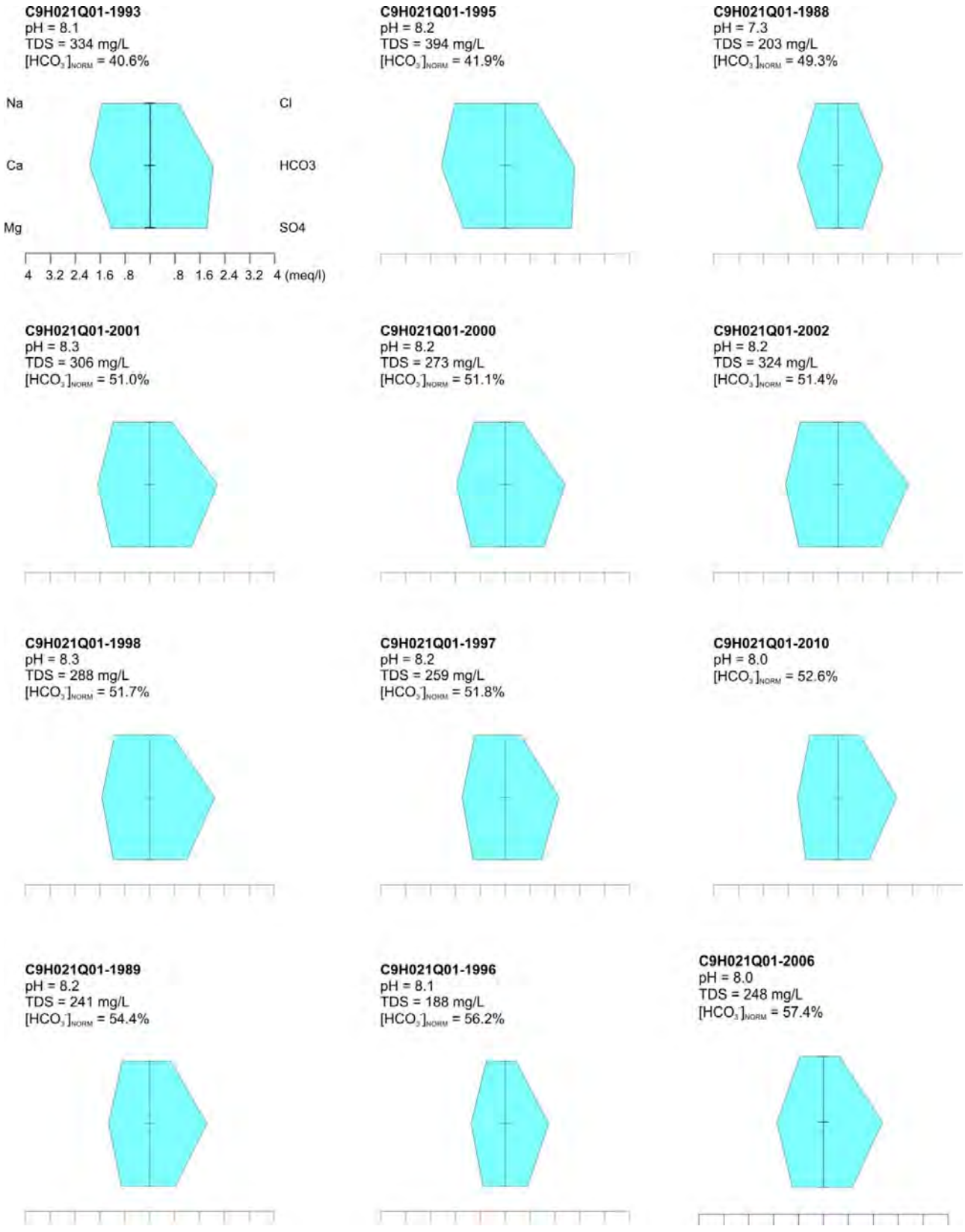

FIGURE 4-10: STIFF DIAGRAMS FOR STATION C9H021Q01 PLACED IN ORDER OF INCREASING $[(HCO_3)]_{NORM}$VALUES. THIS STATION SHOWS AN INCREASE IN TDS WITH DECREASING $[(HCO_3)]_{NORM}$, WHICH INDICATES POLLUTION AS MAIN CONTRIBUTING FACTOR TO THE WATER QUALITY

The cation trends are distinct, although two particular observations are made using the example of monitoring station C1H012 and C9H021 (above and below the Vaal Dam): (1) for station C1H012 it is observed that with increasing $[(HCO_3)]_{norm}$ the TDS is increasing. Generally, high TDS is explained by a high (HCO_3), as well as Ca and Mg values. Na and Cl do not vary significantly with increasing $[(HCO_3)]_{norm}$.

For the second trend (2), for station C9H021, it is observed that with an increasing $[(HCO_3)]_{norm}$ the TDS is decreasing. Generally, low TDS is explained by a low (HCO_3), as well as Ca and Mg values. All values vary significantly with increasing $[(HCO_3)]_{norm.}$ These trends indicate that station C1H012 has a typical chemical weathering pattern with HCO_3 concentrations a great deal higher than SO_4, and that station C9H021 has a greater anthropogenic influence starting lower and increasing as the $[(HCO_3)^-]_{norm}$ decreases.

4.6 SALT BALANCE

The salt balance equation used to determine the salt load of the catchment is:

Salt load = Flow (Mm^3/annum) x Concentration (mg/ℓ)

The salt loads were included to investigate further the controlling factors of Vaal River water chemistry as well as to indicate if the previous conclusions could be supported when the flow of the river was taken into consideration. The data was obtained from DWS Hydrological survey database with 85% reliability and 15% patched data.

Figure 4-11 to Figure 4-16 are a representation of the stations on the Vaal River with the relative TDS salt loads, sulphate loads bicarbonate loads and chloride loads for two distinctive periods. The chloride levels are very low in comparison with the rest and does not display prominent in the figures. It must be noted that there is a break between the stations, as the missing stations did not have sufficient data over the selected periods for the representation of historic and more recent data. Please refer to Figure 1-5, Figure 1-6 and Figure 1-7 for background. The stations in the figures are arranged from east (upstream) to west (downstream) on the Vaal River. A full table of the data is included in Appendix 4.

The two time periods represented in Figure 4-11 to Figure 4-15 are 1985 – 1990 and 2000 – 2005, these periods were selected to represent historic data as well as more recent data. It is common practice for industry to look at concentrations of the ions in effluent. However, load distribution of ions is not always taken into consideration. As time

progresses and more salts are added to the Vaal River, without consideration of loads, the concentration of salts in the water increases pushing up the overall load of the river. To attempt to reduce this effect, Phase 2 of the Lesotho Highlands project will be introduced in the near future. However, this would only reduce the buffer capacity of the rivers for a certain amount of time, diluting the effect temporarily.

Figure 4-11 is a TDS profile for the Vaal River. It is clear from the stacked diagram that the combination of [$(HCO_3)^-$] and [$(SO_4)^{2}$] ions accounts for approximately 70 to 80% of the TDS, indicating that the major drivers of the TDS character is the [$(HCO_3)^-$] and [$(SO_4)^{2}$] ions as indicated in previous results. The Si ions were not included in Figure 4-11 as it is only a representation to support the chemical weathering of the [$(HCO_3)^-$]. The correlation between [$(HCO_3)^-$] vs TDS and [$(SO_4)^{2}$] vs TDS is presented in Appendix 4.

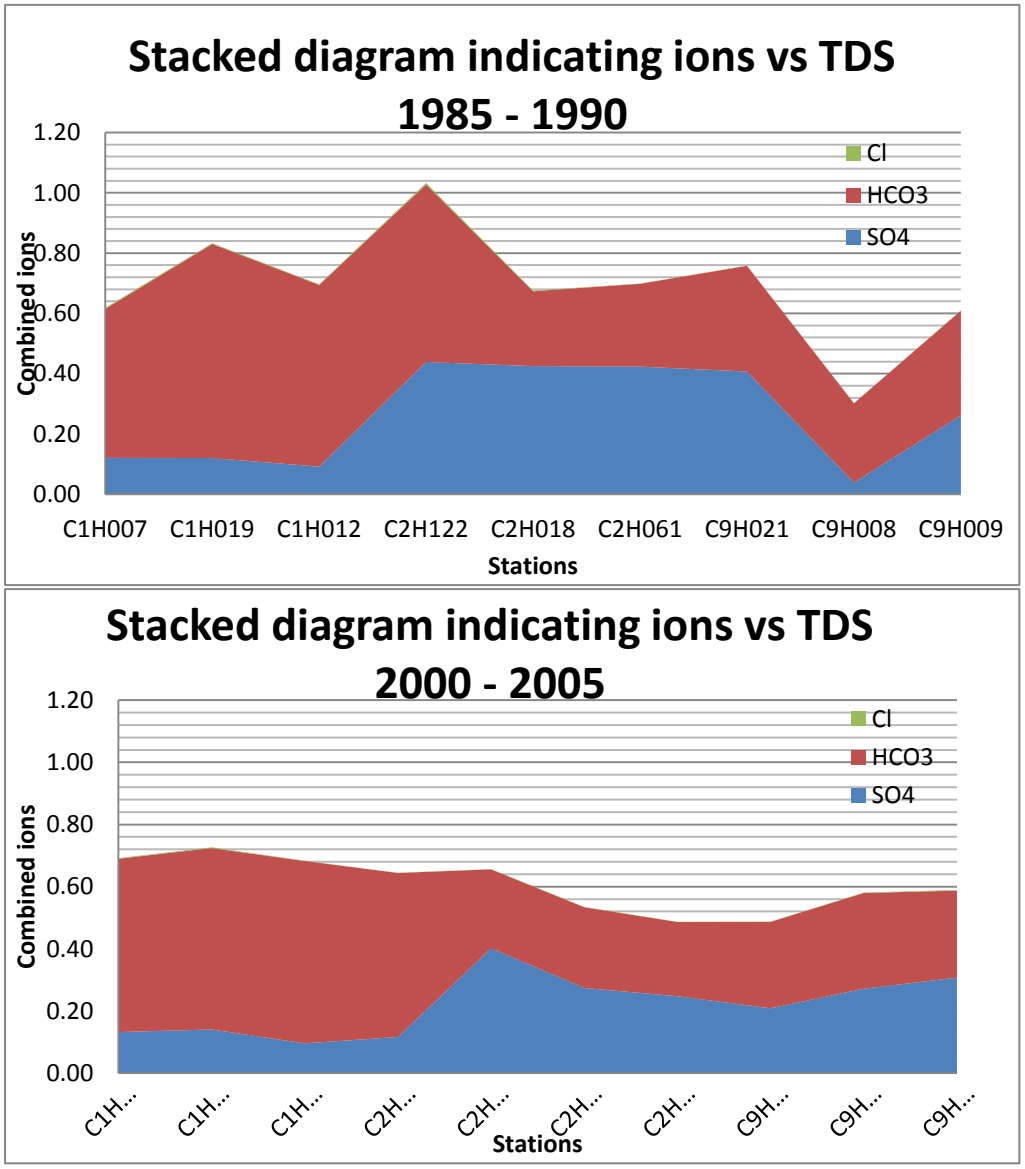

FIGURE 4-11: STACKED DIAGRAMS INDICATING HCO_3, SO_4 AND CL RELATIVE TO TDS FOR THE SELECTED TIME PERIODS

From the geology (section 1.5) and the schematic representation in Figure 4-12, it can be see that the TDS from weathering of the geology also defines three groups. Group 1 having low TDS concentrations indicating the chemical load to be low. Group 2 comprising medium TDS values indicating the chemical load has increased. Lastly group 3 remaining in the medium TDS values, indicating the chemical load has not increased significantly further downstream or the presence of additional water introduced to the system. This is an indication of the baseline values for TDS from the chemical weathering which is supported by the historic data (1985 – 1990), as the anthropogenic influences are less than at present particularly when the loads are taken into consideration. Consistent with Figure 1-7 and Table 1-4, the different lithologies were given a number to coincide with the TDS concentrations: low – 0.5, medium 1, medium-high 2 and high 3, as indicated in Figure 4-12.

Figure 4-13 is an indication of the TDS load as the stations progress from east to west (downstream) on the Vaal River. There is a clear composition change indication with regards to the three different groups as discussed in the previous sections. Figure 4-14 is an indication of the distribution of the [$(HCO_3)^-$] and [$(SO_4)^{2}$] ions contributing to the controlling factors of the Vaal River chemistry. Included in Figure 4-15 is the Si loads to verify the chemical weathering indicated by the [$(HCO_3)^-$] loads, as well as the Cl ions representing further anthropogenic influences. It should be noted that the Cl loads are small in comparison to the [$(HCO_3)^-$] and [$(SO_4)^{2}$] ions, also indicated in Figure 4-11, and is thus not one of the controlling factors. The salt load analysis supports the conclusions in section 4.3 from the ternary diagrams as well as in section 4.4 from the Stiff diagrams.

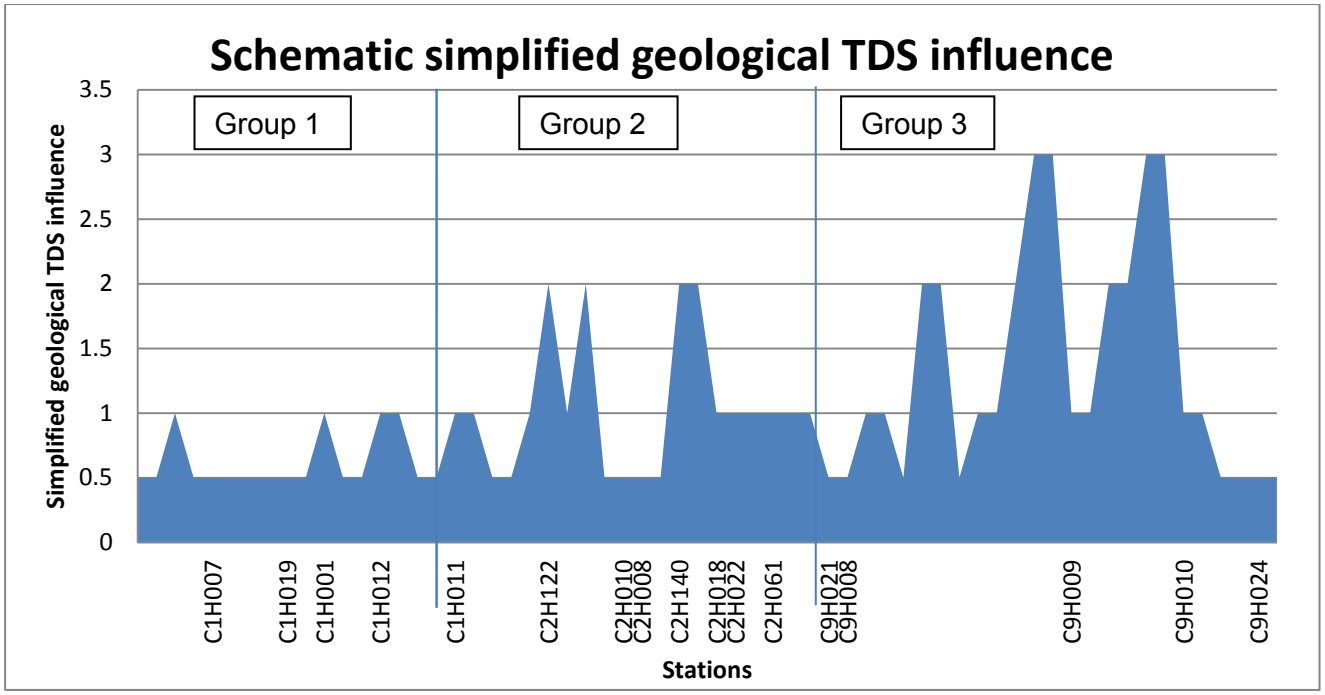

FIGURE 4-12: SCHEMATIC REPRESENTATION OF THE TDS FROM CHEMICAL WEATHERING OF THE GEOLOGICAL STRUCTURES ALONG THE VAAL RIVER (EAST TO WEST)

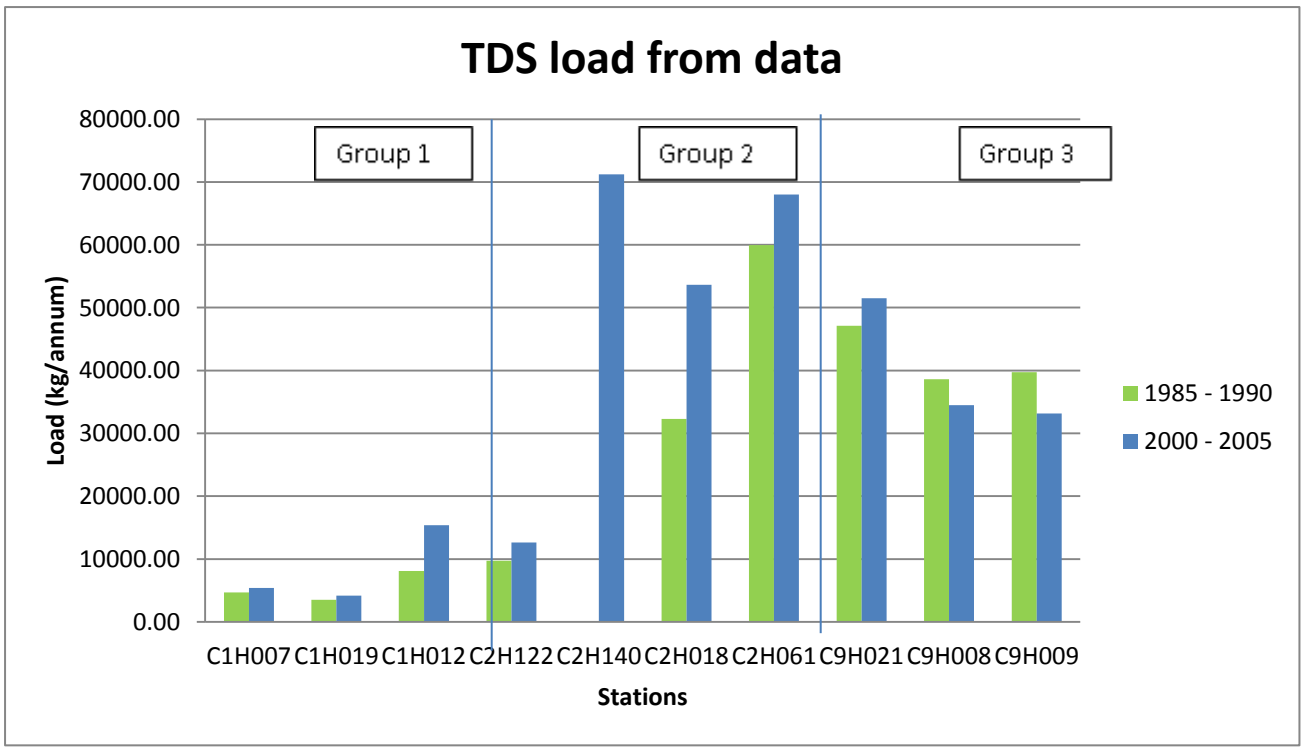

FIGURE 4-13: TDS LOADS FOR THE SELECTED STATIONS FOR THE TWO TIME PERIODS

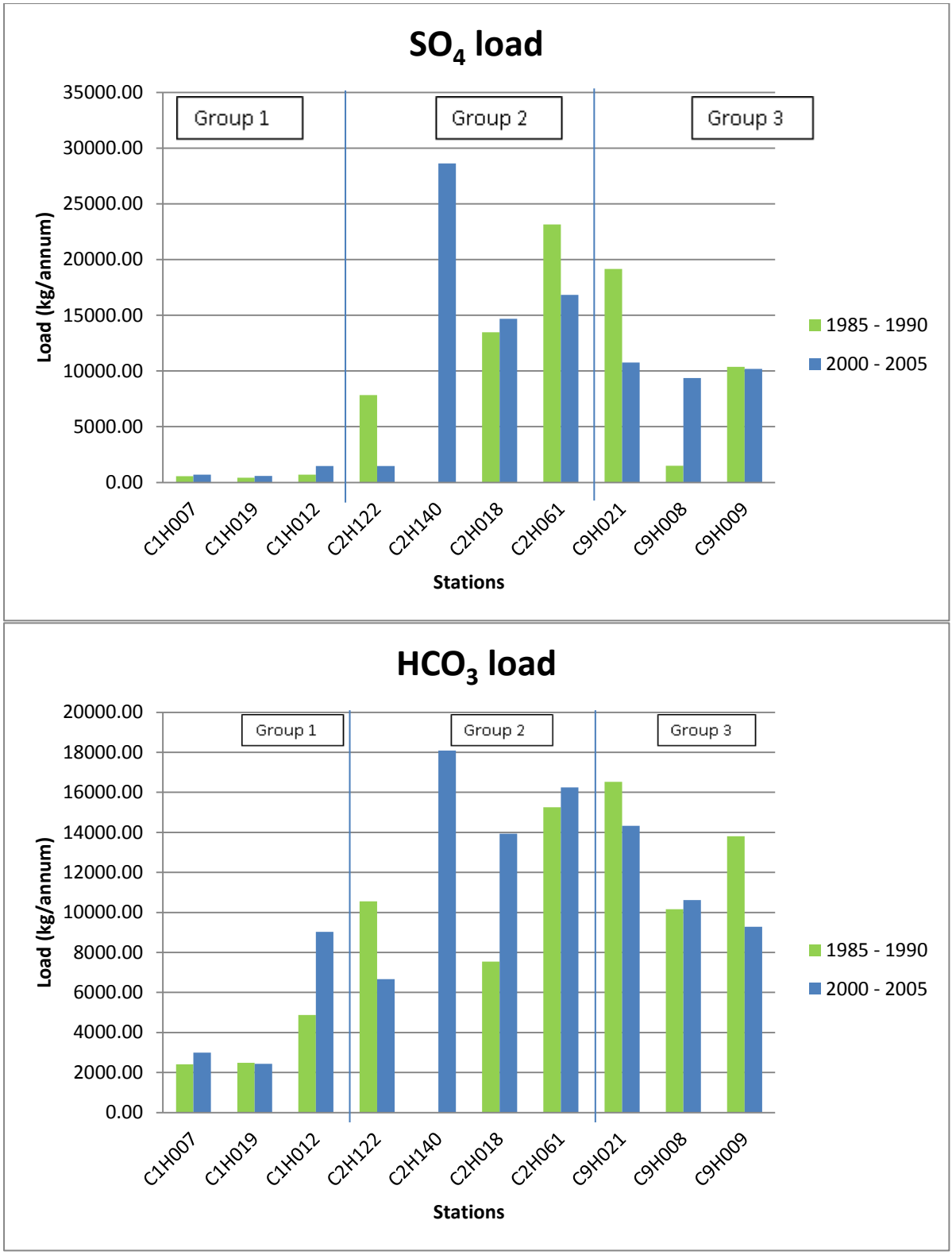

FIGURE 4-14: SO_4 AND HCO_3 LOADS FOR THE SELECTED STATIONS FOR THE TIME PERIODS

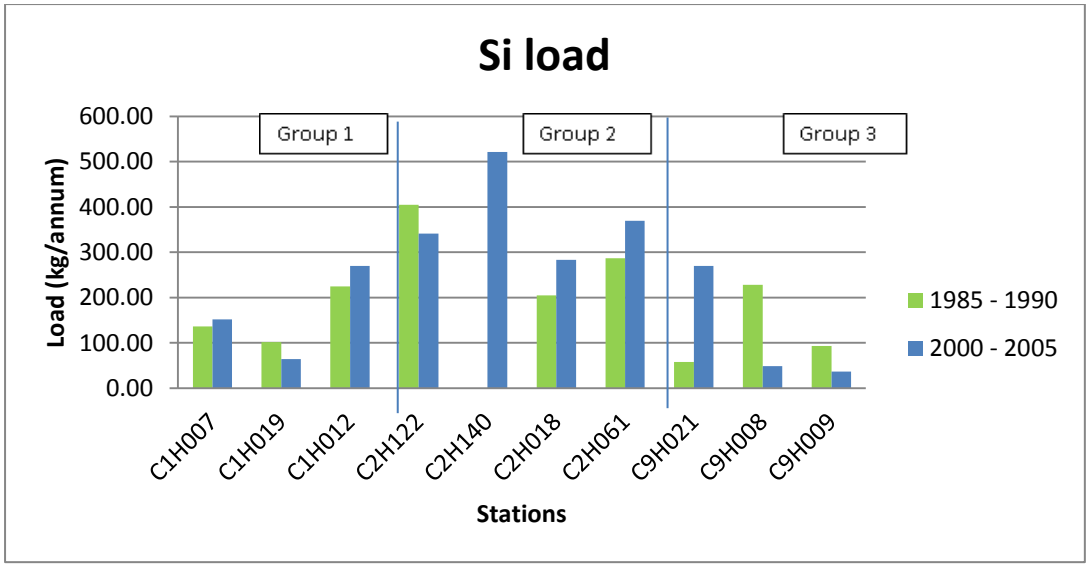

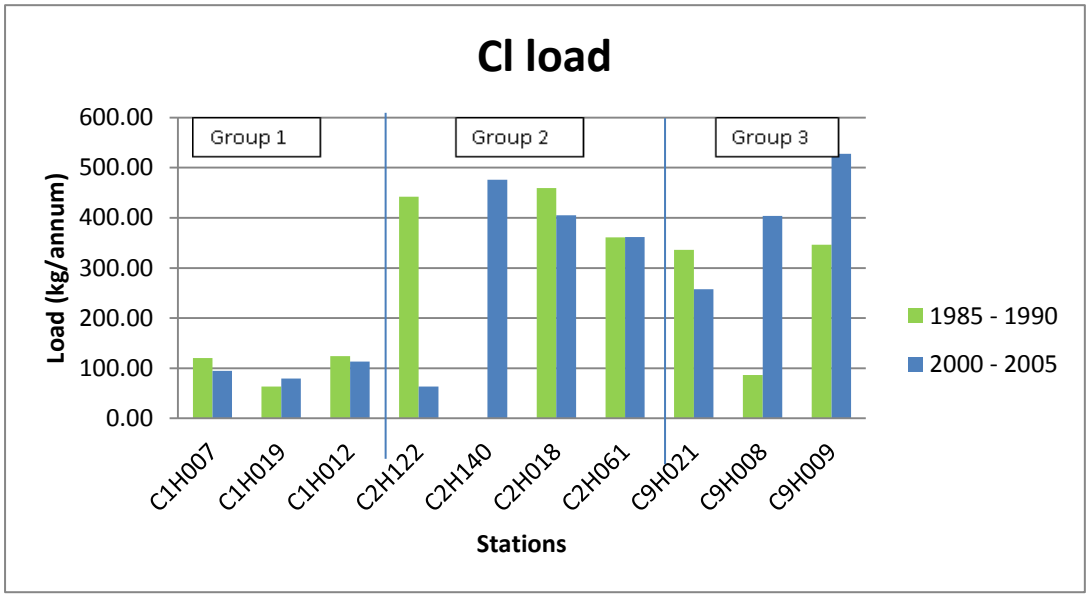

FIGURE 4-15: SI AND CL LOADS REPRESENTING THE SELECTED STATIONS IN THE TIME **PREIODS**

There is a clear spike indicated at station C2H140 in [$(HCO_3)^-$]. This increase in bicarbonate could be an indication of the dolomites associated with the C2 catchment area.

Carbonates play an important role in acid buffering reactions they neutralise acid generated from sulphide oxidation in mining related activities in particular. Calcite neutralises acid by dissolving and complexing with hydrogen ions to form bicarbonate $(HCO_3)^-$ (Lottermoser, 2010). Szramek *et al.,* (2011) indicate that calcite and dolomite weathering end members can be identified or distinguished due to the differences in carbonate source. Dolomite weathers preferentially over calcite, except for pure limestone catchments, the [$(HCO_3)^-$] concentration can be attributed to nearly equal

proportions by mass of dolomite relative to calcite mineral weathering (Szramek *et al.,* 2011).

There are few previous studies on dolomite weathering within surface systems. Typically both lithologies (dolomite and limestone) are lumped as carbonates (Meybeck, 1987; Amiotte Suchet *et al*., 2003; Dürr *et al*., 2005). Recent research in temperate zone glacial drift deposits of mixed carbonate and silicate mineralogy suggests that the contributions from dolomite relative to calcite weathering have been underestimated (Szramek and Walter 2004; Williams *et al*. 2007; Jin *et al.* 2009).

Weathering of the carbonate minerals via sulphuric acid is a possibility in carbonate terrains. Oxidation of pyrite, typically present in carbonate lithologies, produces sulphuric acid, which then causes dissolution of carbonate minerals (Drever, 1997; Langmuir, 1997; Hercod *et al.,* 1998). It should also be noted that dolomite dissolution can be accelerated by reactions with nitric acid produced as a by-product of nitrification of N-fertilizers (Pacheco *et al.,* 2013).

From the study by Szramek *et al.,* (2011) the tributary streams clearly revealed that there are dominant carbonate lithologies (dolomite or calcite) within individual catchments. The lower ion values from the study indicated a directly corresponding ratio to limited dolomite within the catchment. The tributaries with a higher abundance of dolomite indicated that the dolomite weathering contributed to each catchment and that the majority of the samples had ratios indicating a higher degree of dolomite to calcite weathering. It is however important to note that carbonate weathering intensity alone cannot determine the degree of dolomite mineral weathering within a catchment and a number of other factors were investigated. However, it is evident that with the introduction of a dolomite dominated lithology, bicarbonate in the system will increase correspondingly and any remaining cations not accounted for by rain, evaporites or silicates were attributed to carbonate weathering (Moquet *et al.,* 2011).

The effect of load versus the effect of concentrations of the ions in the Vaal River is depicted in Figure 4-16. A clear indication of dilution can be seen in the last group (group 3), indicating that the load decreases although the concentration increased. This is the short term effect the Leshoto Highlands project will have on the middel section, represented by group 2.

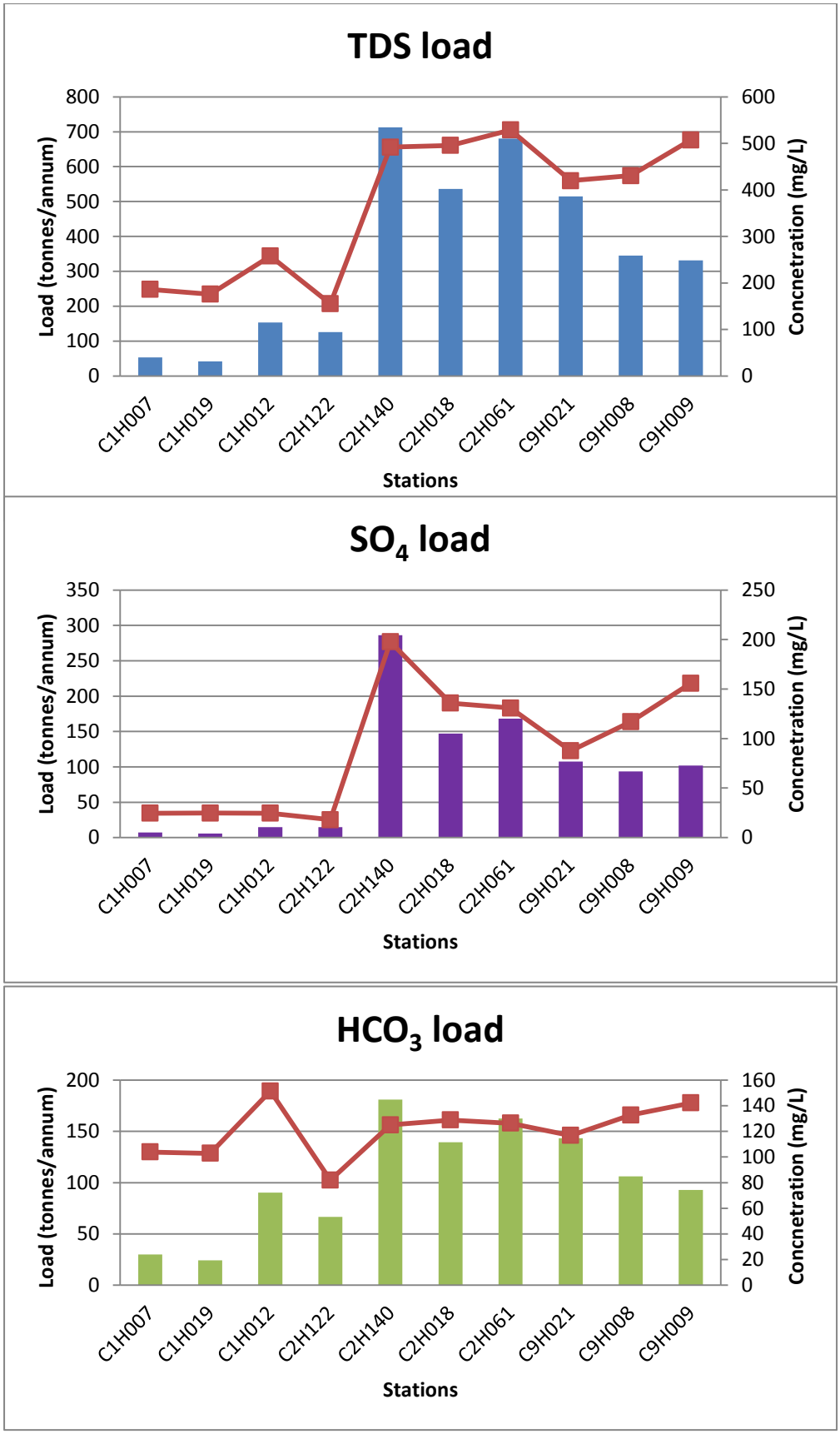

FIGURE 4-16: IONIC LOADS VS CONCENTRATIONS FOR THE 2000 - 2005 TIME PERIOD

The stations in the C1 catchment show a steady increase in all concentrations. The overall land cover in the C1 catchment is cultivated and natural, with few towns present (Figure 1-5 and Figure 1-6). The mining and industrial activities in the catchment are minimal. The simplified geology (Figure 1-7 and Figure 4-12) indicates that the geological TDS contribution is low to medium. A steady increase in salt load is expected as the area is developed. The chemical weathering as well as the anthropogenic influences increase with the progression from east towards the Vaal Dam (westerly direction). However, the overall concentrations are within the same range and approximately two times lower than group 2.

The stations in catchment C2 have a significant increase in salt load between C1 and C2. Before monitoring station C2H122, the water from the Secunda/Evander area joins the Vaal Dam. There are a number of industrial and mining related activities associated with these towns. The simplified geology indicates a medium/high dominated TDS influence (Figure 4-12). This is not as significant as the load from the industrial areas, however the [$(HCO_3)^-$] influence from the dolomites is picked up in this group. As the stations progress further west, the salt load increases. This could either be an indication of the industrial activities associated with the Johannesburg region draining into the Vaal River before C2H018, or the load carried through from the Vaal Dam and the upstream catchments. The geological TDS influence indicates low TDS concentrations, which can thus be considered not to be the influencing factor in group 2. However, as the C2 stations progress west, the drainage line does include areas with high TDS influence. The anthropogenic influence indicates a sharp increase between catchments C1 and C2. The river proceeding in a westerly direction, preceding the Vaal Dam. This trend is also evident in the chemical weathering load of catchment C2. The trend observed is a dominant indication of increase in overall ion concentration influencing the TDS concentrations. Together with the increase in concentration, this is an indication of the salt load of the Vaal River where there is a sharp increasing trend which verifies the data already proven without the influence of the water flow present.

The C9 catchment has a decline in salt load. This could be an indication of numerous tributaries entering after the last station in the C2 catchment. There is a steady decrease in load but an increase in concentration from the first station (C9H021) towards the last station. The region drains over an area with high and low TDS influence (Figure 1-7 and Figure 4-12), but the area has little industrial activity. The land cover consists of mainly natural and cultivated land. The salt load could be inferred from the geological influences, as other influences are minimal, or could be the residual influence from the upstream

influences. The trend for the chemical weathering and anthropogenic influences, in catchment C9, also strengthens the TDS (salt load) trend.

This chapter discussed the implied trends in the different diagrams. In the Conclusion all the trends will be compared and an overall water quality trend will be evaluated for the Vaal River.

5 DISCUSSION AND CONCLUSION

5.1 INTRODUCTION

The water used from the Vaal River is one of the most important sources and resources in South Africa, and in order to meet the user demands in terms of quantity and quality, in the absence of adequate natural recharge to the system, is supplemented with pristine quality water from the Lesotho Highlands and Tugela systems.

Given the importance of the Vaal River system to South Africa, the Department of Water Affairs (DWA), have established an extensive network of monitoring stations. This study has utilised available water quality data to specifically evaluate and establish the inorganic water chemistry of the Vaal River system.

Due to the Vaal River running through the economic heartland of South Africa (DWAF, 2007 and King, 2004), some of the area around the upper basin is highly industrialised and residentially developed. These areas utilise the Vaal River system water and contribute return flows both directly or indirectly (i.e. mine water and industrial discharges and sewage works discharges, as well as urban runoff), whilst some of the basin, particularly in the lower reaches, but not exclusively, is under agriculture and much of which draws water from the Vaal River system for irrigation and contributes land impacted return flow/runoff (DEAT, 2007).

Numerous geochemical diagrams were used for the characterisation of the water chemistry of the Vaal River. There upon several other geochemical diagrams were created to further discuss the different influences on the Vaal River. Water chemistry composition was calculated using the median values of the cations and anions calculated for each station, adapted from the DWA data obtained.

From this study it was identified that the water chemistry of the Vaal River system is naturally and anthropogenically (man-made influences) controlled by:

- Chemical weathering of siliceous sediment, intrusive igneous rocks and metamorphic rocks (Na^+, K^+, Mg^{2+}, Ca^{2+} and $(HCO_3)^-$.
- Input from urban and agricultural areas affect the concentration of $(SO_4)^{2-}$ and Cl^-, as indicated by a decrease in the $[(HCO_3)^-]/[Na^+]$ ratio.

5.2 DISCUSSION OF RESULTS

Based on the characterisation of the water chemistry, three inferred groups were identified along the length of the Vaal River.

- Group 1: Catchments C1, C6, C7 and C8
- Group 2: Catchment C2, C3 and C4
- Group 3: Catchment C9

The identification of the two controllers, natural weathering and anthropogenic factors, is demonstrated by the various inorganic water quality ratio assessment methodologies, as presented in the body of the report. These appear to demonstrate three largely distinct groups of inorganic water quality, largely represented by the monitoring stations above, and below the Vaal Dam, and after the Vet River confluence, as discussed.

5.3 GENERAL INORGANIC CHEMISTRY TRENDS ALONG THE VAAL RIVER

Methods of presenting inorganic water quality data have been generated from the DWA water quality data for the various monitoring stations along the Vaal River. These include the following diagrams:

- Gibbs,
- Gaillardet,
- Activity-activity,
- Ternary,
- Stiff,
- Na + K, and
- Natural vs. anthropogenic diagrams.

The different methods of presenting inorganic water quality use different inorganic element or salt components, and different comparison approaches. It is evident that the different methods do demonstrate some differences in the inorganic water quality composition and ratios along the Vaal River.

Whilst the inorganic water quality grouping of monitoring stations above, and below, the Vaal Dam and after the Vet River confluence is generally well indicated by the various inorganic water quality presentation methods, it is noted that with the Gibbs, Gaillardet and activity-activity diagrams the groups are not quite as well defined as with the other diagrams.

The Vaal River monitoring station inorganic water quality data are situated in two groups in the Gibbs and Gaillardet diagrams.

(1) Mainly in the rock weathering dominated field of the Gibbs diagrams and are closer to the siliclastic dominant field in the Gaillardet mixing diagram, moving towards the carbonate dominant field.

(2) The second set of stations are mainly situated in the rock dominated field of the Gibbs diagrams progressing towards the evaporation dominated field and are slightly away from the siliclastic dominated field, progressing towards the evaporation dominated field in the Gaillardet mixing diagram. The concentrations of ions are slightly higher overall in this group.

All the activity-activity diagrams are an indication of typical South African weathering, taking into consideration climate and geology, and the contribution from the on-going exposure of geology within the watercourse and surrounding land use to weathering activity. No advanced weathering has occurred, with the primary weathering product being kaolinite.

For the ternary, Stiff, Na + K and natural vs. anthropogenic diagrams, the overall average structure of the water chemistry composition was calculated using the median values of the cations and anions from the data obtained from DWA. The figure of the natural TDS influence (Figure 1-7) was combined with the mining activities in the Vaal Catchment to create Figure 5-1, a combined map of activities in the Vaal River. This combined figure will be used as a summary diagram to indicate the influences for the three dominating groups within the catchment.

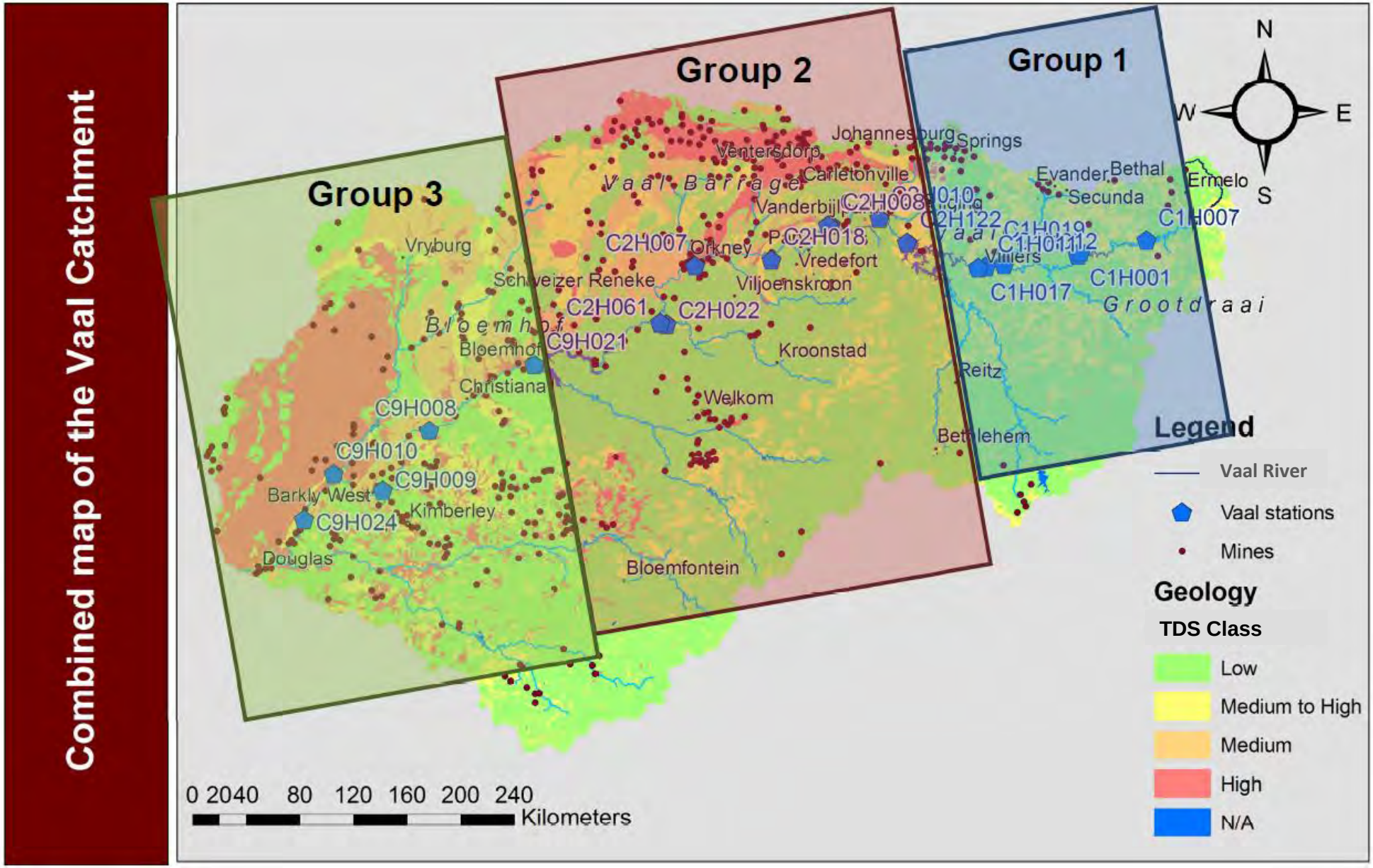

FIGURE 5-1: A COMBINED REPRESENTATIVE FIGURE OF THE SIMPLIFIED GEOLOGY, OR NATURAL TDS INFLUENCE, AND THE MINING ACTIVITIES IN THE VAAL CATCHMENT

5.4 GROUP 1

These stations are representative of the easterly section of the Vaal River, from Breyten/Ermelo towards the Vaal Dam (Figure 5-1 stations C1H007 to C1H011). This section of the Vaal River is dominated mostly by mining activities near the towns of Ermelo and Evander. Catchment

- The bicarbonate values when plotted for each of the monitoring stations suggest little variation, and the entire data set plot in the region of 65 to 75 bicarbonate concentration. This is seen for each station over the full period of monitoring, implying that there is no significant increase or decrease in the relative bicarbonate concentration over time.
- The Stiff diagrams imply that there is a trend in element composition as the $Ca^{2+}\approx Mg^{2+}> Na^{+}$ and the corresponding can be seen in the anions, $(HCO_3)^{-}>>(SO_4)^{2-} >Cl^{-}$, with a low to medium ion concentration shape.
- The Na + K diagrams for group 1 monitoring stations suggest an apparent trend where all the data are grouped together on the $2([Mg^{2+}] + [Ca^{2+}])/([HCO_3])^{-} = 1$ vertical line.
- The natural vs. anthropogenic diagrams in this group indicate the monitoring stations are largely grouped together with a positive correlation between TDS and bicarbonate concentrations. This positive correlation is described as when there is an increase in bicarbonate there will be an increase in TDS.

Group 1 stations appear to suggest a higher influence in chemical weathering than the group 2 stations. This is considered to be typically the influence of the weathering of rocks such as granites, shales and metamorphic rocks. The increase in bicarbonate concentration, again suggests a positive increase in TDS values.

A brief groundwater comparison was completed, with figures included in Appendix 4. Sections were selected for the groundwater comparison using the sections of the catchments. Groundwater section 1 boreholes are in the same vicinity as group 1 catchment C1. The anion ternary diagram accompanying the Piper diagram indicates the same conclusion as with the surface water. The area is dominated by chemical weathering of rocks.

5.5 GROUP 2

These stations are representative of the middle section of the Vaal River, from below the Vaal Dam area, through the Vredefort-Klerksdorp areas towards the Vals River confluence at Klipplaatsdrif, indicated by stations C2H008 to C2H061 in Figure 5-1. This section of the Vaal River is dominated mostly by mining activities. These mining areas include Secunda, Ventersdorp, and Carletonville.

- The inferred trends for the ternary diagrams appear to suggest a sharp decline in bicarbonate concentrations, where the trend is more towards the $SO_{4\ norm}$ region. The group 2 station data do not appear to remain as consistent as with group1 stations. However there is a large increase in overall ion concentrations from group 1 to group 2. The trends observed are not a yearly progression trend; as the positions are random and not a defined progression trend.
- There also appears to be a trend in the Stiff diagrams as the Na^{+}> Ca^{2+} >Mg^{2+} and the corresponding trend can be seen in the anions, $(SO_4)^{2-}$>> $(HCO_3)^{-}$>Cl^{-}. Overall the concentrations have increased, as observed from the sharp increase between group 1 and group 2.
- Similarly, for the group 2 stations, the Na + K diagrams imply a positive correlation, with an increase in Na + K. There is a corresponding increase in the Ca + Mg concentrations, as well as all the data plotting in the contaminated region of the diagram. The data plot is random and does not present a progressive yearly trend.

Group 2 appear to suggest a greater contribution from SO_4 influences than group 1. The TDS bicarbonate concentrations tend to be more narrowly aligned, although the correlation appears to still be negative.

A brief groundwater comparison was completed, with figures included in Appendix 4. Groundwater section 2 and 3 boreholes are in the same overall area shown in the surface water group 2, catchment C2. The anion ternary diagram accompanying the Piper diagram indicates the groundwater appears to be over a wide spread range. Further division of the boreholes are in groundwater section 7. Section 2 and 3 had predominant chemical weathering regions with influences from anthropogenic areas. Section 7 and 8 is an indication of where the natural chemical weathering areas are.

Together with the brief groundwater inspection, the groundwater quality indicates mostly natural weathering influences. The group 2 area is dominated by industrial and mining areas and as a result this is seen in the surface water.

5.6 GROUP 3

These stations are representative of the westerly section of the Vaal River, from the Bloemhof area, near the Vet River confluence towards Schmidtsdrift, after the Harts River confluence (C9H021 to C9H024 in Figure 5-1). This section of the Vaal River is dominated mostly by agricultural activities.

- The inferred trends for the ternary diagrams appear to suggest an incline towards the bicarbonate concentrations, where the trend is moving away from the $SO_{4\ norm}$ region. The group 3 station data do not appear to remain consistent as with group1 and 2 stations.
- There appears to be no apparent trend in the Stiff diagrams. Overall the ion concentrations have increased, as observed from the sharp increase.
- For the group 3 stations, the Na + K diagrams imply that with an increase in Na + K, there is no increase or decrease in the Ca + Mg concentrations. All the data do plot in the contaminated region of the diagram. The data plot is random and does not present a progressive yearly trend.
- With the natural vs. anthropogenic diagrams in this group there appears to be a negative correlation between TDS and bicarbonate concentrations. This negative correlation is described as when there is an increase in bicarbonate there will be a decrease in TDS.

Group 3 appears to suggest an influence from both the bicarbonate and the SO_4 regions. The TDS bicarbonate concentrations tend to be more narrowly aligned although the correlation appears still to be negative. The decrease in bicarbonate concentrations suggests a negative trend with TDS increasing.

A brief groundwater comparison was completed, with figures included in Appendix 4. Groundwater sections 4 and 5 boreholes are in the same vicinity of group 3 catchment C9. The anion ternary diagram accompanying the Piper diagram indicates that the groundwater appears to be over a wide spread range. However, it appears to be more dominant in the natural weathering region.

Further division of the boreholes is in groundwater section 6. Section 4 and 5 had predominantly chemical weathering regions with influences from anthropogenic areas.

Section 6 is an indication of where the natural chemical weathering areas are the most dominant. Figure 1-7 in Chapter 1, section 6, indicates as being in a high TDS region. However, the Stiff diagrams are not an indication that the groundwater has a high TDS level. Together with the brief groundwater inspection, the groundwater quality indicates mostly natural weathering influences.

The group 3 area is dominated by agricultural areas and fewer mines, however the influence of group 2 cannot be disregarded.

5.7 OVERALL CONCLUSIONS

Given the emotive statements in the press in recent years, it was expected that it may be possible to identify such increasing SO_4 loads derived from anthropogenic influence along the Vaal River demonstrated by trends in the inorganic quality from a more natural historical contribution towards the current time. However, the water quality data for the Vaal River indicate a material increase in anthropogenic influence on the inorganic water quality, specifically associated with the group 2 stations, and further implies that natural weathering controls the water quality to a greater degree. This relative importance may change if the anthropogenic factors do increase their relative contribution to inorganic load, and sulphate in particular.

The current study, based on DWA monitoring data for the Vaal River, suggests that the upper (easterly) section of the Vaal River has a definite chemical weathering influence, whilst the bottom (westerly) station evaluated for the Vaal River again suggests a dominance of chemical weathering, and that the relative significance of anthropogenic influences decreases towards the last monitoring station.

From the presentation of the inorganic water quality data, according to the established methods used in this study, it can also be concluded that the TDS cannot be used as a stand-alone chemical index parameter to measure pollution, but that the inorganic components contributing to the overall TDS need to be considered on their individual and collaborative basis.

It is common practice in articles such as McCarthy (2011), to use increased TDS as an indication of anthropogenic inorganic water pollution, and particularly in discussing AMD and industrial discharges to the Vaal River. However, the current evaluation of the DWA monitoring data for the Vaal River, as represented by Figure 4-8, combined with the second set of Stiff diagrams (Figure 4-9 and Figure 4-10), suggest that an increase in

TDS does not necessarily imply that the water is polluted by anthropogenic activities, and natural weathering remains a primary controlling factor for the Vaal River inorganic water quality. It might be expected that the TDS increase with a decrease in bicarbonate concentrations should indicate anthropogenic influences, however it is not seen in the Stiff diagrams.

The two identified stations illustrate that the TDS values vary as the bicarbonate values decrease, whilst the width of the Stiff diagrams is also an indication of the TDS concentration. The TDS increases with an increase in the overall ion concentration, if either the bicarbonate concentration or SO_4 concentration increase, the TDS increases despite the SO_4 influences.

Therefore this study resulted in the following primary conclusions, (1) The water quality of the Vaal River varies geographically in three distinct groups, and this however ties in with (2) the controlling factors of Vaal River water chemistry, which also divides into the three groups. Geographically is can be concluded that the chemical weathering is an indication of the three different groups (Figure 4-12) with strong anthropogenic influences in the middle group. The water chemistry for the Vaal River is, as indicated, controlled by two processes, namely chemical weathering and anthropogenic influences. The prominent indication of the difference in these two influences can be seen between group 1 and group 2, as group 2 has more developed areas associated with the catchment than group 1.

A secondary conclusion from this study emerged with the introduction of the natural versus anthropogenic effect diagrams in section 4.5. The investigation indicated that TDS alone is not an accurate representation of anthropogenic influence (or poor water quality) on inorganic water quality of the Vaal River. The natural weathering, or geological influences, appears to play a more dominant role in certain sections or catchments throughout the Vaal River with lower contributions from anthropogenic influences (section 4.5). Thus, the background TDS could indicate high TDS concentrations, but not reflect anthropogenic influences in these catchments. When using TDS as an indication of water quality, cognisance should be taken of the surrounding area with regards to geology and the anthropogenic influences.

5.8 RECOMMENDATIONS

This study has focused on the inorganic water quality characterisation of the Vaal River. The inorganic characterisation of the Vaal River form this study can be used as

a comparison for future studies, as well as giving rise to a number of questions, all beyond the scope of this study. Most of these require detailed research in their own capacity and further studies will benefit the classification of the water quality of the Vaal River and South African surface water. All data used and diagrams completed for this study can be used as reference for further studies. Such studies or questions would include;

- Inorganic classification of individual tributaries of the catchment
- Industrial load influence in the catchment combined with the inorganic classification
- The practical contribution of various sources e.g. industrial, agricultural, sewage, etc. to the Vaal River inorganic quality; and
- The practical influence of the good quality water from the Lesotho Highlands and Tugela Transfer schemes to the Vaal River inorganic quality.

6 REFERENCES

AGRICULTURAL GEOREFERENCED INFORMATION SYSTEM (AGIS). Department of Agriculture, Forestry and Fisheries. Pretoria. Online: http://www.agis.agric.za [Date of access: 10 Jan. 2009].

AMIOTTE SUCHET, P., PROBST, J.L. and LUDWIG, W. 2003. Worldwide distribution of continental rock lithology: Implications for the atmospheric/soil CO2 uptake by continental weathering and alkalinity river transport to the oceans. *Global Biogeochem Cycles* 17:1038.

ASHTON, P.J. 2002. Avoiding Conflicts over Africa's Water Resources. *A Journal of the Human Environment* 31(3):236-242.

APPELO, C.A.J. and POSTMA, D. 1993. Geochemistry, Groundwater and Pollution. Rotterdam: Balkema Publishers.

BRAUNE, E. and ROGERS, K.H. 1987. The Vaal River catchment: Problems and research needs. Published in South African National Scientific Programmes (SANSP) Report no 143.

BLUTH, G.J.S. and KUMP, L.R. 1993. Lithologic and climatologic controls of river chemistry. *Geochimicaet Cosmochimica Acta.* 58 (10):2341-2359.

BLOWES, D.W., PTACEK, C.J., BENNER S.G., WAYBRANT, K.R. and BAIN, J.G. 1998. Permeable reactive barriers for the treatment of mine tailings drainage water. In: *MERKEL, B. and HELLING, C. Proceedings of International Conference and Workshop Uranium Mining and Hydrology vol. 2.* Freiberg: Germany.

CARTE BLANCHE. 2009. SA Water. Online: http://www.puresa.co.za/SAWater/CarteBlanche.aspx [Date of access: 2 Aug. 2012].

CORTECCI, G., DINELLI, E., BENCINI, A., ADORDNI-BRACCESI, A. and LA RUFFA, G. 2002. Natural and anthropogenic SO_4 sources in the Arno river catchment, northern Tuscany, Italy: a chemical and isotopic reconnaissance. *Applied Geochemistry* 17: 79 – 92.

DENNIS, I and DENNIS, R. 2012. Integrated water management course [Hand out correspondence].MSc and PhD Block Sessions, North-West University Potchefstroom.

DEPARTMENT OF WATER AFFAIRS AND FORESTRY (DWAF). 2009. Vaal River System: Large Bulk Water Supply Reconciliation Strategy. Report number P RSA C000/00/4406/09.

DEPARTMENT ENVIRONMENTAL AFFAIRS AND TOURISM (DEAT). 2007. South Africa Environmental Outlook; A report on the state of the environment.

DEPARTMENT OF WATER AFFAIRS[1] (DWA[1]). 2011. Orange River Basin. Online: http://www.dwa.gov.za/orange/intro.aspx [Date of access: 21 Apr. 2011].

DEPARTMENT OF WATER AFFAIRS[2] (DWA[2]). 2011. Department warns illegal water users. Media Release. Online: http://www.dwa.gov.za/ [Date of access: 21 Apr. 2011].

DEPARTMENT OF WATER AFFAIRS (DWA). 2013. Long-term Strategy for the Management of Acid Mine Drainage of the Witwatersrand. Online: http://www.dwa.gov.za/ [Date of access: 21 Sep. 2013].

DüRR, H.H., MEYBECK, M. and DüRR, S.H. 2005. Lithologic composition of the earth's continental surfaces derived from a new digital map emphasizing riverine material transfer. *Global Biogeochem Cycles* 19:GB4S10.

DREVER, J.I. 1997. The geochemistry of natural waters: surface and groundwater environments. Prentice-Hall: New Jersey.

EBY, G.N. 2004. Principles of Environmental Geochemistry. Thomson Brooks/Cola, Pacific Grove; California.

ESPANA, S.J., PAMO, E.L., SANTOFIMIA, E., ADUVIRE, O., REYES, J. and BARETTINO, D. 2005. Acid mine drainage in the Iberian Pyrite Belt (Odiel Riverwatershed, Huelva, SW Spain): Geochemistry, mineralogy and environmental implications. *Applied Geochemistry* 20: 1320-1356.

FLüGEL, WA. 1995. River Salination due to Dryland Agriculture in the Western Cape Province, Republic of South Africa. *Environment International* 21(5):679 - 686

GAILLARDET, J., DUPRE, B., LOUVAT, P. and ALLE'GRE, C.J. 1999. Global silicate weathering and CO consumption rates deduced from the chemistry of large rivers. *Chemical Geology* 159: 3-30.

GELDENHUIS, S. and BELL, F.G., 1998. Acid mine drainage at a coal mine in the eastern Transvaal, South Africa. *Environmental Geology* 34: 2/3

GIBBS, R.J. 1970. Mechanisms controlling world water chemistry. *Science, New series* 170 (3962): 1088-1090.

HEM, J.D. 1989. Study and Interpretation of the Chemical Characteristics of Natural Water. 5th Edition. United States Government: US Geological Survey.

HENDERSON, P. 1984. General geochemical properties and abundances of the rare earth elements. *In: P. Henderson (Editor), Rare Earth Element Geochemistry. Developments in Geochemistry* New York: Elsevier.

HERCOD, D.J., BRADY, P.V. and GREGORY, R.T. 1998. Catchment-scale coupling between pyrite oxidation and calcite weathering. *ChemGeol 151:259–276.*

HUIZENGA, J. M. 2011. Characterisation of the inorganic chemistry of surface waters in South Africa. *Water SA* 37: 401-410.

INTIERRARMG, 2013. Map - Mines and Mineral Deposits of Africa. IntierraRMG.

JIN, L., OGRINC, N., HAMILTON, S.K., SZRAMEK, K., KANDUCˇ, T. and WALTER, L.M. 2009. Inorganic carbon isotope systematics in soil profiles undergoing silicate and carbonate weathering (Southern Michigan, USA). *ChemGeol 264:139–153.*

KHAKIBOS. 2013. By 2014 Vaal River Will Be Polluted. Online: http://www.khakibos.co.za/by-2014-vaal-river-will-be-polluted/ [Date of access: 2 Jun. 2013].

KING, N. 2004.Chapter 9: The economic value of water in South Africa. In *Sustainable Options: Development lessons from applied environmental economics.* Cape Town: UCT Press.

LANGMUIR, D. 1997. Aqueous environmental geochemistry. Prentice-Hall: New Jersey.

LI, S., XU, Z., WANG, H., WANG, J. and ZHANG, Q. 2009. Geochemistry of the upper Han River basin, China 3: Anthropogenic inputs and chemical weathering to the dissolved load. *Chemical Geology.*264: 89-95.

LOTTERMOSER, B. 2010 Mine Wastes: Characterization, Treatment and Environmental Impacts, 3rd Edition. Springer: Heidelberg.

McCARTHY, T.S. 2011. The impact of acid mine drainage in South Africa. *South African Journal of Science* 107(5/6).

McCARTHY, T. and RUBIDGE, B. 2005. The Story of Earth and Life; A South African perspective on a 4.6-billion-year journey. Cape Town: Struik.

McGREGOR, R.G., BLOWES, D.W., JAMBOR, J.L, and ROBERTSON, W.D. 1998. The solid-phase controls on mobility of heavy metals at the copper cliff tailings area, Sudbury, Ontario, Canada. *Journal Contaminant Hydrology* 33: 247-271.

MEYBECK, M. 1987. Global chemical weathering of surficial rocks estimated from river dissolved loads. *Am J Sci 287:401–428.*

MOQUET, J-S., CRAVE, A., VIERS, J., SEYLER, P., ARMIJOS, E., BOURREL, L., CHAVARRI,E., LAGANE,C., LARAQUE, A., CASIMIRO, W.S.L., POMBOSA, R., NORIEGA, L., VERA, A. and GUYOT, J-P. 2011. Chemical weathering and atmospheric/soil CO2 uptake in the Andean and Foreland Amazon basins. *Chemical Geology 287: 1–26.*

NEWS 24. 2007. Pollution crisis at Vaal River. Online: http://www.news24.com/SciTech/News/Pollution-crisis-at-Vaal-River-20071120 [Date of access: 2 Aug. 2012].

O'KEEFE, J.H., UYS, M. And BRUTON, M.N. 1992. Freshwater Systems. In *FUGGLE, R.F. and RABIE, M.A. Environmental Management in South Africa.* Cape Town: Juta.

PACHECO, F.A.L, LANDIM, P.M.B and SZOCS, T. 2013. Anthropogenic impacts on mineral weathering: A statistical perspective. *Applied Geochemistry 36: 34–48.*

PLANT, J.D., SMITH, D., SMITH B. and WILLIAMS, D. 2001.Environmental geochemistry at global scale. *Applied Geochemistry* 16: 1291-1308.

RABIE, M.A and DAY, J.A. 2000. Rivers. *In FUGGLE, R.F. and RABIE, M.A.* 2000. *Environmental Management in South Africa. 3rd Edition.*Cape Town; Juta.

SAFE WATER DRINKING FOUNDATION (SWDF). 2009. Mining and Water Pollution. Online: http//:www.safewater.org [Date of access: 17Sep. 2011].

SINGER, P.C. and STUMM, W. 1970. Acid mine drainage: rate-determining step. *Science* 167: 1121-1123.

STIFF, H.A. Jr. 1951.The interpretation of chemical water analysis by means of patterns. *Journal of Petroleum Technology* 3: 15-17.

STUMM, W. and MORGAN, J.J. 1996. Aquatic Chemistry, Chemical Equilibrium in Natural Waters Third edition. Wiley: New York.

SZRAMEK ,K. and WALTER, L.M. 2004. Impact of carbonate precipitation on riverine inorganic carbon mass transport from a mid-continent, forested watershed. *Aquatic Geochem 10:99–137.*

SZRAMEK, K., WALTER, L.M., KANDUCˇ, T. and OGRINC, N. 2011.Dolomite Versus Calcite Weathering in Hydrogeochemically Diverse Watersheds Established on Bedded Carbonates (Sava and Socˇa Rivers, Slovenia). *AquatGeochem 17: 357–396.*

THE TIMES. 2012. Vaal River polluted by 2014.Online: http://news.howzit.msn.com/vaal-river-polluted-by-2014 [Date of access: 2 Aug 2012].

TUTU, H., McCARTHY, T.S. and CUKROWSKA, E. 2008. The chemical characteristics of acid mine drainage with particular reference to source, distribution and remediation: The Witwatersrand Basin, South Africa as a case study. *Applied Geology*23:3666-3684

WEBSTER, K.S., WEBSTER, J.G. and QUAADGRAS, N. 1994. The Adsorption of Cu, Pb and Zn onto Impure Iron Oxides. *Institute of Environmental Science and Research Ltd.*

WILLIAMS, E., SZRAMEK, K., JIN, L., KU, T.C.W. and WALTER, L.M. 2007. The carbonate system geochemistry of shallow groundwater/surface water systems in temperate glaciated watersheds (Michigan, USA): significance of open system dolomite weathering. *GeolSoc Am Bull 119:511–528.*

WOOD, A. 2013. Environmental Consultant, Personal communication. SRK Consulting. May 2013.

7 APPENDICES

Appendix 1 SAMPLING STATIONS AND DATA

TABLE 1: DETAILS OF THE FIFTEEN SAMPLE STATIONS ALONG THE VAAL RIVER (FROM EAST TO WEST) OBTAINED FROM DWA

Nr	Monitoring point name	Location	Latitude	Longitude	Number of samples	First sample date	Last sample date
1	C1H001	Vaal River	26.9424	29.2639	349	1975/10/13	1995/11/08
2	C1H002	Primary Tributary	27.1698	29.2333	1230	1974/01/06	2011/05/24
3	C1H004	Primary Tributary	26.6279	29.0245	1513	1975/10/02	2011/10/03
4	C1H007	Vaal River	26.8411	29.7234	1568	1974/01/16	2011/10/11
5	C1H008	Primary Tributary	26.8613	28.8846	1334	1975/11/24	2011/10/03
6	C1H010	Primary Tributary	27.0744	28.5653	232	1976/10/11	1997/09/11
7	C1H011	Vaal River	27.0194	28.6455	110	1976/09/27	1999/10/07
8	C1H012	Vaal River	27.0023	28.7653	1125	1985/11/04	2011/09/20
9	C1H015	Primary Tributary	27.1745	29.2357	443	1995/05/23	2011/10/10
10	C1H017	Vaal River	27.0231	28.5939	1147	1975/11/16	2011/08/03
11	C1H019	Vaal River	26.9216	29.2813	421	1979/10/23	2011/02/22
12	C1H020	Vaal River	26.8672	29.2178	928	1979/07/10	2011/09/15
13	C2H001	Primary Tributary	26.6443	27.0903	1387	1979/10/01	2011/06/30
14	C2H004	Primary Tributary	26.6708	28.0304	919	1984/03/22	2008/11/12
15	C2H005	Primary Tributary	26.7287	27.7180	1071	1984/03/08	2009/01/13
16	C2H007	Vaal River	27.0101	26.6981	1519	1979/05/29	2011/06/22
17	C2H008	Vaal River	26.7358	27.6083	627	1975/08/20	1997/03/06
18	C2H010	Vaal River	26.6897	27.9361	176	1993/10/04	1999/05/31
19	C2H014	Primary Tributary	26.8244	27.9255	438	1984/11/29	2006/11/10
20	C2H015	Primary Tributary	26.6438	27.9644	544	1984/03/08	1998/11/02
21	C2H018	Vaal River	26.9706	27.2097	1780	1973/01/01	2011/08/15
22	C2H021	Primary Tributary	26.4541	28.0855	357	1977/12/21	1999/05/17
23	C2H022	Vaal River	27.3978	26.5056	2714	1974/01/21	2011/05/26
24	C2H061	Vaal River	27.3897	26.4639	1661	1972/05/14	2011/10/20
25	C2H065	Primary Tributary	27.3700	26.3508	762	1972/02/23	2011/09/28
26	C2H070	Primary Tributary	26.6405	28.2300	372	1977/12/21	2008/05/10
27	C2H071	Primary Tributary	26.6199	27.9805	891	1985/08/08	1999/12/06
28	C2H073	Primary Tributary	26.9847	26.6323	1357	1980/03/31	2011/09/20

Nr	Monitoring point name	Location	Latitude	Longitude	Number of samples	First sample date	Last sample date
29	C2H084	Primary Tributary	26.8744	26.6583	447	1979/08/20	2011/04/05
30	C2H085	Primary Tributary	26.8805	26.9643	1342	1986/09/02	2011/08/25
31	C2H122	Vaal River	26.8535	28.1214	768	1982/05/30	2011/11/16
32	C2H136	Primary Tributary	26.4508	28.0893	172	1993/10/04	1999/05/17
33	C2H140	Vaal River	26.7383	27.5920	671	1996/05/01	2011/10/12
34	C2H141	Primary Tributary	26.4537	28.0858	689	1996/08/05	2011/09/26
35	C2H234	Primary Tributary	26.6941	28.1073	587	1998/12/14	2011/05/16
36	C3H003	Primary Tributary	27.5735	24.7460	401	1972/08/31	2011/02/08
37	C3H007	Primary Tributary	27.9032	24.6151	912	1972/09/04	2011/06/24
38	C3H013	Primary Tributary	28.1629	24.4707	721	1972/08/30	1998/07/02
39	C3H016	Primary Tributary	28.3865	24.2971	291	1993/01/14	2011/06/23
40	C4H004	Primary Tributary	27.9350	26.1244	899	1972/11/23	2011/07/27
41	C4H016	Primary Tributary	28.1172	26.7192	196	1995/11/03	2011/09/21
42	C4H017	Primary Tributary	28.1167	26.7253	143	1995/11/03	2011/08/23
43	C6H001	Primary Tributary	27.4414	26.9858	728	1980/01/07	2011/05/25
44	C6H002	Primary Tributary	27.3986	26.6133	852	1973/04/11	2011/11/17
45	C6H003	Primary Tributary	27.4000	26.6256	494	1974/01/21	2010/11/10
46	C6H007	Primary Tributary	27.6714	27.2369	759	1995/04/04	2011/11/17
47	C7H006	Primary Tributary	27.0463	27.0046	703	1978/08/07	2011/06/23
48	C8H001	Primary Tributary	27.2717	28.4911	1447	1974/01/15	2011/10/05
49	C8H004	Primary Tributary	27.7005	28.3214	583	1975/11/20	2010/11/03
50	C8H005	Primary Tributary	28.3758	28.8603	676	1975/11/21	2011/12/07
51	C8H007	Primary Tributary	28.1910	28.3439	118	1975/11/19	1996/11/21
52	C8H011	Primary Tributary	28.1613	28.8744	1282	1975/11/21	2011/10/05
53	C8H012	Primary Tributary	28.0850	28.8369	346	1978/10/12	2011/07/14
54	C8H014	Primary Tributary	27.8149	28.7831	349	1975/11/20	1992/11/03
55	C8H020	Primary Tributary	27.6897	28.3750	755	1978/01/01	2011/09/15
56	C8H022	Primary Tributary	27.2986	28.4958	393	1979/04/30	2011/06/01
57	C8H023	Primary Tributary	28.0231	28.9947	1060	1978/11/02	2011/06/07
58	C8H026	Primary Tributary	27.4308	28.5264	1085	1985/03/21	2011/04/20

Nr	Monitoring point name	Location	Latitude	Longitude	Number of samples	First sample date	Last sample date
59	C8H027	Primary Tributary	27.3014	28.5856	1202	1985/03/21	2011/08/03
60	C8H028	Primary Tributary	27.8028	28.7675	486	1993/01/05	2011/08/02
61	C9H008	Vaal River	28.1146	24.9149	705	1972/11/23	2011/01/20
62	C9H009	Vaal River	28.5162	24.6007	763	1972/11/24	2009/01/22
63	C9H010	Vaal River	28.4062	24.2712	547	1975/09/08	2010/10/28
64	C9H021	Vaal River	27.6696	25.6177	1596	1972/11/23	2011/08/11
65	C9H024	Vaal River	28.7115	24.0729	176	1995/06/01	2009/01/08

TABLE 2: Data for Monitoring Stations

Nr	Station Name	TDS mg/l	Na/ (Na+ Ca)	[Ca]/ [Na]	[HCO3]/ [Na]	Log [Mg]/ [H]2	Log [Ca]/ [H]2	Log [Na]/ [H]	Log [K]/ [H]	Log [Si]	Weath- ering	SO4 cont.	Cl cont.	Na mg/l	K mg/l	Mg mg/l	Ca mg/l	HCO3 mg/l	SO4 mg/l	Cl mg/l
1	C1H001	78.69	0.06	0.31	1.21	0.90	0.886	0.477	0.464	0.86	12.29	6.74	6.75	4.72	0.91	5.47	7.08	50.44	7.39	4.54
2	C1H002	111.38	0.08	0.21	0.81	1.16	1.13	0.63	0.00	0.00	10.04	7.07	5.35	10.34	0.97	6.72	10.08	69.99	12.14	12.94
3	C1H004	234.08	0.08	0.12	0.48	1.06	1.07	0.59	0.57	0.00	12.10	8.42	9.62	50.68	3.34	5.65	13.26	46.43	68.45	61.14
4	C1H007	90.27	0.06	0.92	3.06	1.03	1.02	0.58	0.50	0.00	9.06	7.14	4.50	8.76	0.89	5.53	7.69	45.84	16.53	7.00
5	C1H008	183.66	0.07	0.12	0.48	1.28	1.28	0.73	0.66	0.00	10.60	7.90	7.33	30.53	2.11	6.82	12.54	60.97	48.60	31.03
6	C1H010	140.56	0.08	0.17	0.76	1.48	1.46	0.78	0.61	0.21	11.66	6.36	8.49	11.01	1.08	10.66	12.72	92.86	11.25	12.22
7	C1H011	103.97	0.08	0.23	1.06	0.93	0.92	0.57	0.45	0.21	14.16	6.37	9.26	16.79	1.49	5.39	8.75	51.49	18.62	20.06
8	C1H012	107.23	0.05	0.13	0.55	1.11	1.09	0.60	0.49	0.00	7.34	5.44	4.46	10.89	0.81	6.49	8.18	59.22	11.02	11.23
9	C1H015	109.01	0.06	0.21	0.72	0.78	0.76	0.44	0.35	0.00	7.96	5.83	3.02	6.89	0.78	6.33	8.65	64.65	6.34	3.53
10	C1H017	114.39	0.07	0.15	0.65	1.02	1.00	0.57	0.46	0.00	8.49	5.73	5.07	14.83	1.18	6.48	9.02	58.60	18.75	11.71
11	C1H019	29.49	0.05	0.16	0.56	0.86	0.84	0.45	0.40	0.33	4.98	4.29	3.30	2.86	0.44	2.12	2.78	18.41	6.13	2.30
12	C1H020	44.38	0.04	0.14	0.48	0.78	0.78	0.41	0.37	0.34	4.37	3.54	3.61	2.41	0.41	1.62	2.24	14.55	5.16	2.84
13	C2H001	128.19	0.06	0.62	2.31	0.66	0.66	0.33	0.35	0.13	7.44	5.99	2.42	5.36	1.10	6.38	8.87	50.84	23.61	6.59
14	C2H004	460.35	0.09	0.19	50.11	1.00	1.02	0.59	0.52	1.31	9.51	14.46	8.60	54.89	4.54	22.56	62.88	60.47	257.01	56.07
15	C2H005	246.69	0.09	0.27	0.32	0.81	0.82	0.45	0.45	1.04	8.65	12.71	7.62	39.62	5.23	7.24	33.24	30.29	144.40	39.28
16	C2H007	217.80	0.05	0.25	0.86	1.12	1.11	0.63	0.61	0.54	9.86	9.13	3.74	22.71	3.35	10.45	22.52	32.69	93.00	24.49
17	C2H008	270.34	0.07	0.25	0.47	1.16	1.16	0.66	0.66	0.62	12.63	13.22	4.60	38.37	5.18	8.81	36.83	34.91	148.44	36.67
18	C2H010	195.81	0.04	0.44	0.78	0.62	0.63	0.42	0.35	1.66	11.66	10.01	6.32	17.64	3.31	6.67	18.34	26.06	72.71	25.56
19	C2H014	304.34	0.15	0.32	1.67	1.28	1.28	0.85	0.58	0.97	16.33	14.61	11.62	70.21	2.37	9.48	26.65	111.05	95.69	55.41
20	C2H015	175.92	0.06	0.16	0.21	0.99	0.99	0.52	0.52	0.21	7.69	10.23	4.00	21.41	2.98	7.15	23.15	28.73	96.90	24.75
21	C2H018	220.12	0.05	0.13	0.60	1.19	1.20	0.67	0.69	1.19	11.71	9.82	4.06	22.95	4.03	7.33	20.45	33.15	78.13	24.09
22	C2H021	222.55	0.06	0.16	0.19	0.77	0.77	0.41	0.44	0.96	7.26	10.59	4.78	19.48	3.22	10.43	26.84	24.81	114.88	19.82
23	C2H022	204.63	0.06	0.16	0.58	0.96	0.94	0.56	0.52	0.71	13.02	11.93	4.89	23.70	3.18	13.20	19.98	32.15	102.29	23.22
24	C2H061	225.74	0.06	0.15	0.56	1.18	1.18	0.67	0.65	1.04	12.23	10.24	4.45	23.83	3.59	10.79	19.42	34.44	86.91	26.56
25	C2H065	194.43	0.10	0.26	0.78	1.21	1.13	0.71	0.53	1.44	8.89	7.16	6.24	19.37	1.34	9.07	12.92	92.66	24.65	16.64
26	C2H070	390.68	0.10	0.18	0.34	1.29	1.33	0.74	0.71	1.23	9.44	11.09	8.07	70.09	5.05	16.35	41.30	61.21	173.74	83.67
27	C2H071	148.85	0.06	0.16	0.20	0.67	0.66	0.35	0.37	0.83	7.56	10.32	4.23	15.22	2.89	6.31	18.80	27.84	82.24	16.95
28	C2H073	318.37	0.10	0.39	1.86	0.78	0.78	0.51	0.48	0.24	19.61	13.22	7.14	42.87	7.67	12.81	30.41	50.23	132.46	52.40
29	C2H084	134.56	0.09	0.75	3.69	1.03	0.99	0.54	0.52	0.31	13.82	9.96	5.56	12.16	1.88	10.34	12.64	66.43	45.67	16.78
30	C2H085	160.45	12.19	12.18	12.15	11.93	11.93	12.06	12.09	12.33	12.11	12.23	12.36	16.90	12.35	13.85	14.79	49.17	37.45	19.10

Nr	Station Name	TDS mg/l	Na/ (Na+ Ca)	[Ca]/ [Na]	[HCO3]/ [Na]	Log [Mg]/ [H]2	Log [Ca]/ [H]2	Log [Na]/ [H]	Log [K]/ [H]	Log [Si]	Weath- ering	SO4 cont.	Cl cont.	Na mg/l	K mg/l	Mg mg/l	Ca mg/l	HCO3 mg/l	SO4 mg/l	Cl mg/l
31	C2H122	44.18	0.05	0.16	0.59	1.06	1.06	0.56	0.51	0.42	5.73	5.22	4.63	3.44	0.49	1.77	3.06	20.16	6.59	2.85
32	C2H136	260.51	0.07	0.54	0.38	0.54	0.54	0.32	0.28	1.61	6.03	12.39	7.31	17.63	2.71	10.05	22.66	26.29	114.29	25.62
33	C2H140	191.86	0.04	0.10	0.44	0.77	0.78	0.47	0.43	0.40	8.77	6.66	3.47	18.41	3.09	5.77	16.01	25.82	53.75	20.10
34	C2H141	176.05	0.06	0.16	0.16	0.56	0.55	0.30	0.30	0.16	5.22	7.82	3.64	11.75	2.78	4.66	11.70	23.88	42.41	11.78
35	C2H234	521.94	0.05	0.10	0.28	0.69	0.70	0.45	0.35	0.43	8.14	9.26	2.40	52.98	3.36	18.63	49.01	53.79	218.03	44.35
36	C3H003	273.00	0.13	0.33	0.87	1.10	1.02	0.68	0.54	1.21	14.70	13.02	5.92	44.24	3.03	14.53	10.99	75.60	76.31	39.82
37	C3H007	312.59	0.07	0.15	0.49	1.01	0.98	0.59	0.50	0.65	9.73	8.90	4.29	33.88	1.81	18.22	19.41	50.56	106.04	48.82
38	C3H013	401.87	0.07	0.18	0.55	0.79	0.76	0.44	0.40	1.73	12.41	9.85	4.83	43.39	2.08	18.41	11.62	43.22	113.85	60.81
39	C3H016	334.73	0.06	0.08	0.21	0.55	0.51	0.32	0.28	0.52	5.69	4.42	4.98	50.50	2.06	20.42	10.01	28.93	103.06	68.69
40	C4H004	213.02	0.06	0.88	2.44	1.21	1.20	0.69	0.59	0.44	18.85	8.04	13.39	28.90	1.52	8.18	17.16	36.25	43.01	60.00
41	C4H016	435.35	0.05	0.08	0.30	0.91	0.90	0.53	0.47	0.38	10.09	4.30	8.97	68.19	5.33	17.14	32.79	54.64	84.07	136.77
42	C4H017	566.03	0.06	0.11	0.48	0.74	0.72	0.50	0.52	0.46	14.20	5.75	15.15	81.59	4.45	31.40	55.35	60.85	83.77	276.62
43	C6H001	187.16	0.10	0.17	0.62	1.28	1.25	0.78	0.67	0.44	9.46	4.96	8.70	28.37	3.74	6.12	10.69	75.04	14.48	28.05
44	C6H002	247.35	0.09	0.21	0.72	1.30	1.27	0.79	0.68	0.53	12.30	8.43	6.75	34.48	5.11	11.80	16.81	84.54	55.73	37.55
45	C6H003	265.76	0.08	0.18	0.70	1.26	1.22	0.77	0.66	0.89	12.61	7.11	7.36	37.96	4.46	12.58	18.32	81.64	56.10	43.19
46	C6H007	109.96	0.06	0.13	0.41	0.75	0.74	0.45	0.35	0.27	5.95	5.18	3.15	9.58	1.17	4.14	7.01	47.62	10.77	6.18
47	C7H006	103.45	0.07	0.36	1.52	1.17	1.17	0.67	0.55	0.22	9.40	7.80	5.75	10.71	1.18	5.25	9.12	53.17	16.55	10.03
48	C8H001	101.15	0.10	1.70	4.27	1.06	1.06	0.59	0.51	0.45	9.59	7.21	5.62	6.90	1.24	7.07	10.44	55.42	13.58	7.23
49	C8H004	117.10	0.07	0.21	0.70	1.22	1.22	0.68	0.58	0.62	9.05	5.95	6.55	13.80	1.70	4.66	10.51	66.40	7.79	12.09
50	C8H005	80.95	0.09	1.04	2.82	1.12	1.12	0.67	0.65	1.11	11.95	7.43	7.38	7.98	1.79	3.98	8.99	35.69	15.50	9.79
51	C8H007	165.52	0.08	0.23	0.67	0.63	0.64	0.39	0.26	1.53	5.24	5.05	2.48	10.47	1.33	5.25	16.70	94.18	5.39	3.94
52	C8H011	92.57	0.06	0.32	1.03	1.09	1.07	0.62	0.55	0.35	9.19	6.28	4.99	6.12	1.23	4.72	9.41	55.95	4.77	5.63
53	C8H012	106.58	0.06	0.10	0.36	1.17	1.17	0.64	0.52	0.25	8.22	6.28	4.32	15.15	1.25	3.28	6.90	62.99	8.97	5.44
54	C8H014	122.73	18.50	18.49	18.40	18.14	18.13	18.31	18.36	18.73	19.61	19.83	19.21	23.99	18.42	18.75	20.08	78.08	19.66	18.97
55	C8H020	76.56	0.13	4.36	14.27	0.82	0.81	0.61	0.53	0.14	6.61	5.19	3.67	9.29	1.85	2.77	5.69	41.62	6.91	4.39
56	C8H022	52.75	0.11	1.04	3.23	0.99	1.01	0.50	0.47	1.72	7.91	6.48	3.56	4.28	1.17	2.38	4.61	28.63	5.76	2.36
57	C8H023	86.39	0.06	0.16	0.58	1.25	1.21	0.66	0.54	0.21	11.16	8.94	5.81	8.54	1.42	3.68	7.88	52.35	6.50	4.85
58	C8H026	110.26	0.14	3.27	9.55	0.93	0.90	0.68	0.60	0.11	7.37	5.87	4.33	11.40	2.23	5.43	9.26	66.07	8.05	6.46
59	C8H027	98.49	0.07	0.29	0.98	1.17	1.14	0.66	0.53	0.23	8.07	6.20	4.90	7.38	0.74	5.50	9.67	60.90	6.68	4.65
60	C8H028	90.51	0.07	0.25	0.86	1.00	0.97	0.60	0.47	1.78	7.64	6.47	3.65	7.70	1.11	4.36	8.22	51.55	4.76	5.79

Nr	Station Name	TDS mg/l	Na/ (Na+ Ca)	[Ca]/ [Na]	[HCO3]/ [Na]	Log [Mg]/ [H]2	Log [Ca]/ [H]2	Log [Na]/ [H]	Log [K]/ [H]	Log [Si]	Weath- ering	SO4 cont.	Cl cont.	Na mg/l	K mg/l	Mg mg/l	Ca mg/l	HCO3 mg/l	SO4 mg/l	Cl mg/l
61	C9H008	154.66	0.06	0.17	0.59	0.90	0.88	0.53	0.51	0.77	11.22	8.20	4.41	19.27	3.13	6.98	11.79	21.77	54.49	21.04
62	C9H009	198.85	0.08	0.19	0.66	0.97	0.93	0.57	0.54	1.72	13.56	9.02	5.67	24.54	3.36	8.95	10.04	21.81	63.00	28.79
63	C9H010	127.07	0.08	0.19	0.54	1.00	0.97	0.56	0.56	0.75	11.03	9.08	4.78	20.88	3.07	8.56	6.84	32.27	53.72	26.94
64	C9H021	147.89	0.06	0.15	0.60	0.98	0.98	0.55	0.54	0.90	13.11	9.63	5.39	17.17	2.68	7.54	13.14	21.61	60.89	20.04
65	C9H024	186.41	0.11	0.18	0.49	0.47	0.45	0.31	0.26	0.44	10.42	5.17	6.62	34.05	3.06	13.37	6.91	21.57	69.74	42.58

Appendix 2 SURFACE WATER MONITORING MAPS AND DIAGRAMS

Catchment C1

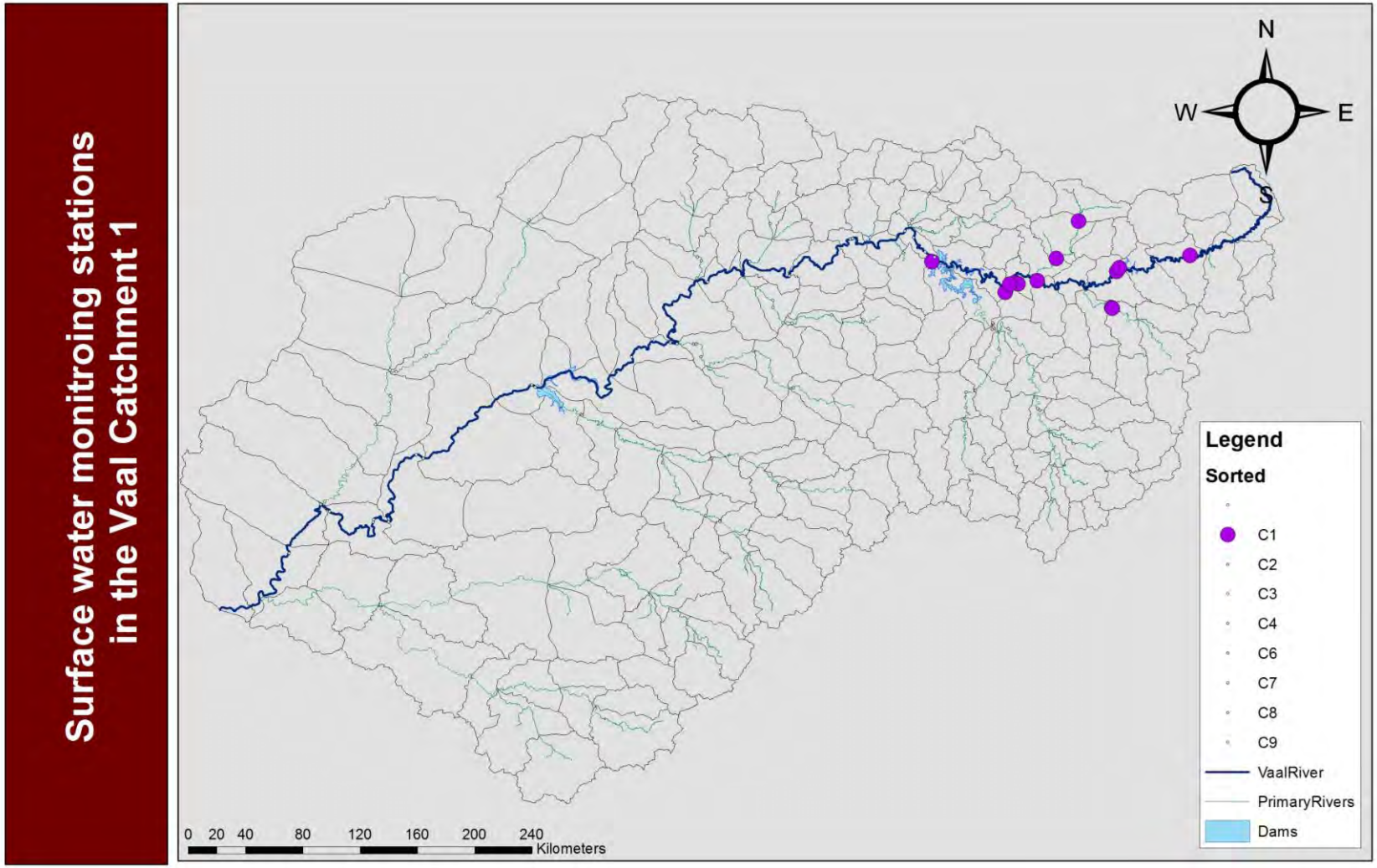

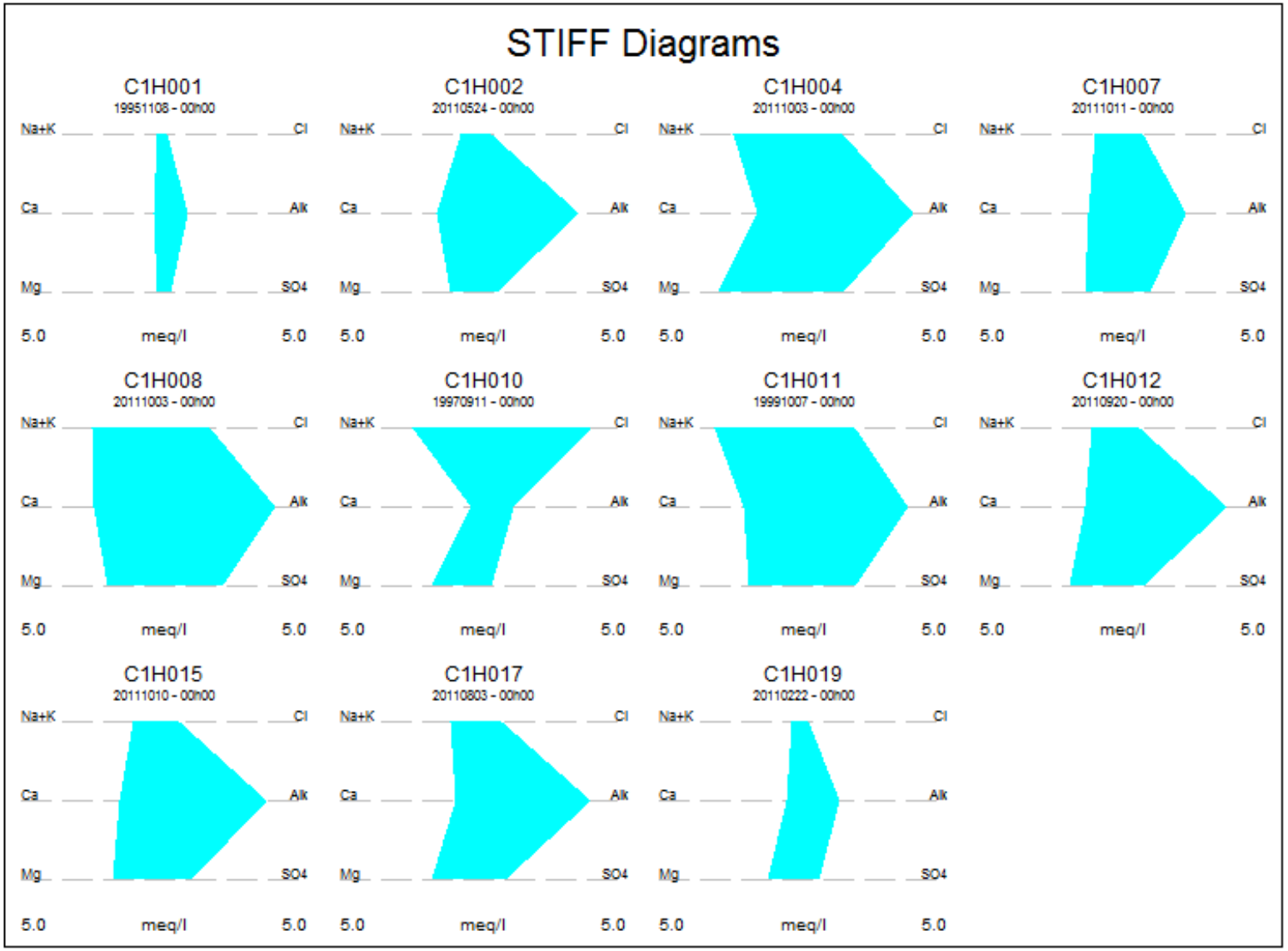
STIFF Diagrams
C1H001
19951108 - 00h00
C1H002
20110524 - 00h00
C1H004
20111003 - 00h00
C1H007
20111011 - 00h00
C1H008
20111003 - 00h00
C1H010
19970911 - 00h00
C1H011
19991007 - 00h00
C1H012
20110920 - 00h00
C1H015
20111010 - 00h00
C1H017
20110803 - 00h00
C1H019
20110222 - 00h00
Na+K
Cl
Ca
Alk
Mg
SO4
5.0
meq/l
5.0

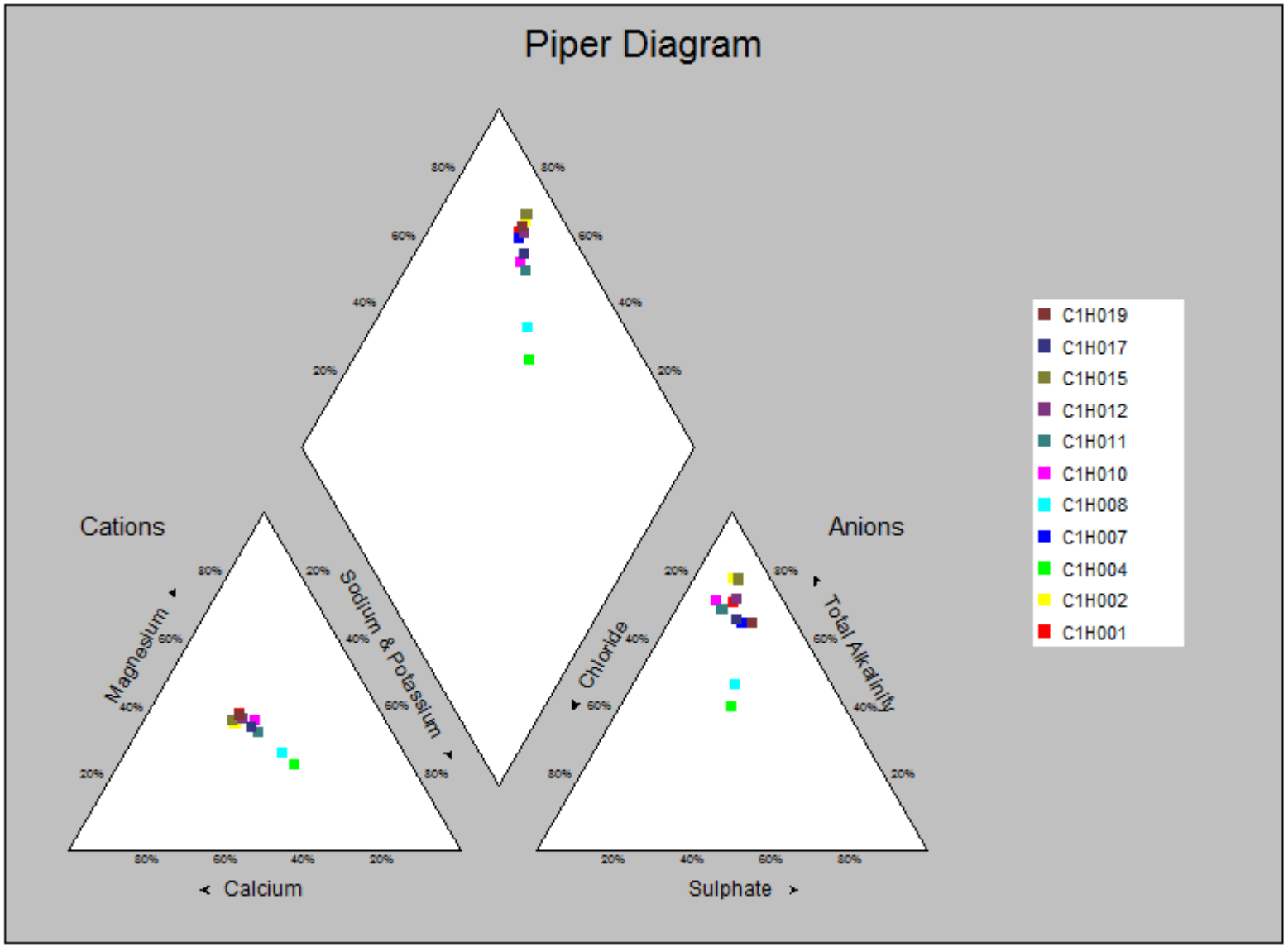
Piper Diagram
Cations
Anions
Magnesium
Sodium & Potassium
Chloride
Total Alkalinity
Calcium
Sulphate
80%
60%
40%
20%
C1H019
C1H017
C1H015
C1H012
C1H011
C1H010
C1H008
C1H007
C1H004
C1H002
C1H001

Catchment C2

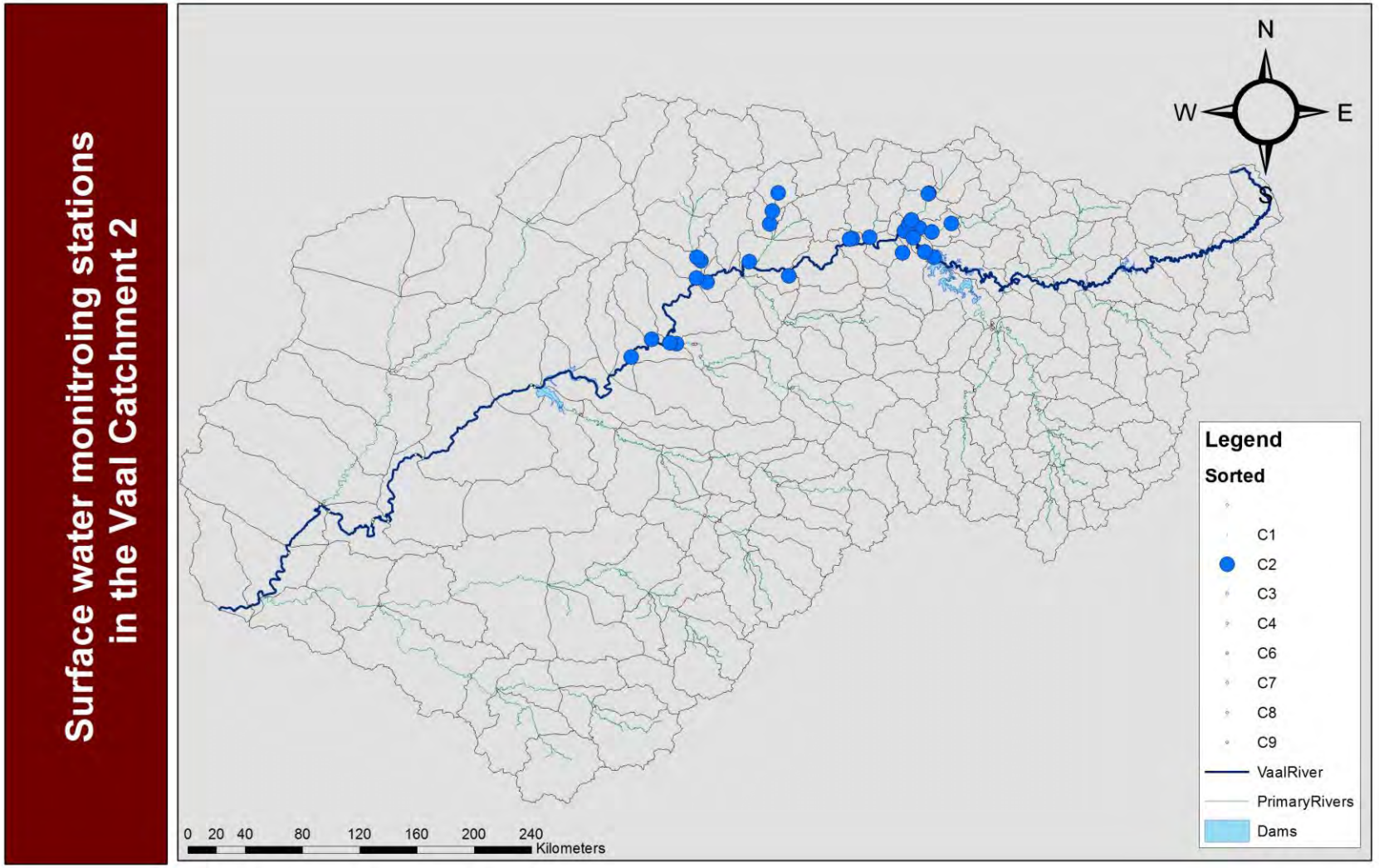

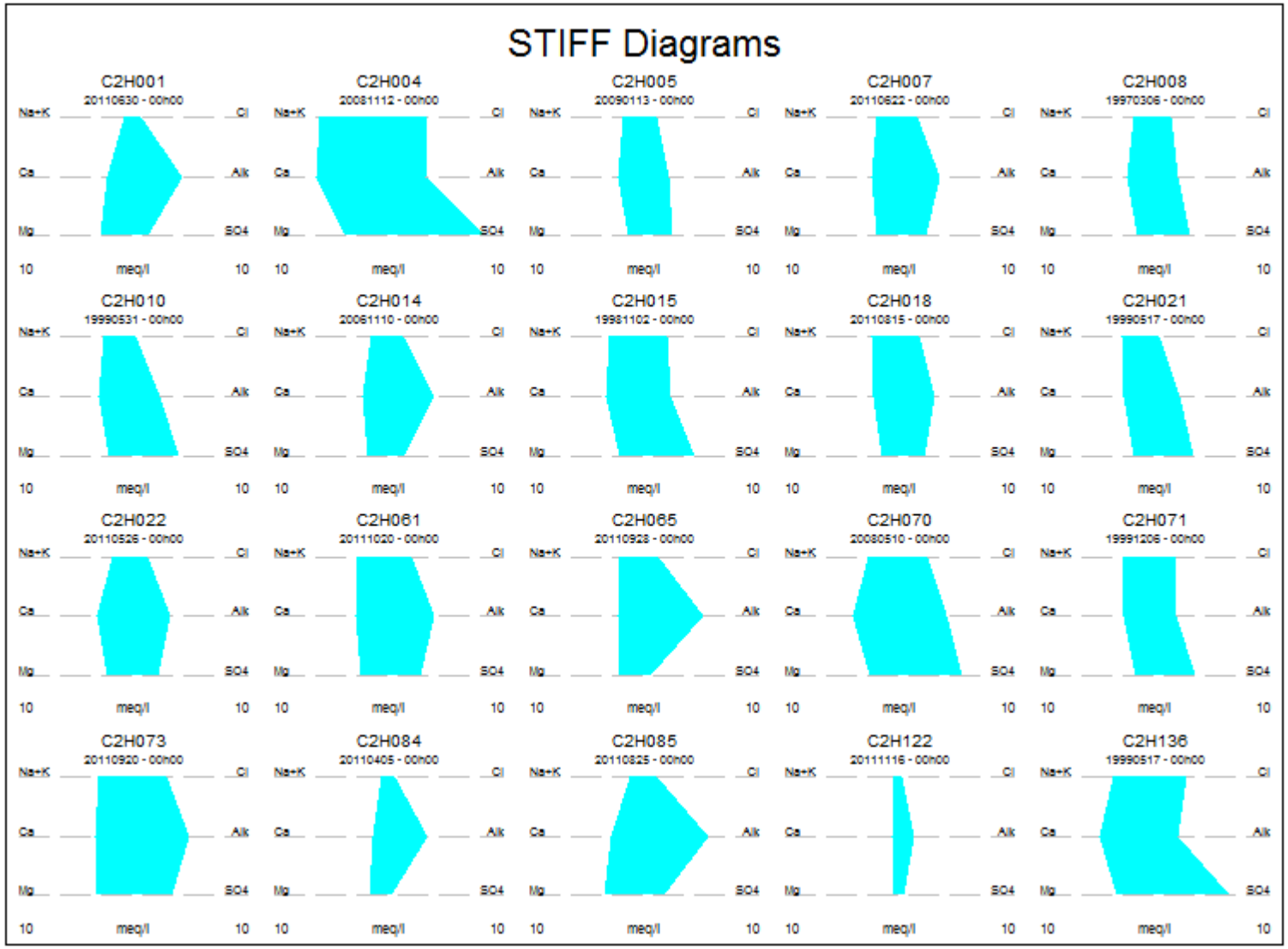
STIFF Diagrams
C2H001
20110630 - 00h00
C2H004
20081112 - 00h00
C2H005
20090113 - 00h00
C2H007
20110622 - 00h00
C2H008
19970306 - 00h00
C2H010
19990531 - 00h00
C2H014
20061110 - 00h00
C2H015
19981102 - 00h00
C2H018
20110815 - 00h00
C2H021
19990517 - 00h00
C2H022
20110526 - 00h00
C2H061
20111020 - 00h00
C2H065
20110928 - 00h00
C2H070
20080510 - 00h00
C2H071
19991206 - 00h00
C2H073
20110920 - 00h00
C2H084
20110405 - 00h00
C2H085
20110825 - 00h00
C2H122
20111116 - 00h00
C2H136
19990517 - 00h00
Na+K
Ca
Mg
Cl
Alk
SO4
10
meq/l

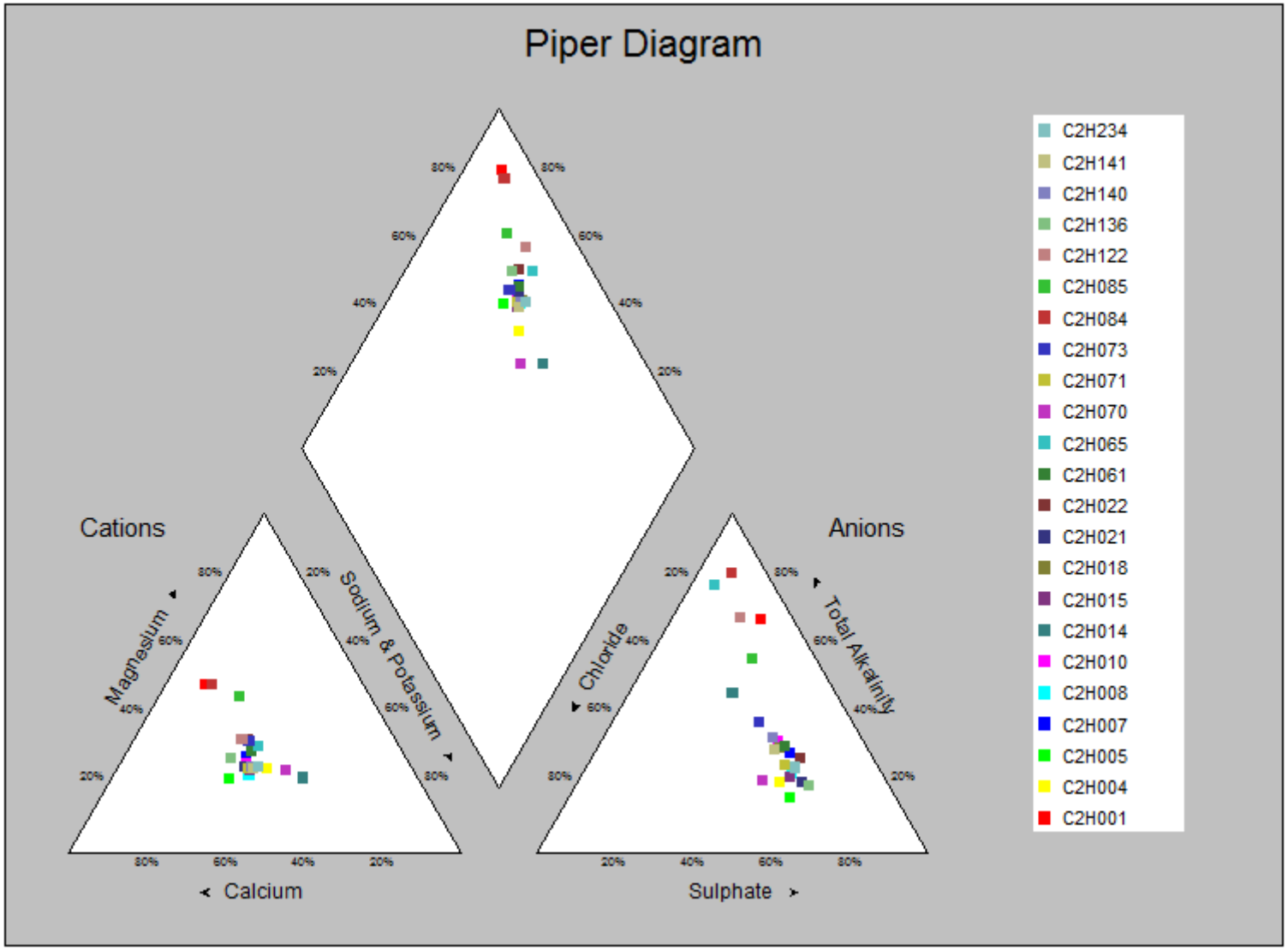
Piper Diagram
Cations
Anions
Magnesium
Sodium & Potassium
Chloride
Total Alkalinity
Calcium
Sulphate
80%
60%
40%
20%
C2H234
C2H141
C2H140
C2H136
C2H122
C2H085
C2H084
C2H073
C2H071
C2H070
C2H065
C2H061
C2H022
C2H021
C2H018
C2H015
C2H014
C2H010
C2H008
C2H007
C2H005
C2H004
C2H001

Catchment C3 + 4

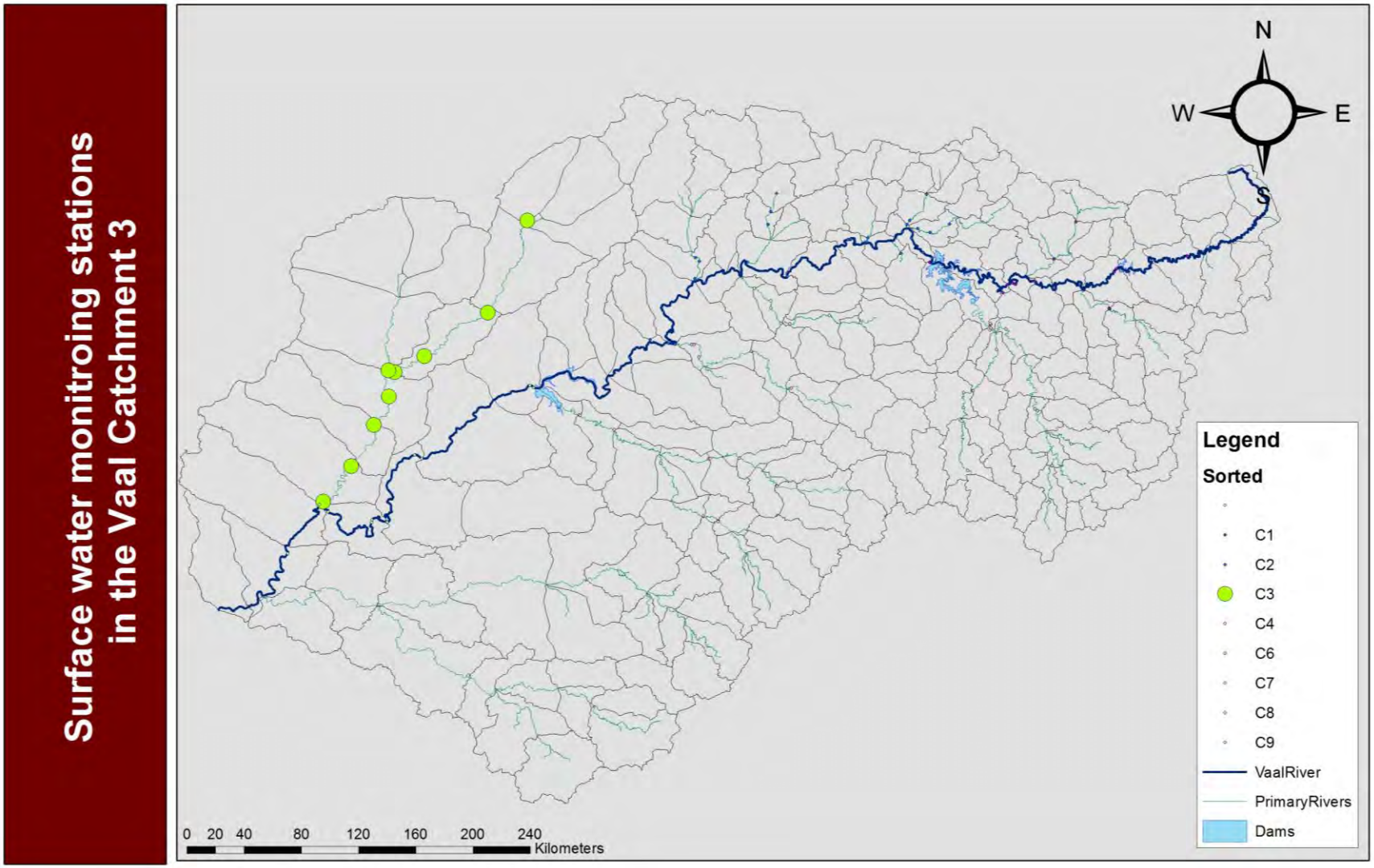

Surface water monitroing stations in the Vaal Catchment 4

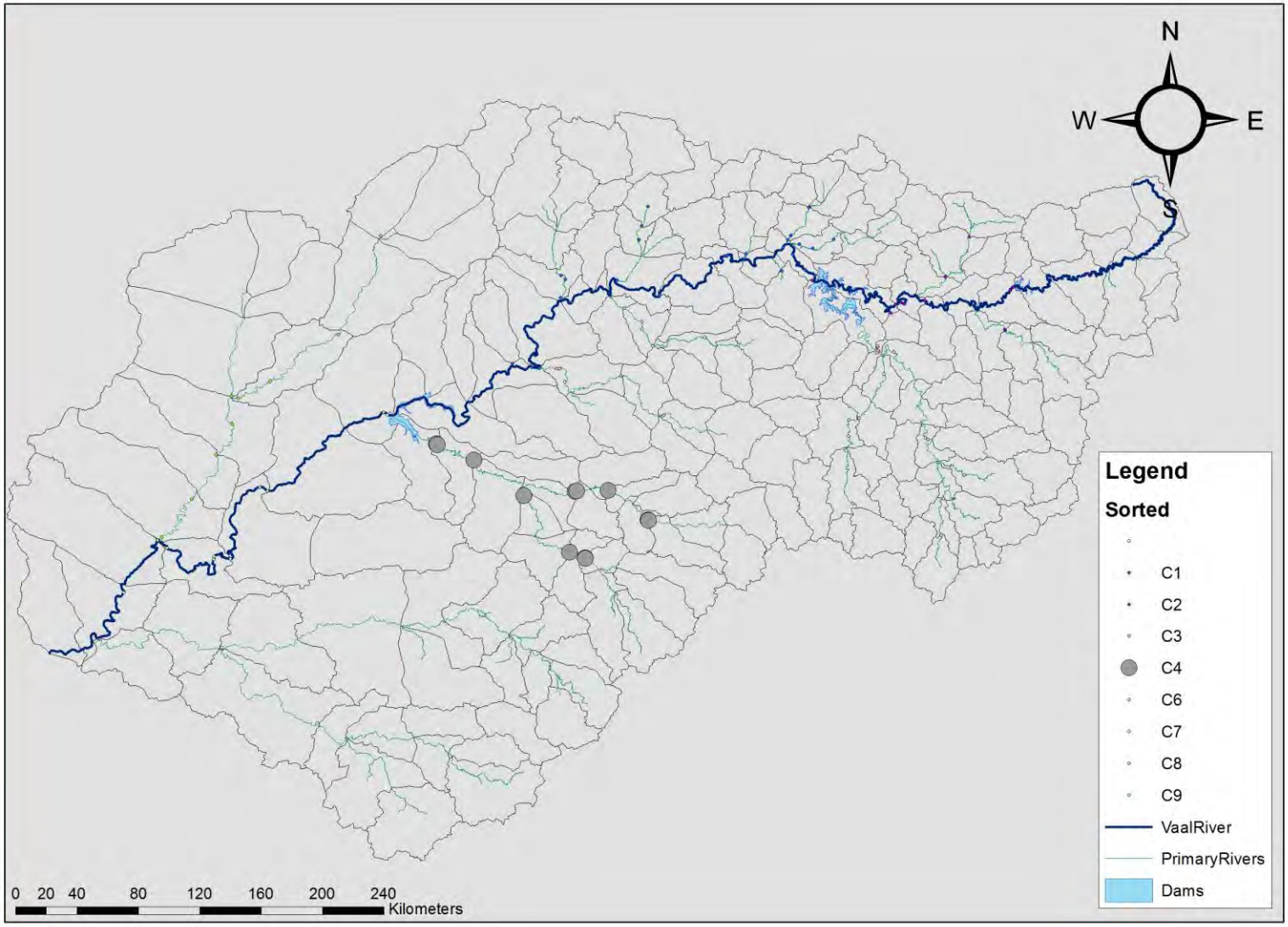

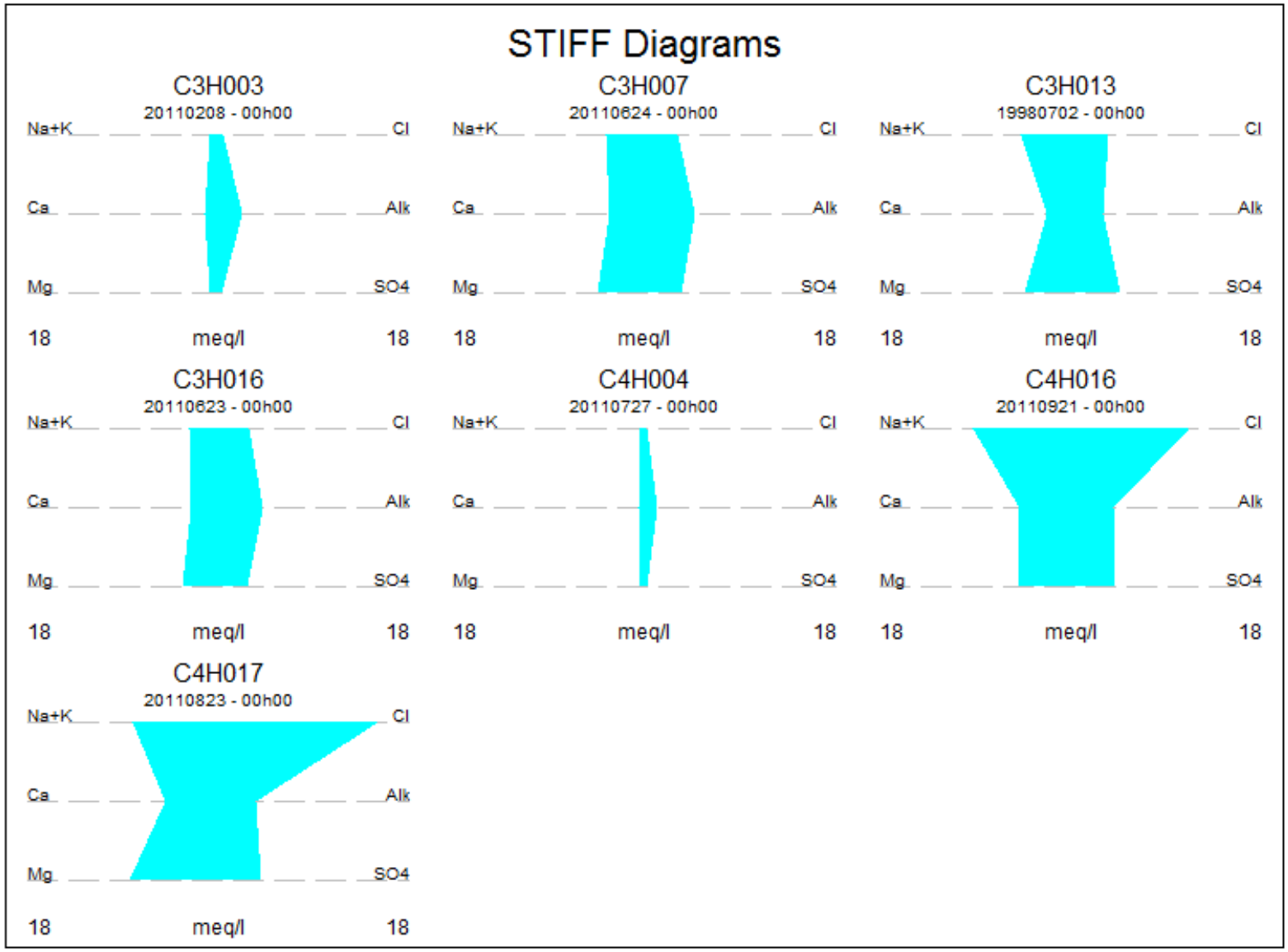
STIFF Diagrams
C3H003
20110208 - 00h00
C3H007
20110624 - 00h00
C3H013
19980702 - 00h00
C3H016
20110623 - 00h00
C4H004
20110727 - 00h00
C4H016
20110921 - 00h00
C4H017
20110823 - 00h00
Na+K
Cl
Ca
Alk
Mg
SO4
18
meq/l
18

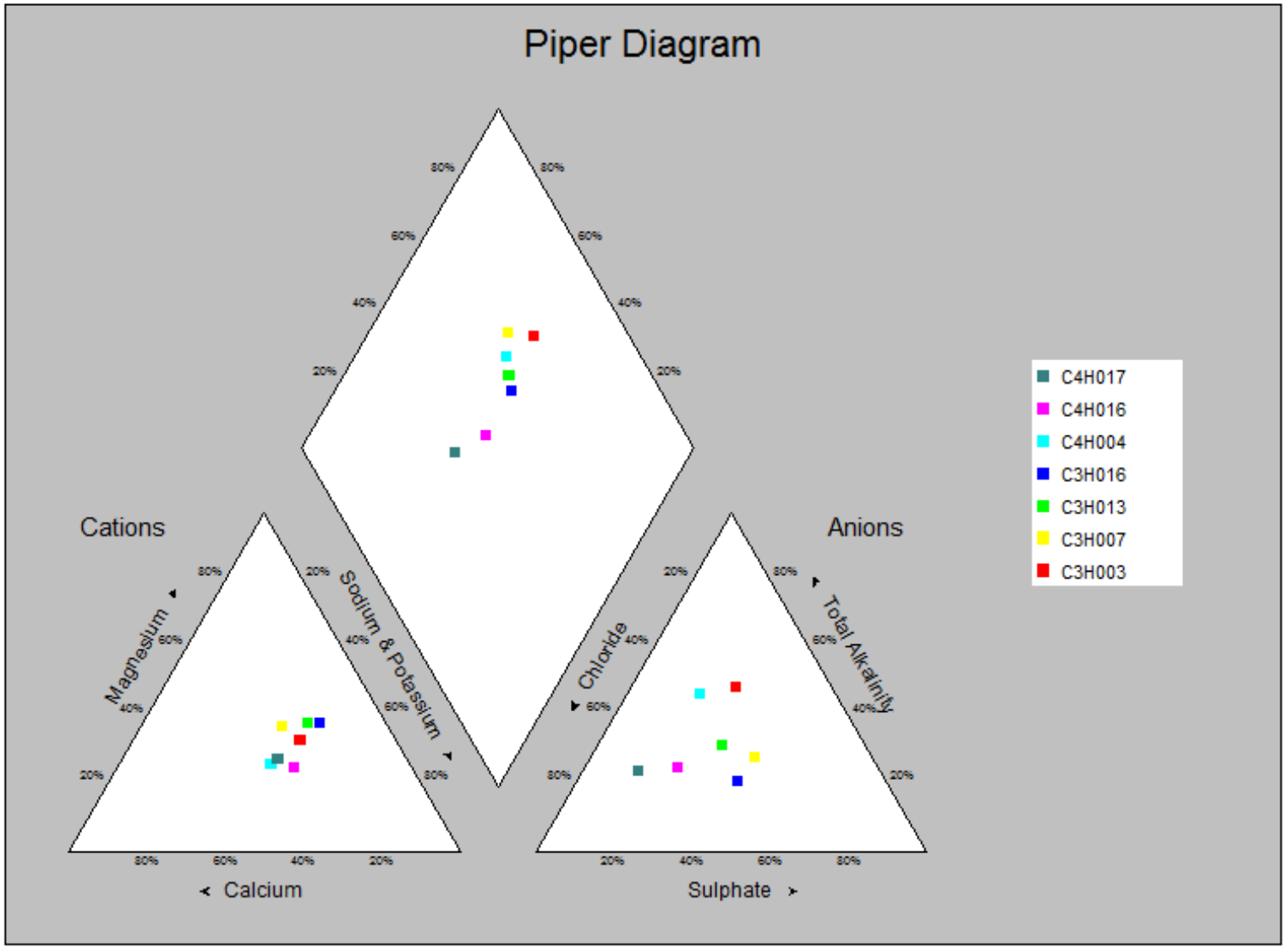
Piper Diagram
Cations
Anions
Magnesium
Sodium & Potassium
Calcium
Chloride
Total Alkalinity
Sulphate
80%
60%
40%
20%
C4H017
C4H016
C4H004
C3H016
C3H013
C3H007
C3H003

Catchment C6 +7

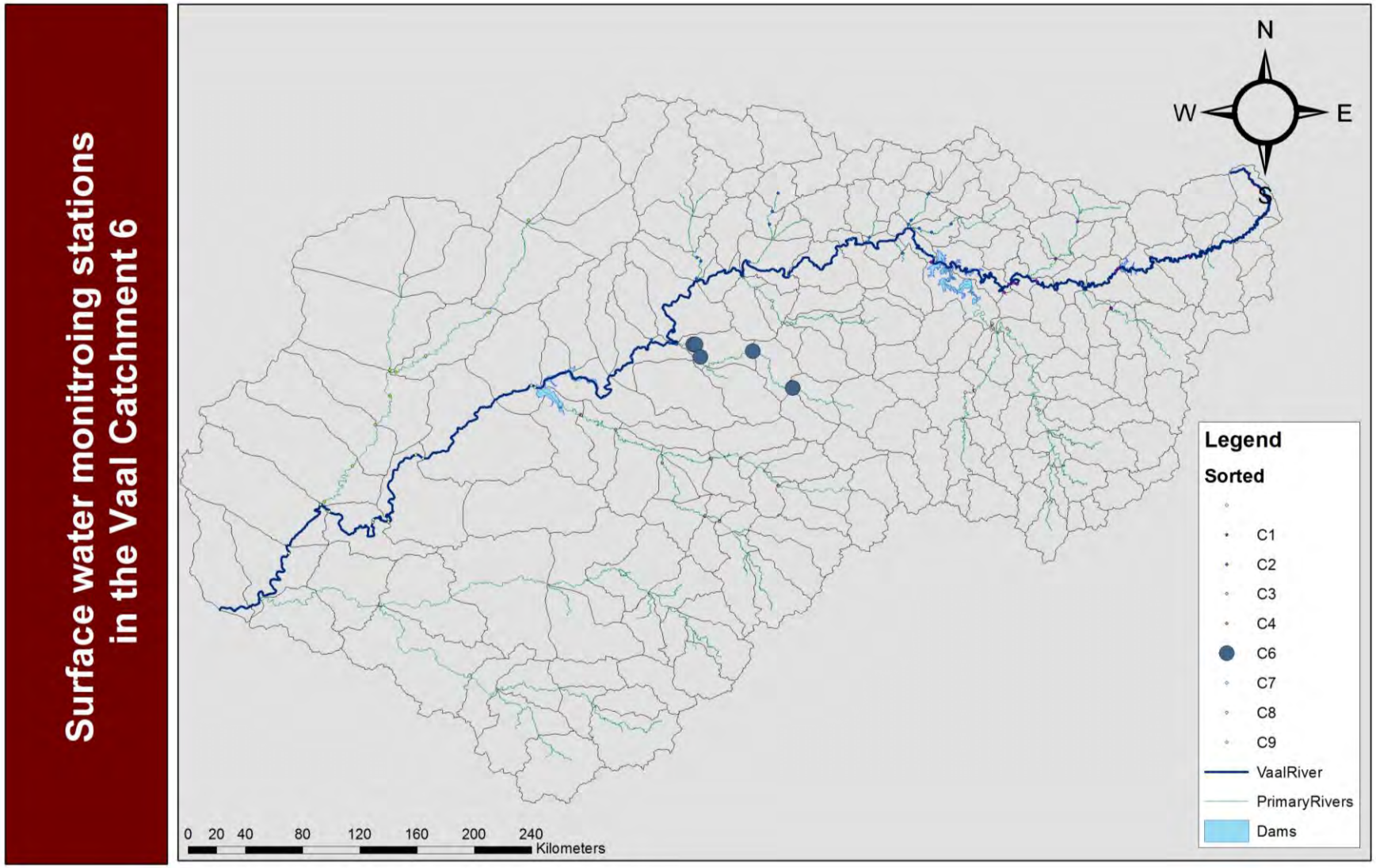

Surface water monitroing stations in the Vaal Catchment 7

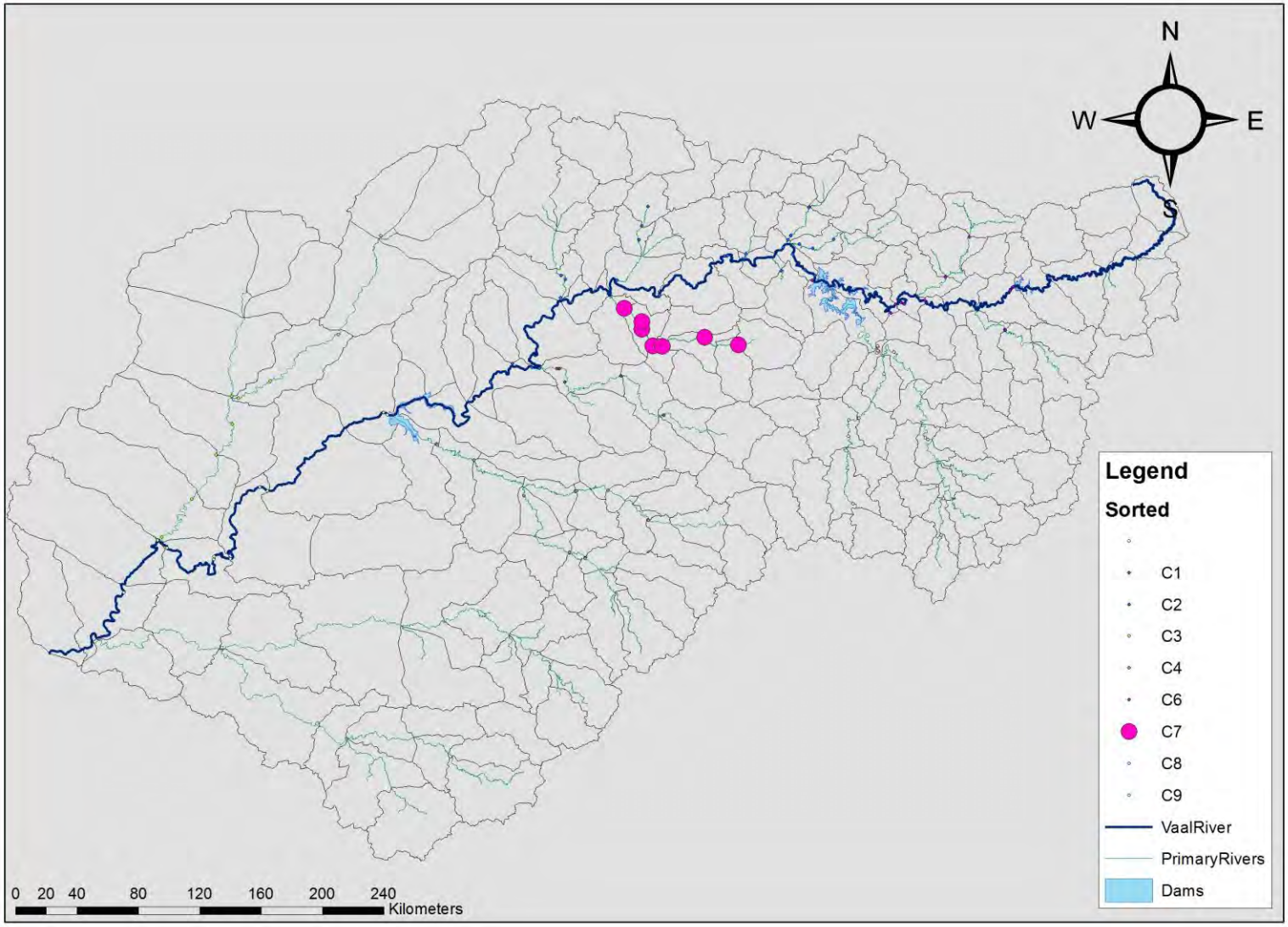

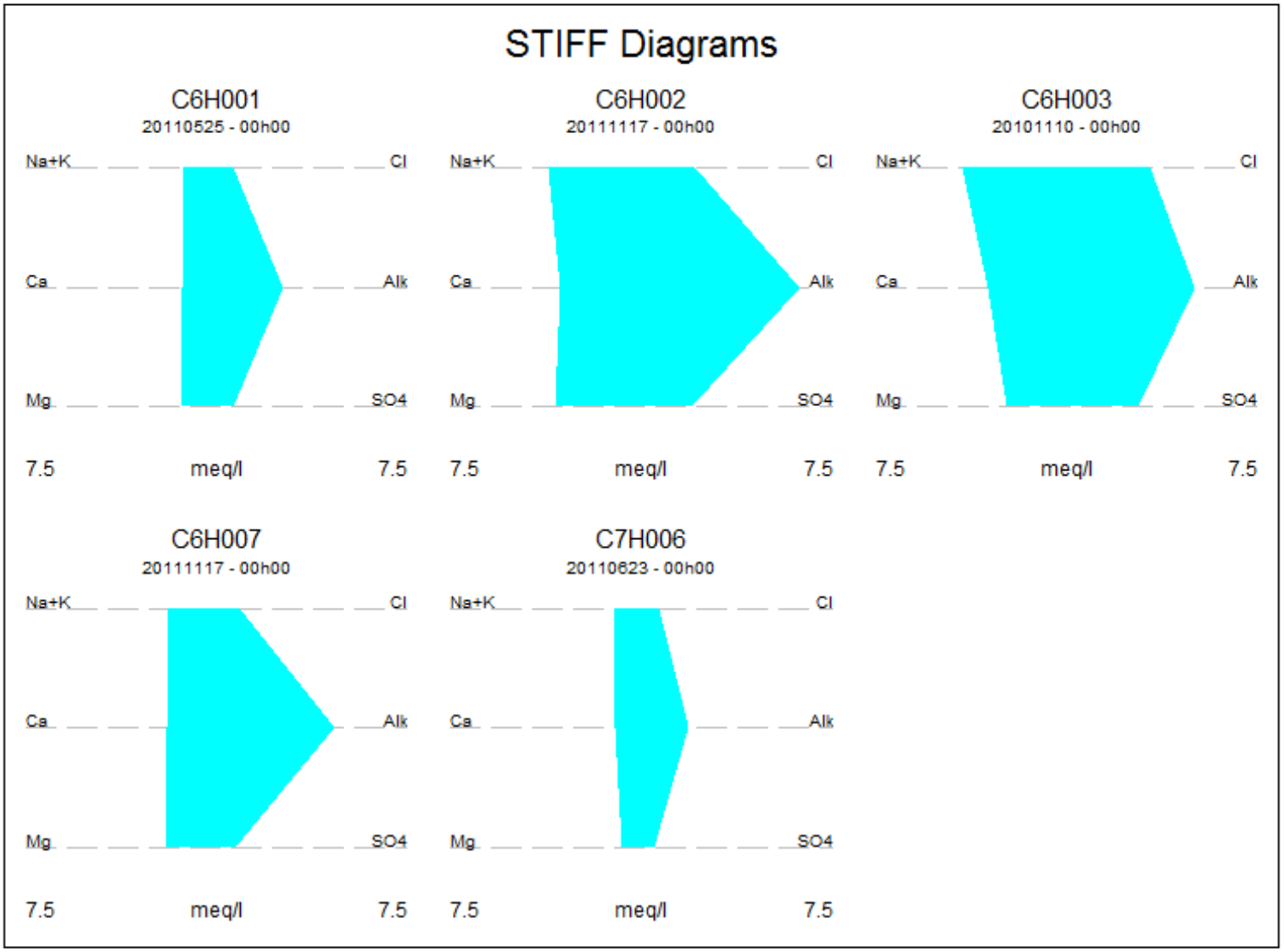
STIFF Diagrams
C6H001
20110525 - 00h00
C6H002
20111117 - 00h00
C6H003
20101110 - 00h00
C6H007
20111117 - 00h00
C7H006
20110623 - 00h00
Na+K
Cl
Ca
Alk
Mg
SO4
7.5
meq/l
7.5

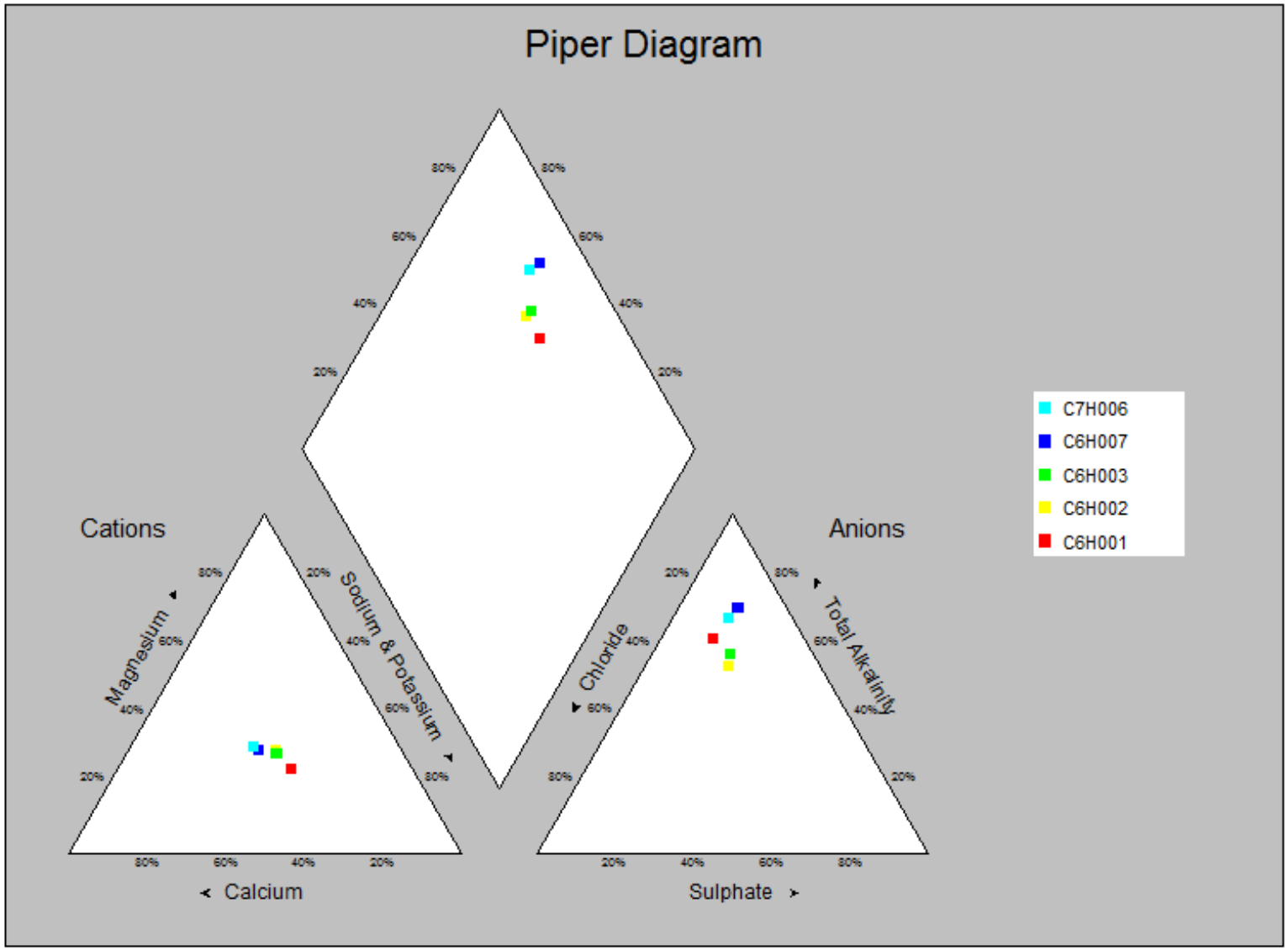
Piper Diagram
Cations
Anions
Magnesium
Sodium & Potassium
Chloride
Total Alkalinity
Calcium
Sulphate
C7H006
C6H007
C6H003
C6H002
C6H001

Catchment C8

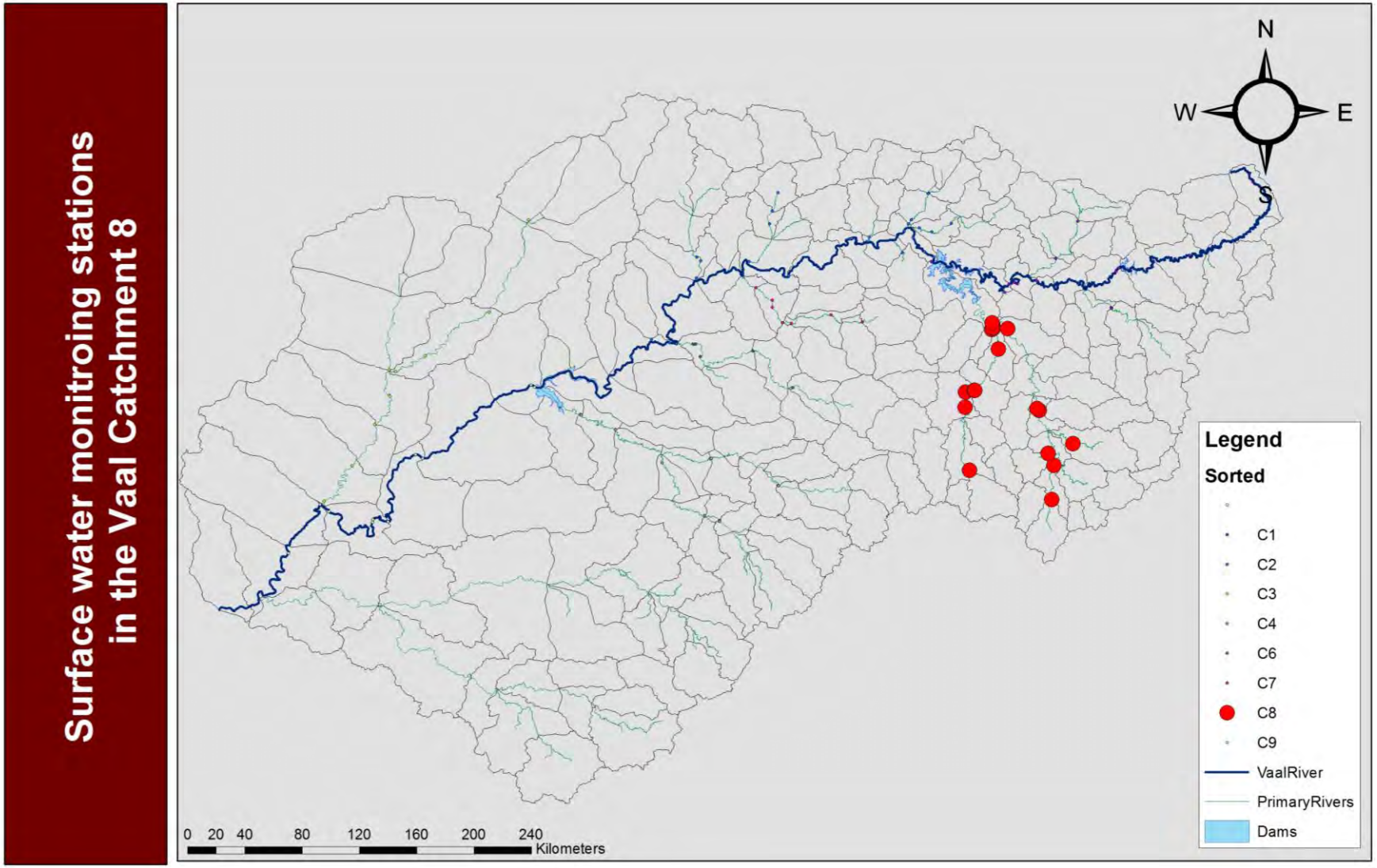

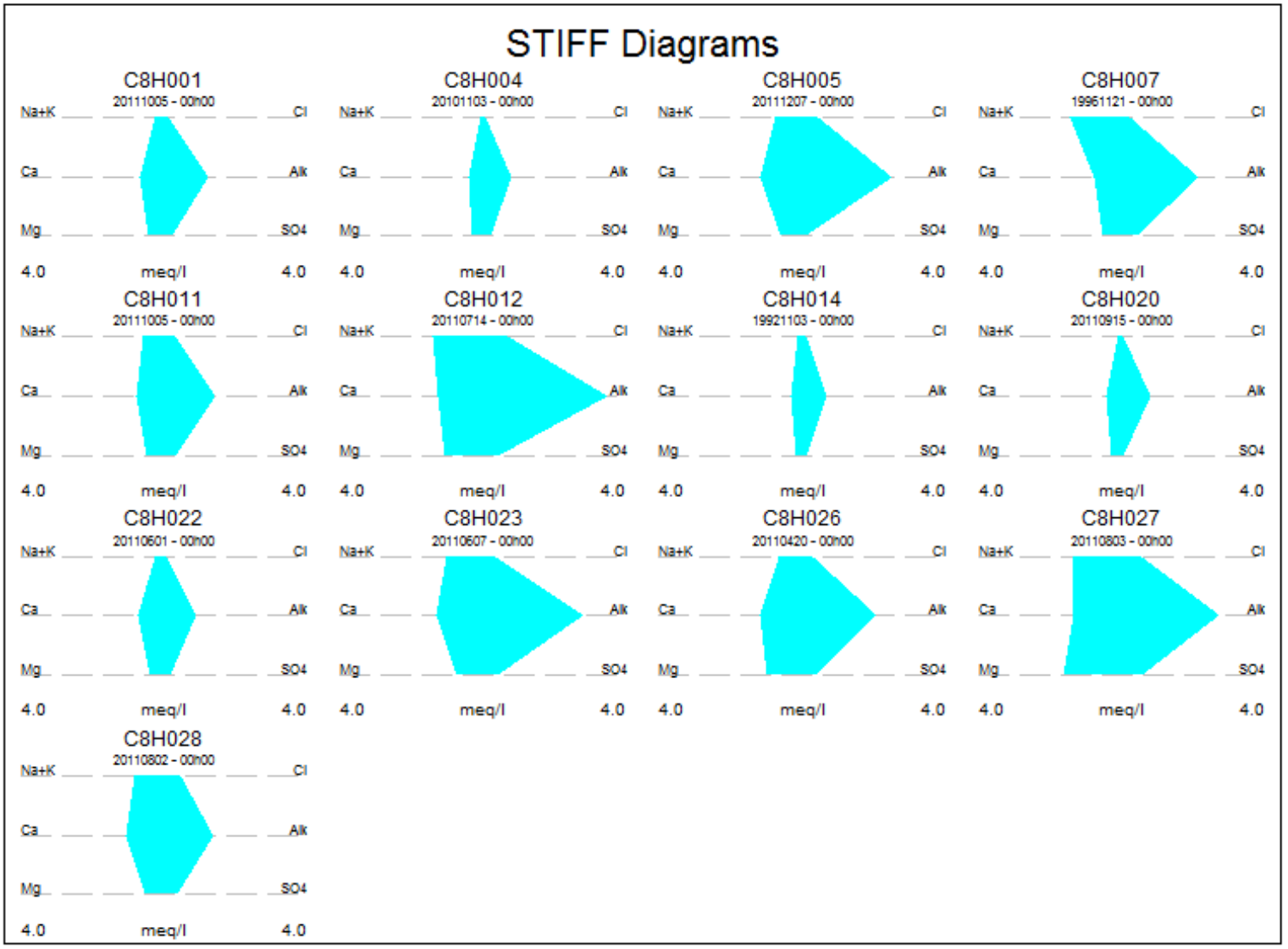
STIFF Diagrams
C8H001
20111005 - 00h00
C8H004
20101103 - 00h00
C8H005
20111207 - 00h00
C8H007
19961121 - 00h00
C8H011
20111005 - 00h00
C8H012
20110714 - 00h00
C8H014
19921103 - 00h00
C8H020
20110915 - 00h00
C8H022
20110601 - 00h00
C8H023
20110607 - 00h00
C8H026
20110420 - 00h00
C8H027
20110803 - 00h00
C8H028
20110802 - 00h00
Na+K
Ca
Mg
Cl
Alk
SO4
4.0
meq/l

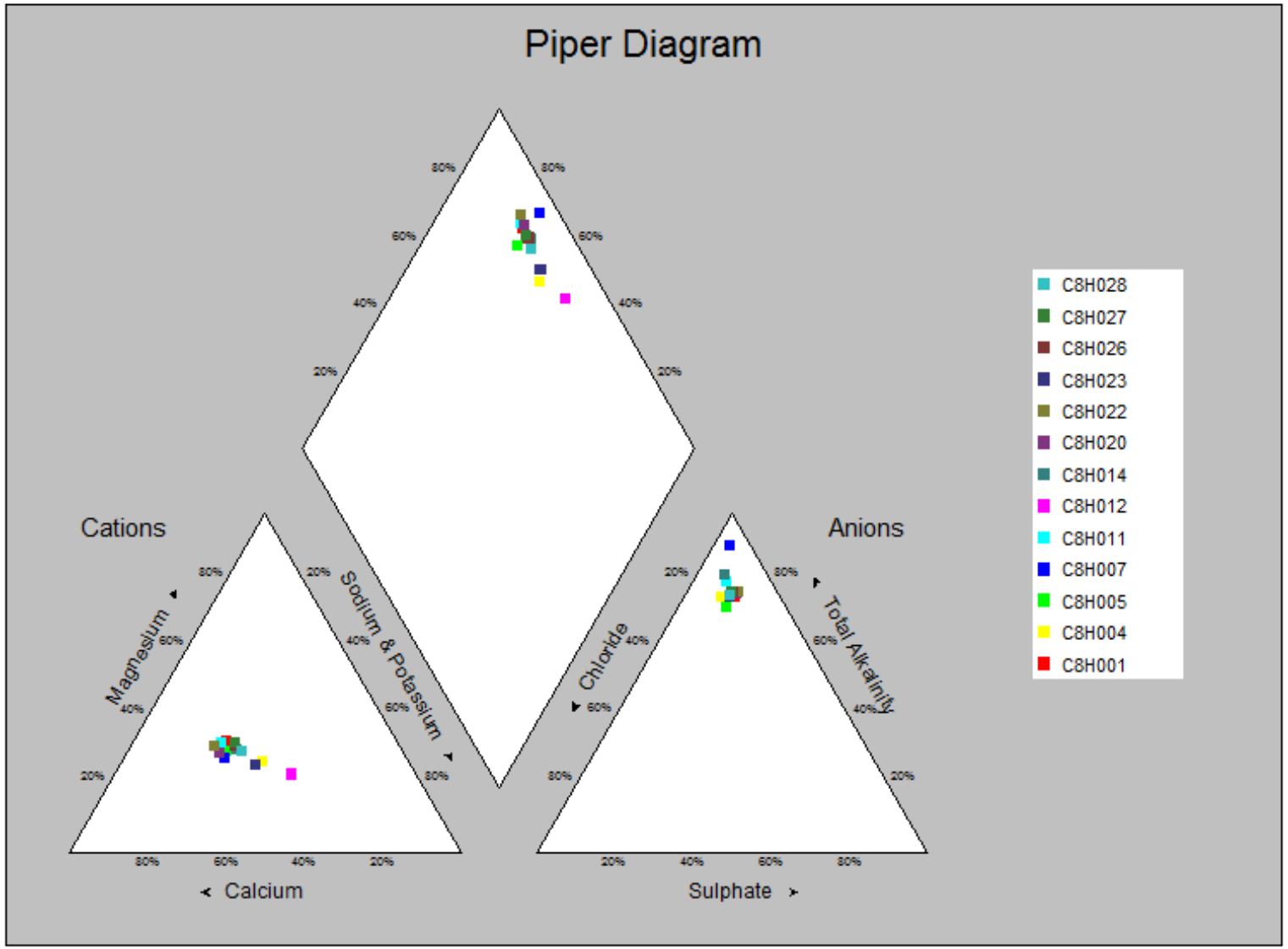
Piper Diagram
Cations
Anions
Magnesium
Sodium & Potassium
Chloride
Total Alkalinity
Calcium
Sulphate
C8H028
C8H027
C8H026
C8H023
C8H022
C8H020
C8H014
C8H012
C8H011
C8H007
C8H005
C8H004
C8H001

Catchment C 9

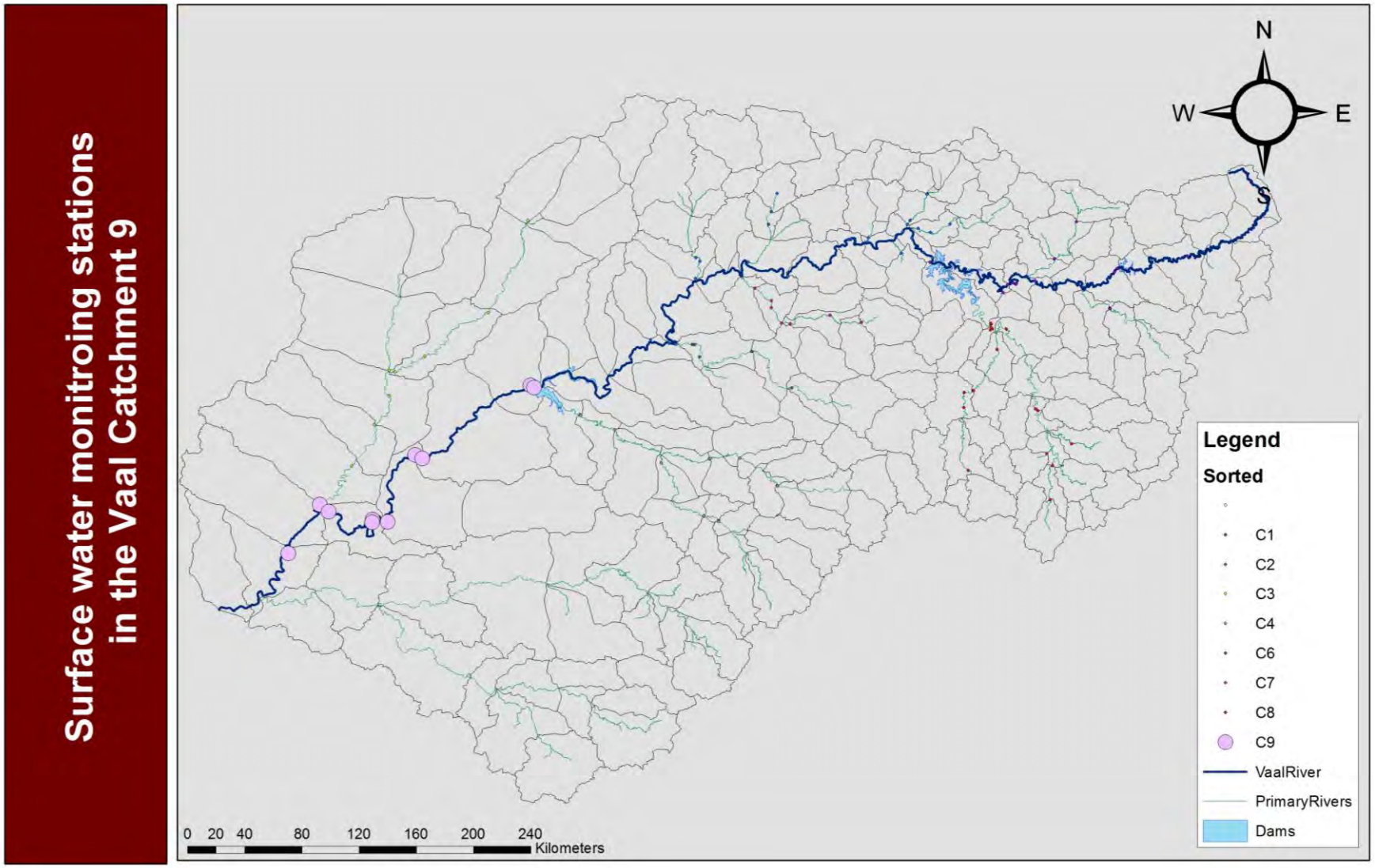

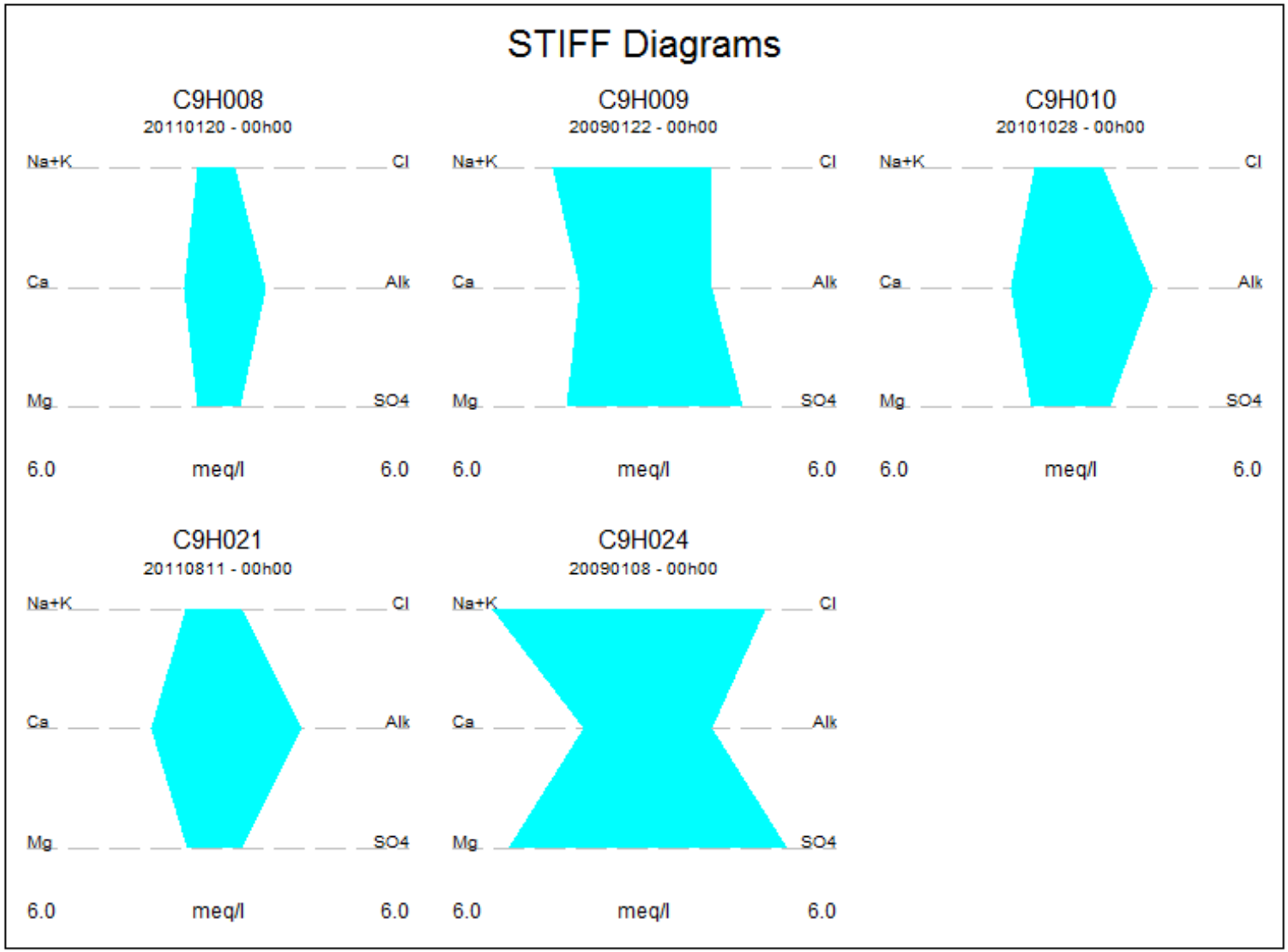
STIFF Diagrams
C9H008
20110120 - 00h00
Na+K
Cl
Ca
Alk
Mg
SO4
6.0
meq/l
6.0
C9H009
20090122 - 00h00
Na+K
Cl
Ca
Alk
Mg
SO4
6.0
meq/l
6.0
C9H010
20101028 - 00h00
Na+K
Cl
Ca
Alk
Mg
SO4
6.0
meq/l
6.0
C9H021
20110811 - 00h00
Na+K
Cl
Ca
Alk
Mg
SO4
6.0
meq/l
6.0
C9H024
20090108 - 00h00
Na+K
Cl
Ca
Alk
Mg
SO4
6.0
meq/l
6.0

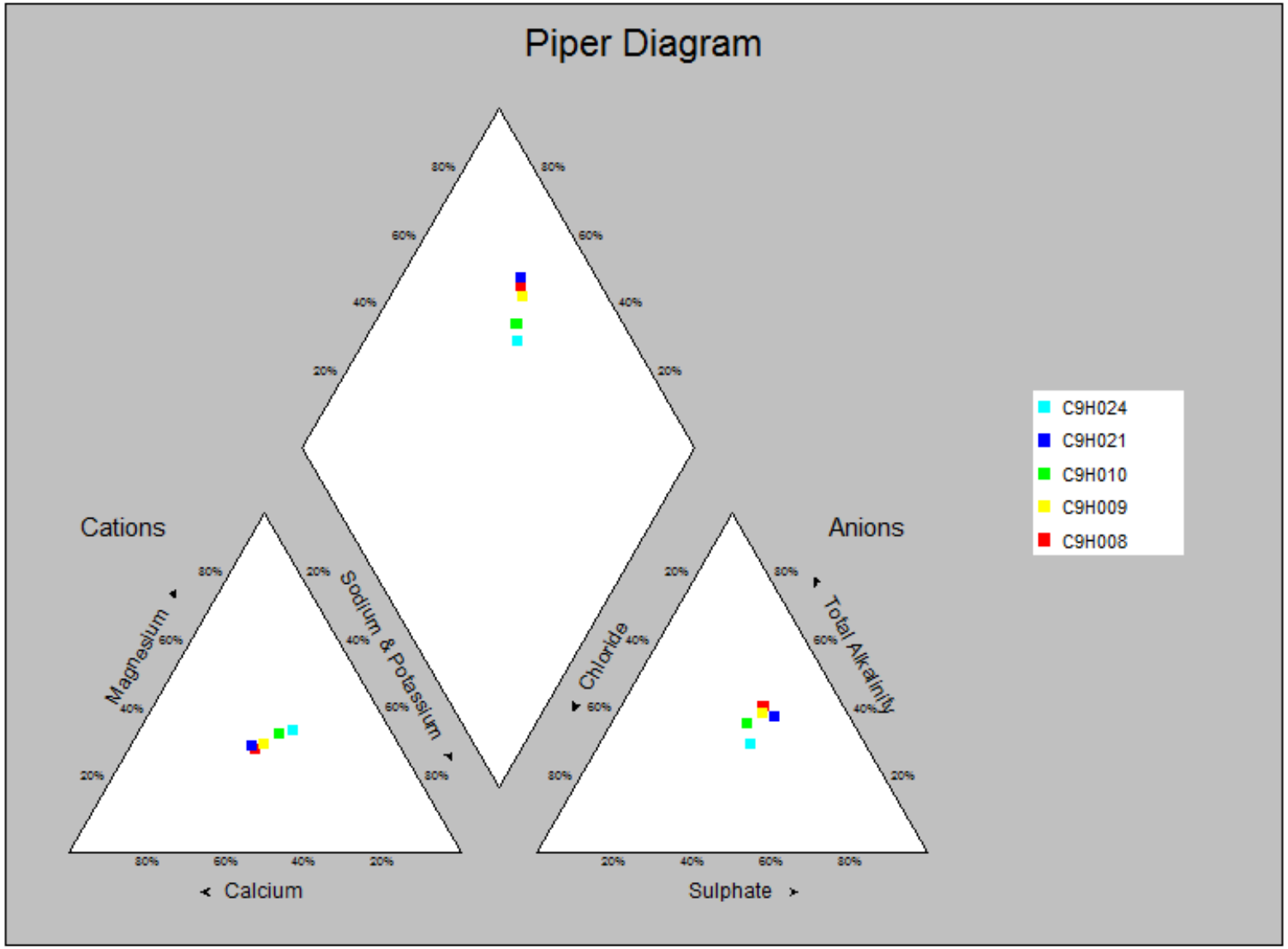
Piper Diagram
Cations
Anions
Magnesium
Sodium & Potassium
Calcium
Chloride
Total Alkalinity
Sulphate
C9H024
C9H021
C9H010
C9H009
C9H008

Appendix 3 TDS VS BICARBONATE FIGURES

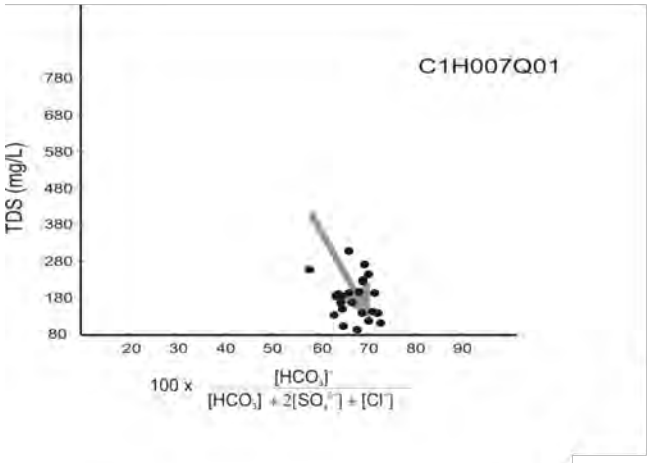

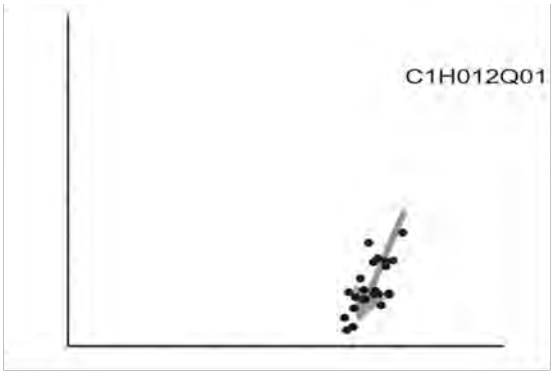

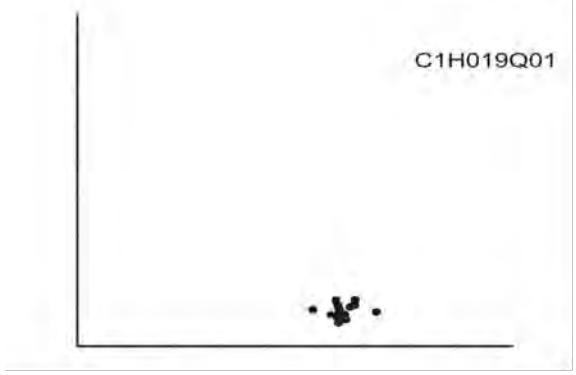

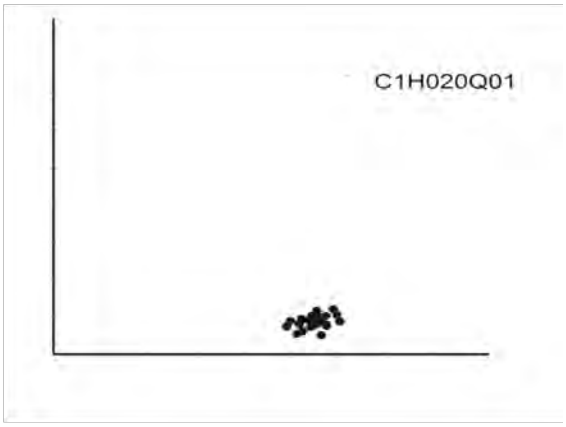

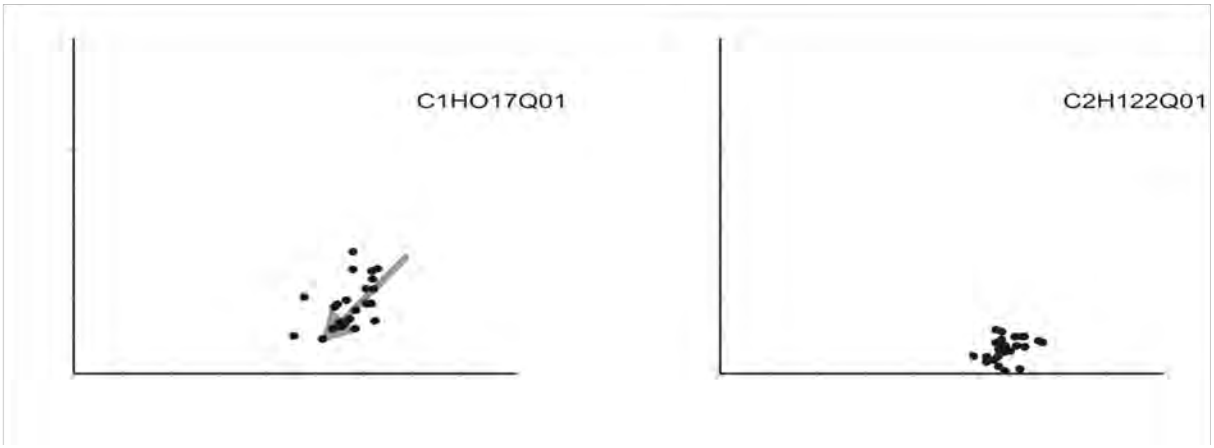

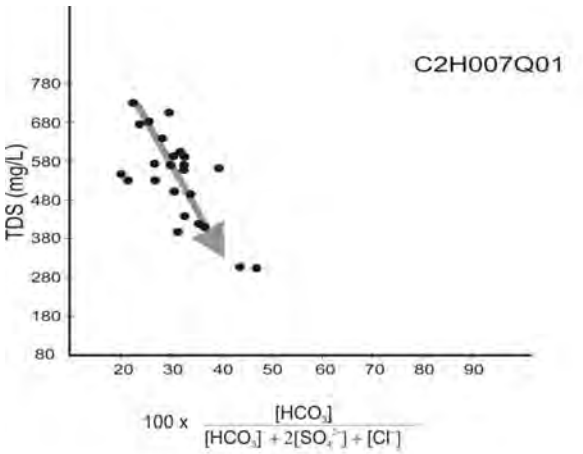
C2H007Q01
TDS (mg/L)
780
680
580
480
380
280
180
80
20
30
40
50
60
70
80
90
100 x [HCO3] / ([HCO3] + 2[SO4 2-] + [Cl-])

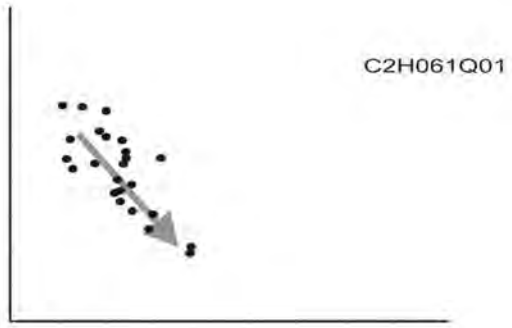
C2H061Q01

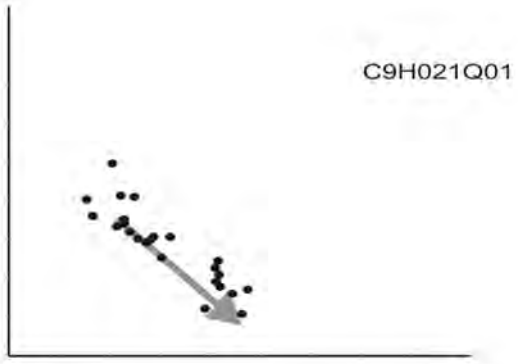
C9H021Q01

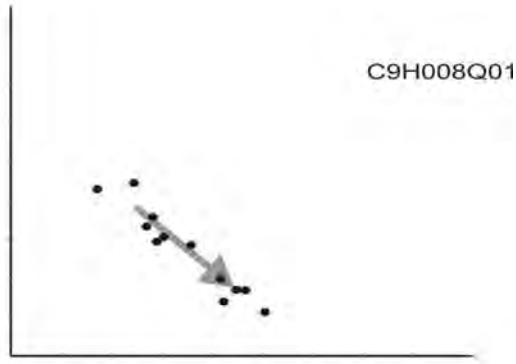
C9H008Q01

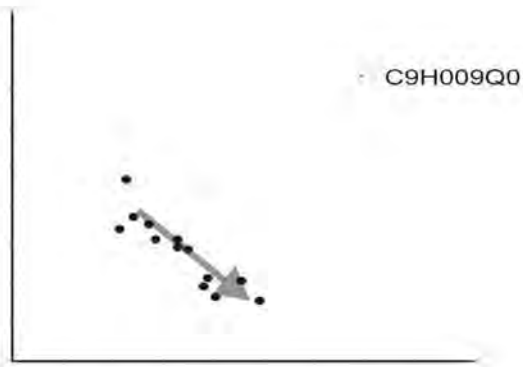
C9H009Q01

Appendix 4 SALT LOAD ANALYSIS

TABLE 3: SALT LOAD OF SELECTED SAMPLE STATIONS ALONG THE VAAL RIVER (FROM EAST TO WEST)

Nr	Monitoring point name	Flow (m^3/a)	TDS* (mg/l)	SO_4 + Cl* (mg/l)	Si (mg/l)
4	C1H007	22.7	27710	5392	11528
11	C1H019	14.9	32041	6050	11858
1	C1H001	2.3	25042	N/A	11069
8	C1H012	39.3	50113	6090	17437
31	C2H122	50.9	109557	23593	53312
17	C2H008	45.6	241746	33455	12592
33	C2H140	89.6	269072	35516	17192
21	C2H018	66.7	242853	34104	15730
23	C2H022	38.9	278988	37715	15663
24	C2H061	82.1	266865	35623	17334
64	C9H021	64.5	130670	21146	14617
61	C9H008	19.9	118064	20370	17592
62	C9H009	14.6	131052	21809	18516
63	C9H010	64.8	185330	26067	16976
65	C9H024	11.6	270660	34614	17245

The data was obtained from DWS Hydrological survey database with 85% reliability and 15% patched data.

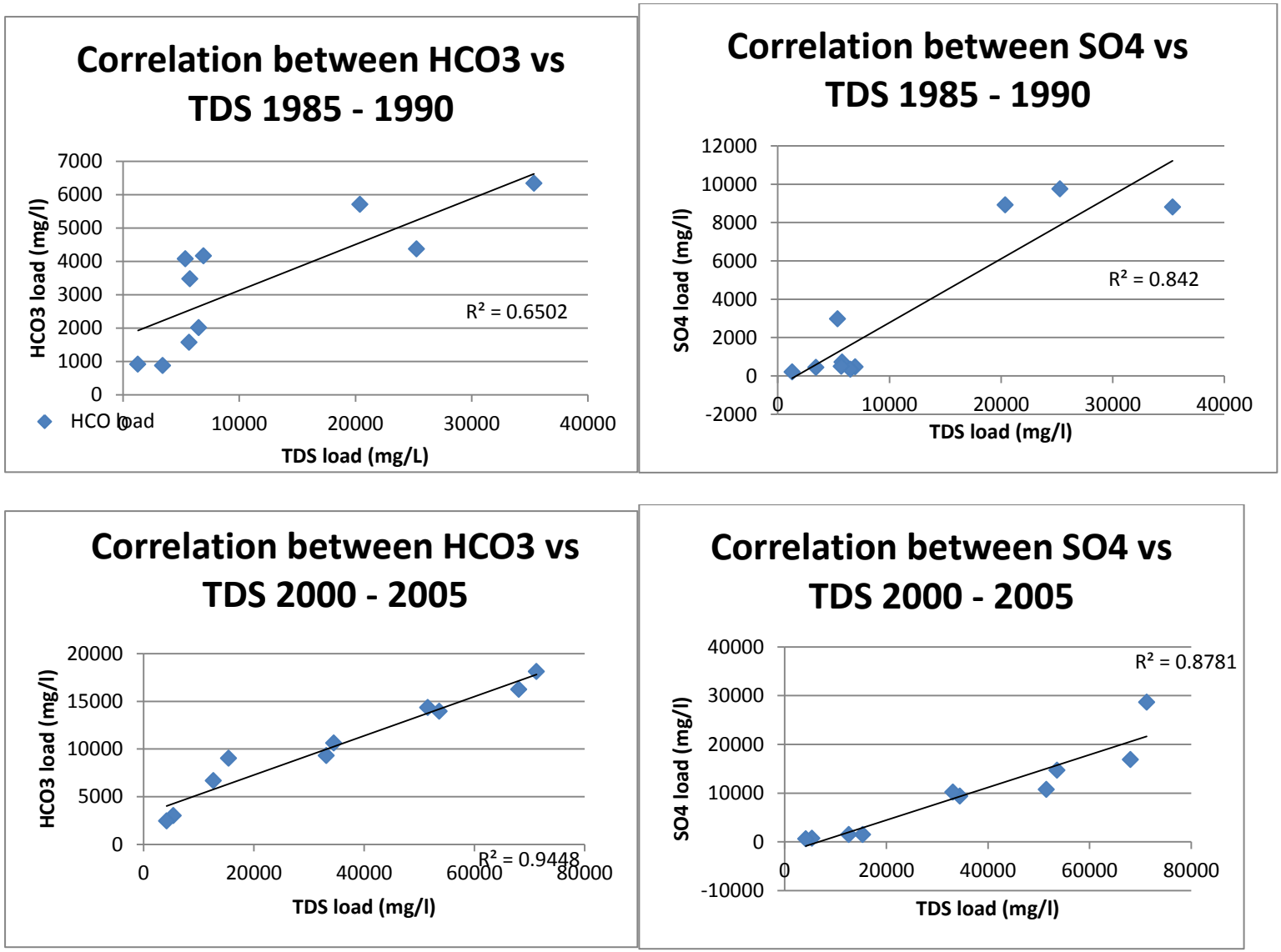

Figure: Selected Sampling Stations Correlations between bicarbonate and TDS

Appendix 5 GROUNDWATER MAPS

Groundwater section 1

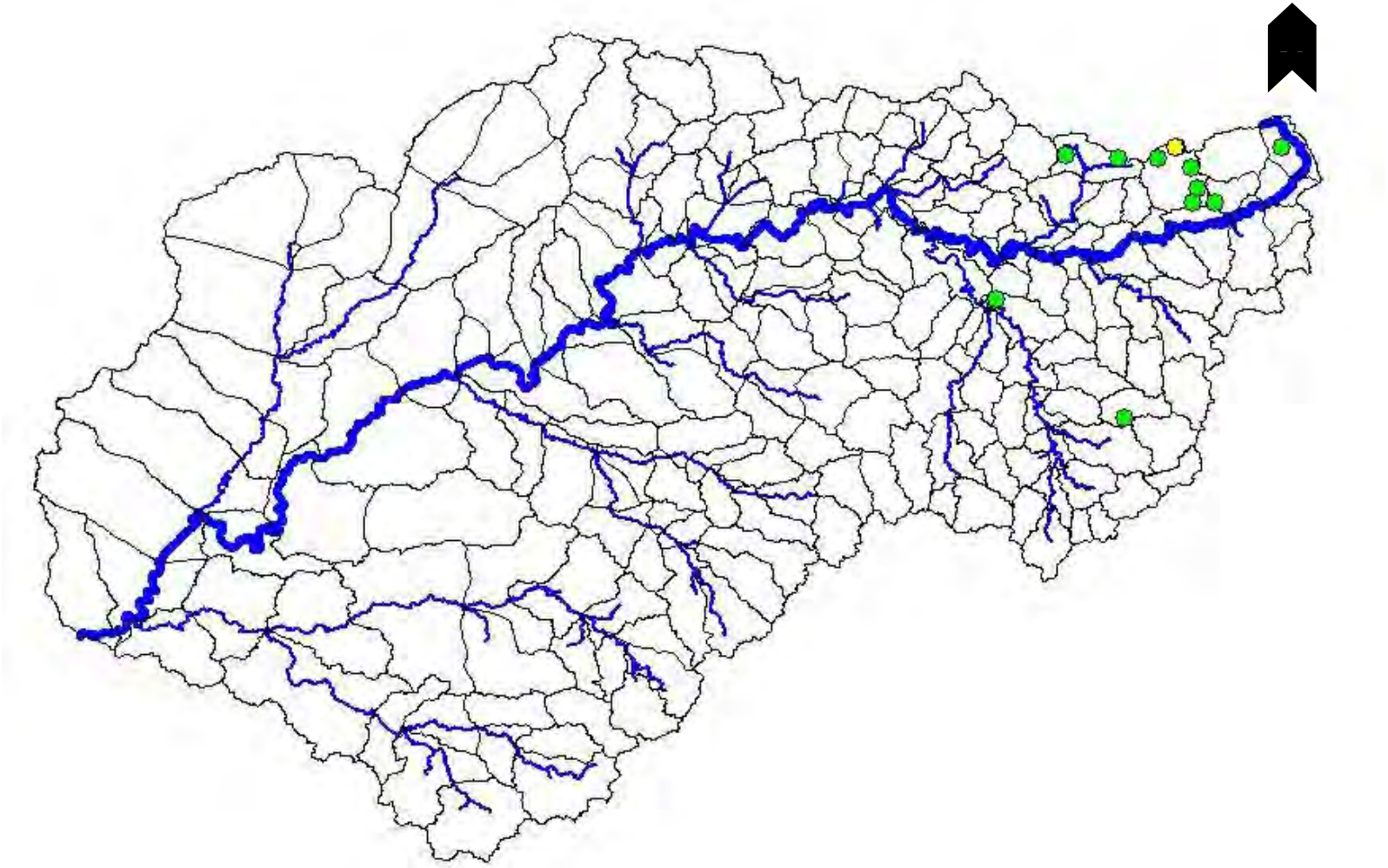

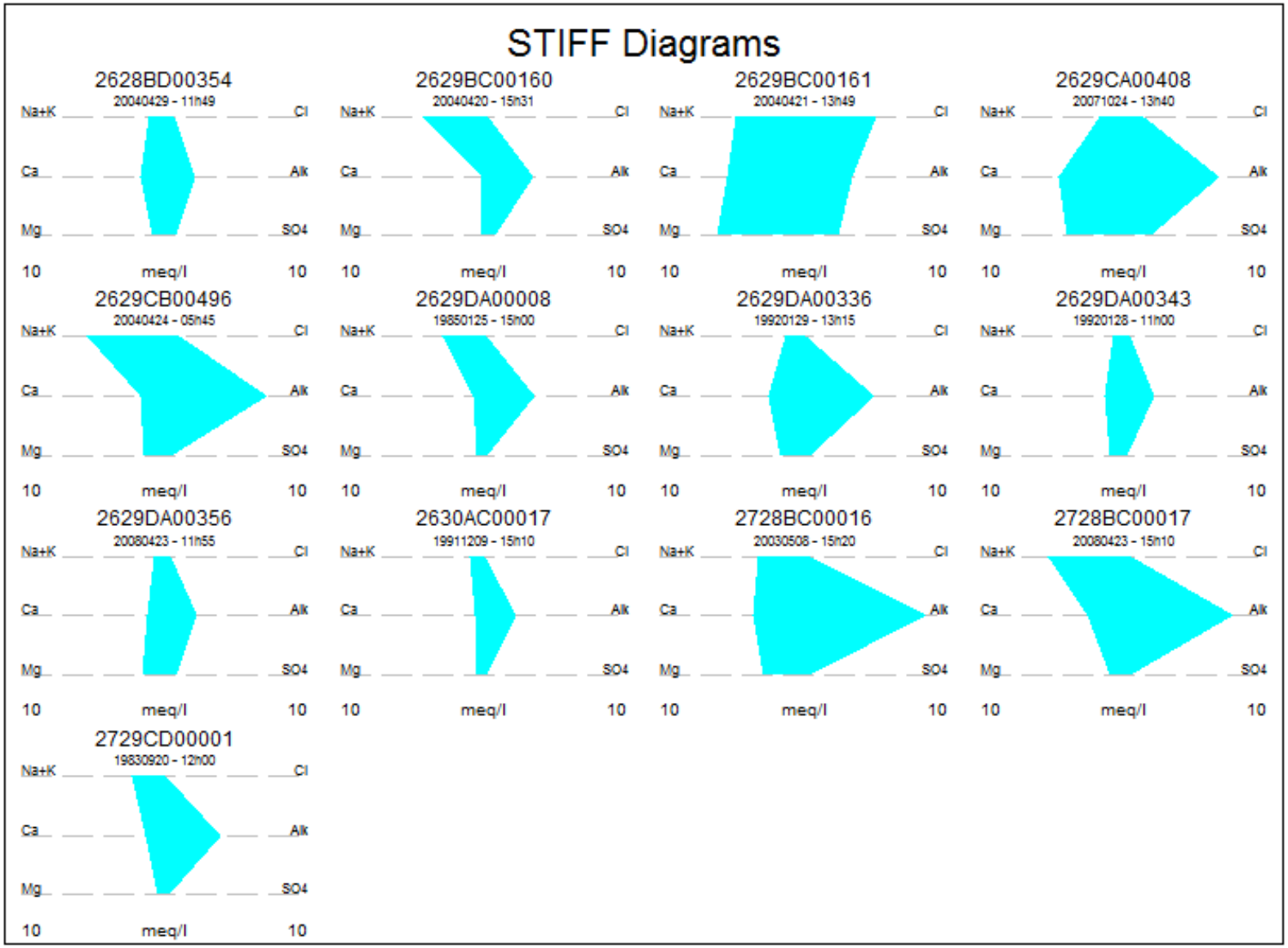
STIFF Diagrams
2628BD00354
20040429 - 11h49
2629BC00160
20040420 - 15h31
2629BC00161
20040421 - 13h49
2629CA00408
20071024 - 13h40
2629CB00496
20040424 - 05h45
2629DA00008
19850125 - 15h00
2629DA00336
19920129 - 13h15
2629DA00343
19920128 - 11h00
2629DA00356
20080423 - 11h55
2630AC00017
19911209 - 15h10
2728BC00016
20030508 - 15h20
2728BC00017
20080423 - 15h10
2729CD00001
19830920 - 12h00
Na+K
Cl
Ca
Alk
Mg
SO4
10
meq/l
10

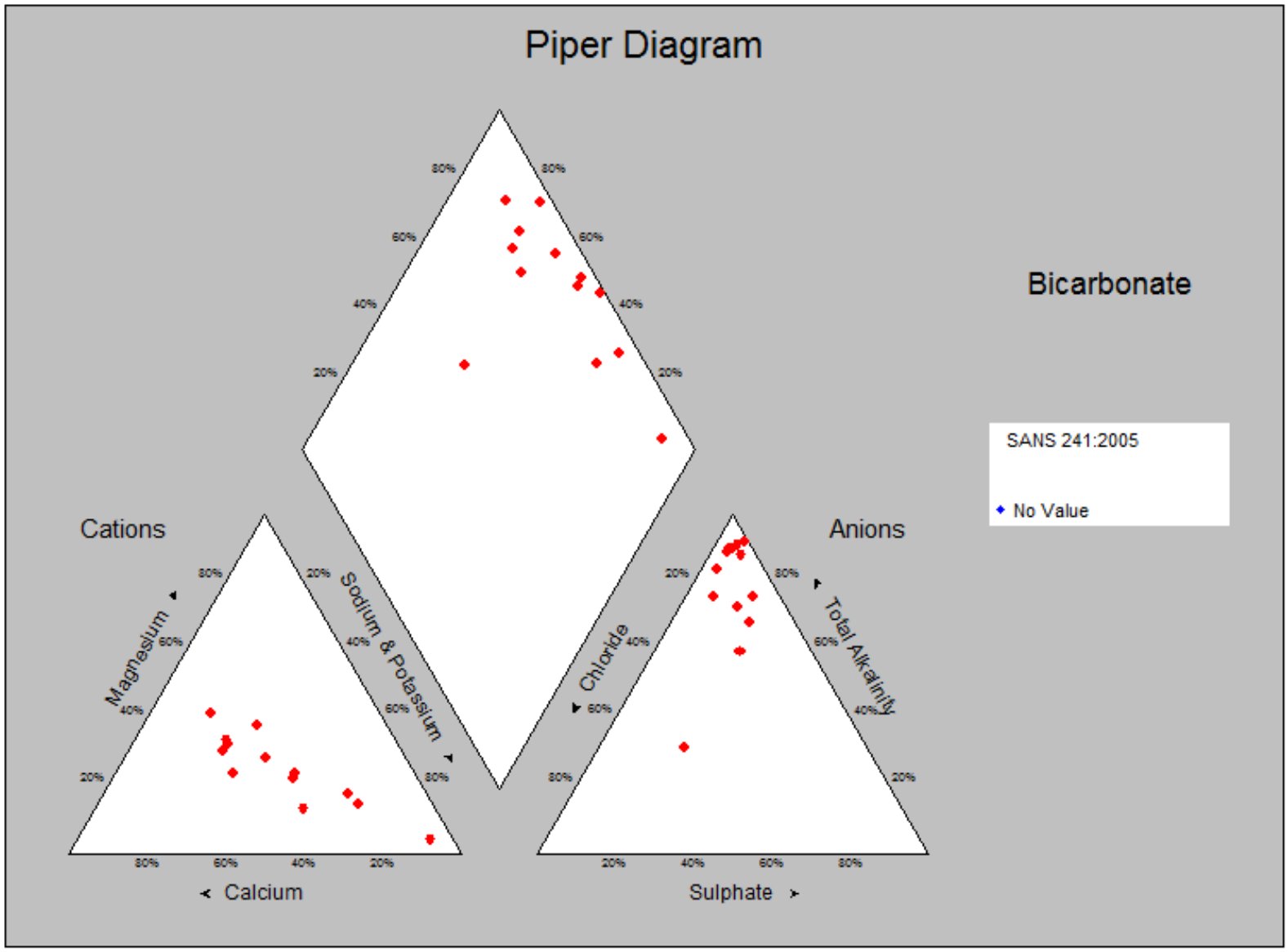
Piper Diagram
Bicarbonate
SANS 241:2005
No Value
Cations
Anions
Magnesium
Sodium & Potassium
Chloride
Total Alkalinity
Calcium
Sulphate
80%
60%
40%
20%

Groundwater section 2

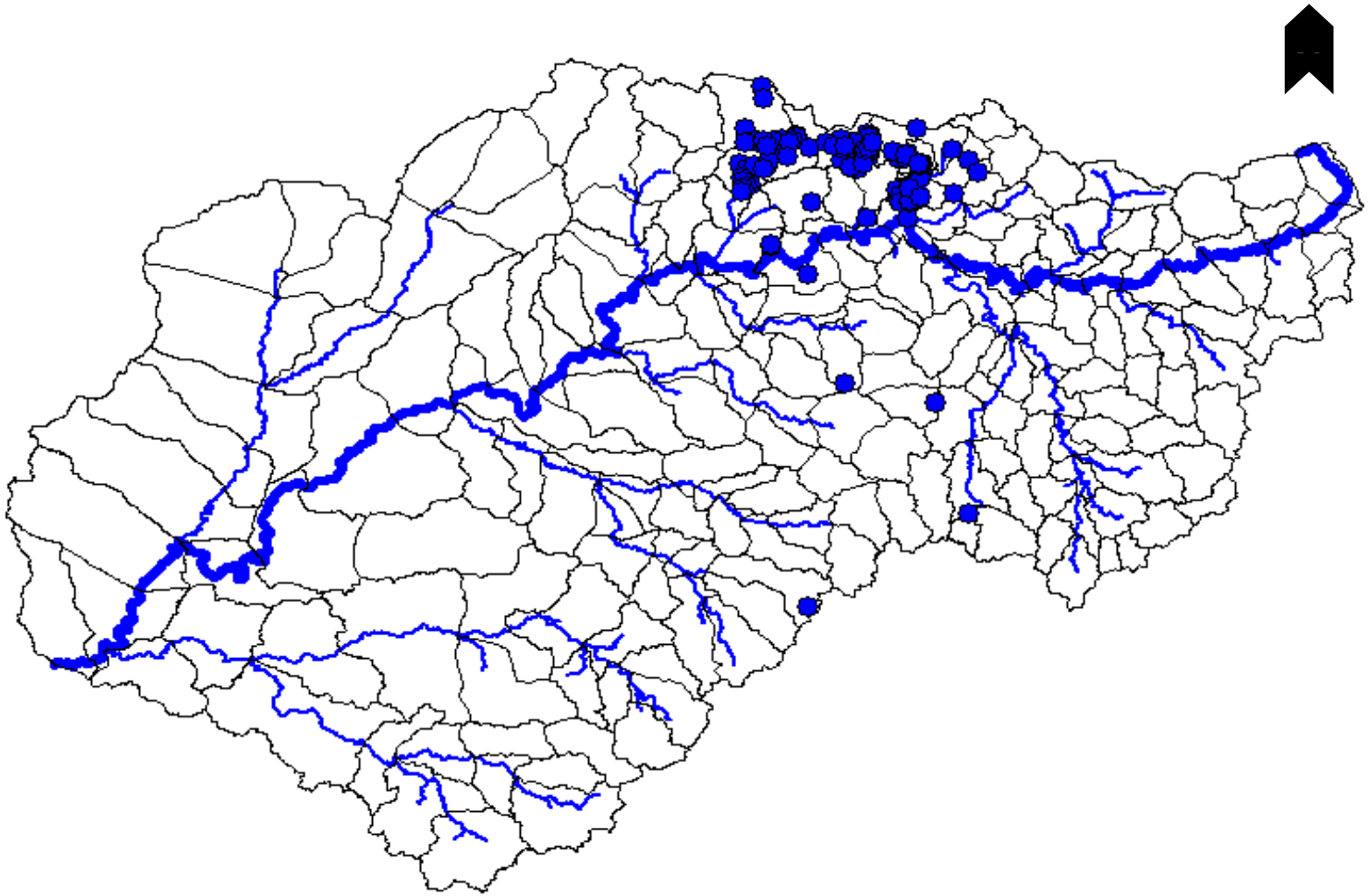

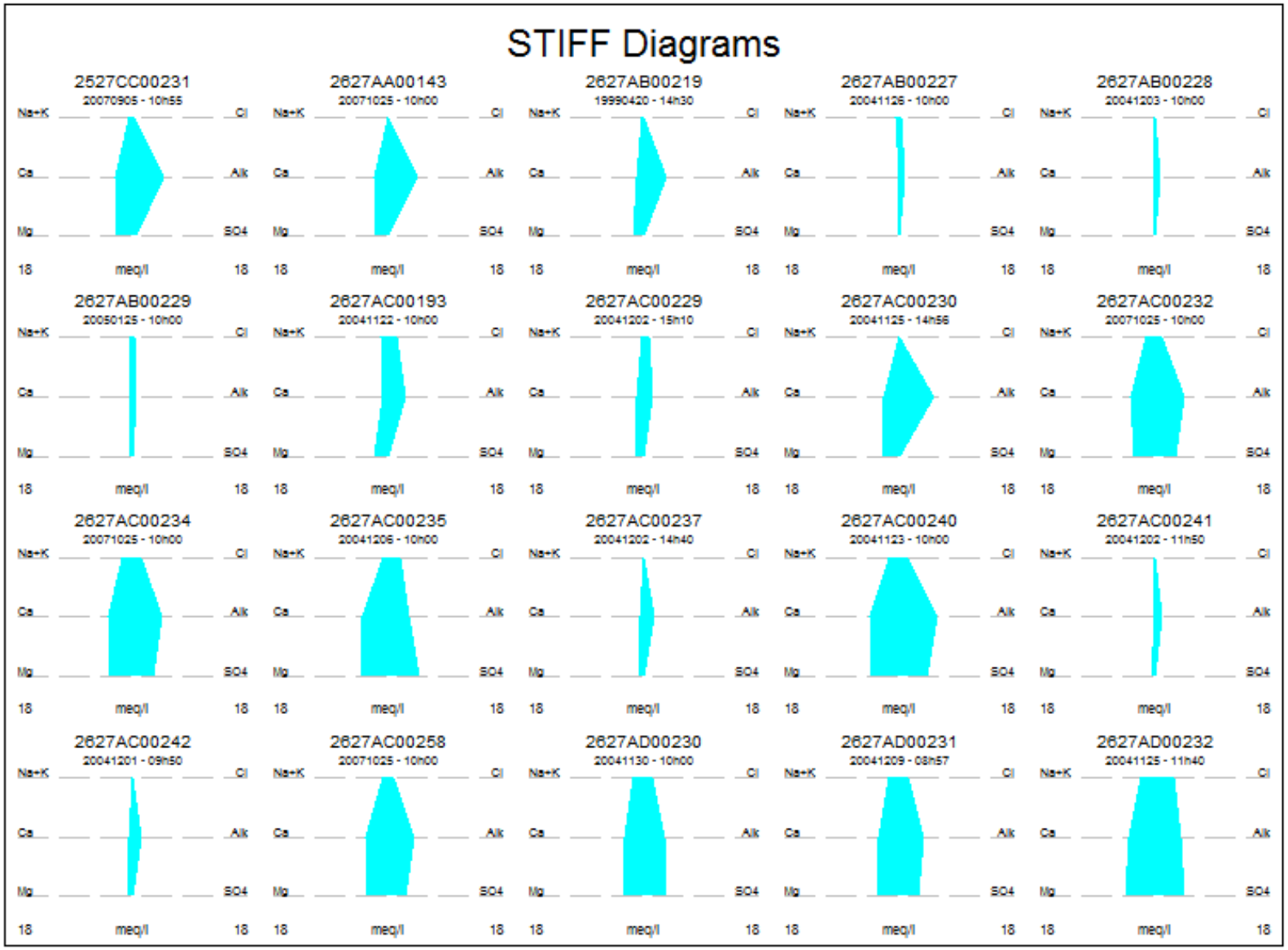
STIFF Diagrams
2527CC00231
20070905 - 10h55
2627AA00143
20071025 - 10h00
2627AB00219
19990420 - 14h30
2627AB00227
20041126 - 10h00
2627AB00228
20041203 - 10h00
2627AB00229
20050125 - 10h00
2627AC00193
20041122 - 10h00
2627AC00229
20041202 - 15h10
2627AC00230
20041125 - 14h56
2627AC00232
20071025 - 10h00
2627AC00234
20071025 - 10h00
2627AC00235
20041206 - 10h00
2627AC00237
20041202 - 14h40
2627AC00240
20041123 - 10h00
2627AC00241
20041202 - 11h50
2627AC00242
20041201 - 09h50
2627AC00258
20071025 - 10h00
2627AD00230
20041130 - 10h00
2627AD00231
20041209 - 08h57
2627AD00232
20041125 - 11h40
Na+K
Ca
Mg
Cl
Alk
SO4
18
meq/l

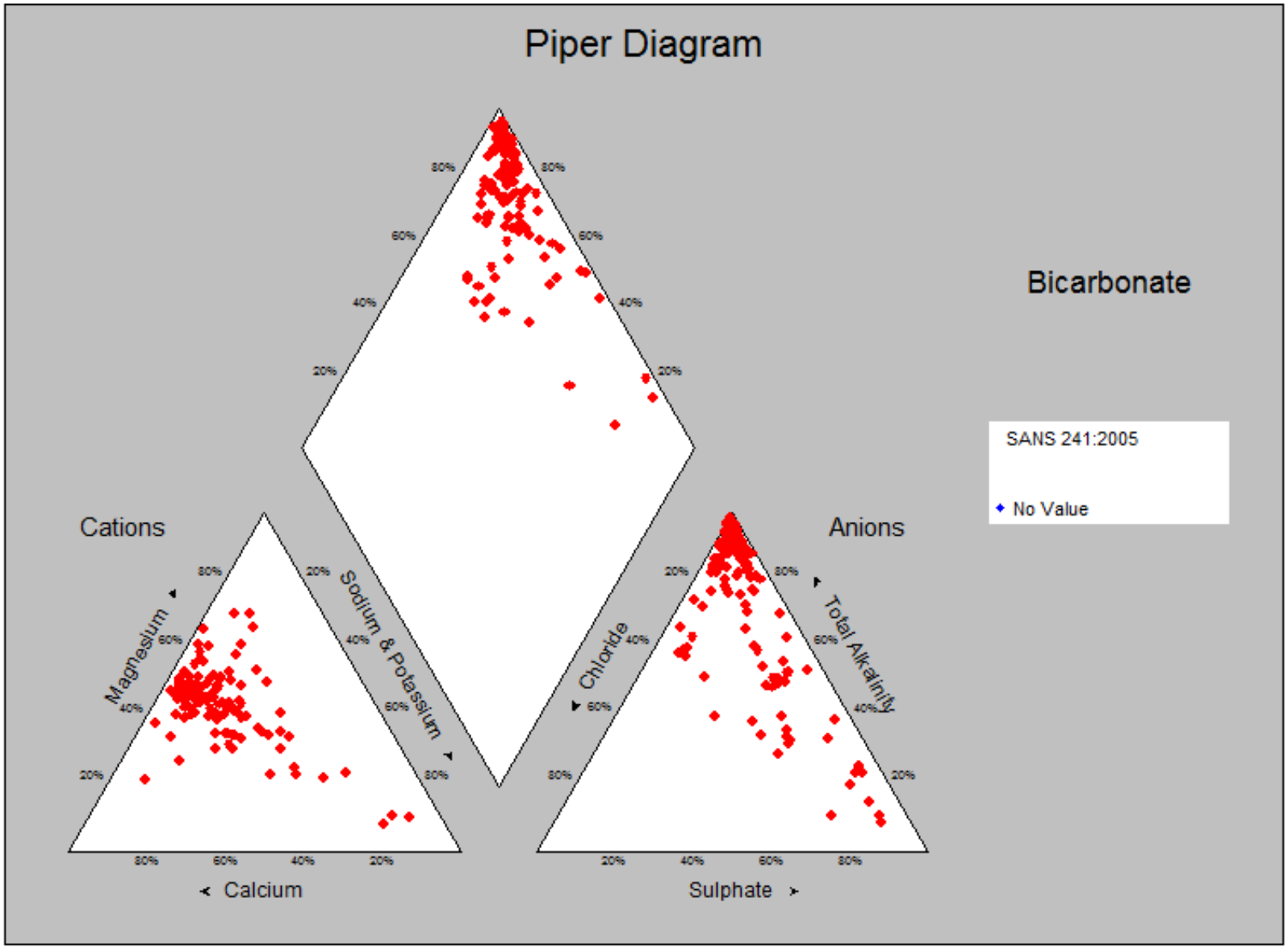
Piper Diagram
Bicarbonate
SANS 241:2005
No Value
Cations
Anions
Magnesium
Sodium & Potassium
Chloride
Total Alkalinity
Calcium
Sulphate
80%
60%
40%
20%

Groundwater section 3

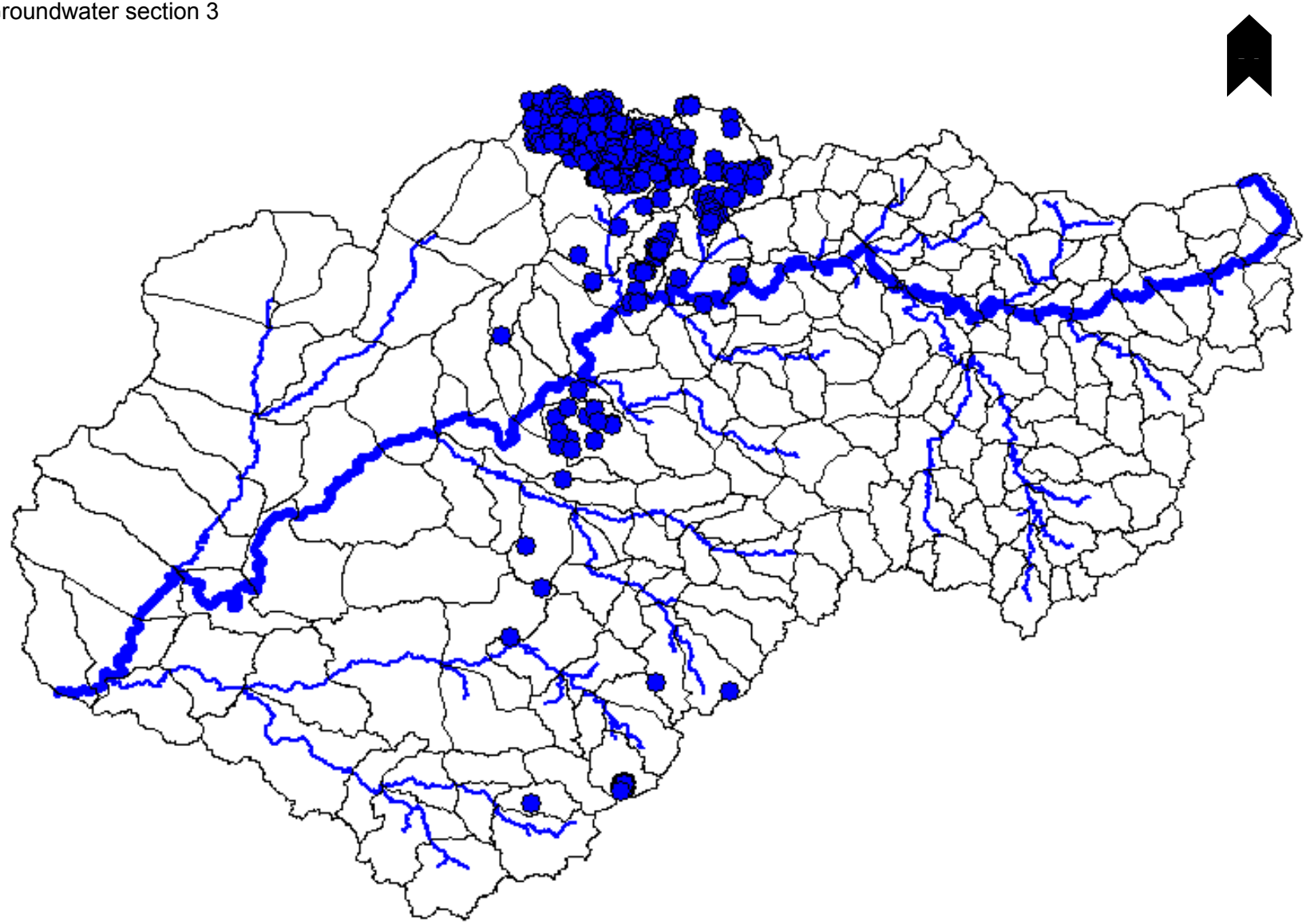

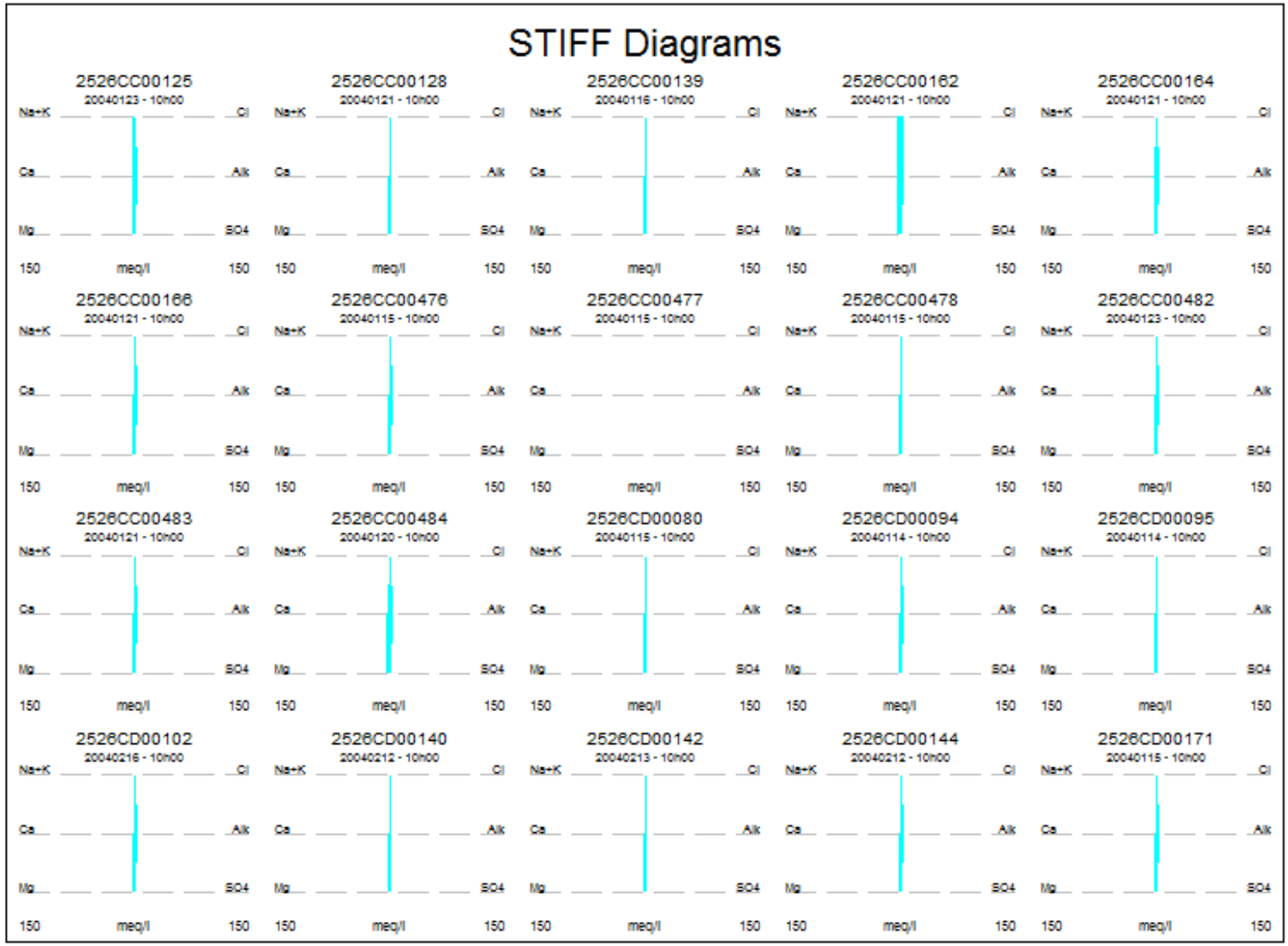
STIFF Diagrams
2526CC00125
20040123 - 10h00
2526CC00128
20040121 - 10h00
2526CC00139
20040116 - 10h00
2526CC00162
20040121 - 10h00
2526CC00164
20040121 - 10h00
2526CC00166
20040121 - 10h00
2526CC00476
20040115 - 10h00
2526CC00477
20040115 - 10h00
2526CC00478
20040115 - 10h00
2526CC00482
20040123 - 10h00
2526CC00483
20040121 - 10h00
2526CC00484
20040120 - 10h00
2526CD00080
20040115 - 10h00
2526CD00094
20040114 - 10h00
2526CD00095
20040114 - 10h00
2526CD00102
20040216 - 10h00
2526CD00140
20040212 - 10h00
2526CD00142
20040213 - 10h00
2526CD00144
20040212 - 10h00
2526CD00171
20040115 - 10h00
Na+K
Cl
Ca
Alk
Mg
SO4
150
meq/l
150

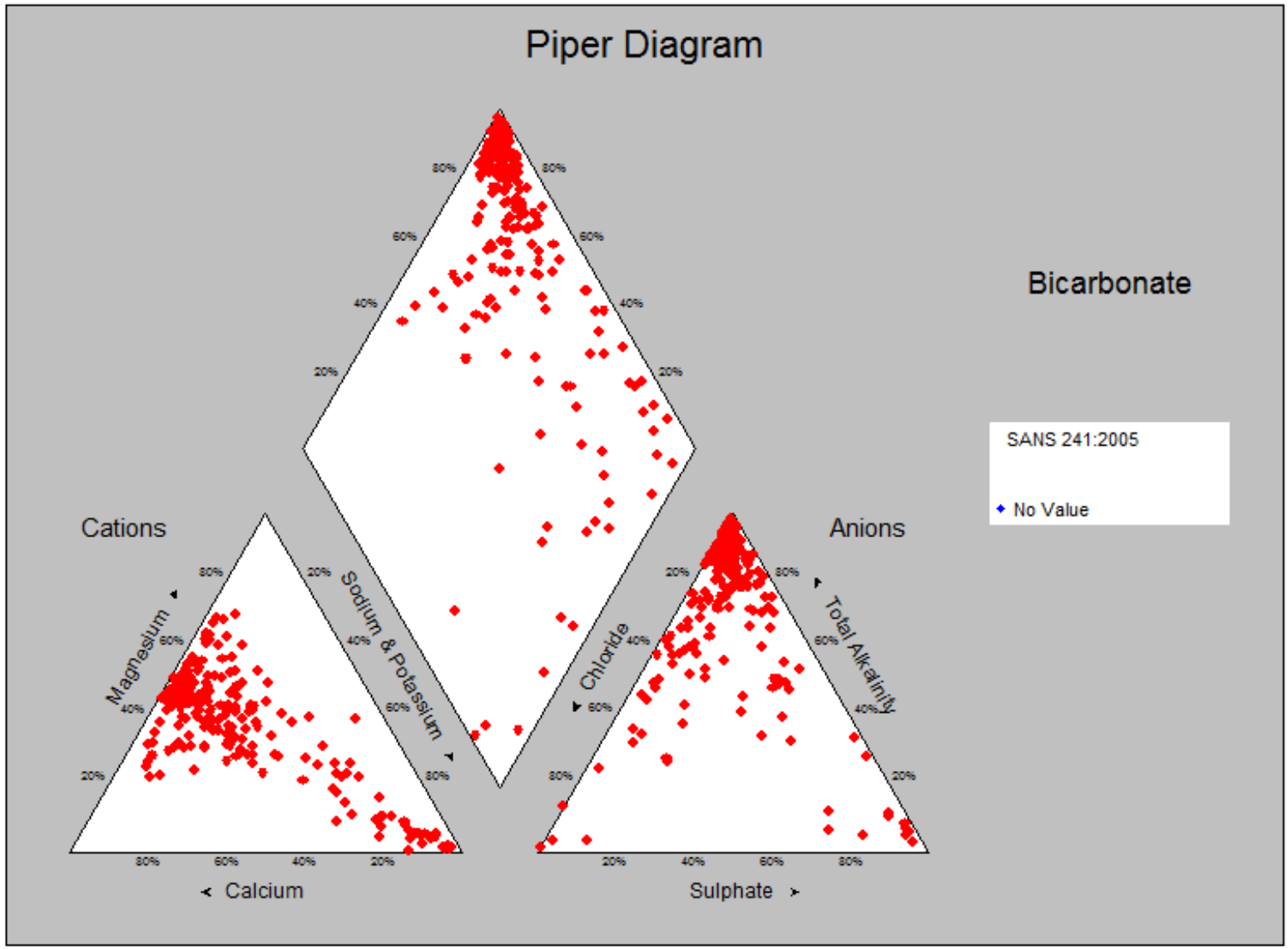
Piper Diagram
Bicarbonate
SANS 241:2005
No Value
Cations
Anions
Magnesium
Sodium & Potassium
Chloride
Total Alkalinity
Calcium
Sulphate
80%
60%
40%
20%

Groundwater section 4

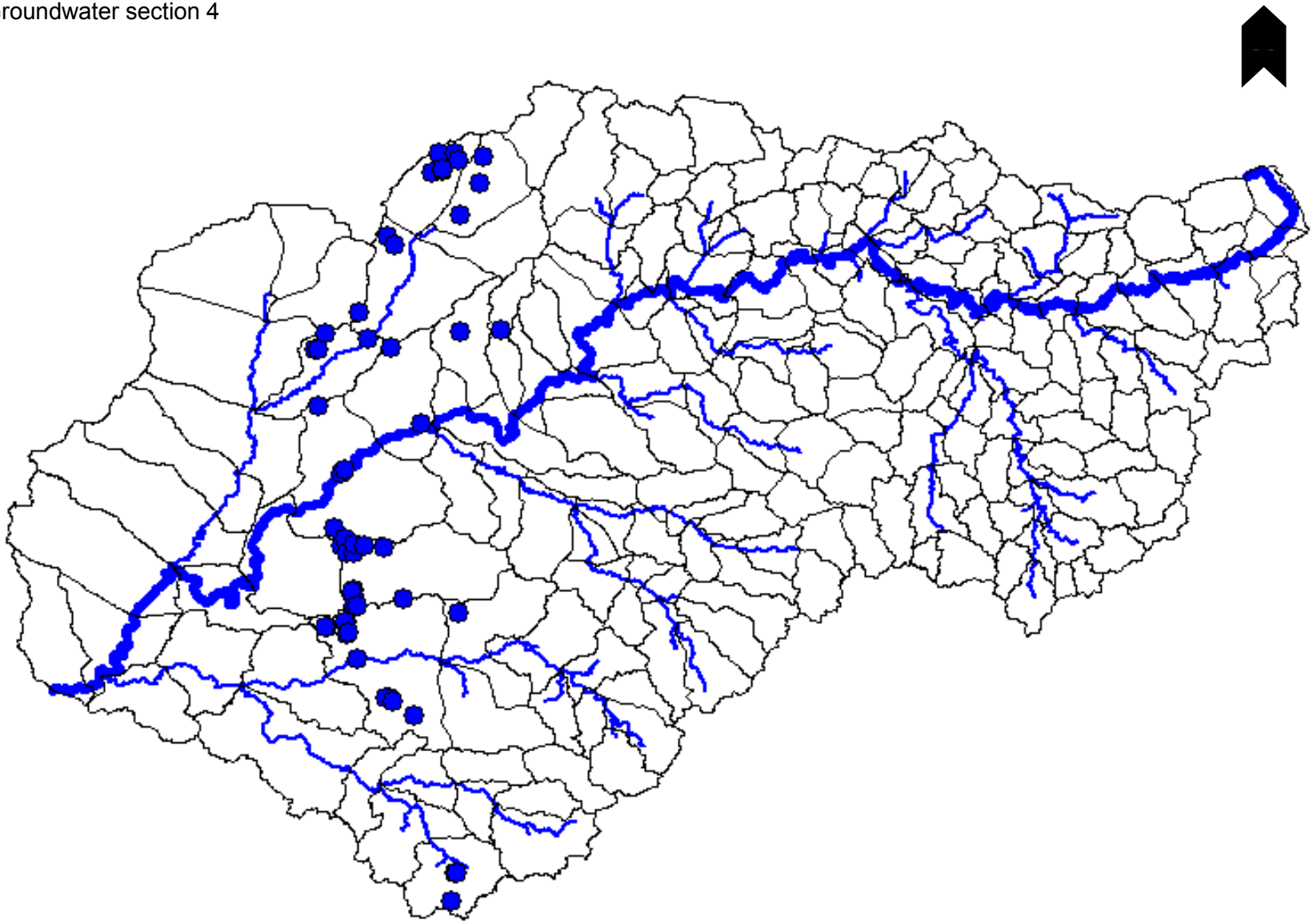

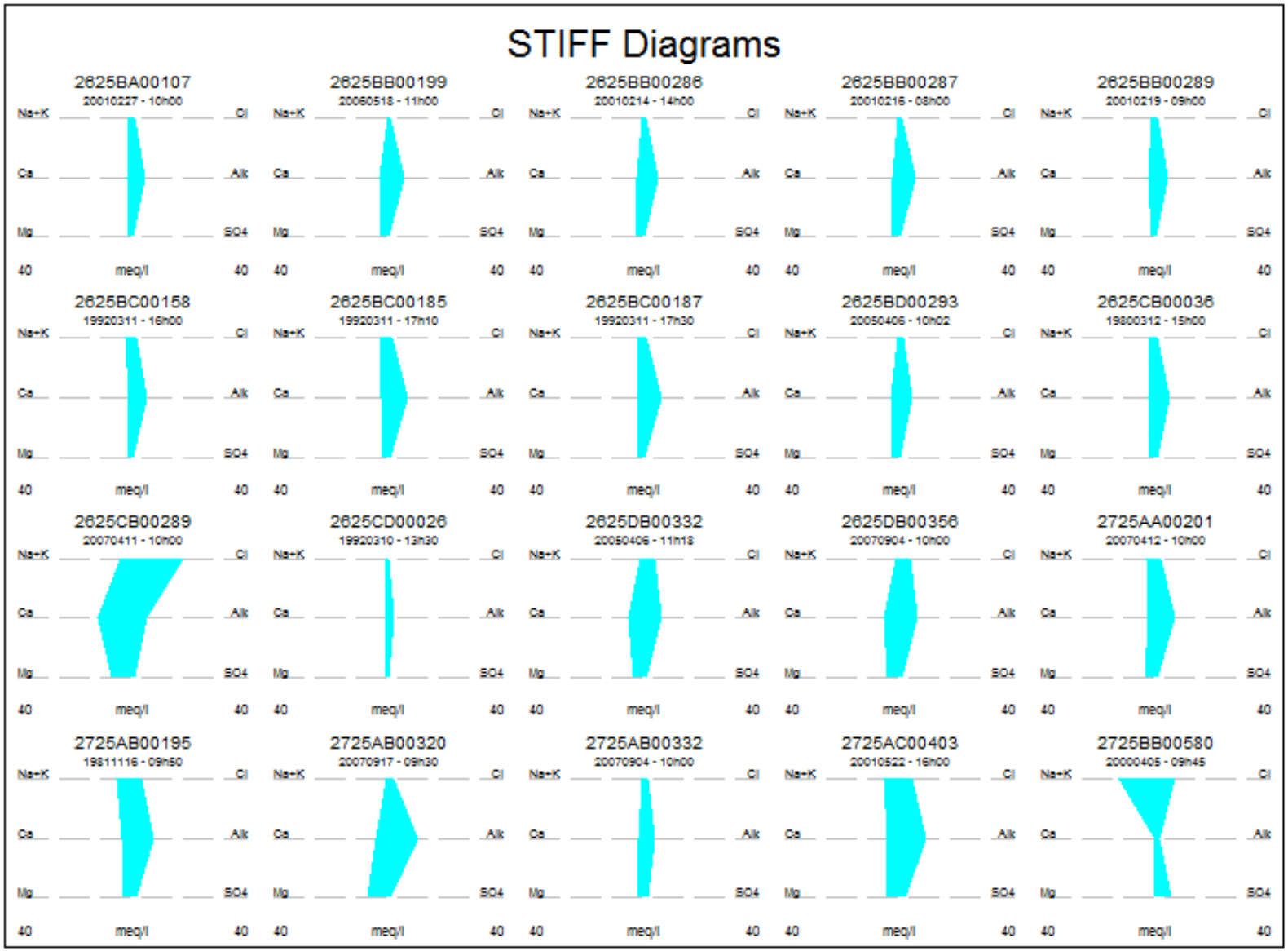
STIFF Diagrams
2625BA00107
20010227 - 10h00
2625BB00199
20060518 - 11h00
2625BB00286
20010214 - 14h00
2625BB00287
20010216 - 08h00
2625BB00289
20010219 - 09h00
2625BC00158
19920311 - 16h00
2625BC00185
19920311 - 17h10
2625BC00187
19920311 - 17h30
2625BD00293
20050406 - 10h02
2625CB00036
19800312 - 15h00
2625CB00289
20070411 - 10h00
2625CD00026
19920310 - 13h30
2625DB00332
20050406 - 11h18
2625DB00356
20070904 - 10h00
2725AA00201
20070412 - 10h00
2725AB00195
19811116 - 09h50
2725AB00320
20070917 - 09h30
2725AB00332
20070904 - 10h00
2725AC00403
20010522 - 16h00
2725BB00580
20000405 - 09h45
Na+K
Ca
Mg
Cl
Alk
SO4
40
meq/l

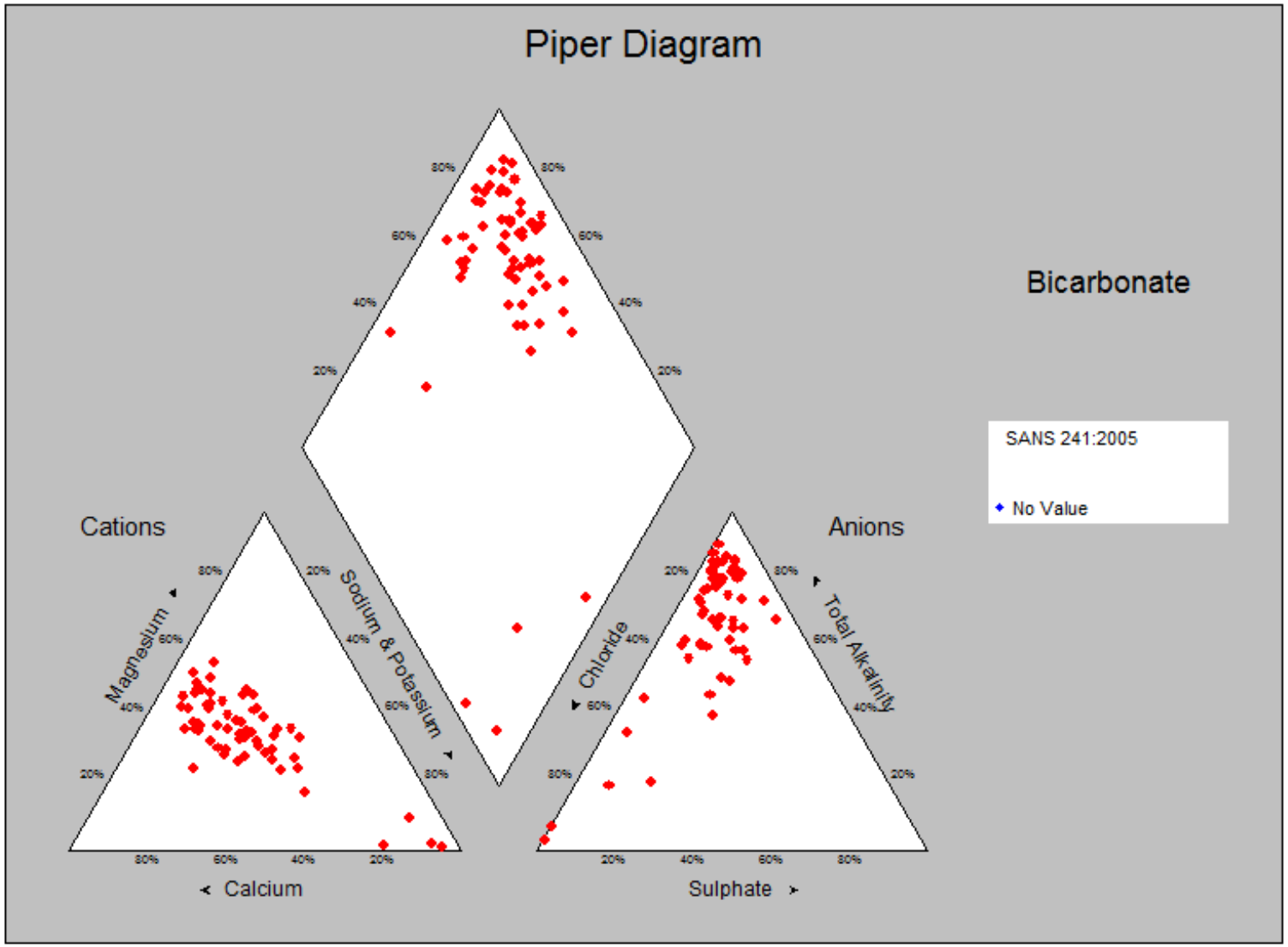
Piper Diagram
Bicarbonate
SANS 241:2005
No Value
Cations
Anions
Magnesium
Sodium & Potassium
Chloride
Total Alkalinity
Calcium
Sulphate
80%
60%
40%
20%

Groundwater section 5

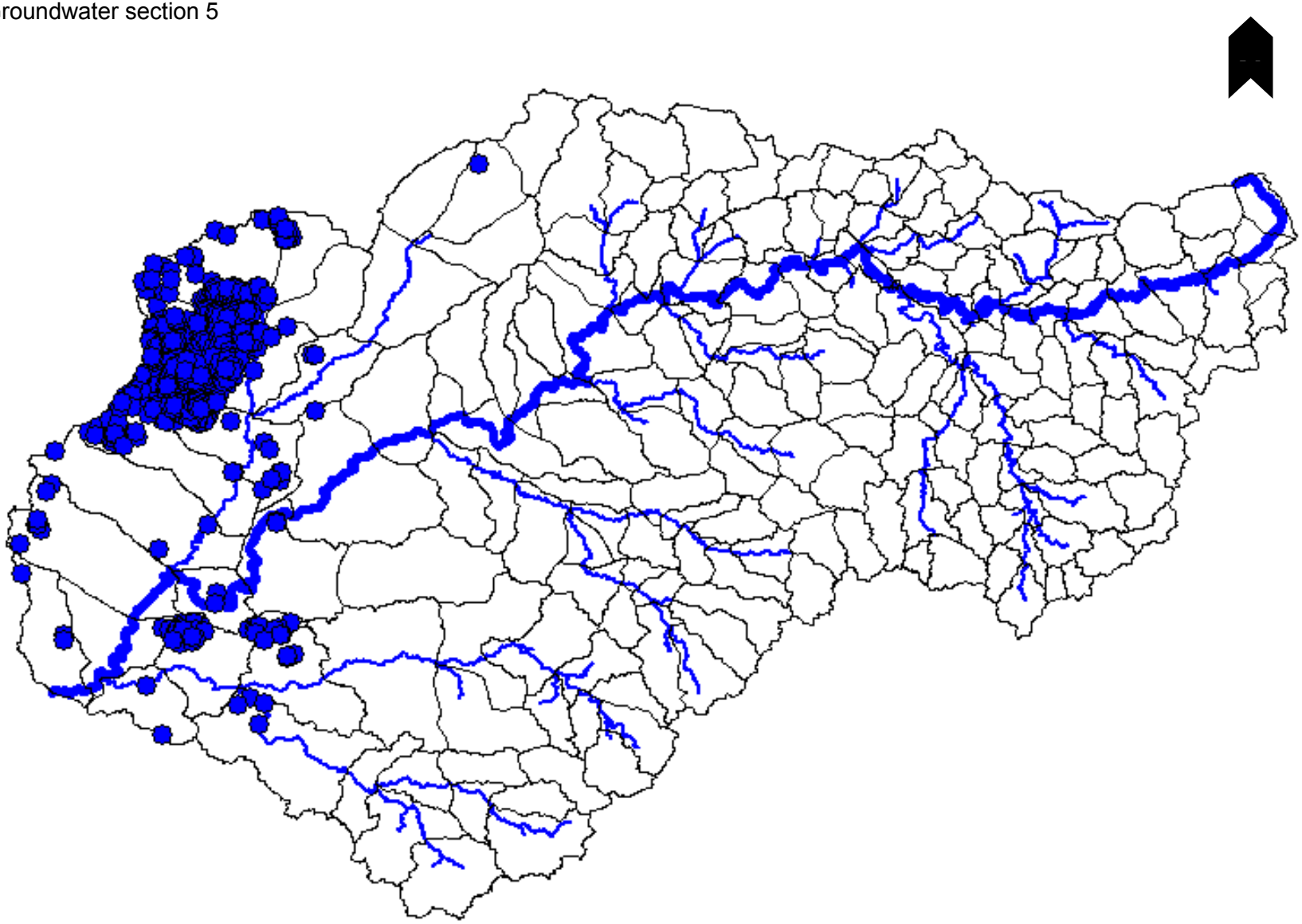

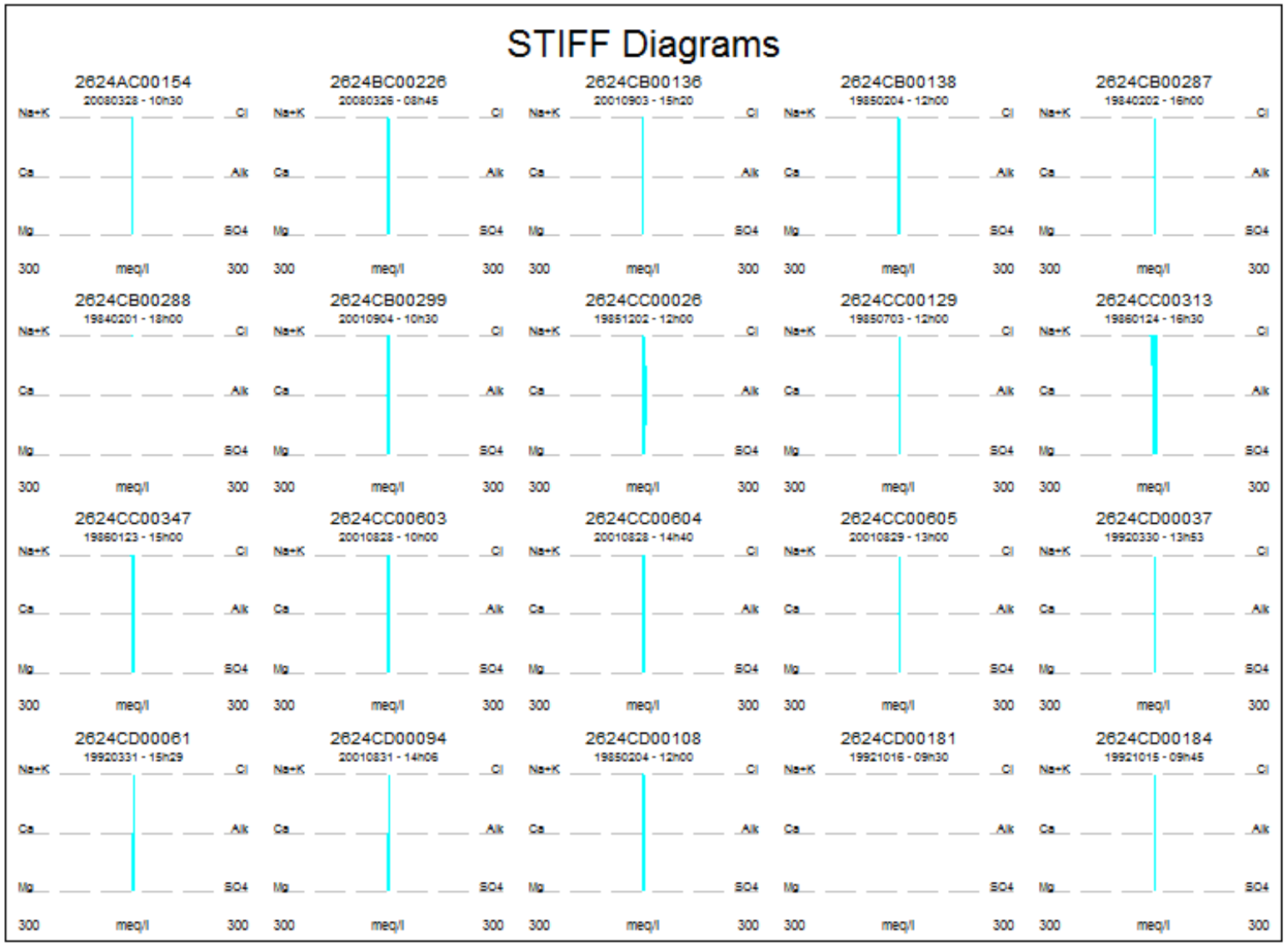
STIFF Diagrams
2624AC00154
20080328 - 10h30
2624BC00226
20080326 - 08h45
2624CB00136
20010903 - 15h20
2624CB00138
19850204 - 12h00
2624CB00287
19840202 - 16h00
2624CB00288
19840201 - 18h00
2624CB00299
20010904 - 10h30
2624CC00026
19851202 - 12h00
2624CC00129
19850703 - 12h00
2624CC00313
19860124 - 16h30
2624CC00347
19860123 - 15h00
2624CC00603
20010828 - 10h00
2624CC00604
20010828 - 14h40
2624CC00605
20010829 - 13h00
2624CD00037
19920330 - 13h53
2624CD00061
19920331 - 15h29
2624CD00094
20010831 - 14h06
2624CD00108
19850204 - 12h00
2624CD00181
19921016 - 09h30
2624CD00184
19921015 - 09h45
Na+K
Cl
Ca
Alk
Mg
SO4
300
meq/l
300

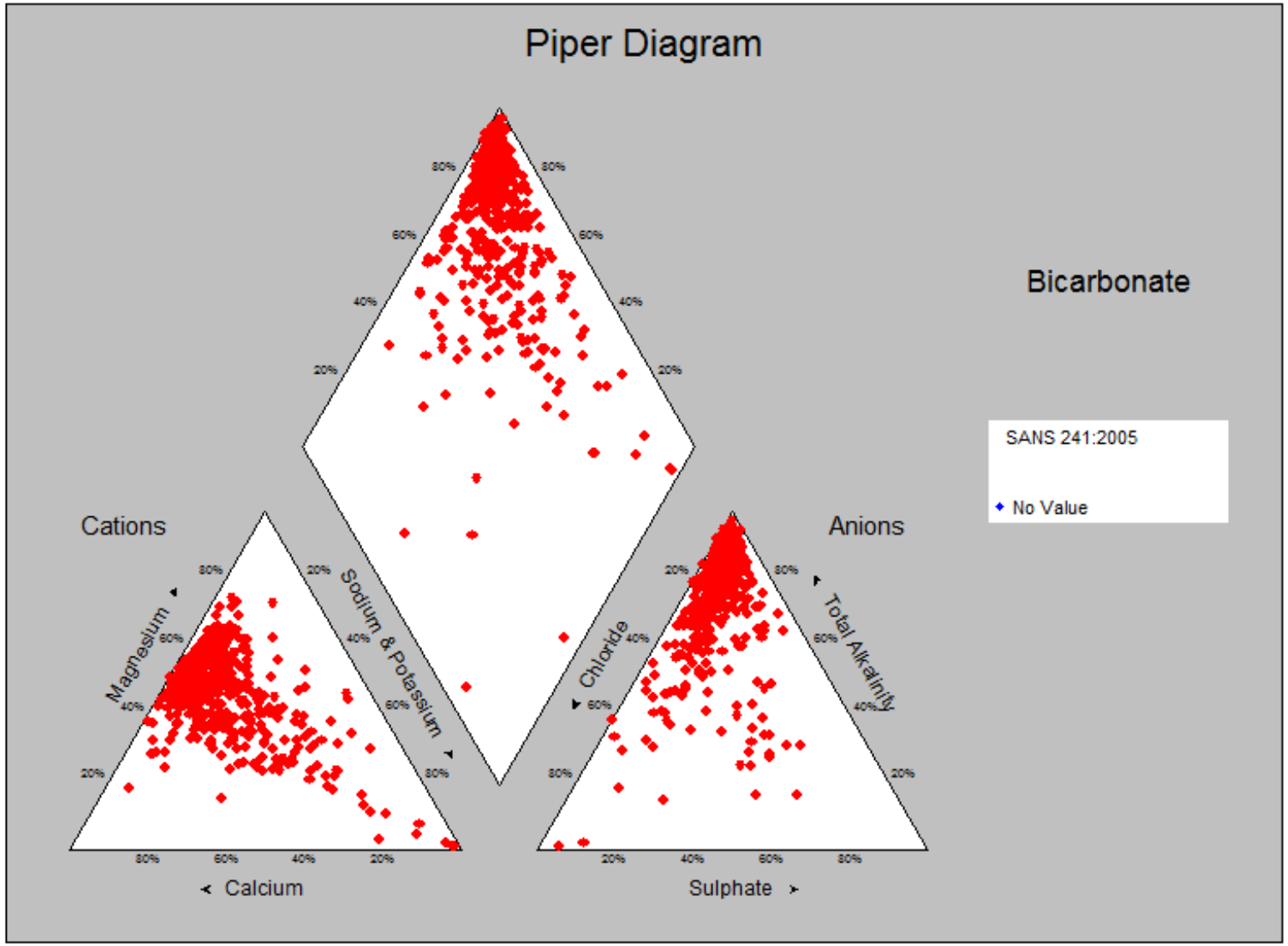
Piper Diagram
Bicarbonate
SANS 241:2005
No Value
Cations
Anions
Magnesium
Sodium & Potassium
Chloride
Total Alkalinity
Calcium
Sulphate
80%
60%
40%
20%

Groundwater section 6

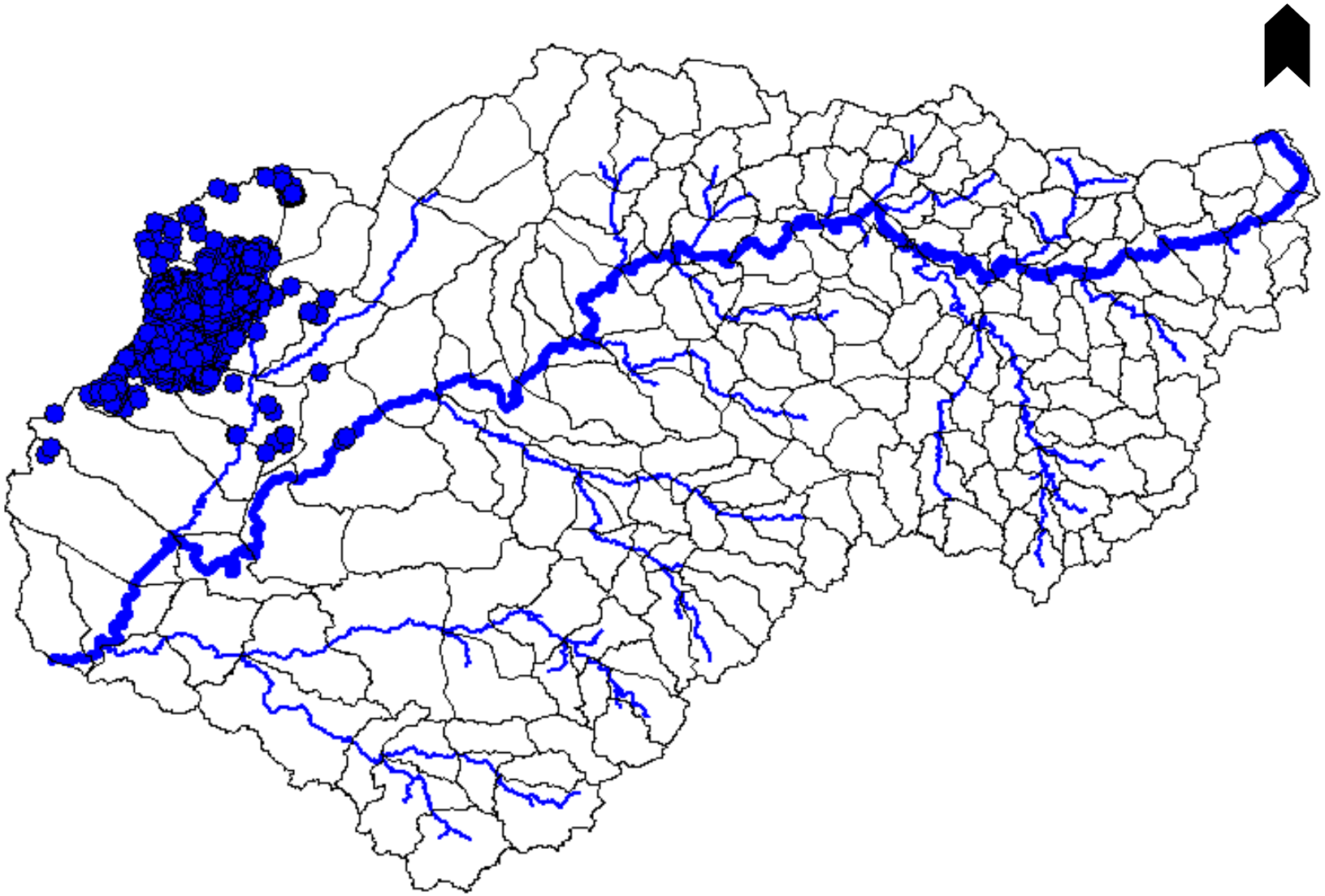

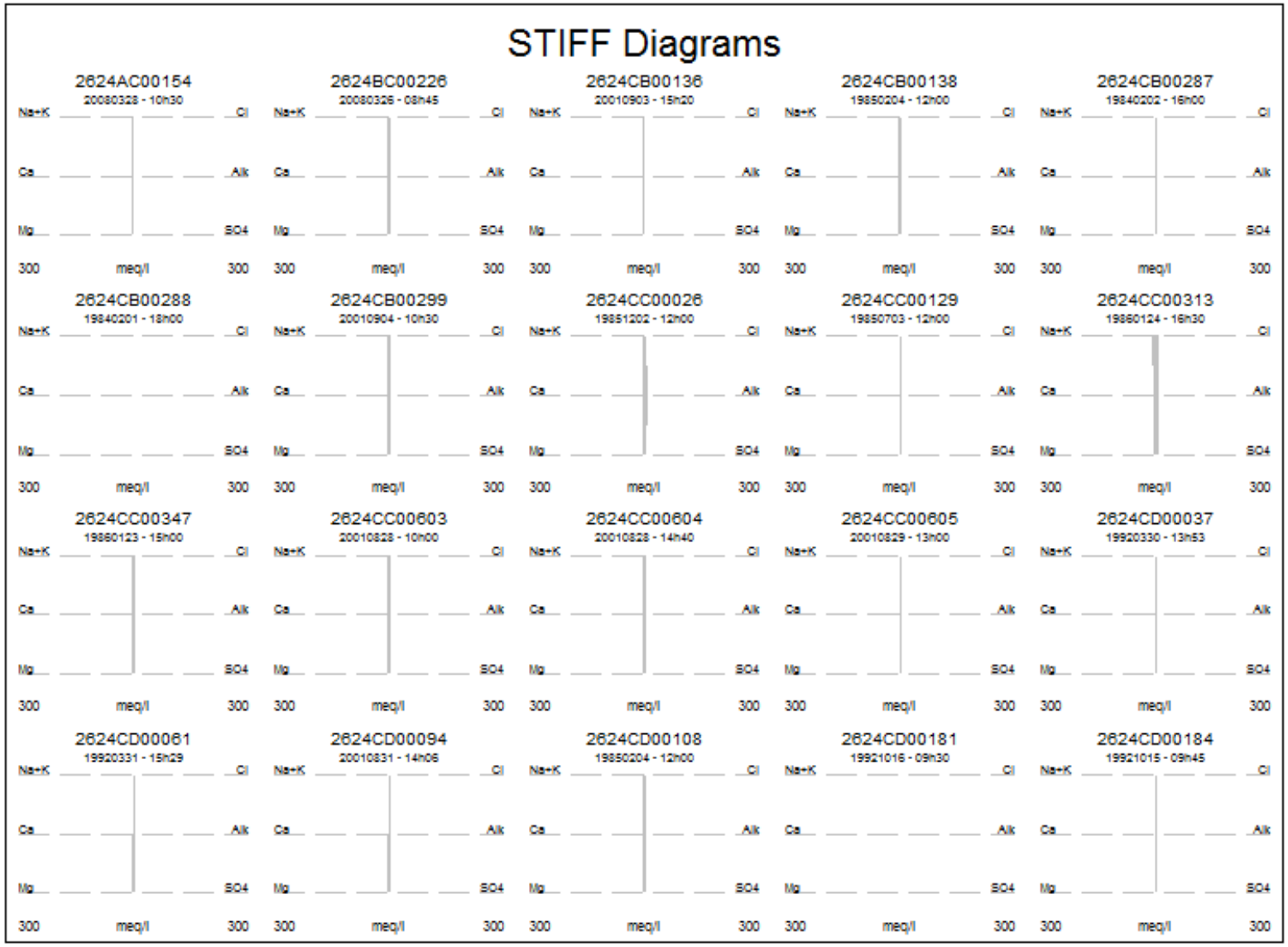
STIFF Diagrams
2624AC00154
20080328 - 10h30
2624BC00226
20080326 - 08h45
2624CB00136
20010903 - 15h20
2624CB00138
19850204 - 12h00
2624CB00287
19840202 - 16h00
2624CB00288
19840201 - 18h00
2624CB00299
20010904 - 10h30
2624CC00026
19851202 - 12h00
2624CC00129
19850703 - 12h00
2624CC00313
19860124 - 16h30
2624CC00347
19860123 - 15h00
2624CC00603
20010828 - 10h00
2624CC00604
20010828 - 14h40
2624CC00605
20010829 - 13h00
2624CD00037
19920330 - 13h53
2624CD00061
19920331 - 15h29
2624CD00094
20010831 - 14h06
2624CD00108
19850204 - 12h00
2624CD00181
19921016 - 09h30
2624CD00184
19921015 - 09h45
Na+K
Ca
Mg
Cl
Alk
SO4
300
meq/l
300

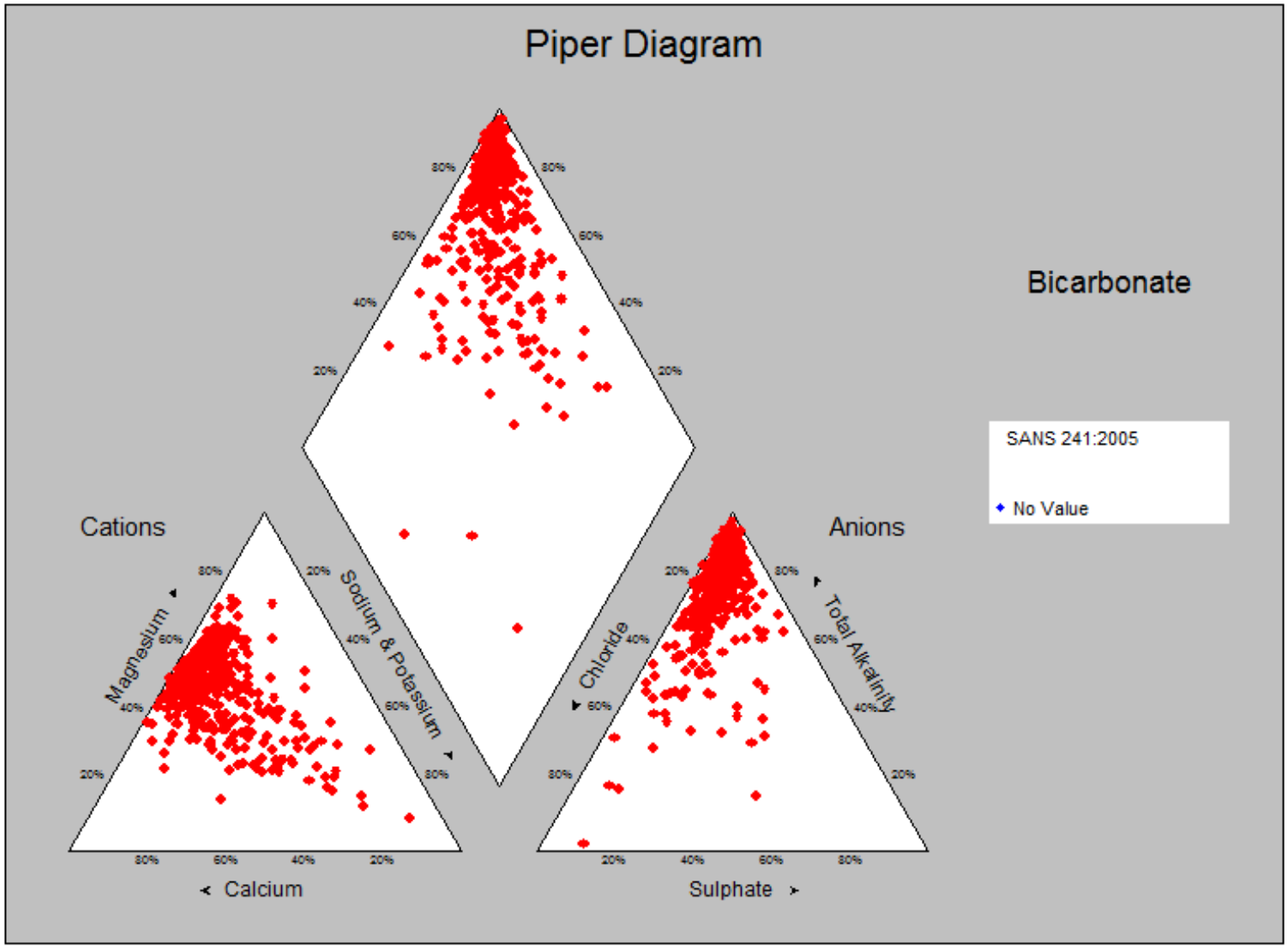
Piper Diagram
Bicarbonate
SANS 241:2005
No Value
Cations
Anions
Magnesium
Sodium & Potassium
Chloride
Total Alkalinity
Calcium
Sulphate
80%
60%
40%
20%

Groundwater section 7

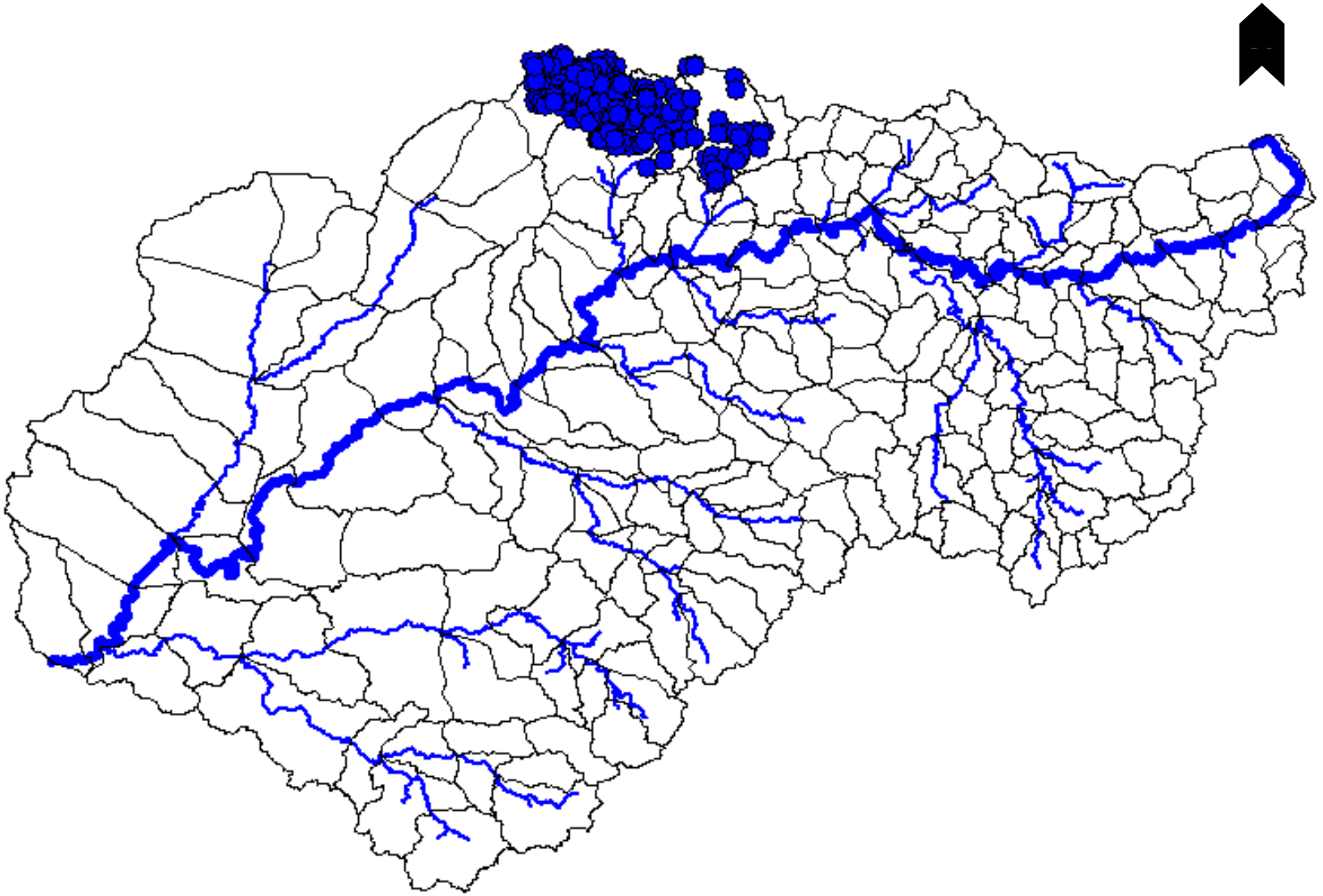

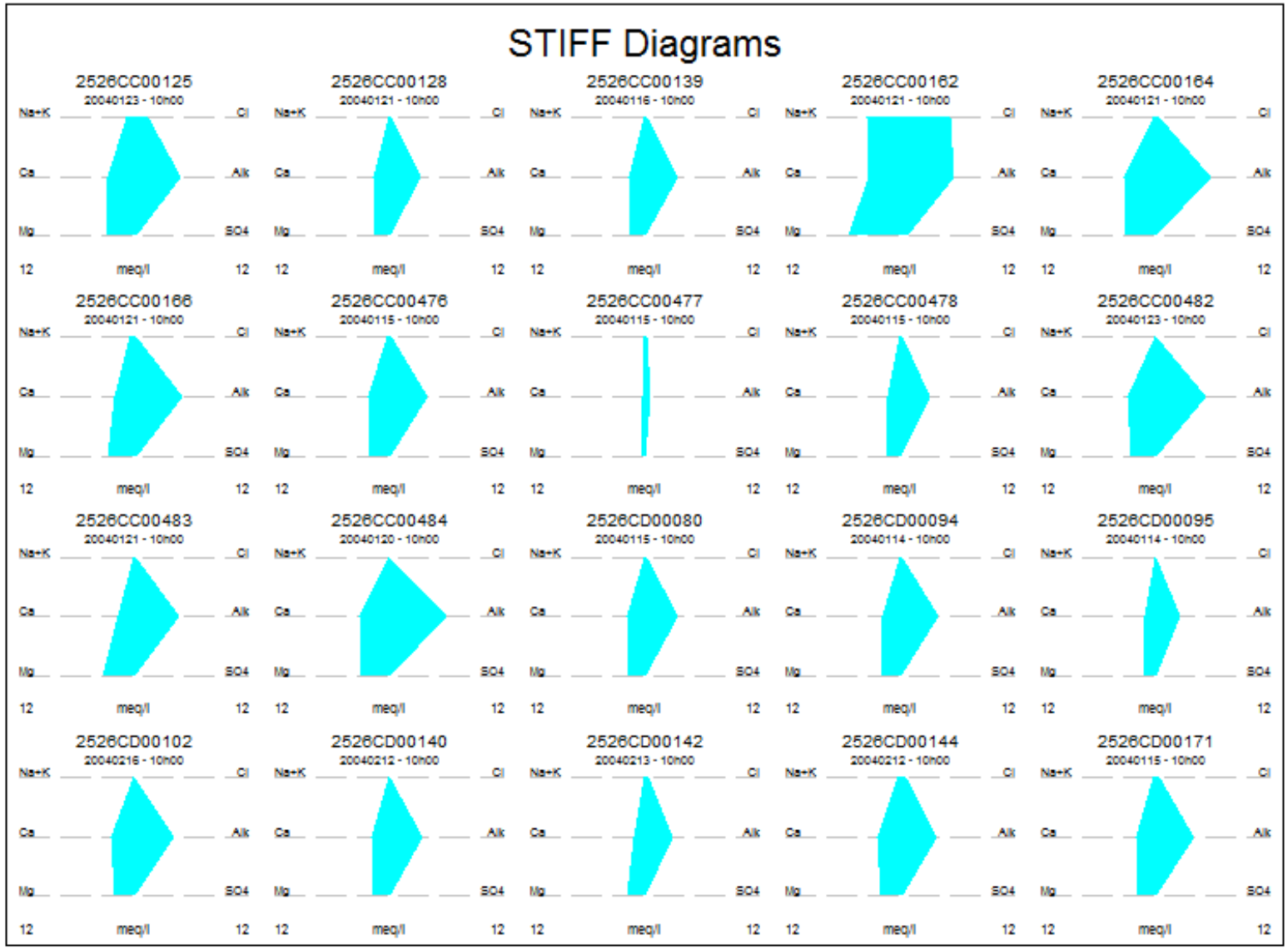
STIFF Diagrams
2526CC00125
20040123 - 10h00
2526CC00128
20040121 - 10h00
2526CC00139
20040116 - 10h00
2526CC00162
20040121 - 10h00
2526CC00164
20040121 - 10h00
2526CC00166
20040121 - 10h00
2526CC00476
20040115 - 10h00
2526CC00477
20040115 - 10h00
2526CC00478
20040115 - 10h00
2526CC00482
20040123 - 10h00
2526CC00483
20040121 - 10h00
2526CC00484
20040120 - 10h00
2526CD00080
20040115 - 10h00
2526CD00094
20040114 - 10h00
2526CD00095
20040114 - 10h00
2526CD00102
20040216 - 10h00
2526CD00140
20040212 - 10h00
2526CD00142
20040213 - 10h00
2526CD00144
20040212 - 10h00
2526CD00171
20040115 - 10h00
Na+K
Ca
Mg
Cl
Alk
SO4
12
meq/l
12

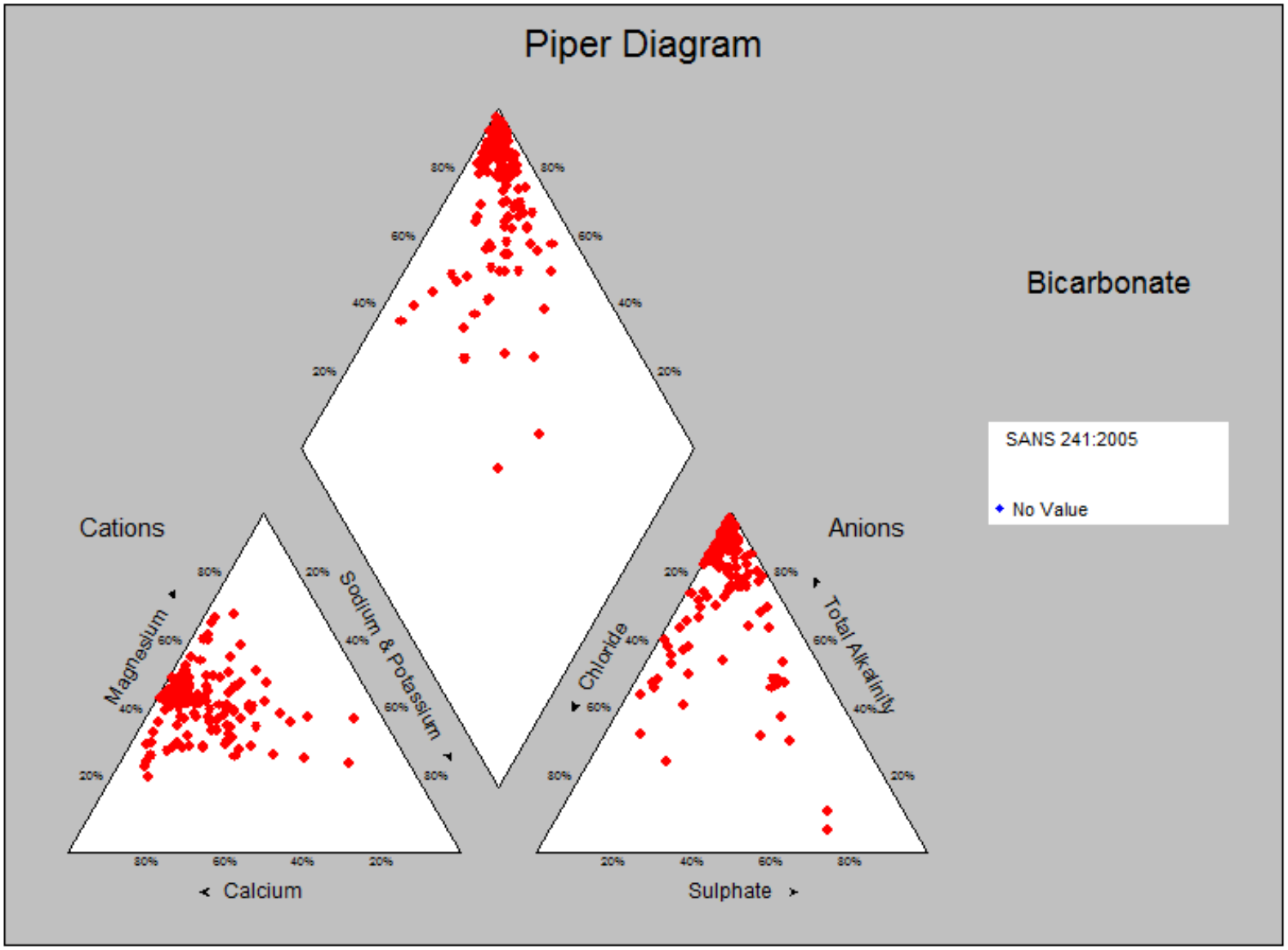
Piper Diagram
Bicarbonate
SANS 241:2005
No Value
Cations
Anions
Magnesium
Sodium & Potassium
Chloride
Total Alkalinity
Calcium
Sulphate
80%
60%
40%
20%

Groundwater section 8

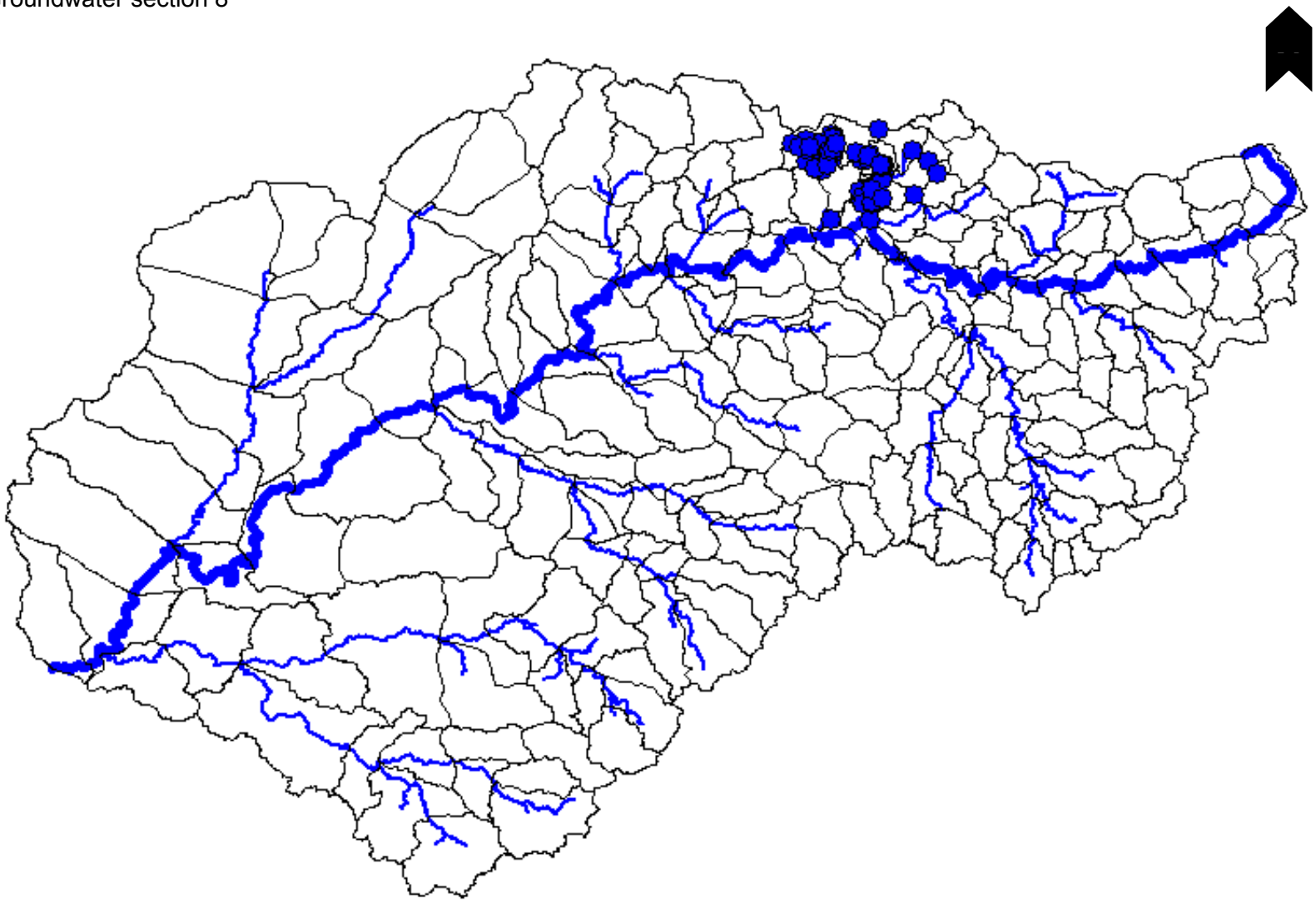

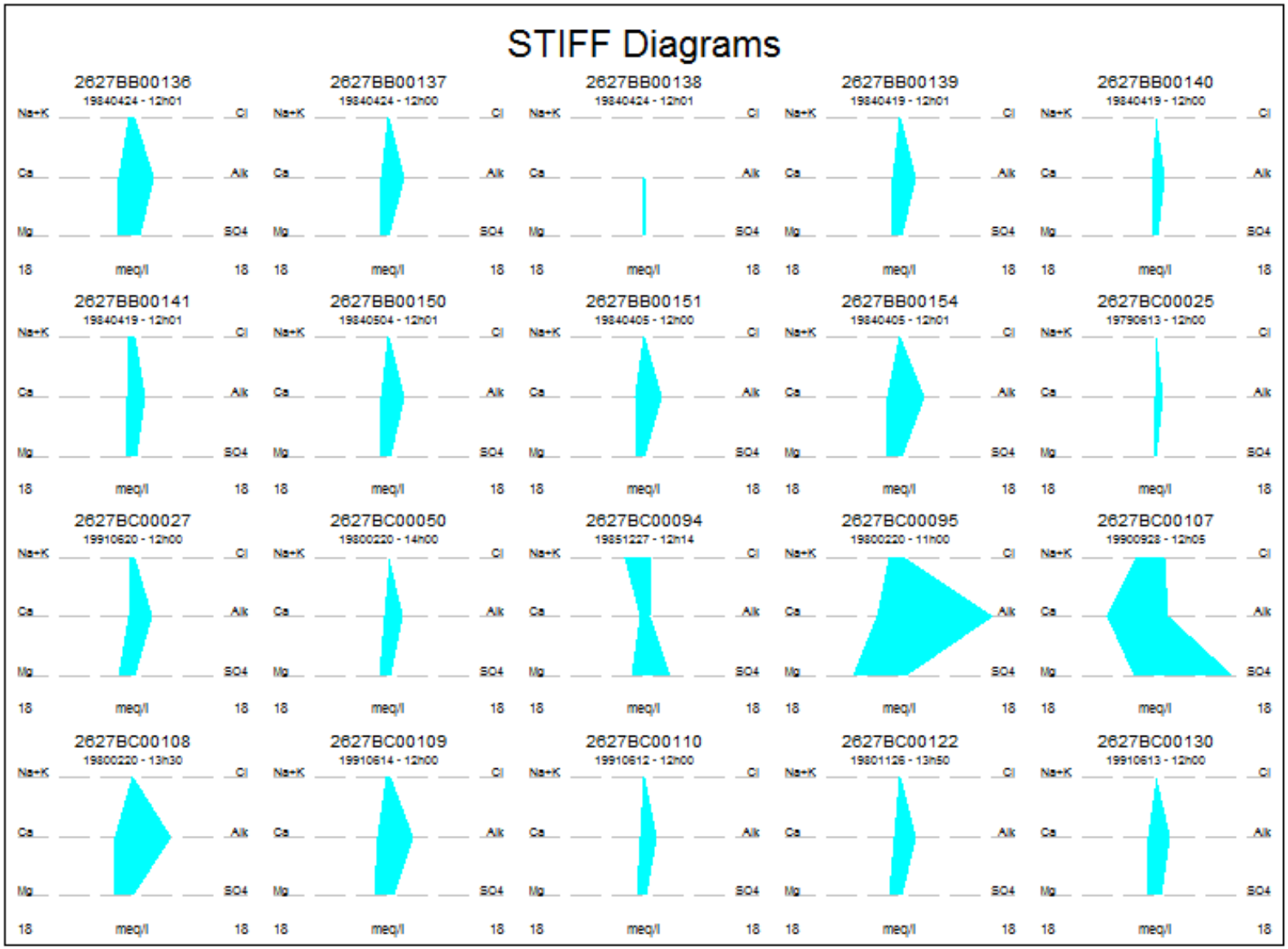
STIFF Diagrams
2627BB00136
19840424 - 12h01
2627BB00137
19840424 - 12h00
2627BB00138
19840424 - 12h01
2627BB00139
19840419 - 12h01
2627BB00140
19840419 - 12h00
2627BB00141
19840419 - 12h01
2627BB00150
19840504 - 12h01
2627BB00151
19840405 - 12h00
2627BB00154
19840405 - 12h01
2627BC00025
19790613 - 12h00
2627BC00027
19910620 - 12h00
2627BC00050
19800220 - 14h00
2627BC00094
19851227 - 12h14
2627BC00095
19800220 - 11h00
2627BC00107
19900928 - 12h05
2627BC00108
19800220 - 13h30
2627BC00109
19910614 - 12h00
2627BC00110
19910612 - 12h00
2627BC00122
19801126 - 13h50
2627BC00130
19910613 - 12h00
Na+K
Ca
Mg
Cl
Alk
SO4
18
meq/l

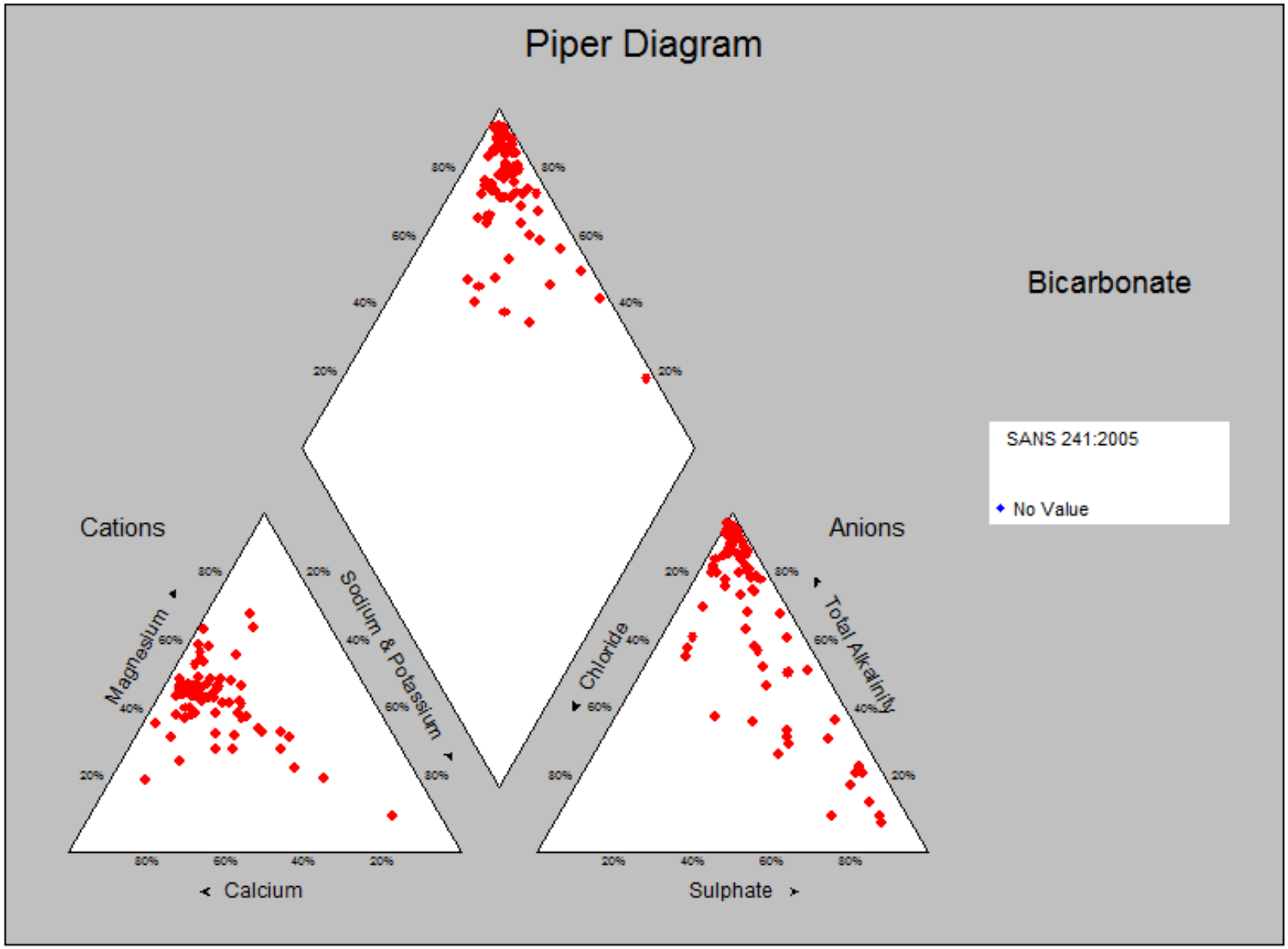
Piper Diagram
Bicarbonate
SANS 241:2005
No Value
Cations
Anions
Magnesium
Sodium & Potassium
Calcium
Chloride
Total Alkalinity
Sulphate
80%
60%
40%
20%